INVESTIGATING THE PROCESS AND REGULATION OF THYMOCYTE EGRESS BY LYMPHOTOXIN BETA RECEPTOR AND THYMIC STROMA

By

Kieran David Jon James

A thesis submitted to the University of Birmingham

For the Degree of DOCTOR OF PHILOSOPHY

Institute of Immunity and Immunotherapy

College of Medical and Dental Science

University of Birmingham

September 2017

ABSTRACT

The thymus is a heterogeneous mix of hematopoietic and stromal cells that function to generate a functional, self-tolerant T-cell pool. Although many of these populations are well studied, the role of non-epithelial stroma remains unclear.

Thymic mesenchyme has been identified as an important regulator of T-cell egress. Studies of lymphotoxin beta-receptor (LTβR) have revealed its critical role in T-cell egress as well as the development and function of lymph node mesenchyme. We hypothesized that LTβR regulation of thymic mesenchyme is critical for T-cell egress. To test this we generated *Wnt-1^{cre}Ltbr^{flox}* mice to delete LTβR on thymic mesenchyme and revealed this to be non-essential for T-cell egress. Moreover, we generated *Foxn-1^{cre}Ltbr^{flox}* mice to delete LTβR on thymic epithelial cell (TEC). Despite the critical role of LTβR in medullary TEC development, T-cell egress was normal. However, deleting LTβR on thymic endothelium using *Flk-1^{cre}Ltbr^{flox}* mice revealed an essential role of LTβR regulation of endothelium to control T-cell egress. Our analysis also revealed that T-cell entry into the perivascular space during T-cell egress occurs stochastically. Collectively our findings highlight a novel role for LTβR regulation of thymic endothelium as a critical pathway of T-cell egress.

ACKNOWLEDGMENTS

Firstly, I would like to express my sincere gratitude to my supervisor Dr. William Jenkinson for the continued support he has provided during the past 4 years of my PhD. I am extremely grateful for all of his help and guidance throughout my time of research and writing of this thesis. I would also like to thank my second supervisor, Professor Graham Anderson, for all of his support and guidance.

Additionally I want to thank everyone within the T-cell development lab for all their help with experiments and general discussions of our work, as well as for all the cakes, biscuits and pick'n'mix, which were always in constant supply. Every member of the T-cell lab has made it such an amazing group to be a part of and have always made being in the lab incredibly fun! Furthermore I would like to thank everyone on the 4th floor of the IBR for making my time as a student so enjoyable.

Lastly I would like to thank all of my family and friends who have been so supportive. I would especially like to thank my parents and Laura for their continued support and encouragement throughout my PhD.

TABLE OF CONTENTS

LIST OF FIGURES

CHAPTER ONE

CHAPTER THREE

CHAPTER FOUR

CHAPTER FIVE

CHAPTER SIX

LIST OF TABLES

ABBREVIATION LIST

-/-	Deficient
2-dGuo	2-deoxyguanosine
3PP	Third pharyngeal pouch
Ab	Antibody
ACKR	Atypical chemokine receptor
Ag	Antigen
Aire	Autoimmune regulator
APC	Antigen presenting cell
BEC	Blood endothelial cell
CCR	C-C chemokine receptor
Cld	Claudin
CLP	Common lymphoid progenitor
CMJ	Corticomedullary junction
cTEC	Cortical thymic epithelial cell
CXCL	CXC chemokine ligand
CXCR	CXC chemokine receptor
DC	Dendritic cell
DLL	Delta-like ligand
ECM	Extracellular matrix
EMT	Epithelial-mesenchymal transition
ETP	Early T-cell progenitor
eYFP	Enhanced yellow fluorescent protein
FCS	Fetal calf serum
FDC	Follicular dendritic cell
FGF	Fibroblast growth factor
Foxo1	Forkhead box protein O1
Foxp3	Forkhead box p3
FRC	Fibroblastic reticular cell
FSP1	Fibroblast specific protein-1
HSA	Heat stable antigen
HSC	Hematopoietic stem cell
ICAM	Intracellular adhesion molecule
IGF	Insulin-like growth factor
iNKT	Invariant natural killer T-cell
IP	Intraperitoneal
IV	Intravenous
Klf2	Krüpple-like factor 2
LEC	Lymphatic endothelial cell
LN	Lymph node
LPP3	Lipid phosphate phosphatase 3
LTi	Lymphoid tissue inducer
LTo	Lymphoid tissue organizer

MHC	Major histocompatibility complex
mKitL	Membrane bound form of Kit ligand
mLN	Mesenteric lymph node
MPP	Multipotent progenitor cell
MRC	Marginal reticular cell
mTEC	Medullary thymic epithelial cell
mTECSC	Medullary thymic epithelial cell stem cell
NC	Neural crest
nTreg	Natural Treg
OPG	Osteoprotegerin
PDGFR	Platelet-derived growth factor receptor
Podoplanin	PDPN
PSGL1	P-selectin glycoprotein ligand 1
RAG	Recombination-activating gene
RANK	Receptor activator of nuclear factor-κB
RORγ	Retinoic acid receptor-related orphan nuclear hormone regulator γ
RTE	Recent thymic emigrant
RTOC	Reaggregate thymic organ culture
Runx	Runt-related transcription factor
S1P	Sphingosine-1-phosphate
S1PR1	S1P receptor 1
SGPL	S1P lyase
SMA	Smooth muscle actin
SPHK	Sphingosine kinase
Spns2	Spinster homolog 2
TCF	T-cell factor
TCR	T-cell receptor
TEC	Thymic epithelial cell
TGFβ	Transforming growth factor
ThPOK	T-helper inducing POZ-Krupple like factor
TNC	Thymic nurse cell
TNFRSF	Tumour necrosis factor receptor super family
TPEC	Thymic portal endothelial cell
TRA	Tissue restricted antigen
Treg	Regulatory T-cell
TSSP	Thymus specific serine protease
VCAM	Vascular cell adhesion molecule

CHAPTER ONE: GENERAL INTRODUCTION

1.1 THYMUS AND THYMOCYTE DEVELOPMENT

1.1.1 Overview Of The Thymus

The thymus is one of two primary lymphoid organs whose function is to support the development of lymphocytes that are essential for the host's adaptive immune protection. The bone marrow is the other primary lymphoid tissue and it functions to support the development of B-cells as well as the generation of T-cell precursors, which migrate to the thymus where they undergo a tightly regulated programme of development. T-cells play a vital role in defending the host against foreign and harmful cells all the while remaining tolerant to the host's own cells thereby preventing autoimmune disease. T-cells can only achieve this by undergoing a highly selective and rigorous developmental program during their development within the thymus.

The importance of the thymus and the role that it plays within the immune system was first discovered in 1961 in a study which revealed that surgical removal of the thymus (thymectomy) resulted in the absence of peripheral T-cells (1). Since this initial observation thymus research has covered many aspects of thymic biology, including the developmental regulation of the organ, the different cell populations that make it up, how it regulates the development of thymocytes (developing T-cells) and how it regulates and achieves a highly effective immune regulatory role whilst ensuring tolerance to self. Together this research has collectively emphasized the essential role that the thymus plays in the development of the T-cell repertoire and its contribution to the immune system.

The thymus regulates the development of T-cells through its unique microenvironment that contains specific cell types, whose organization and function is specialized to educate and screen different thymocyte subsets through their various stages of development. The thymus generates two main types of T-cells differing by their T-cell receptor (TCR); γδ and αβ T-cells.

αβ T-cells are the primary T-cell population generated by the thymus and can be separated into functionally distinct helper T-cells and cytotoxic T-cells based on their expression of the co-receptor CD4 or CD8, respectively. The expression of the co-receptor aids the binding of the TCR to major histocompatibility complex (MHC)–peptide complex by stabilizing the interaction. $CD4^+$ T-cells recognize peptides presented in the context of MHC Class II molecules, while $CD8^+$ T-cells recognize MHC Class I associated peptides and this specificity is important both during the development of the T-cells as well as their function within the periphery. Thymocytes undergo a number of regulated developmental processes during their development within the thymus. Subsequent to cortical thymic epithelial cell (cTEC)-mediated positive selection, T-cell receptor (TCR) bearing $CD4^+$ thymocytes interact with medullary thymic epithelial cells (mTEC) that present self-peptide-MHC class II complexes. Depending on the strength of TCR signaling during this interaction the developing $CD4^+$ T-cell can either continue it's development as a $CD4^+$ T-cell, be selected to differentiate into a regulatory T-cell or be selected for cell death (negative selection) (more detail of this process in Section 1.1.5). Once $CD4^+$ T-cells complete this intrathymic development and enter the periphery the naïve T-cell can become activated by antigenic stimulation as a result of specific TCR interactions with

peptide-MHC complexes presented by antigen presenting cells (APC) coupled with CD3 activation (2). $CD4^+$ T-cells have multiple potential lineages and their differentiation into a specific lineage is dependent on the specific cytokine signaling and transcription factors. Subsets of $CD4^+$ T-cells include: T-helper 1 (Th1), Th2, Th9, Th17, follicular helper T-cells (Tfh) and induced Tregs (iTreg) (2). The signals instructing the differentiation of each lineage are specific and each subset has a particular function within peripheral T-cell immunity. As their name suggests, the main function of $CD4^+$ T-cells is to “help” other cells to kill target cells through their production of various mediators such as cytokines. For example activated Th1 and Th2 cells produce cytokines that stimulate clonal expansion and antibody production by B-cells or both can also activate $CD8^+$ cytotoxic T-cells to kill infected cells (3,4). An exception to this helper role are regulatory T-cells, which are a subclass of $CD4^+$ T-cells which are rescued during negative selection and act in an immunosuppressive manner to curtail immune response.

$CD8^+$ T-cells also undergo intrathymic development similar to $CD4^+$ T-cells but instead interact with self-peptide MHC Class I complexes and are selected for survival or cell death depending on the strength of TCR signaling during this interaction. Once $CD8^+$ cytotoxic T-cells have entered the periphery they are activated by antigenic stimulation of their TCR by cognate endogenous peptides presented by MHC Class I on virally infected cells. Cytotoxic T-cells kill target cells through at least three distinct pathways. Cytotoxic T-cells can produce tumor necrosis factor α which triggers target-cell apoptosis and interferon γ which triggers increased MHC Class I presentation pathway and Fas expression in the target cells enhancing cytotoxic T-cell killing (5,6). Cytotoxic T-cells can also kill target cells

through direct cell-cell contact, either binding Fas on the target cell triggering apoptosis or releasing highly cytotoxic perforins and granzymes directly into the target cell causing apoptosis (7–9).

γδ T-cells are thought to arise during the earliest stages of T-cell development and represent a much smaller fraction of the periphery T-cell pool compared to αβ T-cells. In contrast to αβ T-cells, much less is known of the function and development of γδ T-cells.

These two cell types can be further subdivided into many different subtypes based on their developmental stages and function. The following sections will cover the different cells types and development stages of the αβ T-cell lineage.

1.1.2 Thymic Colonization And Early T-Cell Progenitors

Unlike the bone marrow, which is the site of the generation of B-cell precursors and their development, the thymus is not able to produce its own hematopoietic stem cells to generate T-cell precursors from. Therefore, T-cell development is dependent on the colonization of the thymus by blood-borne progenitor cells (10). The origin of the hemogenic progenitor cell and how it colonizes the thymus differs during different stages of development. At day 12 of gestation (E12), progenitor cell entry occurs prior to vascularization of the thymus, therefore progenitor cells migrate into the thymus via adjacent blood vessels and must migrate through the surrounding mesenchymal layer of the early thymic rudiment to enter the epithelial compartment of the early thymus (11,12). At this early stage the progenitor cells are sourced mainly from the fetal liver (13). However at the post-natal and adult stage the T-cell

progenitor arises from the bone marrow and the developed vasculature of the thymus supports the direct entry of the progenitors into the thymus via blood vessels at the junction between the cortex and the medulla, a region termed the corticomedullary junction (CMJ) (14). Progenitor entry occurs in waves during both embryogenesis and adulthood, during embryogenesis the progenitor cells mainly give rise to γδ T-cells, however at the late stages of embryogenesis and the subsequent post-natal and adult thymus, thymocyte development has largely switched to the αβ T-cell lineage (15,16). As this thesis focuses on aspects of αβ T-cells, the following sections will center on the development of αβ T-cells and their precursors during post-natal and adult stages.

The phenotypic characterization of the hematopoietic progenitor cells that colonize the thymus is poorly understood, in part due to the very small number of these cells that exist within the adult thymus. It is also difficult due to the capacity of multiple different bone marrow borne progenitors such as hematopoietic stem cell (HSCs), multipotent progenitor cells (MPP) and common lymphoid progenitors (CLPs) to give rise to thymus settling progenitors and undergo subsequent T-cell development (17). However more is known about the progenitor cells downstream of the thymus colonizing cells. Commonly referred to as early T-cell progenitors (ETPs), these cells are the earliest progenitor population that has been relatively well defined within the thymus and represent the starting point of intrathymic T-cell development. ETP are found within the DN1 thymocyte population, which are identified as being negative for the co-receptors CD4 and CD8, $CD25^{-}$ and $CD44^{+}$. However the DN1 population contains a mixture of other cell types including those of non-T-cell lineage such as B-

cell progenitors. Therefore ETP are defined as Lineage^{low} (a cocktail of markers including those associated with non-T-cell lineages such as B220 which identifies B-cells) as well as CD25^{-}KIT^{+}Sca-1^{+} (18,19). ETP have multilineage potential, being able to give rise to B-cells as well as T-cells as T lineage commitment does not occur until progeny downstream of the ETP (18).

Colonization of the thymus by these progenitor cells upstream of ETP has been shown to be regulated, at least in part, by adhesive interactions between P-selectin expressed by the thymic endothelial cells and P-selectin glycoprotein ligand 1 (PSGL1) expressed by the progenitor cells (20). Rossi *et. al* showed that mice deficient for PSGL1 had reduced numbers of ETP within the thymus as a consequence of disrupted progenitor cell entry (20). This same study by Rossi *et. al* revealed that the number of thymic progenitors within the thymus regulates the expression of P-selectin, acting as a feedback loop to regulate endothelial-mediated progenitor entry into the thymus (20). This is in accordance with an initial study which observed that the thymus is receptive to progenitor cell entry for a period of ~1 week and refractive for ~3 weeks which allows for the progressive emptying of the microenvironmental niche for the next wave (15). Together these two studies highlight a role of self-regulation of thymocyte progenitor entry into the thymus.

The chemokine receptors C-C chemokine receptor type 7 (CCR7) and 9 (CCR9) both play a role in regulating T-cell progenitor entry into the thymus. Whilst CCR9 regulates progenitor entry, there may be a degree of redundancy in the requirement for this chemokine receptor, as absence of CCR9 when CCR7 is still expressed does

not impact progenitor entry due to CCR7 fully supporting progenitor entry (21). However absence of both CCR9 and CCR7 resulted in a severe reduction of ETP within the double-deficient mouse thymus suggesting a clear role of CCR9 and CCR7 working together to regulate progenitor entry (21).

It has also been shown that lymphotoxin beta receptor (LTβR) can regulate progenitor entry into the thymus, as mice deficient for LTβR have a significant reduction of ETP (22). It is thought that this reduction in T-cell progenitor entry in LTβR-deficient mice is a result of reduced expression of the intracellular adhesion molecule 1 (ICAM-1) and vascular adhesion molecule 1 (VCAM-1) which are both reduced as shown by PCR of thymic mesenchyme and endothelium (22). Interestingly this LTβR-dependent regulation of thymocyte entry was not due to altered P-selectin expression which appeared normal on LTβR-deficient endothelium (22). Consistent with these findings, mAb inhibition of ICAM-1 or VCAM-1, or inhibition of the integrins that these adhesion molecules bind to, impaired the homing of progenitors to the thymus (23). This essential role of LTβR requires interaction between LTβR-expressing stroma and LTβR-ligand-bearing thymocytes providing evidence that thymocytes play a role in regulating T-cell progenitor entry via interactions with thymic endothelium (22,24). Consistent with the thymic endothelial cells' role in regulating progenitor entry via P-selectin, it has been recently shown that LTβR regulates a specific type of endothelial cell, termed thymic portal endothelium, which is significantly reduced in LTβR-deficient mice and therefore these portal endothelial cells are thought to regulate ETP in an LTβR-dependent manner (24).

Upon development from the thymus colonizing T-cell progenitor, ETP undergo further developmental progression that eventually gives rise to T-cell lineage restricted immature DN3 thymocytes which then in turn give rise to $CD4^+CD8^+$ αβ TCR-expressing DP thymocytes that undergo positive selection. The following section will cover how these developmental stages occur as well as how each is regulated in detail. The key stages of the T-cell development programme are summarized within Figure 1.1.

1.1.3 Early Thymocyte Development And T-Cell Lineage Commitment

ETP within the thymus are not yet lineage restricted and still have the capacity to give rise to many non-T-cell lineages such as B-cells, DCs and NK cells (25). T-cell lineage commitment does not occur as a single event; instead commitment occurs over a number of developmental stages between ETP and the T-cell lineage committed DN3 thymocyte population, summarized in Figure 1.1 (26).

The developmental progression begins with ETP defined as $CD4^-CD8^-CD25^-CD44^+CD117^+$ (18,19). ETP develop into DN2 thymocytes, which are $CD4^-CD8^-CD25^+CD44^+CD117^+$ and have lost B-cell potential but still have NK-cell, DC and T-cell lineage potential (27). The DN2 population can be split into two distinct populations termed DN2a and DN2b (28). Using a pLCK-GFP reporter model which reports Lck signaling within the developing thymocyte, Masuda *et. al* were able to show that DN2 cells can be separated by the expression of the pLCK-GFP. GFP^- DN2a cells differentiate and give rise to GFP^+ DN2b which have lost DC lineage potential, marking the key difference between DN2a and DN2b cells (28).

Figure 1.1. T-Cell Development

T-cell progenitors enter the thymus at the cortico-medullary junction (CMJ) via blood vessels, which are surrounded by pericytes, and develop into $CD25^{-}CD44^{+}CD117^{+}$ early T-cell progenitors (ETP). ETP migrate to the inner cortex and develop into $CD25^{+}CD44^{+}$ DN2 cells under the regulation of cortical thymic epithelial cells (cTEC). DN2 thymocytes migrate further into the outer cortex, migrating along a cellular matrix comprised of VCAM-1-expressing cTEC and develop into $CD25^{+}CD44^{-}$ DN3. Development of DN2 into DN3 thymocytes marks T-cell lineage commitment and DN3 express the T-cell receptor (TCR) β chain and a pre-TCRα chain. DN3 cells then develop into pre-DP thymocytes, which begin TCRα chain rearrangement but do not yet express CD4 or CD8 co-receptors. Generation of TCRα and it's pairing with TCRβ forms an αβ TCR which is accompanied with an upregulation of CD4 and CD8 and develop into DP ($CD4^{+}CD8^{+}$) thymocytes. DP thymocytes interact with self-peptide-self-MHC complex-bearing cTEC and undergo positive selection, where successful low affinity interactions between DP TCR and self-peptide MHC on cTEC select the DP cell for survival. Successful positive selection results in commitment and differentiation of $CD4^{+}CD8^{-}$ SP4 and $CD4^{-}CD8^{+}$ SP8 thymocytes, which migrate to the medulla. These SP thymocytes then interact with medullary TEC and undergo negative selection, where SP thymocytes expressing TCRs that bind self-peptide-self-MHC complexes with low affinity survive and SP thymocytes with TCR that bind with high affinity are selected for cell death. These immature SP thymocytes then undergo intrathymic maturation during which they acquire egress-competence and then exit the thymus via blood vessels at the CMJ.

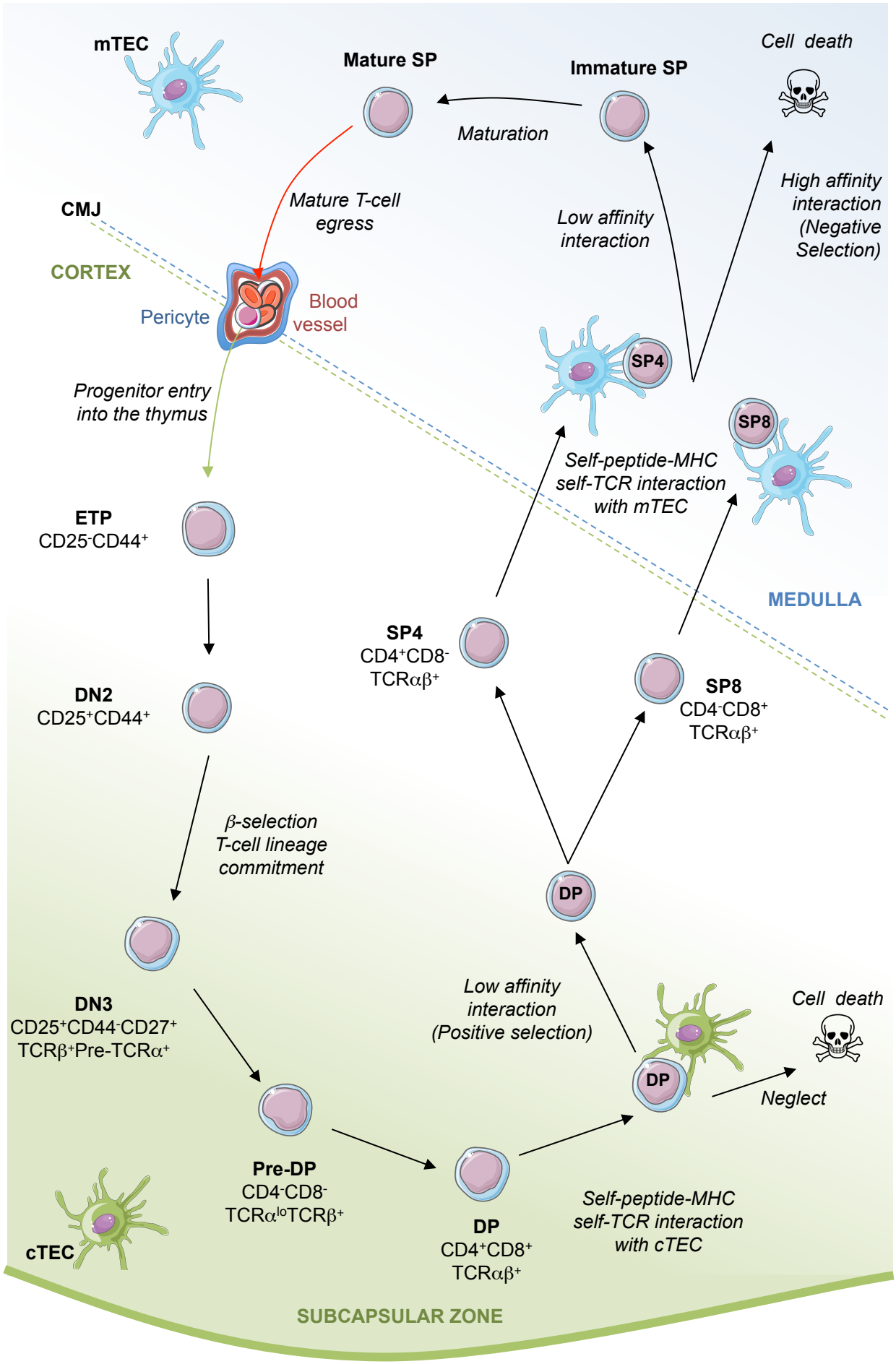
mTEC
Mature SP
Immature SP
Cell death
Maturation
Mature T-cell egress
CMJ
CORTEX
Pericyte
Blood vessel
Low affinity interaction
High affinity interaction (Negative Selection)
SP4
SP8
Progenitor entry into the thymus
Self-peptide-MHC self-TCR interaction with mTEC
ETP
CD25-CD44+
MEDULLA
SP4
CD4+CD8- TCRαβ+
SP8
CD4-CD8+ TCRαβ+
DN2
CD25+CD44+
β-selection T-cell lineage commitment
DP
Low affinity interaction (Positive selection)
Cell death
DN3
CD25+CD44-CD27+ TCRβ+Pre-TCRα+
DP
Neglect
Pre-DP
CD4-CD8- TCRαloTCRβ+
DP
CD4+CD8+ TCRαβ+
Self-peptide-MHC self-TCR interaction with cTEC
cTEC
SUBCAPSULAR ZONE

The developmental transition from ETP to DN2 is regulated by signals from the microenvironment in which the ETP inhabit. ETP are abundant in the perimedullary cortex, a region of the cortex near the CMJ where the thymus colonizing cells enter the thymus (14). These early progenitors spend a long time within the perimedullary cortex, with one study revealing that these cells spend approximately 10 days in this region, during which these cells undergo roughly 1000-fold expansion (29). ETP are in constant contact with stromal cells within the cortex, mainly cortical thymic epithelial cells (cTECs), which support ETP and their development to DN2. ETP/DN2 migrate to the inner cortex under the guidance of the CXC chemokine ligand 12 (CXCL12) expressed by cTEC which binds to its receptor CXC chemokine receptor 4 (CXCR4) expressed by early thymocytes (30). Failure of this signaling results in failure to migrate into the inner cortex and a developmental block at the ETP/DN1 stage, highlighting the requirement of specialized areas within the cortex for the development of different developmental stages of DN thymocytes (30). Kit ligand (KitL) regulates the proliferation and differentiation of DN thymocytes and it has been shown that the membrane bound form of KitL (mKitL) (ligand for Kit, CD117) is produced by cTEC as well as vascular endothelial cells near the CMJ (31,32). ETP are dependent on mKitL produced by cortex-specific vascular endothelial cells for their proliferation and differentiation into DN2 thymocytes (31,33). ETP proliferation and differentiation is also regulated by Notch signaling, notably from delta like ligand 4 (DLL4) produced by cTEC binding to Notch receptors on the ETP, as well as signaling through the interleukin-7 receptor (IL-7R) and IL-7 produced by cTEC (33–35). Constant interaction with cTEC is therefore essential for the development of the ETP-DN2 transition as well as their migration into the inner cortex.

DN2 thymocytes are found throughout the cortex as they make their way from the inner cortex to the outer cortex via chemokine gradient driven migration (14). DN2 cells migrate to the outer cortex using a cellular matrix, rather than an extracellular matrix, comprised of VCAM-1-expressing cTEC which allows the DN2 to remain in contact with cTEC and receive signals from the cTEC as they migrate (36). Similarly to ETP, Kit-KitL interactions regulate proliferation and differentiation of the DN2 cells, however DN2 cells interact with mKitL-expressing cTEC instead of endothelial cells (31,33,34). Notch ligands expressed by cTEC also play a role in regulating proliferation and differentiation of DN2 cells (34). Following a period of proliferation, DN2b develop into DN3 cells which is characterized by a downregulation of CD44 and CD117 expression resulting in a $CD4^{-}CD8^{-}CD25^{+}CD44^{-}$ phenotype (26,28).

Importantly the developmental transition into DN3 thymocytes marks the stage that developing thymocyte precursors commit to the T-cell lineage and become unipotent (26). DN3 thymocytes greatly increase T-cell receptor (TCR) rearrangement, which is initiated at DN2, and generate a fully rearranged TCRβ chain (37). In the context of αβ T-cell development, TCR rearrangement refers to the process of generating a TCR β chain by recombination of segments of Variable, Diversity and Joining, V(D)J, genes occurring at the β loci (38). This occurs through the activity of nucleases and ligases that randomly cut and join, respectively, gene fractions together under the control of recombination-activating gene 1 and 2 (RAG-1 and RAG-2) which are essential for V(D)J rearrangement (39,40). This results in the joining of a random segment from each of the V(D)J regions to generate a combination that encode proteins that form a functional β chain. Mombaerts *et. al* showed in addition to the

essential requirement for either RAG-1 or RAG-2 for V(D)J recombination and subsequent T-cell development, introduction of a single fully rearranged TCRβ gene can convert DN cells to DP, highlighting an essential role of TCRβ expression in DN thymocyte development (39–41).

Only DN3 thymocytes that have successfully generated a TCRβ chain become activated by TCR-dependent selection; identifying heterogeneity within the DN3 compartment (42). DN3 thymocytes that have yet to be selected are $CD27^{lo}$ and termed DN3a, whereas DN3 thymocytes that have undergone TCR-dependent selection upregulate CD27 expression and are termed DN3b (42). For αβ T-cell development, DN3b thymocytes that have successfully generated the TCRβ chain undergo a process termed β selection. This is a process that requires a functional TCRβ chain forming a pre-TCR with an invariant pre-TCRα (pTα) chain, the presence of both TCRβ and pTα is essential for T-cell development (41,43,44). This pre-TCR must be functional for the cells to interact with TCR signaling proteins otherwise cells that fail to produce a pre-TCR die by apoptosis (45). Pre-TCR signals cooperate with Notch signals (Notch/DLL1 interactions), as well as signaling from CXCR4-CXCL12 interactions, to promote cell survival, proliferation and differentiation of the DN3b cells to the DP cell stage (46–48). Following β selection, the DN3b cells undergo extensive proliferation and rapidly downregulate CD25, becoming pre-DP thymocytes (26,49). These pre-DP thymocytes are an intermediary population between DN3b and $CD4^{+}CD8^{+}$ DP thymocytes and begin TCRα chain rearrangement as well as migrate back towards the CMJ. Generation of the TCRα chain and its subsequent pairing with the TCRβ chain forms a mature TCR which is accompanied by

upregulation of CD4 and CD8 expression triggering the rapid progression to DP cells, the development of which will be discussed in further detail in the following section.

1.1.4 Positive Selection

Once DP thymocytes have generated a TCRα chain, it pairs with the TCRβ chain to form an αβ T-cell receptor expressed on the surface of the cell. DP thymocytes that express a functional αβ TCR are selected to continue their development via a process termed positive selection. Positive selection is a crucial step in thymocyte development as it screens the DP thymocyte population to ensure that cells progressing to the next stage of development have a functional T-cell receptor, which is critical to the T-cells overall functions. The importance of this process is highlighted by the fact that only 5-10% of DP thymocytes express low affinity TCR specificities and are therefore selected for cell survival (50,51). During this process, the αβ TCR expressed by the developing DP thymocyte binds to self-peptide self-MHC complexes presented by cTEC and this ability to induce a normal program of positive selection is distinct to cTEC (52). DP thymocytes are programmed for cell death by default but the successful recognition and binding of their TCR to self-peptide MHC complexes induces TCR signaling which promotes their survival (53). Such pro-survival regulators include the retinoic acid receptor-related orphan nuclear hormone regulator γ (RORγ) and trans-acting T-cell factor-1 (TCF-1), with it's co-activator β-catenin, are required for the expression of the anti-apoptotic factor Bcl-x_L (54,55). Absence of either RORγ or TCF-1 results in loss of Bcl-x_L and leads to accelerated spontaneous cell death of the DP thymocytes (54,55). Therefore DP thymocytes are programmed for apoptosis but these transcription factors promote their survival to

maximize the time frame in which DP thymocytes can undergo positive selection (54,55).

It is suggested that the strength of TCR binding to self-peptide MHC complexes determines the cells fate. DP thymocytes with low affinity are selected for survival and continuation of the developmental program. Gene rearrangement occurs during the generation of both the β and α chain to increase the maximum number of random self-peptide TCR specificities. TCRα rearrangement continues even after pairing of the α chain and the β chain to maximize the chances of successful positive selection, until either the cell is selected on having a functional αβ TCR or the cells do not receive a survival signal within the survival timeframe of DP thymocytes (approximately 3-4 days) and die by neglect via programmed cell death (56,57). Upon positive selection, RAG-1 and RAG-2 are downregulated to cease further gene rearrangement (56,57).

Ultimately successful positive selection of DP thymocytes results in the commitment and differentiation into either $CD4^{+}CD8^{-}$ SP4 or $CD4^{-}CD8^{+}$ SP8 thymocytes. SP4 thymocytes recognize MHC Class II whereas SP8 thymocytes recognize MHC Class I (58). Multiple models have been proposed to explain how DP thymocytes commit to either of these two lineages. The two previously prevailing models suggested either an instructional or stochastic program of lineage commitment. The instructional model proposes that the recognition and engagement of a specific class of MHC by the TCR specifically terminates the expression of the mismatched co-receptor molecule and therefore directs the lineage commitment to either SP4 or SP8. This

would suggest that a TCR recognizing MHC Class I promotes the commitment to SP8 by signaling to switch off CD4 expression, whereas a TCR that recognizes MHC Class II promotes the commitment to SP4 by signaling to switch off CD8 expression (58). Whilst initial studies suggested that co-receptors delivered different instructional signals to commit to the appropriate linage, further studies suggested that the strength of the TCR signal determined lineage commitment, with strong TCR signals leading to SP4 commitment and weak signals leading to SP8 lineage commitment (59,60). The stochastic model suggests early lineage commitment to SP4 or SP8 occurs independently of the TCR specificity. Binding of TCR and self-peptide MHC complex provokes down-modulation of the mismatched co-receptor and partial differentiation towards the MHC matched lineage, which a second TCR engagement with a self-peptide MHC complex finalizes this commitment (61,62). However some experimental observations seemed to contradict some of the key principles of these two models leading to an alternative model termed the kinetic signaling model (63,64). The kinetic signaling model proposes that SP4/SP8 lineage commitment is determined by the duration of the TCR signal which is determined by common cytokine receptor γ chains (γ_C) family members, such as IL-7, promoting specific lineage commitment (63). DP thymocytes that have received a TCR signal initially terminate CD8 transcription becoming $CD4^+CD8^{low}$ intermediate thymocytes that, importantly, are not lineage committed (63). If, upon CD8 downregulation, TCR signaling is maintained then the $CD4^+CD8^{low}$ thymocyte will commit to the $CD4^+CD8^-$ SP4 lineage as the TCR interaction must be MHC Class II restricted for continued signaling to occur (63). However if TCR signaling has stopped due to the CD4 expressing cell's TCR interacting with MHC Class I, then the cell becomes

responsive to IL-7 which signals the thymocyte to undergo “co-receptor reversal” (63). This is a process where CD4 transcription is terminated and CD8 transcription is reinstated, leading to a $CD4^{low}CD8^{+}$ thymocytes which then begins to receive TCR signaling and commits to $CD4^{-}CD8^{+}$SP8 lineage (63).

Additional transcription factors have been shown to play a role in lineage commitment for example Runt-related transcription factor 3 (Runx3) and the zinc finger transcription factor T-helper inducing POZ-KruppelV like factor (ThPOK). Runx3 binds and activates CD4 silencers to repress CD4 transcription, directing lineage commitment to SP8 fate (65). Opposing this regulatory role, ThPOK is activated upon MHC Class II engagement and is essential for lineage commitment to SP4 (66,67). ThPOK directly binds CD4 gene silencers, antagonizing their repressive functions to activate the CD4 gene (68). Interestingly this process acts as a positive feedback loop, as ThPOK activation of the CD4 gene results in increased surface expression of CD4, which prolongs TCR engagement with the MHC Class II leading to further ThPOK activation (68).

As well as undergoing positive selection through interactions with self-peptide MHC complexes expressed by cTEC, DP thymocytes upregulate their expression of C-C chemokine receptor 7 (CCR7) following TCR engagement (69–72). The CCR7-ligands CCL19 and CCL21 are expressed by medullary TEC (mTEC) and this drives the migration of DP and newly selected SP thymocytes from the cortex towards the medulla where they undergo the next stage of development (69–71). This requirement of CCR7 is essential for the delocalization of the developing thymocyte

from the cortex to the medulla, however in the absence of CCR7-mediate migration thymocyte development is not impaired, instead thymocytes leave the thymus functionally mature however they have not undergone central tolerance (69–71). This is explained by recent research which has shown that the development of conventional SP4 thymocytes can occur in the absence of the thymic medulla, as seen in mice deficient in RelB-dependent mTEC (72). In addition to CCR7-dependent migration, CCR4 and CCR9 have been suggested to play a role in this cortex to medulla migration. It has been shown that activated DP cells, identified as transiently expressing the activation marker CD69 following TCR stimulation, and SP thymocytes express CCR9 which facilitates migration towards it's ligand CCL25 expressed by cTEC, but importantly PlexinD1 blocks CCL25-mediated migration in these cells allowing the migration against the CCL25 gradient and towards CCR7-ligands in the medulla (73). Similarly CCR4 is reported to be upregulated upon positive selection however analysis of CCR4-deficient mice, CCR7-dificient mice and CCR4;CCR7 double-deficient mice does not support a role for CCR4 in cortex to medulla migration (74). Although this suggests that CCR4 does not have an essential role positive selection findings from Hu *et. al* indicate that CCR4 is required for medullary dependent tolerance potentially through regulating mTEC:dendritic cell interactions (75).

Once DP thymocytes have undergone positive selection, progressed to the next development stage of either SP4 or SP8 lineage commitment and migrated to the medulla they undergo negative selection, a mechanism of central tolerance.

1.1.5 Central Tolerance

Whilst positive selection is a fundamental process in ensuring thymocytes express functional TCRs capable of binding self-peptide MHC complexes, it does not check whether the TCR specificity of each thymocyte could be harmful to self. The random nature of generating a TCR creates a massive range of diversity amongst the TCR specificities and whilst that is good for the diversity of the T-cell repertoire, it also means that within these different TCR specificities there will exist TCRs that will recognize self-peptides and determine the peptide-bearing cell a target. This is the basis of autoimmunity, when the hosts own immune cells recognize the body's tissues and organs as a target. To prevent autoimmunity an additional selection process occurs termed negative selection. Negative selection is key in establishing central tolerance; for T-cells, central tolerance induction is a process that occurs within the thymus to prevent the generation of self-reactive T-cells. Central tolerance includes clonal deletion of autoreactive T-cells by negative selection as well as the generation of regulatory T-cells which act to suppress any self-reactive T-cells that escape into the periphery.

Negative selection occurs through apoptosis of thymocytes bearing high affinity TCRs for self and therefore bind strongly to self-peptide MHC complexes triggering strong TCR signals. Within the apoptosis pathway, BH3-only proteins have been highlighted as playing an essential role in clonal deletion of self-reactive thymocytes. BH3-only proteins are a pro-apoptotic group of the BCL-2 family, a family which includes both pro- and anti-apoptotic members (76). It has been shown that specifically Bim and Puma work in co-operation to regulate the deletion of auto-

reactive thymocytes (77). For example Bim has been shown to be upregulated upon high affinity binding of self-Ags which increases the binding to the pro-survival factor BCL-X_L, inhibiting its functions, leading to apoptosis (76,78).

Interestingly, negative selection occurs both in the cortex and the medulla and therefore occurs at multiple stages of thymocyte development such as early DP development when the cell has just begun to express the TCR within the cortex, through to later stages of SP development within the medulla (53,79,80). Through the use of Bim-deficient mice crossed with a $Nur77^{GFP}$ reporter, a reporter that correlates GFP expression with TCR signal strength, Stritesky *et. al* were able to show that 75% of thymocytes undergoing negative selection are at the DP stage of thymocyte development in the cortex compared to 25% undergoing negative selection at the SP stage in the medulla (81). However the negative selection that occurs within the cortex occurs due to the involvement of rare dendritic cells within the cortex rather than interactions with cTEC (79). On the other hand, negative selection occurring in the medulla is further dependent on mTEC as these stromal cells are specialized for ectopic expression of tissue restricted antigens (TRAs), which are self-peptides that are usually restricted to specific cells within the host's body but mTEC are able to generate these peptides and present them to the developing thymocytes. Antigen presentation can occur either directly by the mTEC or by "antigen hand-over" and presentation by neighboring antigen-presenting cells (APCs) within the medulla such as DCs. The mechanisms that mTEC employ, as well as what makes them specialized for negative selection, are covered in more detail in section 1.2.3.2. In short, the mTEC population as a whole is able to express almost all peripheral

transcripts, presenting these peptides either directly or via APCs within the medulla and therefore can check the TCR specificities of the developing SP thymocytes to eliminate any with specificity to the TRAs. The importance of the medulla for negative selection is highlighted in mice that either lack the ability to migrate to the medulla (CCR7-deficient mice) or mice that lack the medulla all together (such as RelB-deficient mice), both of which result in autoimmunity (69,71,82).

Positive and negative selection are not sequential events where cells must undergo positive selection first before moving on and undergoing negative selection, such an order would suggest that the TCR signal be different during the two processes. Instead a cell can undergo negative selection before it undergoes positive selection, consistent with the fact that negative selection can occur in the cortex (80,83). What decides the difference between positive selection and negative selection is the affinity of the TCR, a high affinity towards self-peptide MHC complexes triggers negative selection whilst low affinity signals positive selection. The intracellular mediator extracellular-signal-regulated kinase (ERK) is a member of the mitogen-activated protein kinase (MAPK) cascade and is involved in both positive and negative selection (84,85). It has been shown that high affinity binding induces high intensity ERK activation, which is associated with cell death indicating its role in negative selection, whereas positive selection stimulates a lower intensity and brief activation of ERK which declines but then gradually increases and is sustained (86). Thus depending on the TCR stimulation of either low or high affinity, the induced activation of ERK differs and the subsequent outcome of positive or negative selection is determined. Similar studies of the MAPK signaling pathway have

highlighted the narrow gap between positive and negative selection in terms of ligand affinity and signaling threshold (87).

High affinity TCR binding does not necessarily mean the thymocyte will undergo negative selection. Instead thymocytes with a high affinity may be directed down an alternative developmental pathways giving rise to non-conventional T-cell subsets such as nTregs or invariant natural killer T-cells (iNKTs) (88). Within the medulla, a small fraction of MHC Class II-restricted thymocytes that receive TCR stimulation from a high affinity TCR self-peptide MHC interaction can be rescued from clonal deletion and develop into natural Treg (nTreg) (88,89). nTreg are a regulatory subtype of SP4 thymocyte that suppress autoreactive T-cells in the periphery and are essential to central tolerance. Upon TCR stimulation within an affinity range between positive and negative selection, thymocytes upregulate CD25 becoming $CD25^{+}Foxp3^{-}$ pre-Treg and then go on to upregulate Forkhead box p3 (Foxp3) to develop into $CD25^{+}Foxp3^{+}$ Treg (90). Foxp3 is essential to the suppressive function of the Treg, for example IL-10 is essential for the function of Treg that suppress inflammatory response toward intestinal antigens and IL-10 has been shown to be a downstream effector mechanism induced by Foxp3 (89–91). The thymic medulla is essential for the development of Treg as shown in RelB-deficient mice which lack a thymic medulla due to perturbed mTEC development, have absent Treg and severe autoimmune defects (72,92,93). Interestingly a recent study found that whilst the thymic medulla is essential for the development of Treg, conventional SP4 thymocytes were present at normal frequencies and appeared phenotypically mature,

as shown by using a system of grafting RelB-deficient thymic lobes into a wildtype (WT) host (72).

Therefore as well as playing a vital role in negative selection of SP thymocytes, mTEC also play an essential role in the development of a regulatory subset of SP4 thymocytes which enforce tolerance within the periphery.

1.1.6 Thymocyte Egress

It has been estimated that developing SP thymocytes stay within the medulla for a period of 4-5 days following development from DP to SP thymocytes (94). During this intramedullary residency, the developing SP thymocytes are exposed to negative selection and Treg specification, as discussed previously, however they also undergo functional and phenotypic maturation prior to their egress from the thymus. The maturation status of the SP thymocyte can be determined by its cell surface expression of a number of maturation markers such as CD69, CD62L, HSA and MHC Class I. Immature SP thymocytes can be identified as $CD69^{+}CD62L^{-}HSA^{+}$ whereas mature SP thymocytes downregulate CD69 and HSA and upregulate CD62L to become $CD69^{-}CD62L^{+}HSA^{-}$ (95). Changes in maturational status of the SP thymocytes is important for its survival and marks the end of negative selection as HSA^{hi} thymocytes are susceptible to tolerance induction whereas HSA^{low} are strongly resistant (96). Additionally, maturation of the SP thymocyte is linked to acquiring key functions such as becoming proliferation-competent and egress-competent (95,97). Xing *et. al* were able to show that the expression profile of CD69 and MHC Class I was able to reveal three populations within SP4 and SP8 thymocytes that were

distinct in their proliferative and egress capabilities (97). $CD69^{+}$MHC Class I^{-} SP thymocytes were the least mature and termed SM, $CD69^{+}$MHC Class I^{+} SP thymocytes were termed M1 and are proliferation-competent and $CD69^{-}$MHC Class I^{+} were termed M2 and are both proliferation- and egress-competent (97). In this study and similar studies of thymocyte egress, a mature cell is deemed egress-competent if it expresses the sphingosine-1-phosphate receptor 1 (S1PR1) (95,97,98). S1PR1 is a G protein-coupled receptor which mediates migration towards a gradient of its ligand, the lipid signaling molecule sphingosine-1-phosphate (S1P) (98). Forkhead box protein O1 (Foxo1) and Krüpple-like factor 2 (Klf2) are transcriptional regulators of S1PR1 expression and are upregulated during thymocyte maturation (99–101). SP thymocyte maturation status was defined on the basis of CD69 and CD62L expression prior to the discovery of S1P-S1PR1 expression, however the definition of immature as $CD69^{+}CD62L^{-}$ and mature as $CD69^{lo}CD62L^{+}$ does coincide with the expression of S1PR1 and the S1PR1 regulating transcription factors. CD62L and S1PR1 are both downstream targets of Klf2 and S1PR1/CD69 expression is linked, therefore as the thymocyte matures, it increases Foxo1 and Klf2 expression which upregulates CD62L as well as S1PR1 expression and concomitantly downregulates CD69 (99–103).

Disruption of the S1P-S1PR1 axis has significant consequences on thymocyte egress as doing so results in reduced thymic output resulting in both reduced T-cells in the periphery and an intrathymic accumulation of mature thymocytes (98). Initial studies revealed the importance of this pathway through the use of the immunomodulator FTY720 which revealed reduced T-cell egress from the thymus

and secondary lymphoid organs due to FTY720 being a potent agonist of S1PR1 which prevents the migration response to the S1P gradient as well as inducing downregulation of the S1PR1 on the SP thymocyte cell surface (104–109). S1P-dependent egress has been shown to require an S1P gradient that is high at the point of exit, both at the vessel that the cell will leave the thymus by and in the blood, which is where the egressing cells will move into when leaving the thymus, whilst remaining low within the rest of the thymic parenchyma (110,111).

Several mouse models have revealed that, within the thymus, the S1P-S1PR1 axis is regulated by multiple cell types and these cells act to maintain the S1P gradient within the thymus. The mechanisms that regulate the S1P gradient mainly fall under two categories; maintaining high levels of S1P by production of S1P at the site of exit or maintaining low levels by degrading or dephosphorylating S1P within the rest of the thymic microenvironment.

S1P production is regulated by two enzymes, sphingosine kinase 1 (SPHK1) and SPHK2 which catalyze the ATP-dependent phosphorylation of sphingosine to generate S1P and both are expressed by thymic pericytes which is consistent with pericytes ensheathing blood vessels at the point of egress (111). Deleting SPHK specifically on thymic pericytes resulted in intrathymic accumulation of mature thymocytes and peripheral T-cell lymphopenia, both of which are indicative of disrupted thymocyte egress and thus highlights the crucial role of thymic mesenchyme in regulating T-cell egress (111).

Thymic epithelial cells have been shown to sustain the intrathymic S1P gradient though the production of lipid phosphate phosphatase 3 (LPP3), a dephosphorylating enzyme which inactivates S1P to maintain low intrathymic S1P levels promoting thymocyte egress (112). Deletion of *Ppa2b*, the gene that encodes LPP3, specifically on TEC results in an intrathymic accumulation of mature thymocytes and interestingly deletion of *Ppa2b* specifically on thymic endothelial cells also results in altered egress (112). Therefore both TEC and endothelium regulate SIP-dependent thymocyte egress through production of LPP3. Furthermore thymic endothelium has also been implicated in regulating S1P-dependent thymocyte egress through the expression of the S1P transporter spinster homolog 2 (Spns2). Spns2 is required for S1P release from endothelial cells, with deletion of Spns2 resulting in intrathymic accumulation of mature thymocytes consistent with an egress defect (113).

In addition to stromal cells, thymocytes and thymic DCs have also been shown to play a role in regulating thymocyte egress, with Zamora-Pineda *et. al* finding that deletion of S1P lyase (SGPL) in bone marrow-derived cells resulted in reduced thymocyte egress and a concomitant intrathymic accumulation of mature SP thymocytes (114). However despite expression of SGPL by radioresistant cells, deletion of *Sgpl* on TEC or endothelium did not alter thymocyte egress (114).

The S1P-S1PR1 axis is regarded as the primary mechanism regulating thymocyte egress however there are additional mechanisms that have been shown to play a role in egress. It was recently shown that IL-4 receptor α (IL-4Rα), which forms part of the type-2 IL-4R complex, is expressed by thymic stromal cells and is essential for

normal S1P-S1PR1-independent thymocyte egress (115). This role of IL-4Rα is dependent on provision of the IL-4R ligands IL-4 and IL-13 by iNKT cells to trigger IL-4R signaling (115). The absence of IL-4R signaling results in an intrathymic accumulation of mature thymocytes, which can be found within the perivascular space, as well as a reduction in recent thymic emigrants (RTE) in the periphery (115). Therefore in addition to the S1P-S1PR1 pathway, type-2 cytokines are an important regulator of T-cell egress suggesting a multifaceted mechanism regulating T-cell egress both at the molecular and cellular level.

The chemokine receptor CCR7 and its ligand CCL19 are essential for T-cell egress within neonates, however this pathway is not required for T-cell egress within adult mice suggesting differing egress mechanisms may exist at different stages of development (69,116). A possible explanation for this difference could be that during development from neonate to adult there is a shift from CCR7-dependent egress mechanisms to mechanisms that are dominant in the adult such as the S1P-S1PR1 pathway and the IL-4Rα pathway. A recent study found that Aire-deficient neonatal mice, which have reduced CCR7-ligand expression, have impaired thymocyte egress but this egress defect is alleviated in adult Aire-deficient mice (117). This study revealed that the S1P-S1PR1 pathway is functional at the neonatal stage but it is not sufficient to correct for the CCR7-dependent egress defect (117). However in Aire-deficient beyond 3 weeks of age, S1PR1 was significantly upregulated on mature thymocytes and this alleviated the T-cell egress defect seen in the younger neonatal Aire-deficient mouse and thus S1PR1-dependent egress becomes the dominant pathway regulating T-cell egress (117).

Another chemokine found within the thymus, CXCR4, was thought to be involved in regulating thymocyte egress. Until recently it was not clear whether CXCR4 was a positive or negative regulator of releasing mature thymocytes from the thymus as there was evidence supporting both as well as these studies being complicated by the embryonic lethality of CXCR4-deficient mice (118–121). However a recent study using $CD4^{cre}CXCR4^{flox}$ mice, which circumvents this embryonic lethality, found no abnormalities in SP thymocyte development or egress, suggesting that CXCR4 is dispensable for thymocyte egress (122).

Whilst these studies provide evidence for the involvement of multiple pathways and cell types in regulating T-cell egress, the precise regulation of this critical process remain relatively unclear and we aim to explore this topic in Chapter 4.

1.2 THYMIC STROMAL MICROENVIRONMENTS

1.2.1 Stromal Populations Of The Thymus

The thymic microenvironment is heterogeneous and essential to the function of the thymus. The primary stromal populations of the thymus are thymic epithelial cells, which include cortical TEC and medullary TEC that are vital to the process of positive and negative selection, respectively, as discussed in previous sections. Due to the importance of the role of TEC a great deal of research has been carried out investigating their development and function, as well as defining the heterogeneity within the cTEC and mTEC compartments based on their expression patterns of transcription factors, chemokines, cytokines and other molecules vital to their function.

However the non-epithelial compartment of thymic stroma remains less well characterized and studied. Non-epithelial cells comprise of endothelial cells, which vascularize the thymus and regulate ETP entry into the thymus. Thymic mesenchyme is the other main non-epithelial population and comprises of cells that contribute to the capsule, trabeculae and septae of the thymus structure as well as fibroblasts, which have been shown to regulate the development of thymic epithelium and thymocytes. Additionally thymic mesenchyme includes thymic pericytes, which support the vasculature as well as thymocyte egress. Further discussion of thymic mesenchyme and their function can be found in section 1.2.5.

1.2.2 The Development And Regulation Of Thymic Epithelial Cells

The most abundant population of thymic stroma are the thymic epithelial cells, which can be separated into cortical thymic epithelial cells (cTEC) and medullary thymic epithelial cells (mTEC) based on their location and function within the thymus. cTEC are restricted to the cortex where they support thymocyte development and screen thymocytes for a functional TCR whereas mTEC are restricted to the medulla and ensure the removal of self-reactive T-cells as well as support the selection of regulatory T-cells. As discussed in previous sections these distinct regions of the thymus are vital for thymocyte development.

1.2.2.1 The regulation of early stages of epithelial cell development

During the earliest stages of thymus development (around E10-E11) the thymus consists of an endodermal-derived epithelial rudiment, which arises from the third pharyngeal pouch (3PP), which is surrounded by neural crest-derived mesenchyme

(123,124). As thymus organogenesis progresses, hematopoietic progenitors migrate through the surrounding NC-derived mesenchyme and colonize the developing thymus (123,125). This early stage colonization initiates the formation of a complex three-dimensional epithelial network, which is characteristic of the thymic epithelial compartment. One of the key transcription factors of thymic epithelial cells, Foxn-1 is expressed by essentially all EpCAM-1^{+} embryonic TEC and plays an important role in the developing thymus. Absence of Foxn-1 in nude mice (nu/nu), which carry a naturally occurring mutation of the Foxn-1 gene, results in athymia (126). Whilst it has been shown that the initial endodermal-to-epithelial transition occurs independently of Foxn-1 signaling, Foxn-1 has been shown to play a key role in multiple aspects of TECs, including differentiation, proliferation and formation of the three-dimensional TEC network (11,127,128). Additionally Foxn-1 has been shown to regulate genes associated with T-cell progenitor recruitment, such as CXCL12 and CCL21 and T-cell progenitor lineage specification, such as delta-like ligand 4 (DLL4) (11,128).

The subsequent lineage specification of the thymic epithelium towards the cTEC and mTEC lineages is a complex process, our understanding of which has greatly benefited from a number of studies in recent years. Adult cTEC and mTEC are clearly distinguishable due to their differential expression of chemokines, cytokines, cell positioning and transcription factors, however embryonic TEC are comparatively less well defined. Clonal assays have shown that a single TEC progenitor taken from an E12 enhanced yellow fluorescent protein (eYFP) reporter mouse thymus and reintroduced into a WT E12 thymus can give rise to cTEC and mTEC, directly

showing that within the embryonic thymus, both cTEC and mTEC arise from a Foxn-1-dependent bipotent TEC progenitor cell (129). A similar study used an *in vivo* approach by creating a null allele of Foxn-1 which was revertible specifically within thymic epithelial cell precursors, with the assumption that the Foxn-1-deficient thymic rudiment still contains thymic epithelial cell precursors (130). Using this inducible model, Bleul *et. al* were able to show that both cTEC and mTEC arise from an upstream bipotent progenitor (130).

The developmental progression of epithelial cells downstream of the bipotent progenitor and the lineage relationship of cTEC and mTEC have been of interest in recent TEC progenitor studies. Baik *et. al* were able to show that the majority of the embryonic TEC population expressed the cTEC marker CD205 but did not express the mTEC-associated marker CD40 ($CD205^{+}CD40^{-}$) and thus are said to have a cTEC-like phenotype (131). This population of $CD205^{+}CD40^{-}$ can then progress through to a $CD205^{+}CD40^{+}$ developmental stage and then to a $CD205^{-}CD40^{+}$ stage suggesting that TEC progenitors serially acquire cTEC and then mTEC lineages (131). *In vivo* analysis of the development capacity of the $CD205^{+}CD40^{-}$ TEC progenitor revealed that these cells can give rise to both cTEC and mTEC lineages, including $AIRE^{+}$ mTEC cells (131). This study showed that TEC progenitors that give rise to both cTEC and mTEC have hallmarks of both the cTEC lineage (CD205 expression) and the mTEC lineage (CD40 expression, as well as RANK expression) (131). A similar observation was found by Ohigashi *et. al* who, using a $\beta5t^{cre}$ x loxP-dependent GFP reporter mouse model, were able to show that almost all mTEC came from a TEC progenitor expressing β5t, supporting the model that the TEC

progenitor has a cTEC-like phenotype or potential pre-commitment to the cTEC lineage (132). These analyses support what is referred to as a “serial progression” model of TEC development, wherein TEC progenitors first acquire cTEC lineage markers, followed by acquisition of mTEC lineage markers and then lineage commitment to mTEC (133). A study by Ribeiro *et. al* revealed that whilst mTEC can be derived from IL-7^+ TEC which are enriched within the cTEC compartment, mTEC can also arise from IL-7^- compartment suggesting an alternative mTEC developmental pathway also exists (134). Whilst these studies provide important insight into the lineage relationship of cortical and medullary epithelia, it still remains to be seen how these populations and their development into lineage committed TEC is regulated.

Downstream of the bipotent TEC progenitor, mTEC stem cells (mTECSCs) have been identified within the embryonic thymus. Identified as Claudin (Cld) 3,4^{hi}SSEA-1^+ TEC, these mTECSCs were shown to posses self-renewal capacity as well as the ability to sustain long-term generation of mTEC and functionally contribute to sustained self-tolerance (135). These mTECSCs are unipotent, only giving rise to mTEC cells and therefore are downstream of the bipotent TEC progenitor (135). Further analysis of this population was recently carried out which showed that the expression of the tumor necrosis factor receptor super family (TNFRSF) member, receptor activator of nuclear factor-κB (RANK), a hallmark characteristic of mTEC, is not expressed within the Cld3,4^{hi}SSEA-1^+ mTECSC population and instead RANK expression is restricted to the SSEA-1^- fraction of Cld3,4^{hi} mTEC progenitors (136,137). Interestingly the induction of RANK expression coincides with

downregulation of the cTEC marker CD205 and upregulation of MHC Class II suggesting that these Cld3,4^{hi}RANK^{+} TEC are mTEC committed progenitor cells that are downstream of the Cld3,4^{hi}SSEA-1^{+} mTECSC (136). Additionally, the findings of Baik *et. al* also revealed that Foxn-1 may play a role in regulating the pool size of the mTECSCs, but neither Foxn-1 or RelB signaling are required for the emergence of the mTECSCs (136). Interestingly RelB is required for the generation of the RANK^{+} mTEC progenitor which is downstream of the mTECSC which reveals a key regulatory step in the development of the mTEC lineage (136). A precursor population has also been identified which gives rise to Aire^{+} mTECS termed pMECs (138). These pMECs express RANK and cTEC molecules and their development into Aire^{+} mTECs has been shown to be dependent on activation of the classical NF-κB signaling pathway via TRAF6-dependedent RANK signaling (138). Akiyama *et. al* showed that the development of the pMECs from their precursors (pro-pMECS) was dependent on non-classical NF-κB activation by RANK and lymphotoxin β receptor (LTβR) signaling (138). Whether these populations of mTECSCs and pro-pMECs/pMECs are directly related has not yet been resolved.

Due to the cTEC-like phenotype of the bipotent progenitor it has been difficult to further separate the developmental stages of the mature cTEC population and therefore knowledge of the development of this TEC subset is less well known. cTEC maturation can be identified through the expression of CD40 and MHC Class II (139).Early CD205^{+} β5t-expressing cTEC progenitors lack expression of CD40 and MHC Class II and the development of these cells are Foxn-1-dependent suggesting they are downstream of the bipotent progenitor (139). The developmental

progression of these cells to mature $CD205^{+}CD40^{hi}$MHC Class II^{hi} cTEC is dependent on the presence of DN1-3 thymocytes however the development of the $CD205^{+}$ progenitor can occur in the absence of these signals (139). Compared to this, the regulation of mTEC development has been much more extensively research and will be the focus of the following section.

1.2.2.2 The regulation of mTEC development

The development of lineage committed, mature mTECs is highly regulated and is dependent on reciprocal interaction with developing thymocytes that reside in the medulla. These reciprocal thymocyte:epithelial interactions are required for both the development of the thymocytes but also for the development of the mTEC and this interaction is often referred to as 'cross-talk' (140).

αβ T-cells have been shown to play a vita role for mTEC development. Research using *Tcrα*$^{-/-}$ mice which cannot generate a functional αβ TCR and therefore lack post-positive selection αβ T-cells have a significant loss of medullary TEC, however the cTEC compartment is normal in these mice (141,142). Loss of SP4 thymocytes has been shown to be essential for the development of a normal medulla. Mice deficient for MHC Class II have a loss of SP4 thymocytes and altered medullary architecture (143). Administration of an anti-TCR mAb into MHC Class II-deficient mice restores SP4 thymocyte development and rescues the medullary phenotype (143,144). Additionally it has been shown that SP4 thymocytes are needed for mTEC proliferation (145). It has even been shown that signals from non-conventional T-cells such as invariant natural killer T-cells (iNKTs) are essential for the development of both mTEC and cTEC (146).

Understanding how these T-cell populations regulate TEC development requires an understanding of the specific signaling pathways involved in thymocyte:epithelial cross-talk and this has been the focus of TEC developmental research for some time. A large focus of this research has revolved around TNFRSF members. This group of receptors has been of major interest due to the important role of many of its members in regulating TEC development. TNFRSF members mediate nuclear factor (NF)κB transcription factors and signaling pathways that have been shown to be highly important in regulating mTEC and medullary organization such as TRAF6, which regulates signaling by TNFRSF members RANK and CD40 which activate the classical NFκB pathway (138,147). Additionally RANK, CD40 and LTβR activate RelB, mediated by NFκB inducing kinase (NIK), and deletion of either RelB or NIK results in defects in medullary organization and mTEC development (92,148).

The LTβR signaling pathway has been shown to play an essential role in the development of peripheral lymphoid organs as well as the maturation of stromal cells within these organs (149,150). With regards to TEC development, Boehm *et. al* were the first to show the requirement for LTβR signaling within the thymus, showing that the LTβR-deficient mouse thymus has a severe medullary disorganization and reduction in UEA-1^{+} mTEC (151). Within the reduced mTEC compartment of *Ltbr*$^{-/-}$ there is a loss of CCL21 and CCL19 expression, reduced numbers of the CCL21-expressing mTEC^{lo} subset and although LTβR does not directly regulate the expression of Aire on mTEC, LTβR-deficient mice do have a reduction in the number of Aire^{+} mTEC^{hi} (152–157).

LTβR has three known ligands, the homotrimer lymphotoxin α ($LT\alpha_3$), heterodimer lymphotoxin $\alpha_1\beta_2$ ($LT\alpha_1\beta_2$) and LIGHT (158). The LTβR ligand LTα is expressed on DP, SP4, SP8 as well as lymphoid tissue inducers (LTi) within the thymus and therefore LTβR:LTβR-ligand signaling is an important process in regulating the development of thymic medullary environment via cross-talk (159). Although LTβR has been shown to not regulate Aire expression by mTEC, it was proposed that LTβR regulates the expression of Fezf2 where it directly induces the expression of Fezf2-dependent TRAs important for negative selection (160). However our recent study showed that the breakdown in tolerance seen in LTβR-deficient mice is in fact due to disrupted regulation of DC frequency and the make up of the DC pool and mTEC continue to express both Aire and Fezf2 in the absence of LTβR (157). As stated above LTβR, along with RANK, is also required for the development of pMECs from their pro-pMEC precursors (138).

Another key regulator of mTEC development is the receptor activator of NFκB (RANK) and its ligand RANKL expressed by lymphocytes. RANKL is expressed by a number of different thymocyte populations within the thymus and RANK:RANKL signaling occurring through cross-talk is highly important in TEC development. RANK signaling was first identified as a key regulator of mTEC development by Rossi *et. al* who's findings revealed that *Rank*$^{-/-}$ mice had a significant reduction of Aire^{+} mTEC, highlighting the essential role of RANK signaling in the development of Aire^{+} mTEC within the embryonic thymus (152). This study also revealed that RANKL provision from $CD4^{+}CD3^{-}$ lymphoid tissue inducer (LTi) cells was playing a role in regulating

the Aire$^+$ mTEC in the embryonic thymus (152). However a similar study published shortly after revealed that RANK-dependent development of Aire$^+$ mTEC in the adult thymus was primarily regulated by RANKL provision by positively selected thymocytes rather than other intrathymic sources of RANKL including LTi suggesting different mechanisms of RANKL provision at different stages of development (161). Additionally Hikosaka *et. al* were also able to show a role for osteoprotegerin (OPG) which is a decoy receptor for RANKL and acts as a negative regulator of mTEC, with mice deficient for OPG having large medullary areas and an increase in Aire$^+$ mTEC (137,161). This is consistent with reports that RANKL is expressed on DP, SP8 and SP4 thymocytes, enriched on the immature CD69$^+$ fraction of SP4 thymocytes, as well as Foxp3$^+$ Treg (159,162). It has also been shown that RANKL is expressed by iNKT cells within the thymus and absence of RANKL$^+$ iNKT cells results in reduced mTEC and Aire$^+$ mTEC and therefore highlighting iNKT cells as a source of RANKL capable of supporting RANK-dependent mTEC development (146).

CD40-deficient mice do not have any overt medullary disorganization or reduction in mTEC or Aire$^+$ mTEC numbers (161). Whilst this observation was shown to be true for CD40-deficient mice, CD40 does play a role in regulating postnatal mTEC development and medullary distribution in cooperation with RANK signaling (162,163). It was also shown that RANK signaling is required for the upregulation of CD40 on mTEC and that CD40 may also regulate mTEC proliferation (162). Highlighting a role for CD40:CD40L interactions and CD40L is expressed by SP thymocytes but is not expressed by Treg (162).

Interestingly, studies have shown that CD80^{lo}MHC Class II^{lo} mTEC (mTEC^{lo}) develop into Aire expressing CD80^{hi}MHC Class II^{hi} mTEC (mTEC^{hi}) (152). However the mTEC^{lo} population has been identified as a mature population itself and therefore is a heterogeneous population that consists of both mature mTECs and immature mTECs that can give rise to mTEC^{hi} cells (152,156). Together these signaling pathways reveal a strict program of thymocyte driven regulation of mTEC development including both Aire^{+} mTEC^{hi} and CCL21^{+} mTEC^{lo}.

1.2.3 The Function Of Thymic Epithelial Cells

As discussed in previous sections, thymic epithelium is vital to the function of the thymus. Through the expression of a range of molecules such as chemokines, cytokines and transcription factors, cTEC and mTEC are able to regulate multiple stages of thymocyte development. The functions and how the cTECs and mTECs are able to carry them out are covered in the following sections 1.2.3.1 and 1.2.3.2.

1.2.3.1 The function of cortical thymic epithelial cells

cTEC, termed for their location within the cortex of the thymus, are a specialized subset of TEC which are commonly identified as Cytokeratin8^{+}CD205^{+}Ly51^{+} TEC. The primary role of cTEC is to regulate the early stages of thymocyte development ranging from ETP to CD4^{+}CD8^{+} (DP) thymocytes and this is evidenced by the specialized genes expressed by cTEC.

A key role of cTEC is during the process of positive selection. As discussed in more detail in section 1.1.4, positive selection is the process where αβ TCR-expressing DP thymocytes are screened to ensure their TCR is functional and able to recognize self-

MHC-peptide complexes with low affinity TCR engagement. Expression of peptides by MHC Class I and II is not limited to cTEC or mTEC, as expression of these molecules within the thymus is vital to both positive and negative selection. However cTEC have the ability to facilitate and regulate the positive selection of developing thymocytes through unique machinery that degrade proteins to provide these self-peptides self-MHC complexes that optimize the process of positive selection.

One of the major molecules associated with this machinery is the thymoproteasome which is a cTEC-specific form of proteasome, other forms include the constitutive proteasome and the immunoproteasome (164). The thymoproteasome is unique in that the β5 (PSMB5) subunit of the constitutive proteasome is replaced by the β5t (PSMB11) subunit (164,165). This incorporation of the β5t subunit is important as the peptides that the β5t-containing thymoproteasome generates have unique cleavage motifs and have low affinity for MHC Class I clefts (165,166). Therefore the thymoproteasome within cTEC facilitates optimum positive selection as only SP8 thymocytes that receive a signal with low-affinity TCR engagement with peptide-MHC Class I complexes are selected for cell survival during positive selection (165). β5t is critical for this function of positive selection of SP8 thymocytes as β5t-deficient mice exhibit significantly impaired CD8 T-cell development characterized by reduced CD8 T-cell numbers, altered TCR repertoire, restricted functional capacity and increased incidence of self-reactive T-cells (165,167,168). Takada *et. al* showed that not only does the low affinity peptides generated by the thymoproteasome facilitate positive selection of SP8 thymocytes but it also fine-tunes the antigen responsiveness of the subsequent mature $CD8^+$ T-cell within the periphery (169). Therefore the cTEC

specific thymoproteasome is highly important in MHC Class I-mediated development of $CD8^+$ T-cells.

cTEC also have machinery specialized for MHC Class II restricted positive selection of SP4 thymocytes. cTEC have been found to express both cathepsin L and thymus specific serine protease (TSSP). Cathepsin L is a lysosomal cysteinal protease which has been previously shown to play a role in MHC Class II αβ heterodimer assembly (170,171). However cathepsin L has also been shown to play a direct role in positive selection of SP4 thymocytes by generating MHC Class II peptide ligands presented by cTEC during positive selection and in line with this role, mice deficient for cathepsin L have impaired SP4 selection (170,171). TSSP is a protease found in cTEC and first proposed by Bowlus *et. al* to have a role in MHC Class II antigen processing (172). More recent analysis showed that TSSP-deficient mice produced normal $CD4^+$ T-cell numbers despite a reduction in the frequency of cTEC expressing high levels of surface MHC Class II (173). However through the use of MHC Class II-restricted TCR transgenic Marilyn or OT-II mice it was shown that TSSP-deficiency impairs the selection of Marilyn and OT-II $CD4^+$ T-cells (173). In a polyclonal setting it was also shown that TSSP-deficiency impaired positive selection of $CD4^+$ T-cells that expressed specific TCRs but was not necessary for the selection of the majority of $CD4^+$ T-cells (174). Thus TSSP is necessary for the selection of some $CD4^+$ T-cell specificities and contributes to the diversification of the $CD4^+$ T-cell repertoire (173,174). TSSP is not required for the selection of SP8 thymocytes consistent with its role in MHC Class II restricted peptides (173). Additionally a process of macroautophagy, the process responsible for the degradation of the majority of

intracellular proteins, occurs within the cTEC which enables MHC Class II peptide loading, which is essential for the selection of specific $CD4^+$ T-cell specificities (175). Autophagy is a process of protein degradation, which occurs during the starvation response as an energy source within the cell however within the thymus macroautophagy can occur in a starvation-independent manner (176). It has been shown that impairment of macroautophagy specifically within TECs disrupts normal selection of MHC Class II-restricted $CD4^+$ T-cells (175).

As well as directly regulating positive selection, cTEC can also regulate positive selection in a slightly different manner. Within the cortex, specialized structures/complexes form between developing DP thymocytes and a single cTEC that engulfs the DP thymocytes. These complexes were first identified by Wekerle *et. al* and were termed 'thymic nurse cells' (TNCs) due to their apparent ability to facilitate lymphocyte survival and differentiation (177). It was later revealed that the primary function of TNCs was to aid DP thymocytes through positive selection by providing an environment for the DP thymocyte cell to undergo a second TCRα rearrangement and thus increasing the odds of positive selection (178). Despite this role, the same study showed that TNCs are not essential for positive selection and therefore their role is more involved in optimizing the process of positive selection than supporting it (178). Together these studies highlight the multiple functional roles cTEC posses to regulate positive selection.

cTEC have also been shown to be involved in early stages of thymocyte development prior to positive selection. One of the main characteristic molecules of

cTEC is the notch signaling ligand delta-like ligand 4 (DLL4), which is abundant in cTEC, and Notch1-DLL4 interactions are essential for driving T-cell lineage commitment of thymocyte progenitors (179,180). The importance of DLL4 is evident when it is deleted specifically on TEC, such as with the Foxn-1^{cre}Dll4^{flox} mouse model, which results in a complete block of T-cell development and loss of T-cell progenitors (180,181). Interestingly there is a role of these thymocyte-cTEC interactions in regulating the expression of DLL4 by cTEC, as these interactions induce downregulation of DLL4 and therefore suggests a mechanism of feedback of DP thymocytes regulating thymopoiesis (179). cTEC produce the cytokines interleukin-7 (IL-7) and kit-ligand (also referred to as stem cell factor) which have both been shown to promote early thymocyte survival, differentiation and proliferation within the cortex (31,33,34,134). Downstream of early T-cell progenitors, cTEC regulate DP thymocyte development through production of transforming growth factor β (TGFβ), which regulates the cell cycle progression and differentiation of DP thymocytes from their CD4^{-}CD8^{lo} precursors (182).

cTEC also express a number of chemokines which are involved in regulating the early stages of thymocyte development. cTEC have been shown to express CCL25 (CCR9-ligand) which regulates thymus colonization by lymphoid progenitors both at the pre-vascularization stage of thymus development as well as in the adult thymus (21,183). This regulation was shown to occur in conjunction with CCL21 (CCR7-ligand) which is not expressed by cTEC and therefore cTEC works in conjunction with other stromal populations to regulate thymus colonization in a CCL25 and CCL21-dependent manner (21,183). Connected to these two chemokines, cTEC also

express the atypical chemokine receptor 4 (ACKR4, formerly known as CCX-CKR1 or CCRL1) which binds CCL21 and CCL25, as well as CCL19, and has been shown to regulate thymus colonization by T-cell progenitors, although ACKR4 has been shown to not play a role in T-cell development (184,185). The CXCR4 ligand CXCL12, expressed by cTEC, also promotes early thymocyte survival. CXCR4 is expressed by all thymocyte progenitors and absence of CXCR4 results in reduced survival of DN3 thymocytes and mislocalization of T-cell progenitors (30,186).

Therefore cTEC have essential functions within the cortex of the thymus to regulate early stages of thymocyte development as well as the positive selection of DP thymocytes to generate SP4 and SP8 thymocytes. Despite the numerous functions of cTEC in positive selection as well as migration of early T-cell progenitors and their downstream populations, there is very little heterogeneity identified within the cTEC compartment, perhaps due to incomplete phenotypic characterization of cTEC. Therefore, cTEC heterogeneity is not as distinct in comparison to the clear separation of function seen in different mTEC populations.

1.2.3.2 The function of medullary thymic epithelial cells

mTEC, termed for their location within the medulla of the thymus, are the other primary population of TEC and are commonly identified using the following markers: UEA-1, Cytokeratin-5 and MTS10.

As mentioned previously, cTECs have multiple functions, but due to the rather limited phenotypic markers used to characterize them, cTEC generally do not separate into

distinct populations. mTEC on the other hand can be broadly separated into two compartments based on their expression of CD80 and MHC Class II. $mTEC^{lo}$ are identified as $CD80^{-}$MHC Class II^{lo} and $mTEC^{hi}$ are identified as $CD80^{+}$MHC Class II^{hi} (187–189). This distinction into $mTEC^{lo}$ and $mTEC^{hi}$ extends beyond phenotypic description as each population has been shown to have specific, as well as shared, functions within the thymus.

As previously discussed in Section 1.1.5, mTEC are essential in establishing central tolerance as they are optimized to remove self-reactive T-cells by producing tissue-restricted antigens (TRAs) as well as being essential to the development of natural regulatory T-cells (nTregs). The ability to express such a vast array of self-Ags is often referred to as “promiscuous gene expression”, and is a major contributing factor whereby mTEC are able to identify developing SP thymocytes that carry TCRs specific to self-Ags and delete them (190).

The autoimmune regulator Aire is a transcription factor which is expressed specifically within the $mTEC^{hi}$ subpopulation and regulates the expression of TRAs within the thymus (187,190,191). Aire has been shown to be functionally important in both humans and mice, with human patients that carry a genetic mutation of Aire suffering from autoimmune-polyendocrinopathy-candidiasis-ectodermal dystrophy (APECED) and Aire-deficient mice exhibiting a similar autoimmune disorder (191–193). Aire has been shown to be required for the deletion of specific self-reactive clones of T-cells carrying TCRs specific to Aire-dependent genes (191). It has also been shown that $Aire^{+}$ mTEC co-express both Aire-dependent genes as well as Aire-

independent genes (194). As well as Aire, mTEC express the transcription factor Fez family zinc-finger 2 (Fezf2) which has been shown to promote promiscuous gene expression of Aire-independent TRAs (160). Fezf2-deficient mice were shown to exhibit autoimmune deficiencies highlighting this transcription factor as a key regulator of central tolerance induction (160). Unlike Aire, Fezf2 expression was not restricted to a specific subset of mTEC, with expression present in $mTEC^{lo}$ and $mTEC^{hi}$ as well as being present in all $Aire^{+}$ $mTEC^{hi}$ (160).

As well as a direct role of Aire in regulating tolerance, Aire has been shown to have additional functions within the medulla. As discussed in section 1.1.5, during negative selection self-antigens are presented to the developing thymocytes directly by mTEC but also indirectly through cross-presentation to thymic dendritic cells (DCs). As well as playing a role in the generation of TRAs cross-presented to the DCs, Aire may play an indirect role in this process by regulating thymic DC positioning. It was shown that the chemokine XCL1, whose receptor XCR1 is expressed on thymic DC, is expressed on $mTEC^{hi}$ and it's expression is diminished in mTEC of Aire-deficient mice (195). This alteration of XCL1 expression in Aire-deficient mice was accompanied by a lack of medullary accumulation of thymic DCs similar to that seen in XCL1-deficient mice suggesting Aire plays an important role in regulating XCR1-XCL1 mediated thymic DC positioning (195). Interestingly this same study revealed that both the XCL1-deficient and Aire-deficient mice have reduced natural Treg (nTreg) development suggesting a role for Aire in regulating this process as well (195). Therefore the defective tolerance induction in Aire-deficient mice may also be due to altered cross-presentation of Ags to DCs as well as defective nTreg

generation. In support of this, Hubert *et. al* found that Aire regulates the transfer of Ags derived from mTEC to DCs (196). Aire also influences other chemokines such as the ligands for CCR4 and CCR7, which are involved in thymocyte migration following positive selection. Although the mechanisms involved in this regulation are not clear, Aire-deficient mTEC have reduced levels of CCR4-ligands and CCR7-ligands which are expressed by $mTEC^{hi}$ and $mTEC^{lo}$, respectively, and given that Aire expression is restricted to $mTEC^{hi}$ this suggests Aire can regulate the expression of chemokines on other mTECs (197).

CCL21 expression by $mTEC^{lo}$ is a key characteristic of $mTEC^{lo}$ and is extremely important in the positioning of thymocytes within the thymus. In mice with absent CCR7-CCR7-ligand interactions such as CCR7-deficient or plt/plt mice, the latter is a mouse model carrying a natural mutation which results in absent CCR7-ligands, post-positive selection thymocytes are not able to migrate to the medulla (69). Within these mice T-cell development appears to progress normally which is consistent with recent studies showing that conventional T-cell development does not depend on mTEC interactions, however the T-cells generated in the thymus of these mice do not undergo a full negative selection program and results in autoreactive T-cells in the periphery of these mice (69,70,82). However CCR7 controls the balance of nTreg and Treg precursors as well as the development of iNKT cells highlighting a key role of CCR7-ligand expression by $mTEC^{lo}$ in the development of non-conventional SP4 thymocyte populations (74).

An additional function of mTEC is also evident and pertains to the later stages of thymocyte development during thymocyte egress. As discussed in section 1.1.6,

thymocyte egress occurs once the developing thymocytes have undergone negative selection and have reached egress competence by downregulating CD69 and upregulating the S1P receptor S1PR1 (97,100,102,103). These S1PR1-bearing thymocytes then follow a S1P-gradient to the site of exit where they undergo S1P-dependent exit from the thymus into the blood. There are multiple cell types that regulate this process, one of which are mTEC that produce the enzyme LPP3 which degrades intrathymic S1P to maintain low levels in the medulla relative to the site of egress (112). It has been shown that deletion of this enzyme selectively in mTEC, through the use of *Ppap2b*^{flox} mice crossed with *Keratin14*^{cre} mice which selectively targeted deletion of the *Ppap2b* gene to mTEC, resulted in an intrathymic accumulation of mature SP4 thymocyte indicative of their inability to exit the thymus as well as increased intrathymic levels of S1P (112). Therefore not only do mTEC regulate the selection of developing thymocytes but they also regulate the final stage of their time within the medulla before joining the peripheral T-cell pool.

1.2.4 Non-Epithelial Thymic Stroma

Non-epithelial stroma encompasses a diverse mix of cells types, which can be separated into the broad headings of endothelial cells and mesenchymal cells. In contrast to our current understanding of thymic epithelial cells, the development, characterization and function of these non-epithelial stroma populations remains relatively poorly defined.

The importance of mesenchyme within the thymus was identified early on in thymic research. Early findings of Auerbach *et al.* revealed that enzymatic separation of

mesenchyme and epithelium led to inability of either compartment to develop and only together could they from a lobular, lymphoid tissue (198,199). In additional studies, the removal of neural crest (NC)-derived mesenchyme resulted in significantly reduced thymic size and mass revealing an essential role of thymic mesenchyme in the development of the thymus organ (123,198,199). The thymic mesenchyme has since been shown to play a key role in the earliest stages of fetal thymic development, however the role that thymic mesenchyme plays within the adult is less well defined. The current understanding of the roles of thymic mesenchyme in both embryonic and adult stages of thymus development and function are discussed in more detail in the following section.

1.2.5 The Role Of Thymic Mesenchyme

1.2.5.1 The role of thymic mesenchyme in the embryonic thymus

A lot of what is known regarding the role of thymic mesenchyme centers on its involvement during thymus organogenesis. As mentioned above, there is an essential requirement for thymic mesenchyme during the development of the thymus. During thymus organogenesis, the endoderm-derived thymic epithelial rudiment is enveloped within a layer of migratory mesenchyme cells derived from the cardiac neural crest (123,125,200). After a short period of development, these NC-derived mesenchyme cells then colonize the thymic epithelial rudiment and form part of the stromal compartment of the thymus organ (125,201). Removal of thymic mesenchyme during early thymus organogenesis through *in ovo* and *in vitro* experiments resulted in defective thymus development, where thymic size was significantly reduced (199,201,202). Thymic mesenchyme also plays a role during

the positioning of the organ during thymus organogenesis as well as regulating thymus lobule formation (203). It has been shown that NC-derived mesenchyme regulates the separation of the thymus from the pharynx as well as its migration into the anterior mediastinum (204). During this early stage of thymus organogenesis, an absence of NC-derived mesenchyme results in altered thymus/parathyroid domain distribution where the border of the thymus shifts causing an increase of the thymus domain (204).

Following the role of thymic mesenchyme in the earlier stages of thymic development there is also a role for thymic mesenchyme during later stages once the thymic rudiment is more developed. It has been shown that platelet-derived growth factor receptor α (PDGFRα) (also CD140a) expressing thymic mesenchyme supports the expansion of TEC during the early stage of thymic development (202). This is an important process that ensures the availability of sufficient intrathymic niches to support a normal programme of thymocyte development. Depletion of the PDGFRα^{+} thymic mesenchyme around day 12 of embryogenesis (E12) results in a hypoplastic thymus and it has been shown that the production of insulin-like growth factors 1 and 2 (IGF1 and IGF2) by the thymic mesenchyme regulate TEC proliferation at this stage (202). It has also been shown that thymic mesenchyme also regulates epithelial cell proliferation through the production of fibroblast growth factors 7 and 10 (FGF7 and FGF10) at a slightly later stage of thymus development (E14) and this regulation was dependent on sustained interactions with thymic mesenchyme (201). However Jenkinson *et. al* also revealed that TEC differentiation occurs independently of sustained interactions with thymic mesenchyme, suggesting thymic mesenchyme

may not regulate TEC development or cTEC/mTEC lineage commitment, however these studies cannot rule out thymic mesenchyme providing a transitory signal for TEC development prior to its removal in these experimental settings (201,202,205). In line with this, despite an absence of thymic mesenchyme, or deletion of FGF10, there is sufficient differentiation of TEC within the hypoplastic thymus to support $CD4^+CD8^+$ (DP) and a small amount of SP thymocyte development (201,202,205). In contrast to these studies, IGF production by thymic mesenchyme has been shown to induce MHC Class II expression on TEC during early stages of embryogenesis, which may explain why there is not a full programme of thymocyte development in the hypoplastic thymi with differentiated TEC (201,205–208). The development of the reaggregate thymic organ culture (RTOC) technique aided the investigation of the role of thymic mesenchyme in regulating early thymocyte development. Anderson *et. al* demonstrated that thymic mesenchyme is required for the development of thymocytes up until the $CD25^+CD44^-$ precursor stage of development but development beyond this can be supported by TEC in the absence of thymic mesenchyme (208,209). The regulation of thymocyte development by thymic mesenchyme was shown to occur through both contact-dependent and -independent processes and one study proposed that the extra cellular matrix (ECM) produced by the thymic mesenchyme may play a role in this regulation (203,209). It has also been shown that *MafB* is strongly expressed by mesenchymal cells within the third pharyngeal pouch and is required for the production of Wnt 3 and BMP4 by thymic mesenchyme, both of which promote CCL21 and CCL25 production by thymic epithelium critical for lymphoid progenitor entry into the developing thymus (210).

Furthermore, in addition to the positive regulation of TEC proliferation through the provision of growth factors, thymic mesenchyme has conversely been shown to negatively regulate TEC proliferation during embryonic development. The findings of Sitnik *et. al* revealed thymic mesenchyme are the primary source of retinoic acid (RA) through the mesenchyme's production of key enzymes for RA within the embryonic thymus and that this production of RA influences TEC proliferation (211). Interestingly this thymic mesenchyme population that expresses RA enzymes also express IGF1 and FGF10 and therefore can both positively and negatively regulate TEC proliferation within the embryonic thymus (201,202,205,211).

1.2.5.2 The role of thymic mesenchyme in the adult thymus

Initial studies have long supported that NC-derived thymic mesenchyme does not persist beyond the embryonic thymus (200,212). It has only been relatively recently shown that this appears to not be the case and in fact NC-derived mesenchyme persists beyond embryogenesis and is detectable within the adult thymus (213). This study utilized NC specific *Wnt-1*^{cre} and *Sox10*^{cre} mouse models, which were both crossed to a *Rosa26*^{eYFP} fate-mapper mouse strain and therefore *Wnt1* and *Sox10* expressing neural crest cells express Cre which deletes the transcription stop in front of the *enhanced yellow fluorescent protein (eYfp)* gene causing the cell and its downstream progeny to express eYFP, identifying the cell as neural crest derived (213). These mouse strains enabled the identification of NC-derived mesenchymal cells within both the fetal and adult thymus (213). Because of this it is not surprising that research of thymic mesenchyme has not been as well investigated and the role

that these cells may play within the adult thymus has been perhaps underappreciated until more recent years.

The development of the MTS-15 antibody aided the identification of thymic mesenchymal fibroblasts within the adult thymus (214). MTS-15^{+} thymic mesenchyme were found at the capsule and trabeculae, where thymic mesenchyme has already been shown to contribute to, as well as around large blood vessels at the CMJ (214). These MTS-15^{+} fibroblasts were PGDFRα^{+}, expressed the growth factors FGF7 and FGF10 which may suggest that these cells are the NC-derived thymic mesenchyme identified in previous studies which regulate thymic epithelial cell proliferation, however the neural crest origin of these MTS-15^{+} thymic mesenchyme was not confirmed (202,214). The MTS-15^{+} cells also express the chemokines CXCL12 and CCL19 suggesting that they may have a role in lymphocyte migration within the thymus (214).

The study from Sitnik *et. al* which showed that the RA producing thymic mesenchyme which regulate TEC proliferation in the embryonic thymus also showed that these cells persist into the adult (211). This suggests that they may have an extended role beyond the support of TEC proliferation in during initial thymus development however this has not yet been directly evaluated (211). In a more recent study Sitnik *et. al* identified a common mesenchymal precursor population within lymph node and thymus mesenchyme, as well as identifying two subsets of thymic mesenchyme that associate with vascular endothelial cells (215). It was proposed that due to the pericyte-like phenotype of these cells as well as their expression of genes associated

with endothelial cell regulation and angiogenesis (such as angiopoietin and VEGF) that these thymic mesenchyme cells may support endothelial cell homeostasis in the adult thymus (215). This is inline with another previous study which showed that NC-derived thymic mesenchyme give rise to pericytes and smooth muscle cells which support thymic blood vessels structurally as well as through the mesenchymal cell's production of VEGF, an endothelial cell mitogen that stimulates endothelial cell proliferation, enabling the formation and sprouting process of blood vessel structures (213,216,217).

As well as their role in supporting the vascular endothelium of the thymus, thymic pericytes have also been shown to regulate the egress of mature thymocytes. During the final stages of thymocyte development the mature thymocytes exit the thymus via blood vessels at the corticomedullary junction (CMJ) (111). Thymic pericytes have been proposed to regulate this process through the production of sphingosine-1-phosphate (S1P) kinase 1 (SPHK1) and SPHK2 which catalyze the ATP-dependent phosphorylation of sphingosine to generate S1P and thereby maintain the intrathymic S1P gradient required for normal thymocyte egress of mature, S1PR1-expressing thymocytes (111).

Whilst these studies highlight important roles for thymic mesenchyme within the adult thymus it is clear that there is still much left to understand about this population phenotypically and functionally. In addition to this little is known about the regulation of the development of the thymic mesenchyme compartment and thus we aim to investigate these two topics within Chapter 3.

1.3 STROMAL MICROENVIRONMENTS OF SECONDARY LYMPHOID TISSUES

1.3.1 Lymph Node Fibroblastic Reticular Cell Function And Development

Peripheral lymphoid tissues are an important component of the immune system. Their primary function is to maintain the naïve lymphocyte population and facilitate the interaction between lymphocytes and antigens. There are a number of peripheral lymphoid organs, each with distinct roles within immune regulation. For the purpose of this research, lymph nodes will be the main focus as their mesenchymal stromal compartments are well studied.

Similar to the thymus, lymph nodes are comprised of a heterogeneous mix of stromal cell subtypes. The stromal populations within the lymph node are primarily mesenchymal and endothelial but, unlike the thymus, do not contain epithelial cells. Typically lymph node stroma are separated into endothelium such as blood and lymphatic endothelium, as well as mesenchyme incorporating fibroblastic reticular cells (FRC), follicular dendritic cells (FDC) and marginal reticular cells (MRC) (218). These different stromal cells reside in distinct regions of the lymph node such as the T-cell zone and the B-cell zone (218). As highlighted in section 1.2.5, there is still much to learn about the cellular and molecular regulation of thymic mesenchyme as well as the functional role mesenchyme may have during thymocyte development within the thymus. Due to the mesenchymal origin of FRCs as well as their localization within the T-cell zone, the current literature surrounding FRCs may provide a platform that might help inform studies elucidating the regulation and functional nature of thymic mesenchyme (219).

Phenotypically FRC are identified as non-hematopoietic (CD45-) stromal cells characterized by their expression of the glycoprotein podoplanin (PDPN) and absence of the platelet endothelial cells adhesion molecule 1 (PECAM-1, commonly referred to as CD31) ($PDPN^{+}CD31^{-}$) (220). They have also been shown to express platelet-derived growth factor α (PDGFRα) and α smooth muscle actin (αSMA) as well as a number of other molecules highlighting the extensive research of this population in recent years (218).

One of the first functional roles attributed to lymph node stroma, including FRCs, is to provide and support the physical structure of the lymph node and to funnel Ags and APCs towards specific lymphocyte populations within the lymph node in order to increase the likelihood of rare T- and B-cells to interact with their cognate Ag and initiate an adaptive immune response (218). FRCs, along with extracellular matrix (ECM), contribute to the structure of the lymph node by creating a 3-dimensional network upon which T-cells and DCs can migrate along as well as compartmentalizing the T-cell zone to ensure suitable localization of lymphocyte populations (219,221). FRCs regulate the migration of T-cells and DCs throughout the T-cell zone through their production of the CCR7-ligands CCL19 and CCL21 (220,222,223). This production of CCR7-ligands also regulates the entry of T-cells from the blood into the lymph node, as found in the naturally occurring mutant mouse strain paucity of lymph node T-cells (*plt/plt*) which lack CCL19 and CCL21 have perturbed T-cell recruitment to lymph nodes (224–226). FRCs also support the survival of T-cells and DCs within the T-cell zone through production of IL-7 which is essential for maintaining T-cell and DC homeostasis, maximizing the time these cells

can spend searching for their cognate Ag (220). Additionally the 3-dimensional network created by the FRCs and ECM creates a conduit system, which transports soluble low molecular weight antigens and chemokines deep into the lymph nodes, delivering these to leukocytes such as B-cells and DCs further facilitating adaptive immune responses (227,228). These functions of the FRC help to ensure that DC cells can receive and present Ags to T-cells within the T-cell zone within the lymph node and aide the screening that the T-cells carry out in order to find their cognate Ag.

Within the thymus, RANK and LTβR signaling have been shown to play a vital role in the development and function of thymic epithelial cells. These two TNFSFR members are also essential for the development of lymph nodes and LN FRCs. During lymph node organogenesis, pre-adipocytes migrate into the lymph node anlage and differentiate into CXCL13-expressing lymphoid tissue organizer (LTo) cells (218). This expression of CXCL13 attracts lymphoid tissue inducer cells (LTi) which express CXCR5 (receptor for CXCL13) causing the LTi to cluster at the site where the lymph node development will occur (150,229). These LTi express both RANK and RANK-ligand and LTi clustering allows RANK signaling to occur between the LTi cells triggering the expression of the LTβR heterotrimeric ligand $LT\alpha_1\beta_2$ (230). LTβR signaling is essential for the initial development of the lymph node mesenchyme precursors from adipocyte precursors as evidenced by LTβR-deficient mice which lack peripheral lymph nodes (149,231). Benezech *et. al* revealed that development from the LTo mesenchymal precursor to an intermediate “primed stromal population”, which expressed intermediate levels of intracellular adhesion molecule 1 (ICAM-1)

and vascular cell adhesion molecule 1 (VCAM-1) (ICAM-1^{int}VCAM-1^{int}), was not dependent on LTβR signaling (232). However further development of this ICAM-1^{int}VCAM-1^{int} to an ICAM-1^{hi}VCAM-1^{hi} mature population was dependent on LTβR signaling and this mature population express key functional molecules such as the chemokines CCL19 and CCL21, as well as the homeostatic regulator IL-7 which are critical for the antiviral immunity (232,233). This emphasizes that RANK and LTβR signaling is essential for the development of functional LN mesenchymal cell development.

Together, the potential shared cellular and molecular similarities displayed by LN and thymic microenvironments raises the interesting question as to whether similar mesenchymal cell types are present within the thymus and whether their developmental regulation and/or function occurs through similar pathways. Such questions will be investigated within Chapter 3.

1.4 GENERAL AIMS

The stromal microenvironment is essential in supporting the development of thymocytes throughout their stepwise maturation progress within the thymus. This microenvironment is a complex and heterogeneous mix of epithelial, mesenchymal and endothelial cells however much of what is known of the thymic stroma focuses on the thymic epithelial compartment. Studies have highlighted the numerous functional roles of mesenchymal cells within peripheral lymph nodes as well as their developmental regulation, however knowledge of thymic mesenchyme in comparison is lacking.

In addition, despite the early identification of the role for LTβR as a potential regulator of T-cell egress, more recent and in-depth analysis of this role has been lacking and thus the precise mechanism whereby LTβR controls normal T-cell egress remains incompletely understood. Therefore, this programme of work seeks to investigate thymic mesenchyme and elucidate the intrathymic role of the LTβR signaling axis by addressing the following three key questions:

1) What are the phenotypic and functional characteristics of thymic mesenchyme?
2) How is thymic mesenchyme regulated at both the cellular and molecular level?
3) What are the cellular and molecular regulators of LTβR-dependent thymocyte egress?

CHAPTER TWO: MATERIALS AND METHODS

2.1 MICE

The mice used within this study were housed and maintained within the [redacted] in accordance with Home Office regulations. Details of all mouse strains, including their phenotype and source, used throughout this study are listed in Table 2.1.

The mice used were either wild type mice used to characterize a normal, un-manipulated thymic microenvironment, or genetically manipulated mice to allow investigations into the functions of genes and mechanisms involved in thymus and T-cell development and function. All adult mice were culled by a schedule one method, primarily cervical dislocation, in accordance with Home Office regulations. For each experiment, mice were age matched and adult mice were classified as 8-12 weeks of age and all mice detailed in Table 2.1 are on a C57BL/6 background. For experiments using embryonic tissues, timed matings were set up and the detection of a vaginal plug indicated successful mating and was classified as day 0 of gestation (embryonic day 0, E0).

Table 2.1 Mouse Strain Information

Mouse Strain	Phenotype	Source
C57BL/6	Wild type.	BMSU
BoyJ	Congenic CD45.1 C57BL/6 Wild type.	BMSU
Balb/c	Wild type.	BMSU
RAG-2-GFP (RAG^{gfp})	Transgenic mice which have a bacterial artificial chromosome (BAC) modified by homologous recombination to encode a green fluorescent protein (GFP) reporter within the *Rag-2* gene (234).	The Jackson Laboratory
Tcra$^{-/-}$	Mice have deletion of *Tcra* which prevents formation of an αβ TCR which results in a loss of αβ T-cells (140).	The Jackson Laboratory
Class ii$^{-/-}$	Deletion of the major histocompatibility complex (MHC) Class II results in absence of CD4 expressing T-cells (235).	Taconic, Germantown, NY
Cd1d$^{-/-}$	Mice carrying mutant *CD1d1* gene have severe loss of invariant natural killer T-cells (iNKT) in thymus spleen and the liver (236). This loss results in a decrease in early IL-4 production by splenic T-cells.	The Jackson Laboratory
Foxp3$^{-/-}$	Mice have a loss of $Foxp3^{+}$ Treg which results in lethal autoimmune syndrome targeting multiple organs (90).	Howard Hughes Medical Institute and Immunology Program, Memorial Sloan-Kettering Cancer Center, New York
Lta$^{-/-}$	Mice lack LTα resulting in defective development of secondary lymphoid organs, including absent Peyer's patches and lymph nodes and disrupted spleen architecture (237).	The Jackson Laboratory
Rank$^{-/-}$	Mice were generated by crossing mice which carried a floxed RANK allele with actin-Cre mice to generate RANK-deficient mice (152). *Rank*$^{-/-}$ mice have stunted limbs and teeth giving a runted appearance and struggle to thrive (238).	Institute of Molecular Biotechnology of the Austrian Academy of Sciences, Institute of Molecular Biology

Table 2.1 Mouse Strain Information Continued…

Mouse Strain	Phenotype	Source
Ltbr$^{-/-}$	Deletion of Ltbr results in mice lacking Peyer's patches, all peripheral lymph nodes and have disrupted architecture including a loss of marginal zones and disorganised T-cell and B-cell zones (149).	Klaus Pfeffer University of Düsseldorf
Ltbr$^{-/-}$*x*RAG-2-GFP (*Ltbr*$^{-/-}$RAG^{gfp})	Mice deficient for LTβR were crossed with RAG-2-GFP reporter mice to study intrathymic dwell time and recent thymic emigrants.	Generated in house at the BMSU
Ltbr$^{fl/fl}$ (*Ltbr*^{flox})	The *Ltbr* allele was flanked with loxP, generated using CreloxP technology (239).	Alexei V. Tumanov University of Chicago
Pdgfrb$^{cre/+}$ (*Pdgfrb*^{cre})	Mice were generated by pronuclear injection of *Pdgfrb* gene fragment and a cDNA encoding Cre recombinase(240). Mice were heterozygous for Cre and were used to target Flox mediated deletion to PDGFRβ-expressing thymic mesenchyme. Mice were also used as controls and have no detrimental phenotype.	Cancer Research Technologies, London
Pdgfrb^{cre}*Ltbr*^{flox}	*Pdgfrb*^{cre} and *Ltbr*^{flox} mice were crossed to specifically delete *Ltbr* in PDGFRβ^{+} cells.	Generated in house at the BMSU
mT/mG	A fate mapper system where all cells express membrane-targeted tdTomato (mT) prior to Cre excision and membrane-targeted EGFP (mG) after Cre excision (241).	The Jackson Laboratory
Pdgfrb^{cre} mT/mG	*Pdgfrb*^{cre} and mT/mG mice were crossed to identify the specificity and efficacy of Cre activity of the *Pdgfrb*^{cre} mouse strain.	Generated in house at the BMSU

Table 2.1 Mouse Strain Information Continued…

Mouse Strain	Phenotype	Source
Wnt-1$^{cre/+}$*2* (*Wnt-1*^{cre})	Mice express *Cre* recombinase under the control of the *Wnt1* promoter (242). Mice were used to target Flox-mediated gene deletion to *Wnt-1*^{cre} expressing thymic mesenchyme. Wnt-1^{cre} mice were used as controls and have no detrimental phenotype.	The Jackson Laboratory
Wnt-1^{cre}mT/mG	*Wnt-1*^{cre} and mT/mG mice were crossed to identify the specificity and efficacy of Cre activity of the *Wnt-1*^{cre} mouse strain.	Generated in house at the BMSU
Wnt-1^{cre}*Ltbr*^{flox}	*Wnt-1*^{cre} and *Ltbr*^{flox} mice were crossed to specifically delete *Ltbr* in PDGFRβ^{+} mesenchyme cells.	Generated in house at the BMSU
Foxn-1$^{cre/+}$ (*Foxn-1*^{cre})	*Cre* was inserted downstream of the *Fonx-1* gene (243). Mice were heterozygous for Cre and were used as controls and have no detrimental phenotype.	The Jackson Laboratory
Foxn-1^{cre}*Ltbr*^{flox}	*Foxn-1*^{cre} and *Ltbr*^{flox} mice were crossed to specifically delete *Ltbr* in Foxn-1^{+} epithelial cells.	Generated in house at the BMSU
Tie2$^{cre/+}$ (*Tie2*^{cre})	Expression of Cre recombinase is driven by the endothelial-specific *Tie2* promoter (244). Mice were heterozygous and were used as controls.	The Jackson Laboratory
Tie2^{cre}*Ltbr*^{flox}	*Tie2*^{cre} and *Ltbr*^{flox} mice were crossed to specifically delete *Ltbr* in Tie2^{+} endothelial cells.	Generated in house at the BMSU
Tie2^{cre}mTmG	*Tie2*^{cre} and mT/mG mice were crossed to identify the specificity and efficacy of Cre activity of the *Tie2*^{cre} mouse strain.	Generated in house at the BMSU
Flk-1$^{cre/+}$ (*Flk-1*^{cre})	Cre recombinase express is driven by expression of *Flk-1* gene (245). *Flk-1*^{cre} mice were used to target endothelial cells. Mice were heterozygous and were used as controls.	The Jackson Laboratory
Flk-1^{cre}mTmG	*Flk-1*^{cre} and mT/mG mice were crossed to identify the specificity and efficacy of Cre activity of the *Flk-1*^{cre} mouse strain.	Generated in house at the BMSU
Flk-1^{cre}*Ltbr*^{flox}	*Flk-1*^{cre} and *Ltbr*^{flox} mice were crossed to specifically delete *Ltbr* in Flk-1^{+} endothelial cells.	Generated in house at the BMSU

2.2 MEDIUM AND TISSUE CULTURE REAGENTS

2.2.1 Medium

Tissues were isolated and handled in a medium of RF10-H (details Table 2.2) and stored on ice prior to processing or culturing. Preparation of single cell suspensions either by mechanical disaggregation or enzymatic digestion, as well as storing of single cell suspensions, were carried out in RF10-H, whereas cell and tissue cultures were placed within a media of Dulbecco's Modified Eagle's Medium (DMEM) (Table 2.3).

2.2.2 Additives

Some experimental conditions required selective depletion of hematopoietic cells to investigate the thymic stroma. To achieve this, fetal thymic organ cultures (FTOC) (further information Section 2.7) were cultured in DMEM with 2-deoxyguanosine (2-dGuo) added, this depletes hematopoietic cells that are rapidly dividing but does not impact thymic stroma resulting in thymic lobes that are empty of thymocytes but retain their stromal populations and structure. A stock solution of 9mM 2-dGuo was stored at -20°C and was added to culture mediums of DMEM to give a final concentration of 1.35mM when required. Unless otherwise stated all media was sourced from Sigma-Aldrich.

Table 2.2 Preparation Of RPMI-1640 Hepes (RF10-H)

Medium and Additives	Volume	Final Concentration
RPMI-1640 + 20mM Hepes, with L-glutamine, without bicarbonate	500ml	-
200mM L-glutamine	5ml	2mM
5000 IU/ml Penicillin and Streptomycin	10ml	100IU/ml
Heat-inactivated fetal calf serum (FCS)	50ml	10%

Table 2.3 Preparation Of DMEM

Medium and Additives	Volume	Final Concentration
Dulbecco's Medium with 3.7g/l bicarbonate, without glutamine	20ml	-
100x non-essential amino acids, containing: L-Alanine 8.9mg/ml L-Asparagine 15mg/ml L-Aspartic acid 13mg/ml Glycine 7.5mg/ml L-Glutamic acid 14.2mg/ml L-Proline 11.5mg/ml L-Serine 10.5mg/ml	200µl	-
1M Hepes	200µl	10mM
$5x10^3$ M2 Mercaptoethanol	200µl	-
200mM L-Glutamine	400µl	4mM
5000 IU/ml	400µl	100 IU/ml
Heat inactivated FCS	2ml	10%

2.3 DISSECTION OF MOUSE TISSUE

Tissues such as thymic lobes, spleens, lymph nodes and kidneys were dissected from adult mice at BMSU and placed into RF10-H on ice. Excess fat or blood was removed from the isolated tissues and which were then stored in RF10-H on ice until the tissue was processed (see section 2.4). For fetal tissues, embryos were removed from pregnant mice on the required day of gestation, separated from the womb and egg sac and washed in RF10-H. Embryonic lobes were then dissected from the embryo under a dissection microscope and transferred into RF10-H until being used, either fresh for thymocyte/stromal cell isolation or for FTOC. Tissues required for cell transfer or cell culture, such as FTOC, were handled and processed within a laminar flow hood to provide a sterile environment, using sterile surgical equipment and sterile RF10-H and DMEM.

2.4 CELL ISOLATION TECHNIQUES

2.4.1 Isolation Of Thymocytes Or Splenocytes

Two methods, either mechanical disaggregation or enzymatic digestion, were used to obtain single cell suspensions of thymocytes or peripheral lymphocytes from the thymus and spleen. For mechanical disaggregation, thymus or spleen were teased apart between two glass slides to release the cells into a petri-dish containing RF10 to obtain a single cell suspension. Alternatively, for enzymatic digestion, tissues were place into 1.5ml eppendorfs containing 1ml RF10-H with 0.4mg/ml DNase1 and 2.5mg/ml Collagenase D added and chopped into fine pieces using scissors to increase surface area, aiding digestion. The enzyme media and tissues were transferred into polypropylene round bottom tubes (BD) and incubated at 37°C using a thermomixer (Eppendorf) to keep the samples agitated. Samples were pipetted up

and down every 5 minutes until all tissue had digested (25-30 minutes) and 30µl of 0.5M EDTA was added to each.

Once a single cell suspension was obtained, cells were filtered through a mesh-membrane filter to remove any cell clumps into 15ml centrifuge tubes (Corning) and centrifuged at 1400rpm for 4 minutes to form a pellet. Thymus samples were then re-suspended in 2ml of staining buffer (500ml PBS + 2ml 0.5M EDTA + 2.5ml FCS) and placed on ice whereas spleen samples were re-suspended in 2ml of red blood cell lysis buffer (Sigma-Aldrich) and left at room temperature for 10 minutes to deplete erythrocytes within the samples. To neutralize the lysis reaction, an equal volume of RF10-H was then added to the cell suspension and centrifuged. If red blood cell lysis was incomplete, this step was repeated, however if lysis was successful the splenocytes were re-suspended in 2ml of staining buffer and placed on ice.

Using Sphero AccuCount cell count beads (SpheroTech), cell counts were acquired by adding 5µl of cell count beads (equivalent to 5000 beads) to 100µl of staining buffer in a FACs tube. 50µl of sample was then added to the count tube, giving a final concentration of 1:40. These samples (FACs tube containing 100µl staining buffer, 5µl of beads and 50µl of sample) were then run on a BD LSR Fortessa flow cytometer to count the number of cells and beads. Total cell numbers were then calculated using the following formula:

$$Total\ cell\ number\ = \left(\left(\frac{Number\ of\ cells}{Number\ of\ beads} \right) \times 5000 \right) \times 40$$

2.4.2 Isolation Of Stromal Cell Populations

For the isolation of stromal cells from the thymus, thymi were place into 1.5ml eppendorfs containing 1ml RF10-H with 0.4mg/ml DNase1 and 2.5mg/ml Collagenase Dispase added and chopped into fine pieces using scissors. The enzyme media and tissues were transferred into polypropylene round bottom tubes (BD) and incubated at 37°C using a thermomixer (Eppendorf) to keep the samples agitated. Samples were pipetted up and down every 5 minutes until all tissue had digested (25-30 minutes) and 30µl of 0.5M EDTA was added to each sample. Once a single cell suspension was obtained, the thymus samples were handled and counted using the same method as used in section 2.4.1. For stromal analysis, CD45- depletion was carried out to enrich the non-hematopoietic stromal cells within the samples. 10µl of anti-CD45 microbeads (Miltenyi Biotec) were added to each sample, vortexed and incubated on ice for 20 minutes. Samples were then passed through primed LS MACs separation columns (Miltenyi Biotec) placed on QuadroMACs separator magnets and collected and placed on ice ready for staining whereas the $CD45^+$ cells retained within the LS MACs separation column were discarded.

2.5 FLOW CYTOMETRY

2.5.1 Antibodies

All primary antibodies used for flow cytometric analysis for this study are listed in Table 2.4 and secondary antibodies are listed in Table 2.5. Antibodies were conjugated with a fluorochrome or were biotinylated, which required a secondary streptavidin antibody for their detection. All antibodies were titrated prior to their use

and the working concentrations for each antibody are stated in Table 2.4 and Table 2.5.

2.5.2 Immunolabeling For Flow Cytometry

Following single cell isolation and cell counting, approximately $5x10^6$ cells from each sample was aliquoted into separate wells of a 96-well plate (Costar) and centrifuged at 1400 RPM for 2 minutes. For experiments investigating rare cell populations, $1x10^7$ cells were stained to increase the number of the rare population to aid analysis. The supernatant was discarded and re-suspended in 50µl ($5x10^6$ cells) or 100µl ($1x10^7$ cells) of antibody mix. All antibody suspensions were made up in staining buffer at the concentrations indicated in Table 2.4 and Table 2.5 and samples were incubated on ice for 30 minutes. Single color controls were prepared for each individual fluorochrome used in the staining combination and these were used to set compensation parameters on the flow cytometer. After 30 minutes incubation on ice, each well was washed with 150µl of staining buffer and centrifuged at 1400RPM for 2 minutes. Following this the supernatant was removed and any secondary or tertiary steps were added in the same method as used for the primary antibody step. Following all necessary antibody staining steps, cells were washed, centrifuged, the supernatant was removed and samples were then re-suspended in 100-200µl of staining buffer and transferred into 12.5ml polystyrene FACS tubes (Becton) to be run on the flow cytometer or stored short-term at 4°C until they were run on the flow cytometer.

2.5.3 Intracellular Immunolabeling For Flow Cytometric Analysis

Intracellular staining of transcription factors such as Foxp3 and Aire required a fixation/permeabilization step to achieve successful detection. Cells were stained for cell surface markers as described in Section 2.5.2. After the final step of surface stain was complete, samples were washed, centrifuged and the supernatant was discarded. Samples were then permeabilized using the eBioscience Foxp3/Transcription Factor Staining Buffer Set (ThermoFisher) in accordance with the manufacturer's protocol. All samples, including single color controls, were re-suspended in 150µl Fixation/Permeabilization solution made up of concentrate and diluent at a 1:3 ratio and were incubated for 45 minutes on ice. Cells were washed twice in 100µl of 10% 10X permeabilization buffer, made up in distilled water. Following permeabilization, cells were stained with either Foxp3 PE or Aire Alexa Fluor 488 (Table 2.4), which were diluted in 10% 10X permeabilization buffer and stained on ice for 30 minutes. Cells were washed and centrifuged twice in 100µl of 10% 10X permeabilization buffer and then finally resuspended in staining buffer and transferred into FACS tube ready for acquisition by flow cytometry. The intracellular staining of CCL21 was carried out in the same manner as Foxp3 and Aire, however the CCL21 primary antibody requires further detection by a secondary goat anti-rabbit Alexa Fluor 647 antibody detailed in Table 2.4 and Table 2.5.

2.5.4 Flow Cytometric Analysis

Samples were run on a BD LSR Fortessa flow cytometer using the accompanying BD FACS diva software and analysis of acquired flow cytometric data was carried out using FlowJo software (version 8.8.6). Voltages for each detection channel, as well as compensation between each fluorochrome was adjusted and set using single

color controls for each fluorochrome. Gating for positive staining was set by using negative control samples which either used isotype controls, fluorescence minus one or samples from knock-out mice lacking the particular protein being stained for, for example using lymphotoxin β receptor (LTβR)-deficient mice to control for LTβR straining levels. The number of events collected during sample acquisition depended on the frequency of the population under investigation. For the majority of samples, $5x10^5$ events were collected, however in instances of rare cells, such as CD4 IV^+ cells, approximately $2\text{-}3x10^6$ events were collected to improve accuracy of the analysis. Forward and side scatter gates were set to exclude any non-viable cells.

Table 2.4 Primary Reagents Used For Flow Cytometry Immunolabeling

Specificity (Clone)	Conjugate	Working Dilution	Supplier
Anti-CD45 (Clone 30-F11)	APC eFluor 780 APC	1:800 1:800	eBioscience eBioscience
Anti-EpCAM-1 (Clone G8.8)	PerCP eFluor 710 APC	1:1000 1:800	eBioscience eBioscience
Anti-TER119 (Clone TER119)	A700	1:200	Biolegend
Anti-Podoplanin (PDPN, gp38) (Clone eBio 8.1.1/8.1.1)	PE PE Cy7	1:800 1:800	eBioscience Biolegend
Anti-CD31 (Clone eBio 390/390)	FITC Bv605	1:300 1:100	eBioscience BioLegend
LIVE/DEAD Fixable Dead Cell Stain Kit	Near-IR	1:1000	Invitrogen
Anti-PDGFRα (Clone APA5)	Biotin	1:200	eBioscience
Anti-PDGFRβ Clone APB5	Biotin	1:200	eBioscience
Anti-Ly-51 (Clone 6C3)	PE	1:200	eBioscience
Anti-Ly-51 (Clone BP-1)	PE	1:200	BD Bioscience
Anti-ICAM-1 (CD54) (Clone YN1/Y.1.7.4)	Pacific Blue	1:200	BioLegend
Anti-VCAM-1 (CD106) (Clone 429)	Biotin	1:200	BioLegend
Rat IgG_{2b}, κ isotype (Clone RTK4530)	Pacific Blue	1:200	BioLegend
Rat IgG_{2a}, κ isotype (Clone eBR2a)	Biotin	1:200	eBioscience
Anti-HSA (CD24) (Clone M1/69)	Biotin PE	1:200 1:500	Pharminogen BD Bioscience
Anti-Sca-1 (Clone D7)	Biotin	1:300	BioLegend
Anti-CD34 (Clone RAM34)	Biotin	1:200	eBioscience
Anti-CD29 (Clone HMβ1-1)	Biotin	1:200	BioLegend
Anti-CD4 (Clone GK1.5)	PE Cy7	1:1500	eBioscience
Anti-CD4 (Clone RM4-5)	Bv711	1:100	BioLegend

Table 2.4 Primary Reagents Used For Flow Cytometry Immunolabeling continued…

Specificity (Clone)	Conjugate	Working Dilution	Supplier
Anti-CD8 (Clone 53-6.7)	PE Bv510	1:200 1:200	eBioscience BioLegend
Anti-PBS-57 Tetramer	APC	1:400	National Institutes of Health Tetramer Core Facility
Anti-FoxP3 (Clone FJK-16s)	PE	1:100	eBioscience
Anti-TCRβ (Clone H57.597)	APC eFluor 780	1:200	eBioscience
Anti-CD25 (Clone eBio3C7)	eFluor 450	1:100	eBioscience
Anti-CD25 (Clone PC61.5)	A700	1:100	eBioscience
Anti-CD69 (Clone H1.2F3)	PerCP-Cy5.5	1:200	eBioscience
Anti-CD62L (Clone MEL-14)	APC	1:1500	BioLegend
Anti-LTβR (Clone eBio3C8)	Biotin	1:200	eBioscience
Anti-UEA-1	Biotin	1:10000	Vector Laboratories
Anti-I^AI^E (MHC Class II) (M5/114.15.2)	Bv421	1:600	Biolegend
Anti-CD80 (Clone 16-10A1)	BV605	1:400	Biolegend
Anti-Aire (Clone 5H12)	Alexa Fluor 488	1:1000	eBioscience
Rabbit IgG Anti-CCL21	-	1:100	Lifespan Biosciences
Anti-CD62p (P-selectin) (Clone RB40.34)	FITC	1:400	BD Bioscience
Anti-Ly6C (Clone HK1.4)	PE Cy7	1:400	Biolegend
Anti-S1PR1 Monoclonal (Clone 713412)	-	1:10	R&D Systems

Table 2.4 Primary Reagents Used For Flow Cytometry Immunolabeling continued…

Specificity (Clone)	Conjugate	Working Dilution	Supplier
Anti-Rat IgG_{2a} (Clone MRG 2a-83)	Biotin	1:100	Biolegend
Anti-CD45.1 (Clone A20)	PE Cy7	1:200	eBioscience
Anti-CD45.2 (Clone 104)	A700	1:200	eBioscience
Anti-CD3 (Clone 145-2C11)	PE	1:50	eBioscience

Table 2.5 Secondary Reagents Used For Flow Cytometry Immunolabeling

Specificity	Conjugate	Working Dilution	Supplier
Streptavidin	PE Cy7	1:1500	eBioscience
Anti-rabbit IgG	Alexa Fluor 647	1:200	Life Technologies

2.6 HIGH SPEED SORTING

Samples were prepared by cell surface labeling by the same method as section 2.5.2. To collect a enough cells to generate reaggregate thymic organ cultures (RTOCs) (detailed in Section 2.8) or for PCR, greater numbers of cells were prepared and therefore the staining volume was increased from 50µl antibody/$5x10^6$ cells to 350µl of antibody/$30x10^6$ cells. Samples bigger than $30x10^6$ were separated prior to staining but importantly stained using the same antibody mix and pooled after staining was complete. Samples were resuspended in 0.5ml of RF10-H and filtered through a 30mm mesh-membrane filter unit (Miltenyi Biotech). Samples were transferred to a polypropylene FACS tube (Becton Dickinson) and stored at 4°C prior to sort. Sorting was carried out using either a MoFlo XDP sorter (Beckman Coulter) or a FACSAria Fusion (BD). Sorted populations were collected into FACS tubes

containing 0.5ml RF10-H, centrifuged, and re-suspended in 1ml of RF10-H. Cells were taken for cell counting as well as to check the cell purity for each of the isolated cell populations by comparing them to the pre-sorted samples, using a BD LSR Fortessa flow cytometer. Isolated cell populations were then centrifuged and washed in PBS to remove residual RF10-H media. If cells were isolated for PCR analysis, samples were centrifuged again, supernatant discarded and snap frozen on dry ice prior to storage in a -80°C freezer.

2.7 FETAL THYMIC ORGAN CULTURE (FTOC)

The FTOC system is a powerful tool that can be used for analysis of thymic stroma and thymocytes, as the cultured thymus can still support normal T-cell development and maintain its structure of the thymic stromal microenvironment *in vitro*. Under sterile conditions within a laminar flow cabinet, thymic lobes were dissected from embryos, typically at day 15 of gestation (E15), and placed on top of a 0.8μm sterile nucleopore filter (Millipore), which lay on top of a sterile anti-wrap sponge support (Medipost Ltd) within DMEM media. Prior to this, the sponge support had been cut to 1cm^2 squares and both the sponges and the nucleopore filters were boiled, separately, for 30 minutes to sterilize and left to air dry within a laminar flow cabinet. Thymic lobes were placed on the filter surface using a mouth-controlled sterile glass pipette. Up to 6 lobes were placed per filter-sponge, two of which were added per 90mm petri dish (Sterilin) containing 4ml of DMEM. For the depletion of hematopoietic cells within the FTOC, 2-dGuo was added to the DMEM medium prior to adding the fetal lobes. 600μl of 2-dGuo stock was added to 4ml of DMEM in a 90mm petri dish. Once the cultures had been set up they were stored in sterile

humidified chambers and gassed with 10% CO_2 for 10 minutes to correct the pH of the culture medium to 7.2-7.4 and then sealed and stored at 37°C for 7 days.

2.8 REAGGREGATE THYMIC ORGAN CULTURE (RTOC)

The generation of RTOCs allows the investigation of specific individual cell types, both hematopoietic and stromal, within an *in vitro* 3-dimensional thymic microenvironment (208,246). The experimental design and generation of the RTOCs used in this study is described in Figure 3.10. For this study, $CD4^+CD8^-TCR\beta^+Tetramer^-Foxp3^-$ SP4 thymocyte, $CD4^+CD8^-TCR\beta^+Tetramer^-Foxp3^+$ regulatory T-cells (Tregs) and $CD4^+CD8^-TCR\beta^+Tetramer^+$ invariant natural killer T-cells (iNKTs) were sorted from adult mice using a MoFlo cell sorter as described in Section 2.6. Under sterile conditions, the isolated populations were mixed with a cell suspension of 2-dGuo-treated FTOC (Section 2.7) that have been digested and $CD45^+$ depleted to enrich for stroma. Thymocyte populations were added at a 3:1 ratio with the 2-dGuo treated, CD45-depleted, FTOC stroma within a 1.5ml eppendorf. The combined cell suspension was centrifuged at 1000rpm for 10 minutes and the supernatant was removed, leaving <5µl of supernatant. The pellet was vortexed and using a finely drawn mouth pipette (finer than typically used for FTOC), the cell suspension was dropped, under a dissection microscope, onto the center of a 0.8µm sterile Whatman filter, which sat on top of a sterile anti-wrap sponge in DMEM. RTOCs were limited to one per filter-sponge and culture conditions were the same used for FTOCs in Section 2.7. RTOCs were cultured for 7 days before enzymatic digestion and analysis of the stromal populations.

2.9 THYMIC KIDNEY CAPSULE TRANSFER

To investigate the contribution of thymic stroma in regulating thymocyte egress *Ltbr*$^{+/+}$ or *Ltbr*$^{-/-}$ E15 2-dGuo-treated FTOC lobes were transferred under the kidney capsule of WT hosts. Mice used for surgery were 6-8 weeks old and were weighed prior to surgery to ensure the correct dose of analgesia was administered as well as to monitor weight changes of the mice following the surgical procedure. Mice were anaesthetized using a chamber containing 4% isoflurane (May and Barker, Degenham, UK) carried within oxygen. Once mice were unconscious they were transferred onto a heat pad and anesthesia administration was maintained using a facemask. 2mg/kg of pre-operative Buprenorphine (Temgesic, AnimalCare, UK) was administered sub-cutaneously.

Mice were laid on their stomach and using an electric trimmer, fur surrounding the site of incision was removed and the site was cleaned and sterilized using 70% ethanol. Two incisions were made; the first was a small incision into the skin using blunt-ended scissors within the region of the left kidney. The skin and peritoneum in this region were separated and the second incision was made into the peritoneum. The kidney was then carefully drawn out of the body using blunt-ended forceps to grab the fat attached to the kidney. The kidney was maintained outside of the body by the small size of the incision into the skin, which prevented the kidney from reentering the body, and the kidney throughout the manipulation outside of the body was kept hydrated with sterile gauze soaked in PBS. A small incision was then made into the capsule of the kidney and the fetal thymic lobes were transferred under the kidney capsule using an iris cutter, with a maximum of two lobes grafted per kidney.

The kidney was gently drawn back into the body cavity and the peritoneum, followed by the skin, was sutured (Vicryl, 16mm round bodied sutures) and the skin was also sealed using a surgical staple to aide wound closure. The mice were removed from anesthesia and placed into a warming box and visually monitored until they had regained consciousness. BMSU staff monitored the recovery of the mice until they were sacrificed between 6-8 weeks later and the thymus tissue was retrieved from the kidney and processed for FACS analysis.

2.10 GENERATION OF BONE MARROW CHIMERAS

To investigate the role of hematopoietic cell populations in regulating thymocyte egress, CD45.1 WT hosts were reconstituted with either CD45.2 WT or CD45.2 *Ltbr*$^{-/-}$ bone marrow (BM) (experimental design detailed in Figure 4.11). BM was obtained from the femur and tibia of the CD45.2 WT and CD45.2 *Ltbr*$^{-/-}$ donors by flushing the bones with sterile RF10-H using a syringe and a 27-gauge needle under sterile conditions. The BM was flushed into a 35mm petri dish containing RF10-H and the extracted BM was passed through the needle several times to obtain a single cell suspension and the cell suspension was then filtered using a 30mm mesh-membrane filter (Miltenyi Biotech). Samples were centrifuged and re-suspended in 2ml red blood cell lysis buffer (Sigma-Aldrich) and left at room temperature for 10 minutes. An equal volume of RF10-H was added to neutralize the lysis buffer, the sample was centrifuged and then resuspended in RF10-H and counted. Following this, the BM samples were then T-cell depleted, first by staining the samples in 2ml of anti-CD3 PE antibody mix (Table 2.4) to ensure adequate staining of T-cells and samples were incubated for 30 minutes on ice. Samples were then washed, centrifuged and resuspended in sterile staining buffer containing 1:10 dilution of anti-PE microbeads

(Miltenyi Biotec), where 10µl of microbeads was added per $1x10^7$ cells. Samples were incubated on ice for 15 minutes and then passed though a primed LS MACs separation column (Miltenyi Biotec) placed on QuadroMACs separator magnets. The column was washed twice using staining buffer and all $CD3^-$ cells that passed through the column were collected. Samples were centrifuged, resuspended in sterile RF10-H and counted. Aliquots were made in 1.5ml eppendorfs, at a concentration of $5x10^6$ cells/200µl PBS (without calcium and magnesium) and stored on ice until transfer into the host mouse.

CD45.1 WT hosts receiving BM transfers that weighed over 18g were placed onto drinking water containing baytril antibiotic drinking water for one week prior to irradiation. Hosts were irradiated using a CIS IBL 437 Cs-137 irradiator (CIS BIO International, Cedex, France) with two 450 Rad doses over two days (dose one: 10am first day, dose 2: 10am second day) and the bone marrow transfer was performed in the afternoon on the day of the second irradiation. 200µl of BM was transferred intravenously via the tail vein into each host, which had been warmed in a warming box to aid visualization of the tail vein, using a 25-gauge needle and 1ml syringe. BMSU staff monitored the recovery of the mice post-injection and the mice remained on baytril drinking water for a week following BM transfer. The chimera mice were harvest 12 weeks after bone marrow transfer to maximize the amount of time for the thymocytes to accumulate and thymocyte emigration was measured using flow cytometry.

2.11 ANTI-CD4 INTRAVENOUS (IV) LABELING

To measure the frequency of cells within the perivascular space in WT and genetically altered mice an intravenous (IV) labeling approach was used. WT or genetically altered mice were each injected with 1µg of anti-CD4 PE antibody intravenously using a 25-gauge needling attached to a 1ml syringe. The anti-CD4 PE was prepared at a concentration of 1µg of CD4 PE (GK1.5; BioLegend) in 200µl of PBS (without calcium and magnesium). Each mouse was harvested 3 minutes after injection and the thymus was immediately dissected and mechanically dissociated using glass slides in 20ml of RF10-H to dilute any excess, unbound anti-CD4 PE antibody, and stored on ice. Injections were staggered every 3 minutes to ensure enough time to process each sample. As a control for the anti-CD4 IV labeling, a control mouse was first administered FTY720 18 hours prior to anti-CD4 administration. FTY720 blocks sphingosine-1-phosphate mediated egress and entry into the perivascular space, therefore mice receiving FTY720 treatment act as a negative control for PVS labeling by anti-CD4 IV. FTY720 (Sigma Aldrich) was administered at 1mg/mouse and made up in distilled water prior to injection.

2.12 IN VIVO BRDU LABELLING

For *in vivo* labeling of proliferating cells, 1.5mg/mouse of BrdU (Sigma Aldrich) was administered by intraperitoneal injections and mice were harvested 18 hours after. Cells were isolated and stained for cell surface markers as described in Section 2.5.2 in a 96-well plate. Samples were then resuspended in 100µl of BD fix/perm for 30 minutes in the fridge and then washed with 150µl of perm/wash. Cells were spun down, supernatant removed and resuspended in BD Cytoperm buffer Plus for 10 minutes on ice. Cells were then washed in 150µl of perm/wash, spun down,

supernatant removed and resuspended in 100µl of BD fix/perm and incubated on ice for 5 minutes. Following this cells were washed in 150µl of perm/wash, spun down, supernatant removed and resuspended in 100µl of diluted DNAse (30µl of stock DNAse, 70µl PBS with calcium and magnesium) and incubated for 1 hour at 37°C. Samples were then washed with perm/wash, centrifuged, supernatant removed and resuspended in 100µl of anti-BrdU (1:100 dilution in perm/wash buffer) and incubated for 40 minutes at room temperature. The samples were washed a final time and resuspended in staining buffer and stored at 4°C until ran on the Flow Cytometer.

2.13 IMMUNOHISTOLOGY TECHNIQUES

2.13.1 Sectioning And Fixation Of Frozen Tissues

Thymus tissue was harvested from adult mice, cleaned of any excess fat and blood, placed on tin foil sections and frozen down as soon as possible on dry ice. Frozen tissues were then mounted in optimal cutting temperature (OCT) compound onto a microtome. Sections were cut at a thickness of 7µm and mounted onto four spot glass slides (Hendley-Essex) and left to air dry at room temperature for 40 minutes before being fixed in acetone (Sigma Aldrich) for 20minutes at 4°C. Sections where removed from acetone and allowed to air dry for 5-10 minutes and then immediately stained for immunolabeling or stored in sealed bags at -20°C until used for immunolabeling.

2.13.2 Immunolabeling Of Frozen Tissue Sections

Sections freshly removed from acetone following fixation were left to air dry for 5-10 minutes or sections removed from -20°C were left at room temperature to air dry for 30 minutes prior to placing in PBS bath for 10-15 minutes to rehydrate the sections.

The details of the primary antibodies used for staining of frozen sections for confocal analysis are listed in Table 2.6 and secondary antibodies are listed in Table 2.7. Antibodies were made up in PBS containing 1% bovine serum albumin (BSA) and 100µl of each antibody mix was applied to each section, ensuring full coverage of each tissue section and incubated for 30 minutes in a dark, humidified chamber at room temperature. Excess PBS was removed from the edges of the slides as well as between each section before adding antibodies to prevent the antibodies staining multiple sections. Sections were washed within a PBS bath for 10 minutes between each staining step. Once all staining steps were complete the sections were fully emerged in a DAPI (4',6-diamidino-2-phenylindole) solution for 10 seconds to stain the nucleus of the cells throughout the whole section. Sections were immediately washed in a fresh PBS bath for 30 seconds, twice. Excess PBS was removed from the edges of the slides as well as between the sections and then a small drop of DABCO (1,4 diazabicyclooctane), in glycerol at pH 7, or ProLong Gold Antifade Mountant (Life Technologies) was added to each section to prevent fading of the fluorochromes. The slide was mounted with a cover slip (Sigma Aldrich) and sealed using nail varnish around the outer edges of the cover slip and allowed to air dry. Slides were then either imaged shortly after or were stored at -20°C until use.

Table 2.6 Details Of Primary Antibodies Used For Immunohistology

Specificity (Clone)	Host/Isotype	Conjugate	Working Dilution	Supplier
Anti-CD31 (Clone WM-59)	Mouse	Alexa Fluor 488/Biotin	1:100	eBioscience
Anti-PDPN (Clone 8.1.1)	Hamster IgG	-	1:10	Kind gift from Andrew Farr (247)
Anti-ERTR5	Rat IgM	-	1:5	Kind gift from Van Vliet E (248)
Anti-Pancytokeratin Clone C11	Mouse	Alex Fluor 488	1:500	Sigma
Anti-β5t	Rabbit	-	1:100	MBL
Anti-CD8 (Clone 53-6.7)	Rat	Biotin	1:200	eBioscience
Anti-ERTR7	Rat IgG	-	1:10	Kind gift from Van Vliet E (248)

Table 2.7 Details Of Secondary Antibodies Used For Immunohistology

Specificity (Clone)	Host/Isotype	Conjugate	Working Dilution	Supplier
Streptavidin Monoclonal	-	Alexa Fluor 555	1:500	Invitrogen (Thermofisher)
Anti-Rat IgG	Goat	Alexa Fluor 594	1:200	Invitrogen (Thermofisher)
Anti-Rat IgM	Goat	Alexa Fluor 647	1:200	Invitrogen (Thermofisher)
Anti-Hamster IgG	Goat	Alex Fluor 647	1:200	Invitrogen (Thermofisher)
Anti-Rabbit IgG	Chicken	Alex Fluor 647	1:200	Invitrogen (Thermofisher)

2.13.3 Confocal Analysis And Quantitation

To quantify the medullary area within WT, *Ltrb*$^{-/-}$, *Foxn-1*^{cre} and *Foxn-1*^{cre}*Ltbr*^{flox} mice, full tissue immunofluorescence scans were taken using a Zeiss Axio ScanZ1 and each tissue scan was analyzed using Zeiss Zen Blue software to measure the area of each medullary region. Medullas were defined as containing either CD4 or CD8 single positive thymocytes and areas of ERTR5^{+} staining (which stains medullary thymic epithelial cells). Three sections were analyzed per mouse, each from different depths within the tissues for quantitation, with a minimum of three mice per strain. We adopted a previously published method to categorize the medullary areas according to their area in mm^2 and the mean number of medullas within each size category was calculated (249). For the imaging of the perivascular space in Section 5 and thymic mesenchyme in Section 3 images were taken using a Zeiss LSM 780 and analyzed using Zeiss Zen Black software.

2.14 PREPERATION OF SAMPLES FOR GENE EXPRESSION ANALYSIS

All gene expression analysis was carried out in collaboration with S. Parnell, University of Birmingham.

2.14.1 mRNA Extraction And cDNA Synthesis

Prior to their use, all buffers were equilibrated to room temperature. $0.9cm^3$ of lysis/binding buffer was added to a maximum of $1x10^7$ cells and lysed by vigorous vortexing or passing through a 21-gauge needle with care. Lysate was applied on top of Lysate Clear Column in a centrifuge tube and centrifuged at 13,000g for 3 minutes. 50µl of oligo (dT) microbeads were then added to the lysate and gently mixed to allow hybridization of mRNA to oligo (dT) microbeads. A MACSµ column was placed

in a magnetic field of a thermo MACS Separator and primed with 100µl of lysis/binding buffer. Lysate was then added to the column matrix, within which the magnetically labeled mRNA will bind to the column whereas the unwanted protein and DNA will not. To remove the proteins and DNA, the MACSµ columns were rinsed twice with 200µl of lysis/binding buffer and washed four times with 100µl of wash buffer to remove rRNA and DNA. 100µl of equilibration/wash buffer was then added to the column twice and following this the reverse transcription mastermix was added to the top of the column matrix. 1µl of sealing solution was applied to prevent evaporation and the column matrix was incubated for 1 hour at 42°C on the thermo MACs block. The column was then rinsed twice with 100µl equilibration/wash buffer and finally 20µl of release solution was added to the column and incubated at 42°C for 30 minutes. The synthesized cDNA was then eluted with 50µl of cDNA elution buffer, collected in an eppendorf and stored at -20°C until use.

2.14.2 Real Time Quantitative PCR

Real time quantitative PCR was performed using a RotorGene RG-3000 (Qiagen) using SYBR green with primers specific for the variety of genes of interest. Details of the primers used, including the forward 5' and reverse 3' sequences are detailed in Table 2.8. Prior to the amplification of the target genes of interest, β-actin was used as the housekeeping gene for sample normalization. Oligonucleotides of the genes of interest were synthesized by Sigma-Genosys. PCR reactions were performed in replicates within a 15µl reaction buffer containing 7.5µl of 2X qPCR mastermix (Bioline Sensimix NoRox SybrGreen QT 650-05) containing heat-activated Taq polymerase, dNTPs, $MgCl_2$, Sybr green and reaction buffer. The 15µl reaction buffer

also contained 0.15µl (20µM stock concentration) of both forward and reverse primers (final concentration 0.2µM), 6.2µl DNAse-free/RNAse-free, PCR grade water (Life Technologies 10977035) and 1µl cDNA template. β-actin primers were designed and synthesize by QIAGEN (QuantiTect Mm Actb 1SG Primer Assay: QIAGEN QT00095242) and used at a 1x concentration. The amplification program included an initial denaturation step at 95°C for 10 minutes, followed by cycling at 95°C for 15 seconds, 60-62°C (primer pair specific) for 20 seconds and 72°C for 15 seconds (40 cycles). At the end of each cycle the fluorescent signal produced from the amplicon was obtained and at the final amplification a dissociation curve was generated (72-99°C, hold 30 seconds on the first step, then 5 seconds on the next steps), per primer pair, to verify the specificity of the amplicon. The reaction amplification efficiency and Ct values were acquired from Rotor Gene 6.0 software (Qiagen) using standard curves generated from mouse universal cDNA (Biochain). The Pfaffl model was adopted to calculate the relative expression values of each sample, normalized to β-actin. The Pfaffl model was selected as it takes into account gene dependent efficiencies within the amplification process.

2.15 GRAPHS AND STATISTICAL ANALYSIS

All graphs and statistical analysis were generated using GraphPad Prism 6 software. The statistical test carried out is described in the figure legend accompanying each figure throughout this study and only P-values below 0.05 were considered significant.

Table 2.8 Details Of Primers Used For qPCR

Primer	NCBI Reference Sequence	Forward 5' End Sequence	Reverse 3' End Sequence
Fgf10	NM_008002.4	CAGCGGGACCAAGAATGAAG	TGACGGCAACAACTCCGATTT
Il-7	NM_008371.4	TTCCTCCACTGATCCTTGTTCT	AGCAGCTTCCTTTGTATCATCAC
Enpp2	NM_001136077.2	GGAGAATCACACTGGGTAGATGATG	ACGGAGGGCGGACAAAC
Cxcl13	NM_018866.2	CATAGATCGGATTCAAGTTACGCC	TCTTGGTCCAGATCACAACTTCA
Ccl19	NM_011888.2	GCTAATGATGCGGAAGACTG	ACTCACATCGACTCTCTAGG
Ccl21	NM_011124.4	ATCCCGGCAATCCTGTTCTC	GGGGCTTTGTTTCCCTGGG
Sphk1	NM_011451.3	GAGCTCCGAGCTGTTTGCA	TGACACCCCCGCACGTA
Rank	NM_009399.3	GCTGGCTACCACTGGAACTC	GTGCAGTTGGTCCAAGGTTT
Ltbr	NM_010736.3	CAGAGAGCTGGAGGCTGAAC	GGAGCTCCCTCTTCAGGAGT
Lta	NM_010735.2	GCTTGGCACCCCTCCTGTC	GATGCCATGGGTCAAGTGCT
Ltb	NM_008518.2	TGGCAGGAGCTACTTCCCT	TCCAGTCTTTTCTGAGCCTGT
Light	NM_019418.3	GTTTCTCCTGAGACTGCATCAA	TGGCTCCTGTAAGATGTGCTG
Ppap2b	NM_080555.2	GGTGGCCTGCTGCATAGTGTT	TCCTGTCGATGATCCACGGG
Sgpl1	NM_009163.3	TATTGCACCAAATATGAGCC	CTGTTGTTCGATCTTACGTC
Spns2	NM_153060.3	CCATCCTGAGTTTAGGCAACG	GATCACCTTTCTATTGAAGCGGT
Foxo1	NM_019739.3	TGTCAGGCTAAGAGTTAGTGAGCA	GGGTGAAGGGCATCTTTG
Klf2	NM_008452.2	CTCAGCGAGCCTATCTTGCC	CACGTTGTTTAGGTCCTCATCC
S1pr1	NM_007901.5	AAATGCCCCAACGGAGACT	CTGATTTGCTGCGGCTAAATTC
Coro1a	NM_001301374.1	CTCACTGGGGTCTTGTGTCC	GGCTCATCCCATCTGCTCTG

CHAPTER THREE: CHARACTERISATION AND REGULATION OF NON-EPITHELIAL THYMIC STROMA

3.1 INTRODUCTION

The thymic stromal microenvironment is a highly specialized, heterogeneous component of the thymus organ and is essential for the support and regulation at all stages of T-cell development. The thymic stromal compartment is made up of epithelial and non-epithelial cells, with much of what is known about thymic stroma focusing on the epithelial compartment due to the vital functions this subset of stromal cells carry out to generate a functional and self-tolerant T-cell pool.

However the non-epithelial cell populations within the thymus have numerous important functions that make their research an inviting prospect. Studies have highlighted the key role of thymic endothelial cells in regulating the entry of T-cell progenitors through the expression of P-selectin and the adhesion molecules ICAM-1 and VCAM-1 by endothelial cells and absence or blockade of these interactions with T-cell progenitors causes significant reductions in ETP within the thymus (20,22,24). In addition, it was shown that regulation of T cell progenitor entry by thymic endothelial cells was dependent on signaling through the lymphotoxin β receptor (LTβR) (22,24). Furthermore, thymic endothelial cells produce cytokines such as Kit-ligand (KitL), with the membrane-bound form of KitL (mKitL) expressed by endothelial cells within the thymic cortex being required for the proliferation and differentiation of DN1 stage thymocytes (31,33).

The other main non-epithelial stromal population identified within the thymus is the thymic mesenchyme. During embryogenesis, neural-crest (NC)-derived thymic mesenchyme is essential for the normal development of the thymus, with removal of

the thymic mesenchyme resulting in a hypoplastic thymus and an associated disruption of the normal programme of T-cell development (123,199,201,202,208,209). Embryonic thymic mesenchyme also produce a number of growth factors which are essential for the proliferation of the TEC compartment and furthermore thymic mesenchyme has also been implicated in the regulation of MHC Class II expression on TEC during embryogenesis (201,202,205–208). Together these highlight the functional significance of this cellular compartment during thymus development.

Through the use of NC-derived mesenchyme specific *Wnt-1*^{cre} and *Sox10*^{cre} mouse models crossed with a Rosa26 fate-mapper, where fluorescent protein expression was driven by *Wnt-1*^{cre} or *Sox10*^{cre} expression within the NC-derived cells, NC-derived thymic mesenchyme was identified within the adult thymus (213,250). Within the adult, thymic mesenchyme contributes to the structure of the thymus, including provision of a cellular contribution to the capsule of the thymus (214,250). In addition, mesenchymal cells also comprise thymic pericytes, which produce the enzymes SPHK1 and SPHK2. These kinases act to phosphorylate sphingosine to produce sphingosine-1-phosphate (S1P), with this pericyte-mediated production of S1P being essential to maintain the S1P gradient required for mature thymocyte egress (111).

Still, despite what has currently been discovered, much remains unknown about the cellular and molecular developmental regulation, phenotypic heterogeneity and functional roles of thymic mesenchymal populations within the adult thymus, together

highlighting a need for further phenotypic and functional characterization of these cells.

Lymph node (LN) stromal populations can be divided into a number of subpopulations based on their expression of specific phenotypic markers including podoplanin (PDPN) and the platelet endothelial cell adhesion molecule 1 (PECAM-1 or CD31). These two markers can identify a $PDPN^{+}CD31^{-}$ mesenchymal population termed fibroblastic reticular cells (FRCs), which have a number of key functions within the lymph nodes including the maintenance of T-cell homeostasis through the production of interleukin-7 (IL-7), production of migratory signals essential for entry into the lymph node as well as migration to and within the T-cell zone (220,222–226). Additionally the cellular and molecular developmental mechanisms of this LN mesenchymal population, such as signaling through TNFRSF members RANK and LTβR, as well as the requirement for stroma-lymphocyte interactions for their development, share similarities with the mechanisms in place for the development of thymic epithelial stromal cells (149,151,152,161,230–232). Thus studies of LN mesenchymal populations may provide a platform from which investigation of the thymic mesenchyme can be based on.

The following section aims to identify the phenotypic and functional characteristics of the thymic mesenchyme population, as well as the cellular and molecular pathways that regulate them.

3.2 RESULTS

3.2.1 Identifying And Characterizing Non-Epithelial Stromal Populations Within The Adult Murine Thymus

To determine the stromal populations that exist within the non-hematopoietic, non-epithelial compartment of the thymus, flow cytometric analysis was carried out on digested adult mouse thymi and mesenteric lymph nodes (mLN). During development the thymus is derived from the foregut and may potentially share some phenotypic similarities with mLN and therefore was chosen for comparison. Firstly a staining panel was assembled to identify the stromal populations of peripheral lymph nodes. TER119 and CD45 were included to exclude erythrocytes and hematopoietic cells, respectively. Additionally PDPN and CD31 were included to identify the three main LN stromal populations; fibroblastic reticular cells ($PDPN^{+}CD31^{-}$, FRC), lymphatic endothelial cells ($PDPN^{+}CD31^{+}$, LEC) and blood endothelial cells ($PDPN^{+}CD31^{-}$, BEC) and in our hands all three populations were identifiable (Fig 1.A.) (220). In contrast to LN stroma, the thymic stromal compartment consists largely of epithelial cells and therefore in order to exclude epithelial cells from our thymic analysis, the epithelial cell adhesion molecule EpCAM-1 was included in the staining panel (Fig 3.1.B.). Interestingly the non-epithelial stromal population was predominantly made up of $PDPN^{+}CD31^{-}$ mesenchymal cells loosely matching the FRC within the LN (Fig 3.1.B.). In addition, $PDPN^{-}CD31^{+}$ thymic endothelial cells were easily identifiable and consistent with previous reports there were no detectable population of lymphatic stromal cells (Fig 3.1.B.C) (111). From here on in, the term thymic mesenchyme will refer to the $TER119^{-}CD45^{-}EpCAM\text{-}1^{-}CD31^{-}PDPN^{+}$ thymic

Figure 3.1. Identification Of PDPN^{+} Thymic Mesenchyme Within The Non-Epithelial Thymic Stromal Compartment

Adult B6 WT thymi were digested using a Collagenase Dispase and DNase enzyme mix and isolated stromal cells were stained for FACS analysis.

(A) Gating strategy to identify the different lymph node stromal populations based on PDPN and CD31 within lymph nodes; fibroblastic reticular cells (FRC, PDPN^{+}CD31^{-}), lymphatic endothelial cells (LEC, PDPN^{+}CD31^{+}) and blood endothelial cells (BEC, PDPN^{-}CD31^{+}).

(B) Gating strategy of PDPN and CD31 on TER119^{-}CD45^{-}EpCAM-1^{-} thymic non-epithelial stroma to identify PDPN^{+}CD31^{-} mesenchyme and PDPN^{-}CD31^{+} endothelial cells.

(C) Table comparing the presence or absence of the three stromal populations within the thymus and inguinal lymph nodes based on expression of PDPN and CD31.

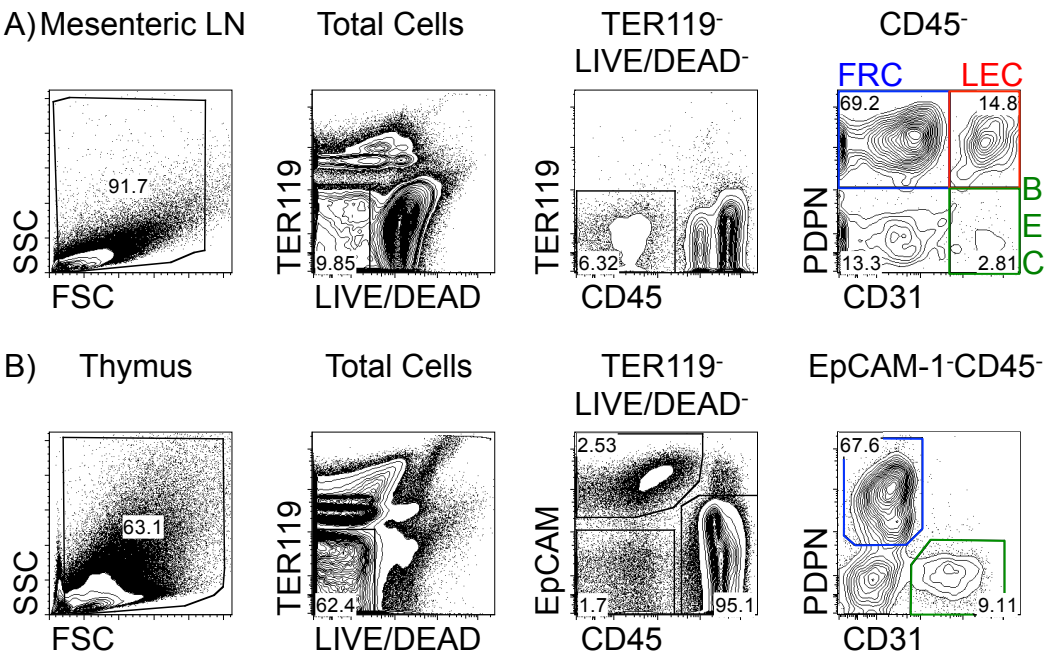

C)

	Stromal Population		
	PDPN$^+$ CD31$^-$	PDPN$^+$ CD31$^+$	PDPN$^-$ CD31$^+$
mLN	✓	✓	✓
Thymus	✓	✗	✓

stromal population and thymic endothelium will refer to the TER119$^-$CD45$^-$EpCAM-1$^-$ CD31$^+$PDPN$^-$ thymic stromal population.

Knowing the cell position within the thymus is important when attempting to understand the role of a stromal population as it can provide context to the cells location relative to other cells in the thymus. Using CD31 and PDPN, as identified above, as well as ER-TR5 (a marker of medullary TEC (mTEC) (248)), β5t (a proteasome subunit expressed by cortical TEC (cTEC) (165)) and pancytokeratin (stains cTEC) we investigated the intrathymic positioning of PDPN$^+$ thymic mesenchyme. Co-staining of CD31, PDPN, ER-TR5 and pancytokeratin revealed that broadly, PDPN is restricted to the medulla where it is expressed by some mTEC but also non-mTEC (Fig 3.2.A.) consistent with flow cytometric analysis (Fig 3.1.B.). PDPN$^+$ cells appeared to surround/ensheath CD31$^+$ endothelial cells both at the cortico-medullary junction and within the cortex in a perivascular manner (Fig 3.2.A.B.). These perivascular PDPN$^+$ cells were present in the medulla, near the cortico-medullary junction (CMJ) where endothelial cells are thought to be the site of thymocyte egress and within the deeper cortex (Fig 3.2.B.). Previous studies have identified a role for thymic mesenchyme contributing to the capsule and septea of the thymus structure and PDPN$^+$ cells were identifiable in both structures (Fig 3.2.C.) (251).

Expression of additional cell surface markers was performed by flow cytometry in order to further characterize the PDPN$^+$CD31$^-$ mesenchymal cells and to also get a

Figure 3.2. Localization Of PDPN^{+} Thymic Mesenchyme

Adult B6 WT thymi were frozen and 7μm think thymus sections were cut and stained for immunofluorescence confocal microscopy.

(A) High resolution image of a thymic area stained for CD31 (white), PDPN (red), ERTR5 (blue) and pancytokeratin (green). Smaller images on the left show single color images for each marker and the larger image on the right is an image of the four combined colors. Scale bars represent 50μm.

(B) High resolution image of a thymic area stained for CD31 (blue), PDPN (red) and pancytokeratin (green). Scale bars represent 50μm.

(C) Low resolution tile scan image of a thymic area stained for ERTR5 (blue), PDPN (red) and b5t (green). Scale bars represent 200μm.

All images are representative of 4 mice from 3 independent experiments.

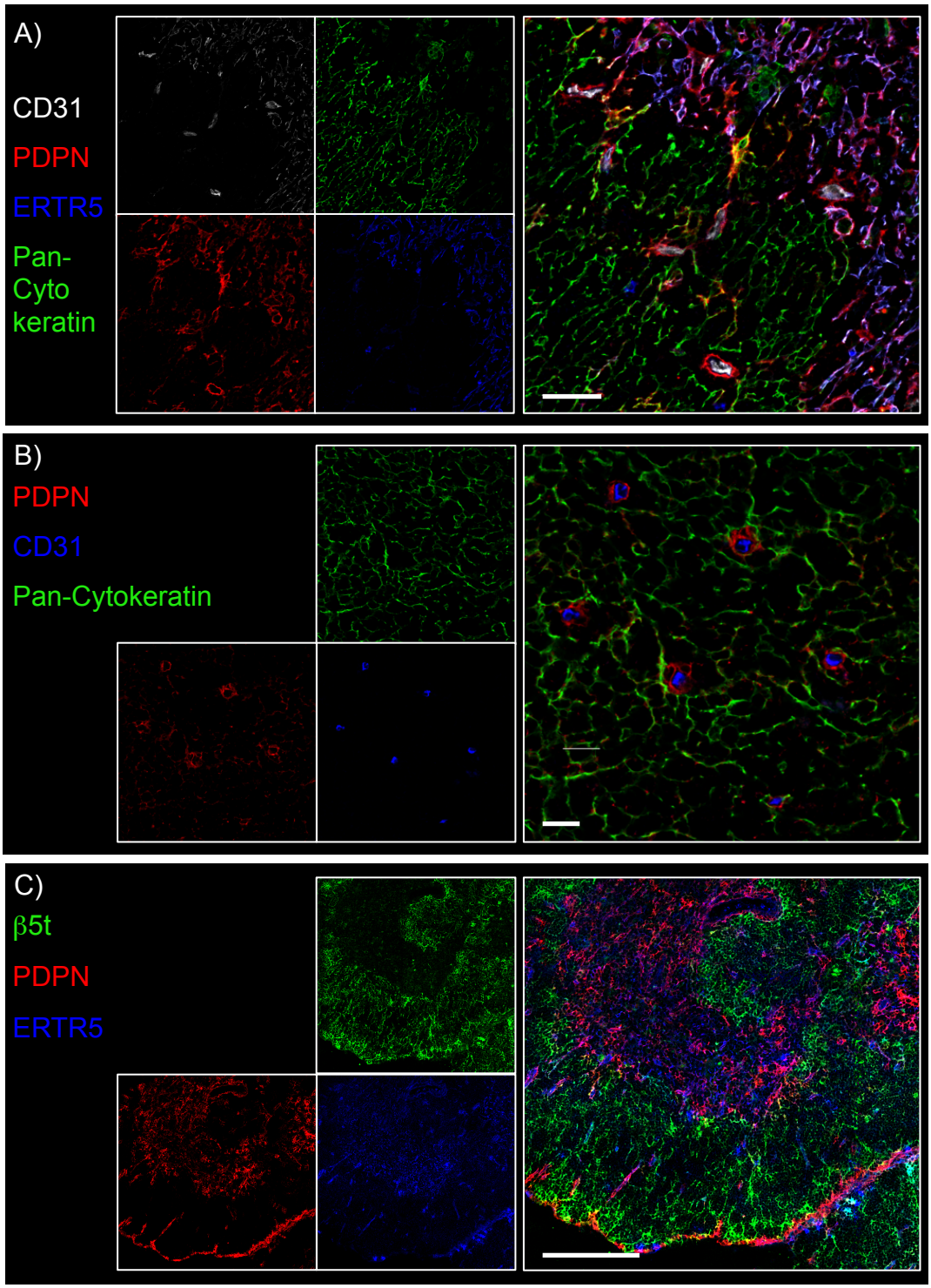
A)
CD31
PDPN
ERTR5
Pan-
Cyto
keratin
B)
PDPN
CD31
Pan-Cytokeratin
C)
β5t
PDPN
ERTR5

better understanding of their potential role within the thymus. Such markers were selected based on reported phenotypes of embryonic thymic mesenchyme (PDGFRα (202)), adult thymic pericytes (PDGFRβ (111,213)) and previously identified cortical thymic mesenchyme (Ly-51) (217). As well as CD24 (heat stable antigen, HSA), Sca-1, CD34 and CD29 which are associated with mesenchymal stem cells and intercellular adhesion moledule-1 (ICAM-1) and vascular cell adhesion molecule (VCAM-1) which have been associated with peripheral lymphoid tissues. Thymic mesenchyme expressed PDGFRα, PDGFRβ, Ly-51, ICAM-1 and VCAM-1 at comparable levels to mLN FRC (Fig 3.3.A.B). Interestingly the expression profile of ICAM-1 and VCAM-1 on thymic mesenchyme mirrors that of lymph node FRC that has previously been reported which separates expression into distinct ICAM-1^{lo}VCAM-1^{lo}, ICAM-1^{int}VCAM-1^{int} and ICAM-1^{hi}VCAM-1^{hi} populations (Fig 3.3.C.). Thymic mesenchyme also expresses Sca-1, CD34 and CD29, markers associated with a adipocyte/pre-adipocyte phenotype whilst not expressing HSA (Fig 3.3.D.) (231).

In addition to cell surface phenotype, $PDPN^{+}$ thymic mesenchyme cells were sorted for qPCR for gene expression analysis to gather additional data on a potential role within the thymus (Fig 3.4.A.). Mesenteric LN FRCs were sorted and run alongside the sorted thymic mesenchyme and genes were selected based on their previously reported roles in thymocyte migration and homeostasis within lymph nodes (Fig 3.4.B.C.). Consistent with previous reports, thymic mesenchyme expressed *Fgf-10* known for a role in supporting TEC during thymus organogenesis (Fig 3.4.C.). Thymic mesenchyme also expressed *Enpp2*, which encodes autotaxin (ATX), an

ectoenzyme that is required for the production of lysophosphatidic acid (LPA) which plays a role in lymphocyte trafficking into lymph nodes and regulation of lymphocyte migration (252,253) (Fig 3.4.C.). *Cxcl13*, *Ccl19* and *Il-7*, which are genes involved in regulating lymphocyte migration and homeostasis were also expressed by thymic mesenchyme (Fig 3.4.C.). To gain a thymic context for the level of expression of these genes, sorted thymic mesenchyme was compared to sorted mTEC isolated from embryonic thymus cultured in fetal thymic organ culture (FTOC) conditions. Interestingly, whilst comparing thymic mesenchyme to mLN revealed a low level of expression of *Ccl19* in thymic mesenchyme, in the context of the thymus thymic mesenchyme expresses higher levels than mTEC and thus thymic mesenchyme may express *Ccl19* at a functionally significant level within the thymus (Fig 3.4.D.). Conversely, whilst compared to mLN, thymic mesenchyme appears to express *Il-7*, comparing to mTEC revealed that thymic mesenchyme express low levels of *Il-7* suggesting mTEC are the primary thymic source of IL-7 (Fig 3.4.D). The localization of mesenchyme and mTEC would suggest that IL-7 production by thymic mesenchyme is redundant (Fig 3.2.A.). Additionally the PCR reveals that thymic mesenchyme is a major source of CXCL13 and ATX within the thymus compared to mTEC (Fig 3.4.D.).

As discussed above, thymic mesenchyme can be separated based on the expression of ICAM-1 and VCAM-1 in a similar manner to LN FRC (Fig 3.3.C.). In LN FRCs, the ICAM-1^{hi}VCAM-1^{hi} population is the functionally mature compartment of the FRCs and follow a developmental transition from ICAM-1^{lo}VCAM-1^{lo} lymphoid tissue organizer cells to ICAM-1^{int}VCAM-1^{int} and finally ICAM-1^{hi}VCAM-1^{hi} (232). In light of

Figure 3.3. Phenotypic Characterization Of Thymic Mesenchyme

Thymi and mesenteric lymph nodes (mLN) were harvested from WT B6 adult mice and digested for stromal analysis by FACS.

(A) Expression profile of PDGFRα, PDGFRβ and Ly-51 on $TER119^{-}CD45^{-}EpCAM\text{-}1^{-}PDPN^{+}CD31^{-}$ thymic mesenchyme (Thymic Mes, red) and $TER119^{-}CD45^{-}PDPN^{+}CD31^{-}$ mLN fibroblastic reticular cells (mLN FRC, blue) compared with staining controls for each tissue.

(B) Expression profile of ICAM-1 and VCAM-1 on $TER119^{-}CD45^{-}EpCAM\text{-}1^{-}PDPN^{+}CD31^{-}$ thymic mesenchyme (Thymic Mes, red) and $TER119^{-}CD45^{-}PDPN^{+}CD31^{-}$ mLN fibroblastic reticular cells (mLN FRC, blue), compared with staining controls for each tissue.

(C) Expression pattern of ICAM-1 and VCAM-1 plotted together on $TER119^{-}CD45^{-}EpCAM\text{-}1^{-}PDPN^{+}CD31^{-}$ thymic mesenchyme and $TER119^{-}CD45^{-}PDPN^{+}CD31^{-}$ mLN fibroblastic reticular cells (mLN FRC), where $ICAM\text{-}1^{lo}VCAM\text{-}1^{lo}$, $ICAM\text{-}1^{int}VCAM\text{-}1^{int}$ and $ICAM\text{-}1^{hi}VCAM\text{-}1^{hi}$ populations are gated.

(D) Expression profile of HSA, Sca-1, CD34 and CD29 on $TER119^{-}CD45^{-}EpCAM\text{-}1^{-}PDPN^{+}CD31^{-}$ thymic mesenchyme (Thymic Mes, red) compared with staining controls and $CD45^{+}$ hematopoietic cells (blue).

All data is typical of three independent repeats.

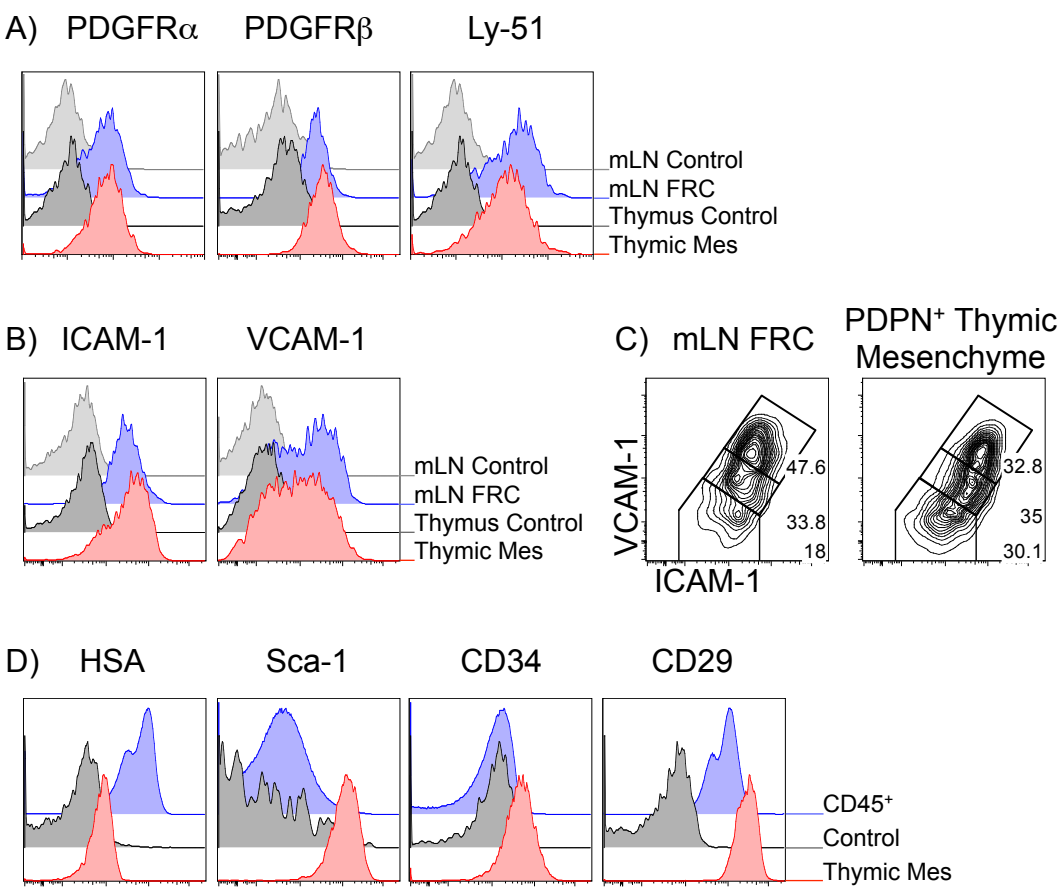
A) PDGFRα PDGFRβ Ly-51
mLN Control
mLN FRC
Thymus Control
Thymic Mes
B) ICAM-1 VCAM-1
mLN Control
mLN FRC
Thymus Control
Thymic Mes
C) mLN FRC
PDPN+ Thymic Mesenchyme
VCAM-1
ICAM-1
47.6
33.8
18
32.8
35
30.1
D) HSA Sca-1 CD34 CD29
CD45+
Control
Thymic Mes

Figure 3.4. Genotypic Analysis And Comparison Of Functional Gene Expression On Thymic Mesenchyme, Epithelium and LN FRCs

(A) Pre sort stained stromal cells and post sort purity check of sorted $PDPN^{+}CD31^{-}$ thymic mesenchyme from adult B6 WT mice.

(B) Pre sort stained stromal cells and post sort purity check of sorted $PDPN^{+}CD31^{-}$ mesenteric lymph node fibroblastic reticular cells from adult B6 WT mice.

(C & D) Quantitative real time PCR was performed on the following populations sorted from adult B6 WT mice for mLN FRC and thymic mesenchyme and FTOC for mTEC:

$CD45^{-}PDPN^{+}CD31^{-}$ **mLN $PDPN^{+}CD31^{-}$** (blue)

$CD45^{-}EpCAM\text{-}1^{-}PDPN^{+}CD31^{-}$ **Thymic $PDPN^{+}CD31^{-}$** (red)

$CD45^{-}EpCAM\text{-}1^{+}UEA\text{-}1^{+}$ **Thymic mTEC** (green) FTOC

Error bars indicate the SEM and mRNA levels were normalized to housekeeping gene β-actin. Data is from at least two independently sorted biological samples; with each gene analyzed a minimum of two times and each PCR ran in triplicates to obtain a SEM.

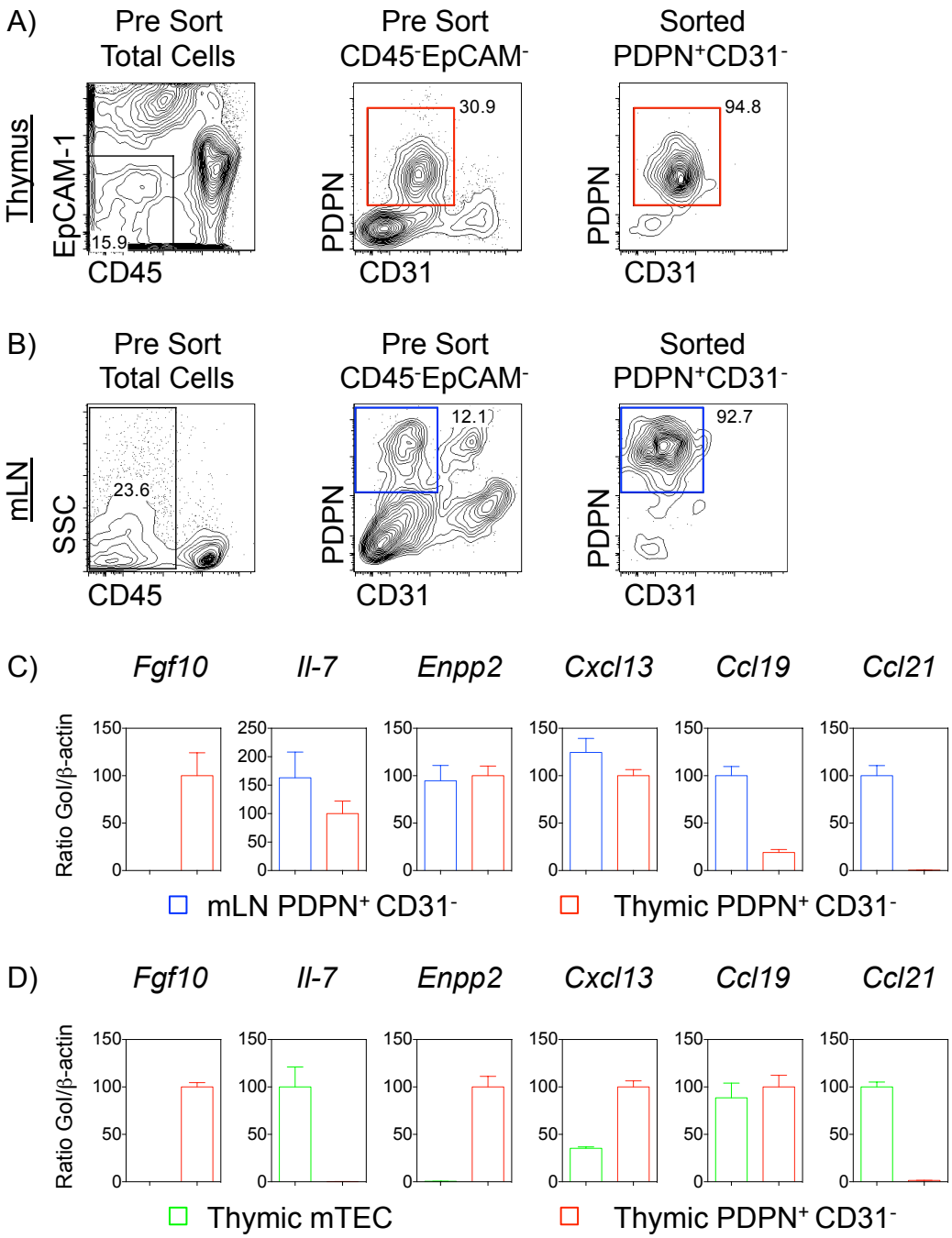
A)
Pre Sort
Total Cells
Pre Sort
CD45-EpCAM-
Sorted
PDPN+CD31-
Thymus
EpCAM-1
15.9
CD45
30.9
PDPN
CD31
94.8
PDPN
CD31
B)
Pre Sort
Total Cells
Pre Sort
CD45-EpCAM-
Sorted
PDPN+CD31-
mLN
SSC
23.6
CD45
12.1
PDPN
CD31
92.7
PDPN
CD31
C)
Fgf10
Il-7
Enpp2
Cxcl13
Ccl19
Ccl21
Ratio Gol/β-actin
mLN PDPN+ CD31-
Thymic PDPN+ CD31-
D)
Fgf10
Il-7
Enpp2
Cxcl13
Ccl19
Ccl21
Ratio Gol/β-actin
Thymic mTEC
Thymic PDPN+ CD31-

this, we studied the temporal emergence and development of the ICAM-1^{hi}VCAM-1^{hi} PDPN^{+} thymic mesenchyme population. We chose developmental time points that included three main stages of development: embryogenesis (embryonic day 14-18, E14-E18), neonatal development (day 0, D0 and day 1, D1) and young adult (week 1, W1 and week 2, W2). Our analysis revealed that the ICAM-1^{hi}VCAM-1^{hi} PDPN^{+} mesenchyme began appearing postnatally around D0-D1 (Fig 3.5.A-B.). Full maturation occurred within the first two weeks of thymus development, where the percentage of ICAM-1^{hi}VCAM-1^{hi} increased to its maximum at W2 (Fig 3.5.C.). Additionally ICAM-1 MFI increased steadily up to W1 (Fig 3.5.D-E.).

This ontogenic analysis suggests a potential precursor-product relationship between the ICAM-1^{lo}VCAM-1^{lo} and ICAM-1^{hi}VCAM-1^{hi} and suggests that ICAM-1^{hi}VCAM-1^{hi} cells may be the mature population of thymic mesenchyme. To test whether ICAM-1^{lo}VCAM-1^{lo} and ICAM-1^{hi}VCAM-1^{hi} are functionally distinct populations, thymic mesenchyme was separated based on the expression of ICAM-1 and VCAM-1 and sorted into two populations, ICAM-1^{lo} PDPN^{+} mesenchyme and ICAM-1^{hi} PDPN^{+} mesenchyme (Fig 3.6.A.B.). Similarly to LN FRC, the ICAM-1^{hi} fraction of thymic mesenchyme appeared to have the highest expression levels of *Ccl19, Enpp2* and *Sphk1* (a kinase involved in regulating thymocyte egress) suggesting that these ICAM-1^{hi}VCAM-1^{hi} mesenchyme cells are vital to the function of the thymic mesenchyme population (Fig 3.6.C.). Interestingly the ICAM-1^{lo} fraction had the highest levels of expression of *Cxcl13* suggesting an important function role of ICAM-1^{lo} expressing mesenchyme in addition to ICAM-1^{hi} (Fig 3.6.C.).

Figure 3.5. Temporal Emergence Of ICAM-1^{hi}VCAM-1^{hi} PDPN^{+} Thymic Mesenchyme During Thymic Development

Thymic lobes were harvested from B6 WT mice from different stages of development: embryonic days 14-18 (E14-E18), neonatal days 0, 1 (D1 and D2) and week 1 and week 2 (W1 and W2). All thymic lobes were digested for FACS analysis of the stromal populations using an enzyme mix of Collagenase D and DNase.

(A) Expression pattern of ICAM-1 and VCAM-1 on TER119^{-}CD45^{-}EpCAM^{-} PDPN^{+}CD31^{-} mesenchyme from embryonic thymi where ICAM-1^{hi}VCAM-1^{hi} population is gated.

(B) Expression pattern of ICAM-1 and VCAM-1 on TER119^{-}CD45^{-}EpCAM^{-} PDPN^{+}CD31^{-} mesenchyme from neonatal thymi where ICAM-1^{hi}VCAM-1^{hi} population is gated.

(C) Percentage and cell number of ICAM-1^{hi}VCAM-1^{hi} cells within the PDPN^{+}CD31^{-} mesenchyme compartment of embryonic and neonatal thymi.

(D) MFI of ICAM-1 on PDPN^{+}CD31^{-} thymic mesenchyme.

(E) Histogram showing the expression of ICAM-1 on PDPN^{+}CD31^{-} thymic mesenchyme from E14 (green), E18 (dark blue), D0 (red), D1 (purple) and W1 (light blue) mice, compared to a isotype staining control.

For E18, D0, D1, W1 and W2 are typical of 2 independent repeats and E14, E15, E16 and E17 were carried out once.

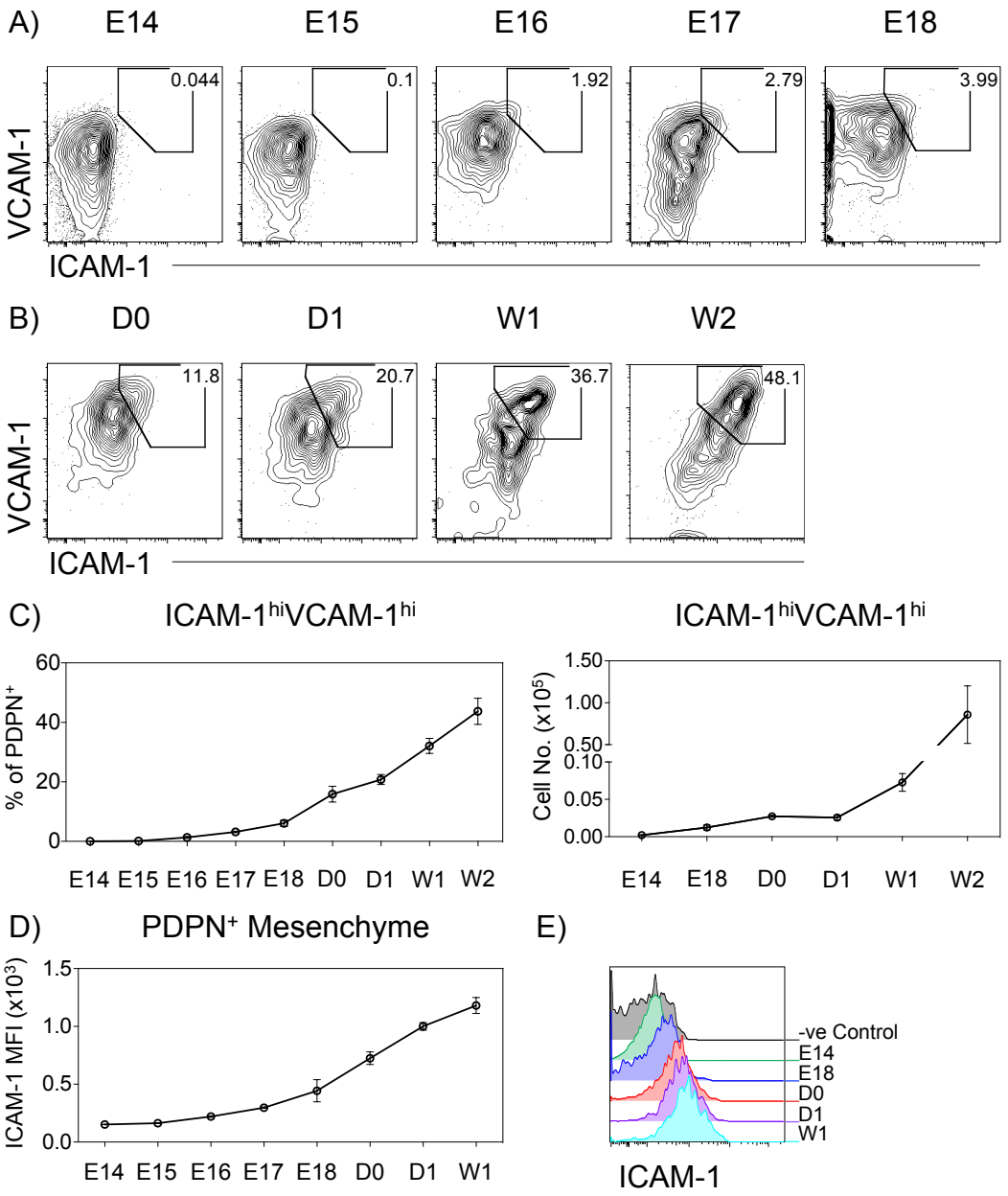
A)
E14
E15
E16
E17
E18
0.044
0.1
1.92
2.79
3.99
VCAM-1
ICAM-1
B)
D0
D1
W1
W2
11.8
20.7
36.7
48.1
VCAM-1
ICAM-1
C)
ICAM-1hiVCAM-1hi
% of PDPN+
60
40
20
0
E14 E15 E16 E17 E18 D0 D1 W1 W2
ICAM-1hiVCAM-1hi
Cell No. (x10^5)
1.50
1.00
0.50
0.10
0.05
0.00
E14 E18 D0 D1 W1 W2
D)
PDPN+ Mesenchyme
ICAM-1 MFI (x10^3)
1.5
1.0
0.5
0.0
E14 E15 E16 E17 E18 D0 D1 W1
E)
-ve Control
E14
E18
D0
D1
W1
ICAM-1

Figure 3.6. Genotypic Analysis ICAM-1^{lo} And ICAM-1^{hi} PDPN^{+} Thymic Mesenchyme

(A) Pre sort stained stromal cells from adult B6 WT mice to identify ICAM-1 and VCAM-1 expressing cells within CD45^{-}EpCAM-1^{-}PDPN^{+} thymic mesenchyme.

(B) Post sort purity checks of sorted ICAM-1^{lo} and ICAM-1^{hi} PDPN^{+} thymic mesenchyme from adult B6 WT mice.

(C) Quantitative real time PCR was performed on the following populations sorted from B6 WT mice:

CD45^{-}EpCAM-1^{-}PDPN^{+}ICAM-1^{lo}VCAM-1^{lo} **ICAM-1^{lo}PDPN^{+}** (blue)

CD45^{-}EpCAM-1^{-}PDPN^{+}ICAM-1^{hi}VCAM-1^{hi} **ICAM-1^{hi}PDPN^{+}** (red)

Error bars indicate the SEM and mRNA levels were normalized to housekeeping gene β-actin. Data is from at least two independently sorted biological samples; with each gene analyzed a minimum of two times and each PCR ran in triplicates to obtain a SEM.

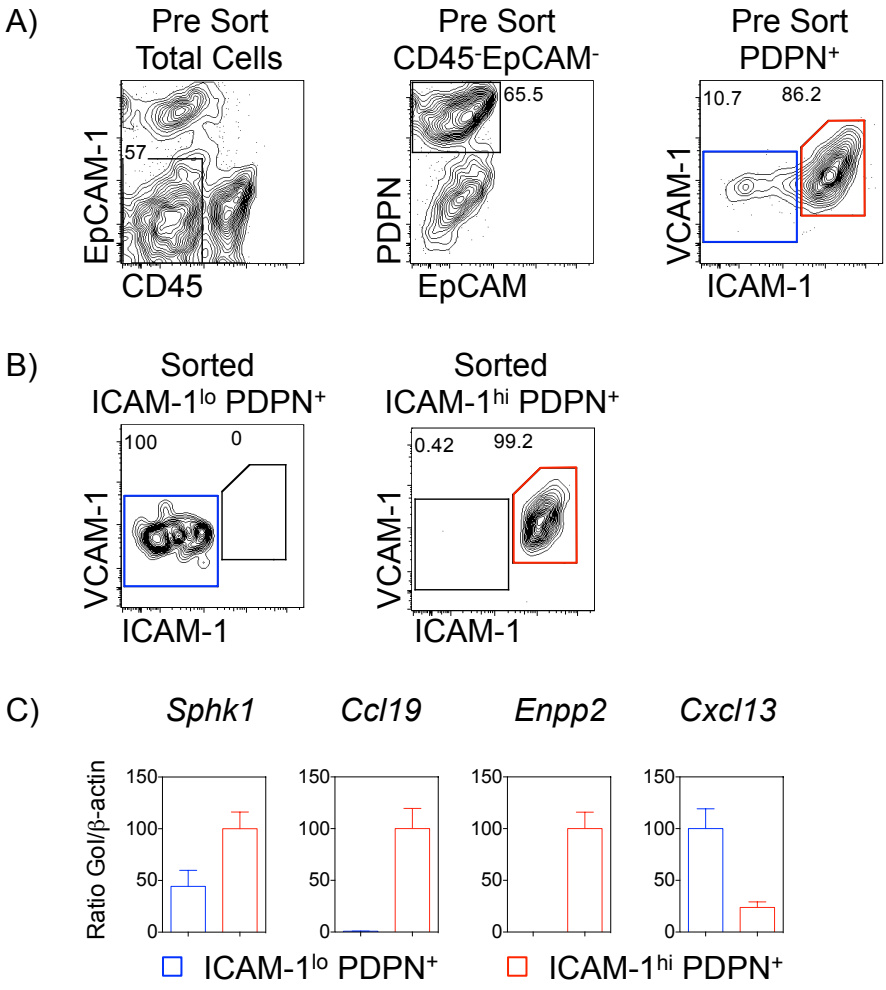
A)
Pre Sort
Total Cells
EpCAM-1
57
CD45
Pre Sort
CD45-EpCAM-
65.5
PDPN
EpCAM
Pre Sort
PDPN+
10.7
86.2
VCAM-1
ICAM-1
B)
Sorted
ICAM-1lo PDPN+
100
0
VCAM-1
ICAM-1
Sorted
ICAM-1hi PDPN+
0.42
99.2
VCAM-1
ICAM-1
C)
Sphk1
Ccl19
Enpp2
Cxcl13
Ratio GoI/β-actin
150
100
50
0
ICAM-1lo PDPN+
ICAM-1hi PDPN+

Collectively these analyses identify a PDPN^{+} thymic mesenchyme population that shares key phenotypic similarities with peripheral lymph node FRCs. The data suggests a role for thymic mesenchyme in supporting thymocyte migration and egress through their expression of key chemotactic factors including *Ccl19*, *Cxcl13*, *Enpp2* and *Sphk1* as well as the cell position within the thymus in both the medulla and surrounding CD31^{+} blood vessels. In addition, this analysis provides evidence of an ICAM-1^{hi}VCAM-1^{hi} fraction of thymic mesenchyme that express key factors linked to a potential role of thymic mesenchyme in thymocyte migration and/or egress.

3.2.2 Thymocyte-Mesenchyme Interactions Are Essential For The Development Of ICAM-1^{hi}VCAM-1^{hi} Thymic Mesenchyme

After identifying the potential functional importance of the ICAM-1^{hi}VCAM-1^{hi} PDPN^{+} mesenchyme as well as the developmental kinetics of how the population arises, we investigated how their development is regulated. We found it interesting that the emergence of the ICAM-1^{hi}VCAM-1^{hi} population coincided with the timing of thymocyte development and subsequent egress of αβ^{+} T-cells, which occurs postnatally. This could suggest cross-talk between mature thymocytes and the developing thymic mesenchyme to trigger their development. To test whether interactions between thymocytes and thymic mesenchyme are required for the development of the ICAM-1^{hi}VCAM-1^{hi} PDPN^{+} thymic mesenchyme, WT FTOCs were cultured either in the absence or presence of 2'-deoxyguanosine (2-dGuo), a compound that is toxic to hematopoietic cells. We found that treatment of FTOC with 2-dGuo led to an almost complete loss of the ICAM-1^{hi}VCAM-1^{hi} expressing PDPN^{+} thymic mesenchyme, evidenced by a reduced proportion of this population (Fig

Figure 3.7. Thymocyte:Mesenchyme Interactions Are Essential For ICAM-1^{hi}VCAM-1^{hi} PDPN^{+} Mesenchyme Development

E15 WT lobes were cultured in fetal thymic organ culture (FTOC) conditions in the presence or absence of 2-deoxyguanosine (2-dGuo) for 5-7 days and then harvested and digested for FACS analysis of the stromal populations.

(A) Expression pattern of PDPN and CD31 on TER119^{-}Viability^{-}CD45^{-}EpCAM-1^{-} non-epithelial stroma where PDPN^{+}CD31^{-} mesenchyme and PDPN^{-}CD31^{+} endothelial cells are gated.

(B) Expression pattern of ICAM-1 and VCAM-1 on PDPN^{+}CD31^{-} mesenchyme where ICAM-1^{hi}VCAM-1^{hi} population is gated.

(C) The percentage of ICAM-1^{hi}VCAM-1^{hi} cells was within the PDPN^{+}CD31^{-} mesenchyme compartment of FTOC (blue circle) and FTOC + 2-dGuo (red square) was calculated.

(D) Histogram showing the expression of ICAM-1 and VCAM-1 on PDPN^{+} thymic mesenchyme and the plotted MFI of each adhesion molecule represented as a ratio of the MFI of FTOC + 2-dGuo:FTOC.

The standard error bars display the SEM and a mann-whitney test was performed in (C) and an unpaired parametric T-tests was performed in (D), where ** denotes a significant difference as $p<0.01$ and *** as $p<0.001$. All data is typical of 3 independent repeats.

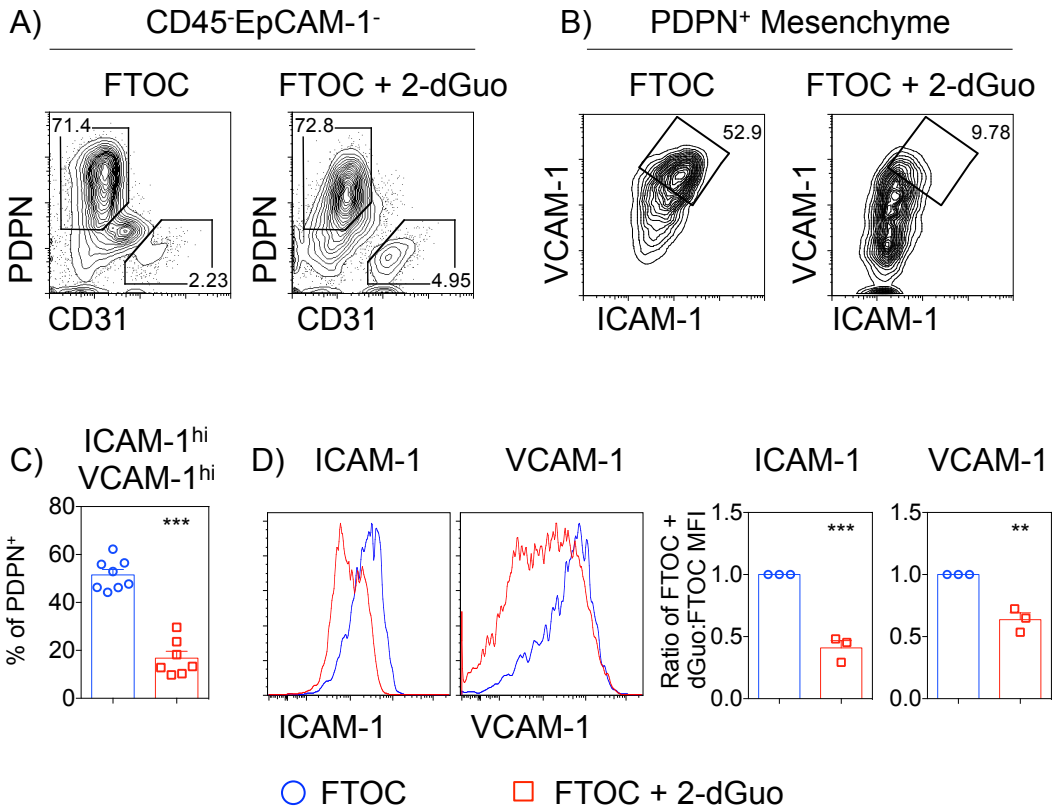
A)
CD45-EpCAM-1-
FTOC
FTOC + 2-dGuo
71.4
2.23
72.8
4.95
PDPN
CD31
B)
PDPN+ Mesenchyme
FTOC
FTOC + 2-dGuo
52.9
9.78
VCAM-1
ICAM-1
C)
ICAM-1hi
VCAM-1hi
% of PDPN+
***
D)
ICAM-1
VCAM-1
Ratio of FTOC + dGuo:FTOC MFI
***
**
FTOC
FTOC + 2-dGuo

3.7.B.C.) and reduced ICAM-1 and VCAM-1 MFI represented as a ratio of 2-dGuo MFI:FTOC MFI (Fig 3.7.D.).

Previous studies have shown there is an essential requirement for $\alpha\beta^+$ thymocyte crosstalk in the development of thymic epithelial stroma, to investigate whether this was also the case for thymic mesenchyme we investigated *Tcra*$^{-/-}$ mice which lack $\alpha\beta^+$ thymocytes (140,254). These mice showed no alterations in total thymic cellularity (Fig 3.8.B.) but they do show a significant reduction in the percentage and cell number of ICAM-1^{hi}VCAM-1^{hi} PDPN$^+$ mesenchyme (Fig 3.8.A.C.). This data reveals that αβ$^+$ T-cells are essential for the development of ICAM-1^{hi}VCAM-1^{hi} PDPN$^+$ thymic mesenchyme and removing hematopoietic cells *in vitro* results in a loss of this population.

The αβ T-cell compartment is a heterogeneous mix of conventional and non-conventional T-cell subsets, many of the cells within this compartment have previously been shown to influence thymic epithelial cells such as SP4 thymocytes, Treg and iNKT cells (145,146). To determine which of these subsets are essential for mesenchyme development we used mouse models where the genes *MHC class ii*, *Cd1d* or *Foxp3* are knocked out, resulting in a loss of CD4$^+$ thymocytes, CD1d$^+$ invariant natural killer T (iNKT) cells or regulatory T-cells (Tregs), respectively. When CD4$^+$ thymocytes were absent in *MHC class ii*$^{-/-}$ there was no difference in total thymic cellularity or the PDPN$^+$ thymic mesenchyme compartment (Fig 3.8.D-F). Fitting with their role in regulating mTEC, there was a reduction in the number and the proportion of ICAM-1^{hi}VCAM-1^{hi}, suggesting a role for SP4 thymocytes in ICAM-

1^{hi}VCAM-1^{hi} thymic mesenchyme development (Fig 3.8.F.) (145). When iNKT cells were absent in the *Cd1d*$^{-/-}$ model there was no evidence of altered PDPN^{+} thymic mesenchyme development (Fig 3.9.A-C) however when Tregs were absent there was a small significant reduction in the proportion of ICAM-1^{hi}VCAM-1^{hi} PDPN^{+} mesenchyme (Fig 3.9.D-E). Together these data support that αβ^{+} T-cells are essential for the development of ICAM-1^{hi}VCAM-1^{hi} PDPN^{+} mesenchyme, but the loss of one specific population is not enough to recapitulate a reduction in ICAM-1^{hi}VCAM-1^{hi} PDPN^{+} thymic mesenchyme with the same severity as seen in the *Tcra*$^{-/-}$ mouse, suggesting there is redundancy among the different αβ T-cell subsets to ensure the development of this population.

The knockout models above test if any one-thymocyte population is essential for the development of ICAM-1^{hi}VCAM-1^{hi} PDPN^{+} mesenchyme, but it does not indicate whether any of the populations alone are sufficient for this process. One approach that enables this analysis is the use of reaggregate thymic organ cultures (RTOCs) to add each of the three thymocyte populations (SP4, iNKT and Tregs) separately to an *in vitro* organ culture. SP4, iNKT and Tregs were sorted and added at a 3:1 ratio with digested 2-dGuo treated FTOC to create RTOCs with different conditions; empty, with total thymocytes added or with SP4, iNKT cells or Tregs added (Fig 3.10.A.). As expected from our previous analysis of 2-dGuo treated FTOC (Fig 7), when no cells were added there were no ICAM-1^{hi} VCAM-1^{hi} cells present highlighting the essential role for continued interactions with thymocyte populations (Fig 3.10.B.C.). Furthermore the addition of total thymocytes restored the ICAM-1^{hi} VCAM-1^{hi} population indicating that the thymic mesenchyme remains responsive to thymocytes

within the RTOC system (Fig 3.10.B.C.). Consistent with the potential redundancy between the T-cell populations highlighted by the knockout mice, just adding one of the sorted thymocyte populations to a RTOC was sufficient to support ICAM-1^{hi} VCAM-1^{hi} development (Fig 3.10.B.C.). Whilst all three populations were sufficient to drive some degree of ICAM-1^{hi} VCAM-1^{hi} development, it did appear that SP4 thymocytes were much better in their ability to induce ICAM-1^{hi} VCAM-1^{hi} development (Fig 3.10.B.C.).

Figure 3.8. αβ^{+} T-cells Are Essential For ICAM-1^{hi}VCAM-1^{hi} PDPN^{+} Thymic Mesenchyme Development

(A) Expression pattern of ICAM-1 and VCAM-1 on TER119^{-}CD45^{-}EpCAM-1^{-} PDPN^{+}CD31^{-} mesenchymal stroma isolated from control (*Tcra*$^{+/+}$, left) and TCRα-deficient (*Tcra*$^{-/-}$, right) mice where ICAM-1^{lo}VCAM-1^{lo}, ICAM-1^{int}VCAM-1^{int} and ICAM-1^{hi}VCAM-1^{hi} populations are gated.

(B) The cell number of total thymus was calculated from *Tcra*$^{+/+}$, (blue, n=10) and *Tcra*$^{-/-}$, (red n=10) mice.

(C) The cell number and percentages of ICAM-1^{lo}VCAM-1^{lo}, ICAM-1^{int}VCAM-1^{int} and ICAM-1^{hi}VCAM-1^{hi} PDPN^{+}CD31^{-} mesenchyme were calculated from *Tcra*$^{+/+}$, (blue, n=10) and *Tcra*$^{-/-}$, (red n=10) mice.

(D) Expression pattern of ICAM-1 and VCAM-1 on TER119^{-}CD45^{-}EpCAM-1^{-} PDPN^{+}CD31^{-} mesenchymal stroma isolated from control (*Class ii*$^{+/+}$, left) and MHC Class II-deficient (*Class ii*$^{-/-}$, right) mice where ICAM-1^{lo}VCAM-1^{lo}, ICAM-1^{int}VCAM-1^{int} and ICAM-1^{hi}VCAM-1^{hi} populations are gated.

(E) The cell number of total thymus was calculated from *Class ii* $^{+/+}$, (blue, n=5) and *Class ii* $^{-/-}$, (red n=5) mice.

(F) The cell number and percentages of ICAM-1^{lo}VCAM-1^{lo}, ICAM-1^{int}VCAM-1^{int} and ICAM-1^{hi}VCAM-1^{hi} PDPN^{+}CD31^{-} mesenchyme were calculated from *Class ii* $^{+/+}$, (blue, n=5) and *Class ii* $^{-/-}$, (red n=5) mice.

The standard error bars display SEM and a mann-whitney test was performed on statistics, where ** denotes p<0.01, *** denotes p<0.001 and **** denotes p<0.0001. All data is typical of three independent repeats.

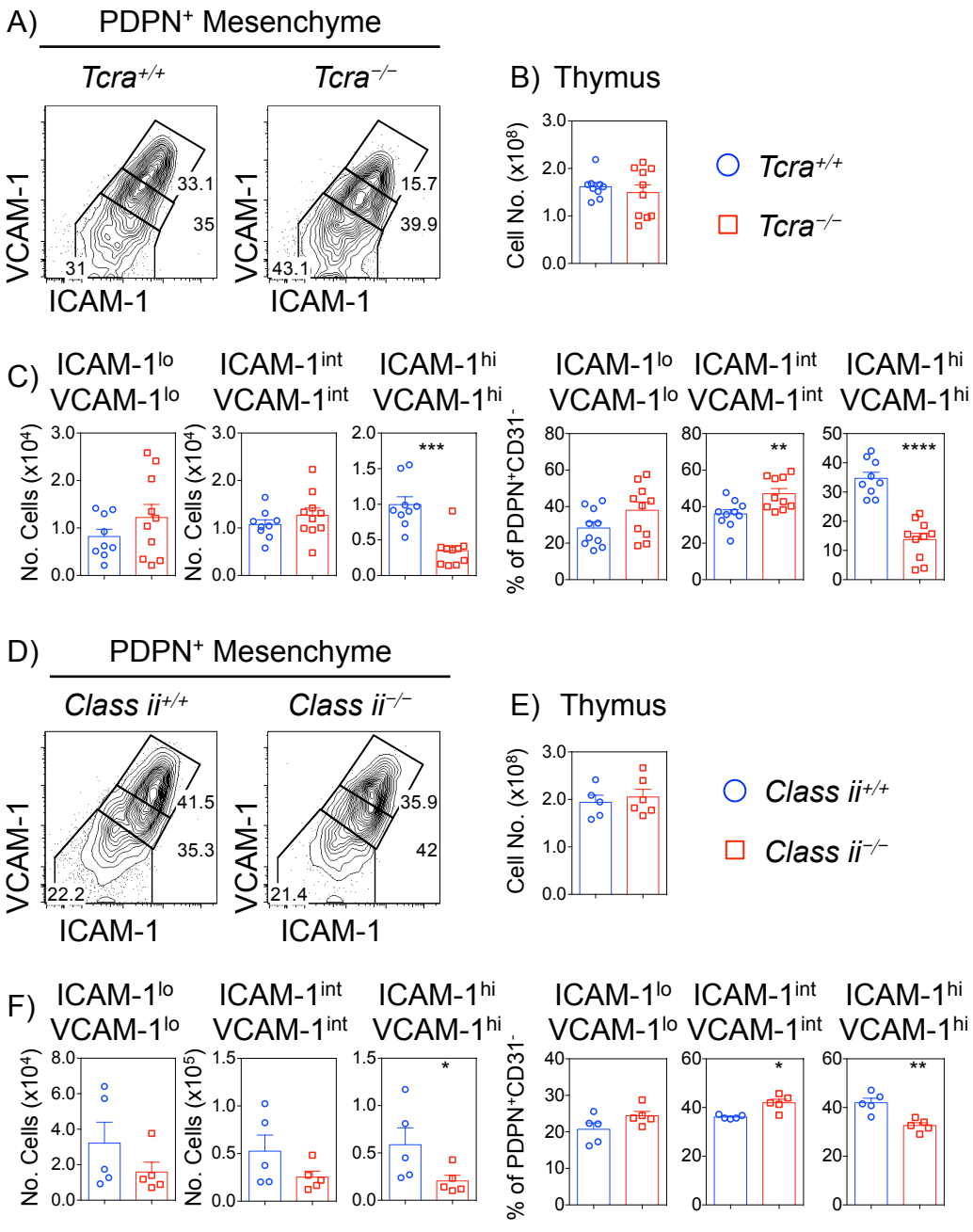
A)
PDPN+ Mesenchyme
Tcra+/+
Tcra−/−
VCAM-1
ICAM-1
33.1
35
31
15.7
39.9
43.1
B) Thymus
Cell No. (x10^8)
Tcra+/+
Tcra−/−
C)
ICAM-1lo VCAM-1lo
ICAM-1int VCAM-1int
ICAM-1hi VCAM-1hi
No. Cells (x10^4)
No. Cells (x10^4)
***
% of PDPN+CD31-
**
****
D)
PDPN+ Mesenchyme
Class ii+/+
Class ii−/−
41.5
35.3
22.2
35.9
42
21.4
E) Thymus
Cell No. (x10^8)
Class ii+/+
Class ii−/−
F)
ICAM-1lo VCAM-1lo
ICAM-1int VCAM-1int
ICAM-1hi VCAM-1hi
No. Cells (x10^4)
No. Cells (x10^5)
*
% of PDPN+CD31-
*
**

Figure 3.9. Deficiency In Foxp3^{+} Treg, But Not iNKT Cells, Impacts ICAM-1^{hi}VCAM-1^{hi} PDPN^{+} Thymic Mesenchyme

(A) Expression pattern of ICAM-1 and VCAM-1 on TER119^{-}CD45^{-}EpCAM-1^{-} PDPN^{+}CD31^{-} mesenchymal stroma isolated from control (*Cd1d*$^{+/+}$, left) and iNKT-deficient (*Cd1d*$^{-/-}$, right) mice where ICAM-1^{lo}VCAM-1^{lo}, ICAM-1^{int}VCAM-1^{int} and ICAM-1^{hi}VCAM-1^{hi} populations are gated.

(B) The cell number of total thymus, were calculated from *Cd1d*$^{+/+}$, (blue, n=8) and *Cd1d*$^{-/-}$, (red n=7) mice.

(C) The cell number and percentages of ICAM-1^{lo}VCAM-1^{lo}, ICAM-1^{int}VCAM-1^{int} and ICAM-1^{hi}VCAM-1^{hi} PDPN^{+} mesenchyme were calculated from *Cd1d*$^{+/+}$, (blue, n=8) and *Cd1d*$^{-/-}$, (red n=7) mice.

(D) Expression pattern of ICAM-1 and VCAM-1 on TER119^{-}CD45^{-}EpCAM-1^{-} PDPN^{+}CD31^{-} mesenchymal stroma isolated from control (*Foxp3*$^{+/+}$, left) and Foxp3^{+} Treg-deficient (*Foxp3*$^{-/-}$, right) mice where ICAM-1^{lo}VCAM-1^{lo}, ICAM-1^{int}VCAM-1^{int} and ICAM-1^{hi}VCAM-1^{hi} populations are gated.

(E) The percentages of ICAM-1^{lo}VCAM-1^{lo}, ICAM-1^{int}VCAM-1^{int} and ICAM-1^{hi}VCAM-1^{hi} PDPN^{+} mesenchyme were calculated from *Foxp3*$^{+/+}$, (blue, n=9) and *Foxp3*$^{-/-}$, (red n=15) mice.

The standard error bars display SEM and a mann-whitney test was performed, where * denotes a statistical difference as $p<0.05$. Data is typical of two independent repeats for *Cd1d*$^{-/-}$ data and three independent repeats for *Foxp3*$^{-/-}$ data.

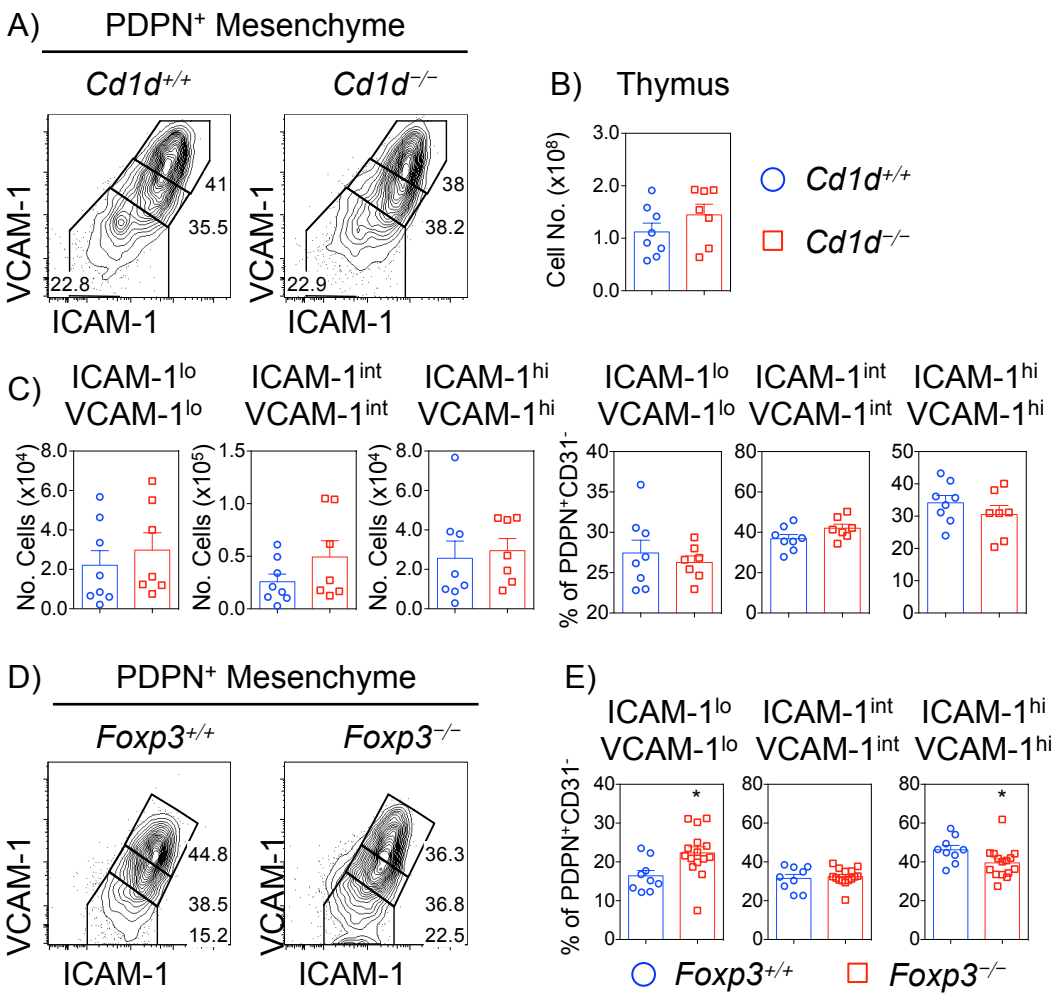
A)
PDPN+ Mesenchyme
Cd1d+/+
Cd1d−/−
VCAM-1
ICAM-1
41
35.5
22.8
38
38.2
22.9
B)
Thymus
Cell No. (x10^8)
Cd1d+/+
Cd1d−/−
C)
ICAM-1lo VCAM-1lo
ICAM-1int VCAM-1int
ICAM-1hi VCAM-1hi
No. Cells (x10^4)
No. Cells (x10^5)
% of PDPN+CD31-
D)
PDPN+ Mesenchyme
Foxp3+/+
Foxp3−/−
44.8
38.5
15.2
36.3
36.8
22.5
E)
Foxp3+/+
Foxp3−/−

Figure 3.10. Redundancy Among Thymocyte Populations Ensures The Development Of ICAM-1^{hi}VCAM-1^{hi} PDPN+ Thymic Mesenchyme

(A) Reaggregate thymic organ cultures (RTOCs) were created by mixing SP4, Treg and iNKT cells, isolated from adult B6 WT mice by highspeed cell sorting, at a 3:1 ratio with a cell suspension of E15 2-dGuo treated FTOC that had been digested and CD45$^+$ cell depleted. The RTOCs were cultured for 7 days and harvested for FACS analysis

(B) Expression pattern of ICAM-1 and VCAM-1 on TER119$^-$CD45$^-$EpCAM-1$^-$ PDPN$^+$CD31$^-$ mesenchymal stroma isolated from RTOCs made with the following conditions:

dGuo **Empty**

dGuo + unsorted thymocytes **+ Thymocytes** (red)

dGuo + CD4$^+$CD8$^-$TCRβ$^+$Tetramer$^-$Foxp3$^-$ **+SP4** (blue)

dGuo + CD4$^+$CD8$^-$TCRβ$^+$Tetramer$^-$Foxp3$^+$ **+Treg** (green)

dGuo + CD4$^+$CD8$^-$TCRβ$^+$Tetramer$^+$ **+iNKT** (purple)

(C) Percentages of ICAM-1^{hi}VCAM-1^{hi} PDPN$^+$ mesenchyme for each of the RTOC conditions.

The standard error bars display SEM and an one-way ANOVA was performed, where * denotes a statistical difference as $p<0.05$, ** denotes $p<0.01$ and *** denotes $p<0.001$. All data is typical of two independent repeats.

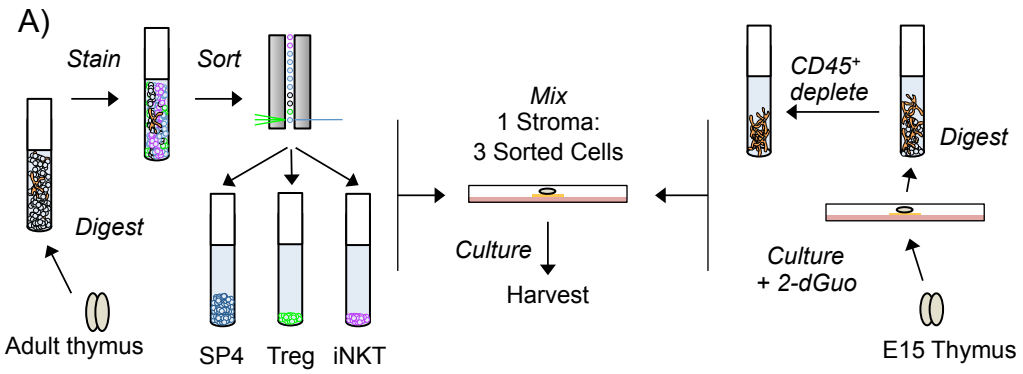
A)
Stain
Sort
Digest
Adult thymus
SP4
Treg
iNKT
Mix
1 Stroma:
3 Sorted Cells
Culture
Harvest
CD45+
deplete
Digest
Culture
+ 2-dGuo
E15 Thymus

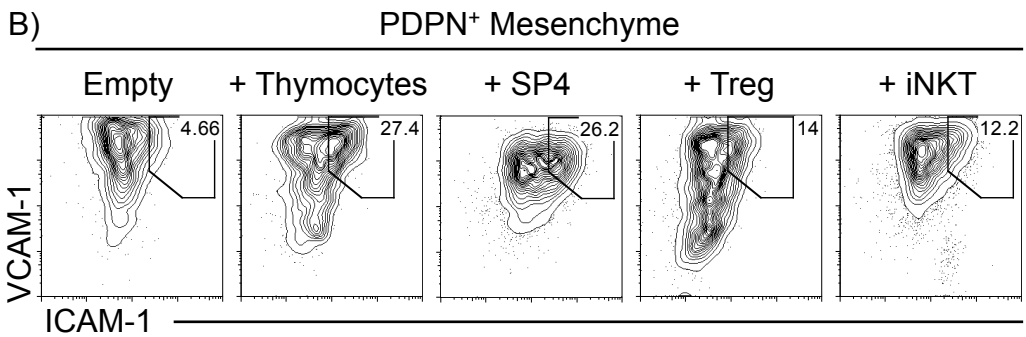
B)
PDPN+ Mesenchyme
Empty
+ Thymocytes
+ SP4
+ Treg
+ iNKT
4.66
27.4
26.2
14
12.2
VCAM-1
ICAM-1

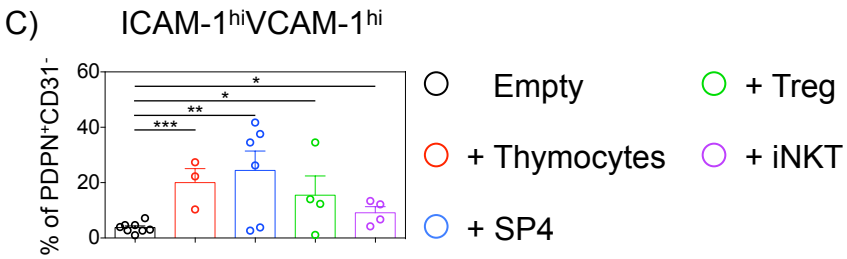
C)
ICAM-1hiVCAM-1hi
% of PDPN+CD31-
60
40
20
0
*
*
**
***
Empty
+ Thymocytes
+ SP4
+ Treg
+ iNKT

3.2.3 Thymocyte Mediated Conditioning Of ICAM-1^{hi}VCAM-1^{hi} Thymic Mesenchyme Occurs Through Signaling Via The Lymphotoxin Beta Receptor Pathway

After identifying thymocytes as a cellular regulator of ICAM-1^{hi}VCAM-1^{hi} mesenchyme conditioning we explored the molecular pathways that may be involved in this process. Members of the tumor necrosis factor receptor superfamily (TNFRSF) have been shown to play a key role in stromal development in both secondary lymphoid tissues as well as the thymus, two of which that are well defined and have been shown to be essential for stromal development are RANK (*Tnfrsf11a*) and lymphotoxin beta receptor (LTβR, *Tnfrsf3*) (149,151,152,161,230–232). To investigate whether these two molecular pathways were involved in the conditioning of ICAM-1^{hi}VCAM-1^{hi} mesenchyme, PCR analysis was carried out on sorted mTEC and PDPN^{+}CD31^{-} mesenchyme for gene expression of *Rank* and *Ltbr*. This analysis revealed that mesenchyme had a high level of gene expression of *Ltbr* but *Rank* was only detectable at very small levels suggesting that RANK signaling may not be involved in mesenchyme conditioning (Fig 3.11.A.). To confirm this, thymi were harvested from mice deficient for RANK (*Rank*$^{-/-}$) and cultured in FTOC conditions for 7-days before being digested for FACs analysis. This approach was taken because RANK is essential for bone development and *Rank*$^{-/-}$ mice have stunted growth of limbs and teeth resulting in a runted appearance and struggle to thrive and thus are culled before reaching adulthood (238). The total mesenchyme population was normal in *Rank*$^{-/-}$ thymi and the proportion and absolute number of ICAM-1^{hi}VCAM-1^{hi} mesenchyme was also normal (Fig 3.11.B.C.). Thus this data along with the PCR

analysis support that RANK signaling is not essential for the development of ICAM-1^{hi}VCAM-1^{hi} mesenchyme.

The PCR analysis also revealed that PDPN^{+}CD31^{-} thymic mesenchyme express high levels of *Ltbr*; to investigate whether LTβR is essential for the development of ICAM-1^{hi}VCAM-1^{hi} mesenchyme the same analysis was carried out on LTβR-deficient mice (*Ltbr*$^{-/-}$). Consistent with its role in secondary lymphoid tissue development there was a significant reduction in the total number of PDPN^{+} thymic mesenchyme (Fig 3.12.A.). This was associated with a massive loss of the number of ICAM-1^{hi}VCAM-1^{hi} cells but there was also a reduction of the ICAM-1^{int}VCAM-1^{int} populations, however percentages show that it is predominantly the ICAM-1^{hi}VCAM-1^{hi} being affected (Fig 3.12.C.D.).

Together the above data reveal an essential role for LTβR, but not RANK, signaling in the development of ICAM-1^{hi}VCAM-1^{hi} thymic mesenchyme and suggests that thymocyte-mesenchyme cross-talk could be occurring through this pathway. To investigate this further, SP4, SP8, iNKT and Tregs were sorted and PCR was carried out to determine the expression of the three known ligands of LTβR, LTα, LTβ and LIGHT (Fig 3.13.A.B). Consistent with previous reports all three ligands were present on all sorted thymocyte populations (Fig 3.13. C). Surprisingly *Lta* and *Light* were expressed at their highest on Treg and iNKT cells, respectively, however the analysis revealed that expression by the other populations was still high.

Figure 3.11. RANK Signaling Is Not Essential For ICAM-1^{hi}VCAM-1^{hi} PDPN^{+} Mesenchyme Development

(A) Quantitative real time PCR was performed on the following populations sorted from B6 WT mice:

TER119^{-}CD45^{-}EpCAM-1^{-}PDPN^{+} **thymic mesenchyme** (red)

CD45^{-}EpCAM-1^{-}UEA-1^{+} **mTEC** (blue)

Error bars indicate the SEM and mRNA levels were normalized to housekeeping gene β-actin. Data is from at least two independently sorted biological samples; with each gene analyzed a minimum of two times and each PCR ran in triplicates to obtain a SEM.

(B) Embryonic thymic lobes were harvested from E15 control (*Rank*$^{+/+}$, left) and RANK-deficient (*Rank*$^{-/-}$, right) mice and cultured in fetal thymic organ culture conditions for 7 days prior to harvesting for FACS analysis. Thymic mesenchyme was identified as TER119^{-}Viability^{-}CD45^{-}EpCAM-1^{-}PDPN^{+}CD31^{-} and the expression pattern of ICAM-1 and VCAM-1 was investigated, where ICAM-1^{hi}VCAM-1^{hi} population is gated.

(C) The percentages and cell number of total thymus, PDPN^{+}CD31^{-} mesenchyme and ICAM-1^{hi}VCAM-1^{hi} PDPN^{+} mesenchyme were calculated from *Rank*$^{+/+}$ (blue, n=7) and *Rank*$^{-/-}$ (red n=9) mice. The standard error bars display SEM and a mann-whitney test was performed. All data is typical of two independent repeats.

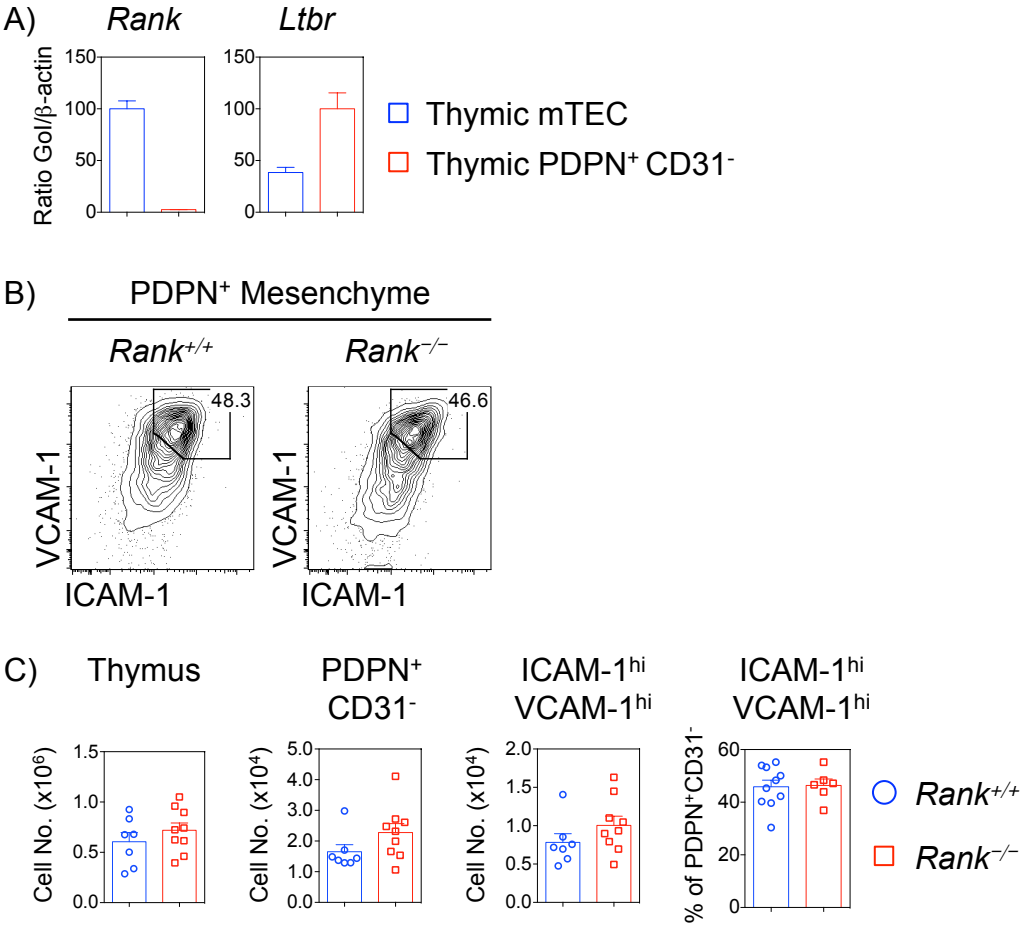
A)
Rank
Ltbr
Ratio Gol/β-actin
150
100
50
0
Thymic mTEC
Thymic PDPN+ CD31-
B)
PDPN+ Mesenchyme
Rank+/+
Rank−/−
48.3
46.6
VCAM-1
ICAM-1
C)
Thymus
PDPN+ CD31-
ICAM-1hi VCAM-1hi
ICAM-1hi VCAM-1hi
Cell No. (x10^6)
Cell No. (x10^4)
% of PDPN+CD31-
Rank+/+
Rank−/−

Figure 3.12. LTβR Signaling Is Essential For ICAM-1^{hi}VCAM-1^{hi} PDPN^{+} Mesenchyme Development

(A) Expression pattern of PDPN and CD31 on non-epithelial stroma, identified as TER119^{-}Viability^{-}CD45^{-}EpCAM-1^{-}, isolated from control (*Ltbr*$^{+/+}$, left) and LTβR-deficient (*Ltbr*$^{-/-}$, right) mice where PDPN^{+}CD31^{-} thymic mesenchyme cells are gated.

(B) Expression pattern of ICAM-1 and VCAM-1 on PDPN^{+}CD31^{-} mesenchymal stroma isolated from control (*Ltbr*$^{+/+}$, left) and LTβR-deficient (*Ltbr*$^{-/-}$, right) mice where ICAM-1^{lo}VCAM-1^{lo}, ICAM-1^{int}VCAM-1^{int} and ICAM-1^{hi}VCAM-1^{hi} populations are gated.

(C) The cell number of total thymus, PDPN^{+}CD31^{-} mesenchyme and ICAM-1^{lo}VCAM-1^{lo}, ICAM-1^{int}VCAM-1^{int} and ICAM-1^{hi}VCAM-1^{hi} PDPN^{+} mesenchyme were calculated from *Ltbr*$^{+/+}$, (blue, n=6) and *Ltbr*$^{-/-}$, (red, n=6) mice.

(D) The percentages of ICAM-1^{lo}VCAM-1^{lo}, ICAM-1^{int}VCAM-1^{int} and ICAM-1^{hi}VCAM-1^{hi} PDPN^{+} mesenchyme were calculated from *Ltbr*$^{+/+}$, (blue, n=6) and *Ltbr*$^{-/-}$, (red, n=6) mice.

The standard error bars display SEM and a mann-whitney test was performed, where * denotes a statistical difference as $p<0.05$ and ** $p<0.01$. All data is typical of two independent repeats.

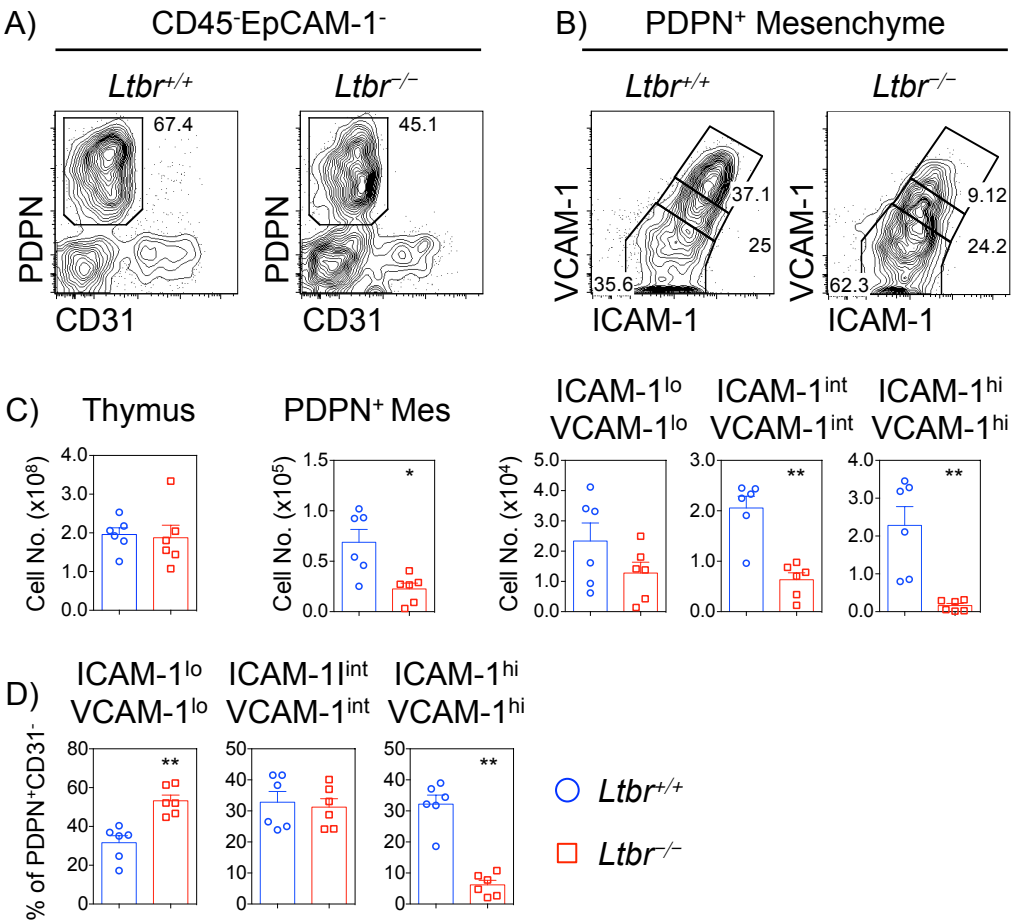
A)
CD45-EpCAM-1-
Ltbr+/+
Ltbr−/−
67.4
45.1
PDPN
CD31
B)
PDPN+ Mesenchyme
37.1
25
35.6
9.12
24.2
62.3
VCAM-1
ICAM-1
C)
Thymus
PDPN+ Mes
ICAM-1lo VCAM-1lo
ICAM-1int VCAM-1int
ICAM-1hi VCAM-1hi
Cell No. (x10^8)
Cell No. (x10^5)
Cell No. (x10^4)
D)
% of PDPN+CD31-
Ltbr+/+
Ltbr−/−

Figure 3.13. Genotypic Analysis Of Lymphotoxin Beta Receptor Ligand Expression On Sorted Thymocyte Populations

(A) Pre sort purity check of stained thymocytes from adult B6 WT mice.

(B) Post sort purity check of thymocytes populations sorted from adult B6 WT mice.

(C) Quantitative real time PCR was performed on the following populations sorted from B6 WT mice:

$CD4^+CD8^-TCR\beta^+$mCD1d PBS-57 $Tetramer^-Foxp3^-$ **cSP4 thymocytes** (red)

$CD4^-CD8^+TCR\beta^+$ **SP8 thymocytes** (blue)

$CD4^+CD8^-TCR\beta^+$mCD1d PBS-57 $Tetramer^-Foxp3^+$ **$Foxp3^+$ Treg** (green)

$CD4^+CD8^-TCR\beta^+$mCD1d PBS-57 $Tetramer^+$ **iNKT cells** (orange)

Error bars indicate the SEM and mRNA levels were normalized to housekeeping gene β-actin. Data is from at least two independently sorted biological samples; with each gene analyzed a minimum of two times and each PCR ran in triplicates to obtain a SEM.

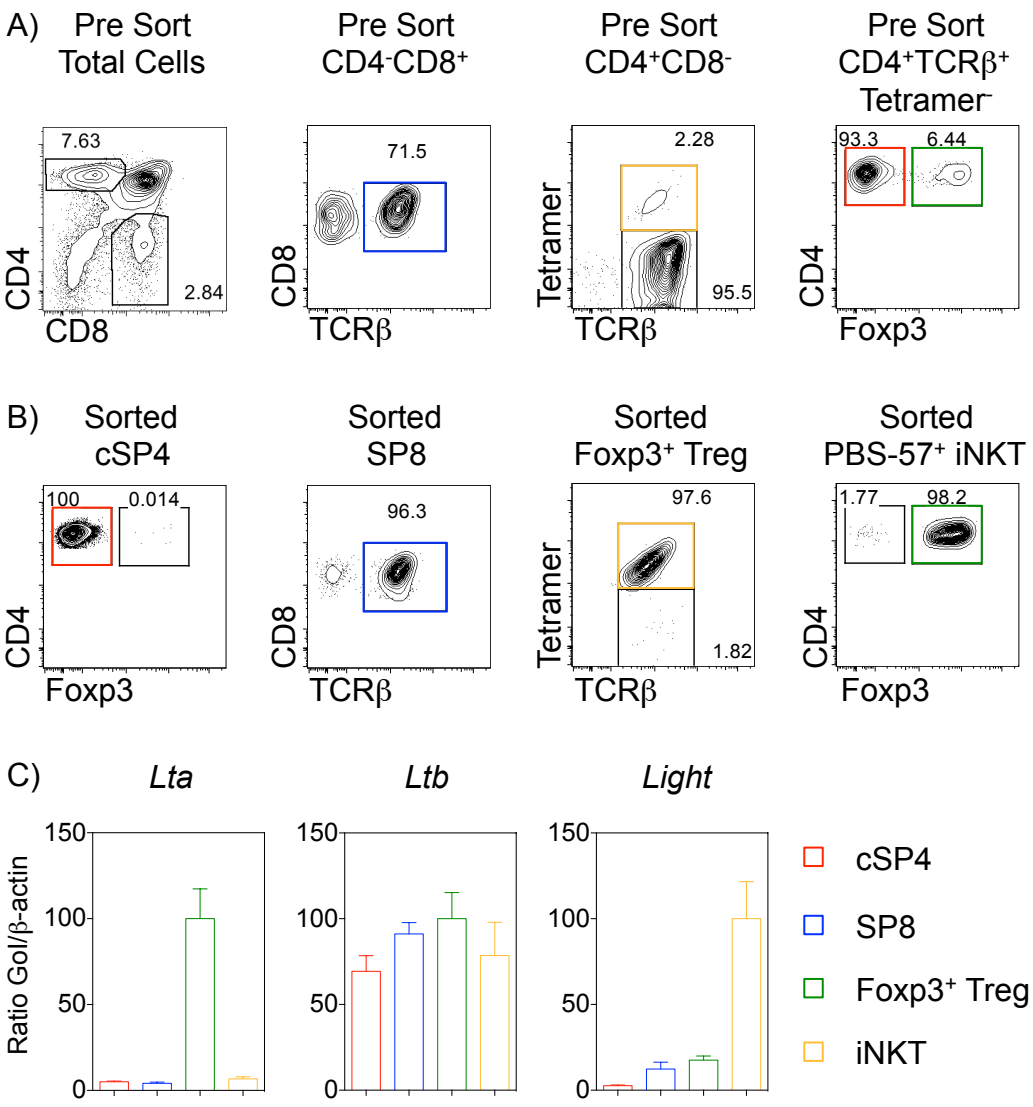
A)
Pre Sort
Total Cells
Pre Sort
CD4-CD8+
Pre Sort
CD4+CD8-
Pre Sort
CD4+TCRβ+
Tetramer-
7.63
2.84
CD4
CD8
71.5
CD8
TCRβ
2.28
95.5
Tetramer
TCRβ
93.3
6.44
CD4
Foxp3
B)
Sorted
cSP4
Sorted
SP8
Sorted
Foxp3+ Treg
Sorted
PBS-57+ iNKT
100
0.014
CD4
Foxp3
96.3
CD8
TCRβ
97.6
1.82
Tetramer
TCRβ
1.77
98.2
CD4
Foxp3
C)
Lta
Ltb
Light
Ratio GoI/β-actin
150
100
50
0
cSP4
SP8
Foxp3+ Treg
iNKT

To further investigate the role of LTβR ligands in ICAM-1^{hi}VCAM-1^{hi} development thymi were harvested from LTα-deficient mice (*Lta*$^{-/-}$). Deletion of *Lta* prevents the formation of the heterodimer and homotrimer forms of the LTβR ligands $LT\alpha_1\beta_2$ and $LT\alpha_3$. Unlike *Ltbr*$^{-/-}$ mice, there was no alteration to the total PDPN$^+$ mesenchyme population in *Lta*$^{-/-}$ mice, which would be consistent with the overall less severe phenotype of *Lta*$^{-/-}$ mice, compared to *Ltbr*$^{-/-}$ mice (Fig 3.14.A.D.) (237). Within the PDPN$^+$ mesenchyme compartment there was a significant, but not complete, reduction in percentage and cell number of the ICAM-1^{hi}VCAM-1^{hi} population (Fig 3.14.B-D.). Additionally there was a significant increase in the number and percentage of the ICAM-1^{lo}VCAM-1^{lo} population as well as the percentage of the ICAM-1^{int}VCAM-1^{int} suggesting the PDPN$^+$ mesenchyme is halted at the earlier development stages (Fig 3.14.B-D.). This data reveals that preventing signaling between LTβR on stroma and $LT\alpha_3$/$LT\alpha_1\beta_2$ on thymocytes inhibits the complete development of ICAM-1^{hi}VCAM-1^{hi} PDPN$^+$ mesenchyme, however signaling via LTβR-LIGHT may compensate for $LT\alpha_3$ and $LT\alpha_1\beta_2$ for the development of the PDPN$^+$ population as a whole.

In the previous analysis we have shown that thymocyte:mesenchyme interactions are essential for the development of ICAM-1^{hi}VCAM-1^{hi} PDPN$^+$ mesenchyme and using the RTOC system we have shown that single thymocyte populations that express LTβR ligands are sufficient for this development. To further understand the role of LTβR in this process we investigated whether stimulation of LTβR in the absence of thymocytes is sufficient to drive the development of ICAM-1^{hi}VCAM-1^{hi} PDPN$^+$ mesenchyme. To achieve this, 2-dGuo-treated FTOC were stimulated *in vitro* with an

Figure 3.14. LTα Expression On Thymocytes Is Essential For ICAM-1^{hi}VCAM-1^{hi} PDPN^{+} Mesenchyme Development

(A) Expression pattern of PDPN and CD31 on non-epithelial stroma, identified as TER119^{-} CD45^{-}EpCAM-1^{-}, isolated from control (*Lta*$^{+/+}$, left) and LTα-deficient (*Lta*$^{-/-}$, right) mice where PDPN^{+}CD31^{-} thymic mesenchyme cells are gated.

(B) Expression pattern of ICAM-1 and VCAM-1 on PDPN^{+}CD31^{-} mesenchymal stroma isolated from control (*Lta*$^{+/+}$, left) and LTα -deficient (*Lta*$^{-/-}$, right) mice where ICAM-1^{lo}VCAM-1^{lo}, ICAM-1^{int}VCAM-1^{int} and ICAM-1^{hi}VCAM-1^{hi} populations are gated.

(C) The cell number of total thymus, PDPN^{+}CD31^{-} mesenchyme and ICAM-1^{lo}VCAM-1^{lo}, ICAM-1^{int}VCAM-1^{int} and ICAM-1^{hi}VCAM-1^{hi} PDPN^{+} mesenchyme were calculated from *Lta*$^{+/+}$, (blue, n=6) and *Lta*$^{-/-}$, (red n=6) mice.

(D) The percentages of ICAM-1^{lo}VCAM-1^{lo}, ICAM-1^{int}VCAM-1^{int} and ICAM-1^{hi}VCAM-1^{hi} PDPN^{+} mesenchyme were calculated from *Lta*$^{+/+}$, (blue, n=6) and *Lta*$^{-/-}$, (red n=6) mice.

The standard error bars display SEM and a mann-whitney test was performed, where * denotes a statistical difference as $p<0.05$ and ** $p<0.01$. All data is typical of three independent repeats.

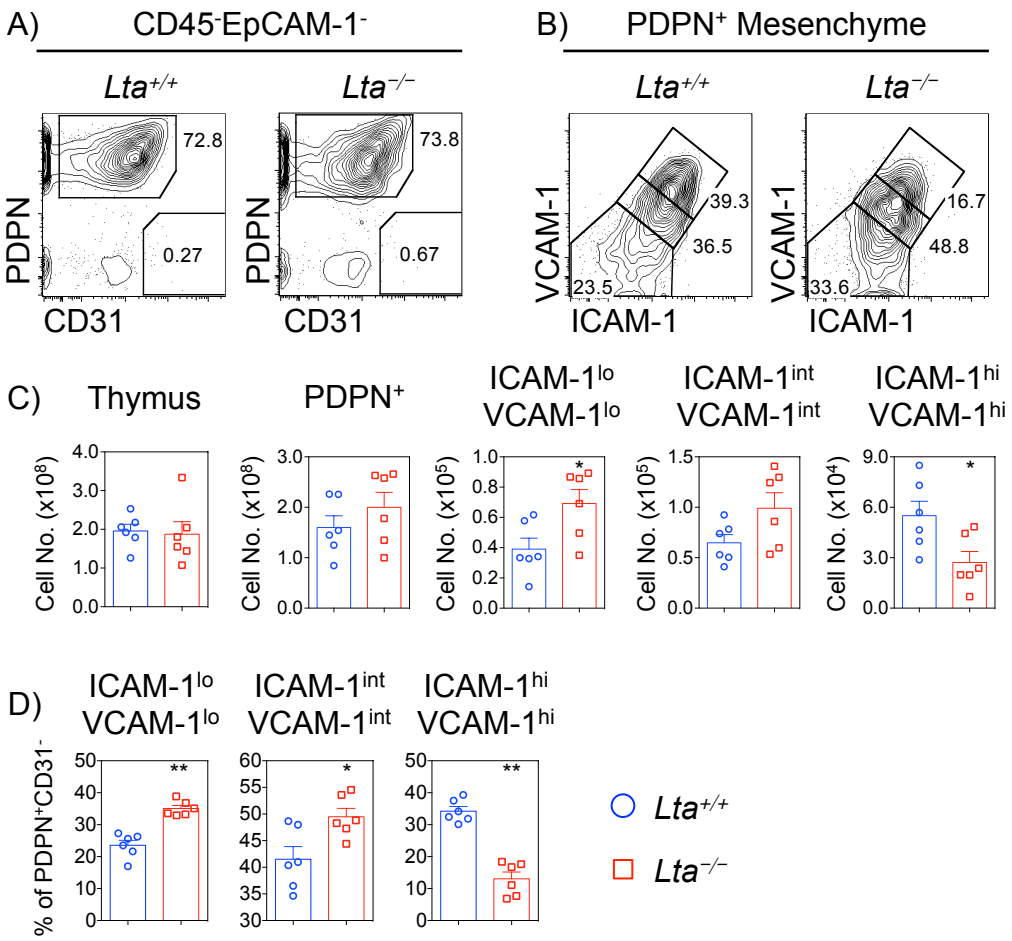
A)
CD45-EpCAM-1-
Lta+/+
Lta−/−
PDPN
CD31
72.8
0.27
73.8
0.67
B)
PDPN+ Mesenchyme
VCAM-1
ICAM-1
39.3
36.5
23.5
16.7
48.8
33.6
C)
Thymus
PDPN+
ICAM-1lo VCAM-1lo
ICAM-1int VCAM-1int
ICAM-1hi VCAM-1hi
Cell No. (x10^8)
Cell No. (x10^5)
Cell No. (x10^4)
D)
% of PDPN+CD31-
Lta+/+
Lta−/−

agonistic anti-LTβR antibody. This stimulation caused a complete restoration of the ICAM-1^{hi}VCAM-1^{hi} population, both absolute numbers and proportions, within the 2-dGuo culture treated with the anti-LTβR antibody (Fig 3.15.A.B.). Interestingly the total number of PDPN^{+} thymic mesenchyme was increased in the stimulated cultures further highlighting a key role for LTβR in the development of the PDPN^{+} mesenchyme as a whole (Fig 3.15.B.). As an *in vivo* test of this hypothesis, *Tcra*$^{-/-}$ mice were stimulated with the same agonistic anti-LTβR antibody injected intraperitoneally for 3 consecutive days. Due to reagent and mouse availability this experiment could only be performed once, however the preliminary results suggest a restoration of the ICAM-1^{hi}VCAM-1^{hi} PDPN^{+} mesenchyme in the stimulated *Tcra*$^{-/-}$ mouse compared to un-stimulated *Tcra*$^{-/-}$ shown by the percentage of ICAM-1^{hi}VCAM-1^{hi} and MFI increase of ICAM-1 and VCAM-1 (Fig 3.15.C-E.). This data suggests that not only is LTβR signaling necessary for the development of ICAM-1^{hi}VCAM-1^{hi} thymic mesenchyme but is also sufficient to support their development.

Following on from these experiments we investigated whether continuous LTβR signaling was required to maintain the ICAM-1^{hi}VCAM-1^{hi} thymic mesenchyme. To do this, a similar *in vivo* stimulation was carried out in the context of thymic recovery in WT mice that had received congenically marked WT bone marrow following lethal total body irradiation (TBI). This experiment was carried out to introduce a period of time where thymocytes were absent within the thymus, which would occur in the initial stages of thymic recovery following TBI and bone marrow reconstitution. Within this experiment mice received two doses of 500 rad irradiation and were subsequently given WT bone marrow and then injected with an isotype or agonistic

Figure 3.15. Stimulation Of LTβR Is Sufficient For ICAM-1^{hi}VCAM-1^{hi} Thymic Mesenchyme Development

(A) 2-dGuo-treated FTOC were cultured in the presence or absence of an agonistic anti-LTβR antibody for 7 days and then harvested for FACS analysis. FACS plots show the expression pattern of ICAM-1 and VCAM-1 on TER119^{-}Viability^{-}CD45^{-} EpCAM-1^{-}PDPN^{+}CD31^{-} thymic mesenchyme where the ICAM-1^{hi}VCAM-1^{hi} population is gated.

(B) The cell number of total thymus, PDPN^{+}CD31^{-} mesenchyme and ICAM-1^{hi}VCAM-1^{hi} PDPN^{+} mesenchyme were calculated, as well as the percentage of ICAM-1^{hi}VCAM-1^{hi}, for + PBS (blue n=7) or + anti LTβR (red n=6).

(C) Adult *Tcra*$^{-/-}$ were injected IP with isotype (left) or 100μg of agonistic anti-LTβR antibody (right) everyday for three days and then harvested for FACS analysis on the fourth day. FACS plots show the expression pattern of PDPN and CD31 on TER119^{-} Viability^{-}CD45^{-}EpCAM^{-} cells for each condition.

(D) Expression pattern of ICAM-1 and VCAM-1 on PDPN^{+}CD31^{-} thymic mesenchyme for *Tcra*$^{-/-}$ with isotype (left) and *Tcra*$^{-/-}$ with anti LTβR (right).

(E) Cell number of total thymus was calculated for *Tcra*$^{-/-}$ with isotype (blue n=3) and *Tcra*$^{-/-}$ with anti LTβR (red n=3).

(F) The percentages of ICAM-1^{hi}VCAM-1^{hi} PDPN^{+} mesenchyme was calculated for *Tcra*$^{-/-}$ with isotype (blue n=3) and *Tcra*$^{-/-}$ with anti LTβR (red n=3).

G) The MFI of ICAM-1 and VCAM-1 on PDPN^{+}CD31^{-} mesenchyme *Tcra*$^{-/-}$ with isotype (blue n=3) and *Tcra*$^{-/-}$ with anti LTβR (red n=3).

The standard error bars display SEM and a mann-whitney test was performed in A&B and an unpaired parametric T-test in C-G. * denotes a statistical difference as $p<0.05$ and ** $p<0.01$. Data is typical of two independent repeats for A&B and only one experiment for C-G.

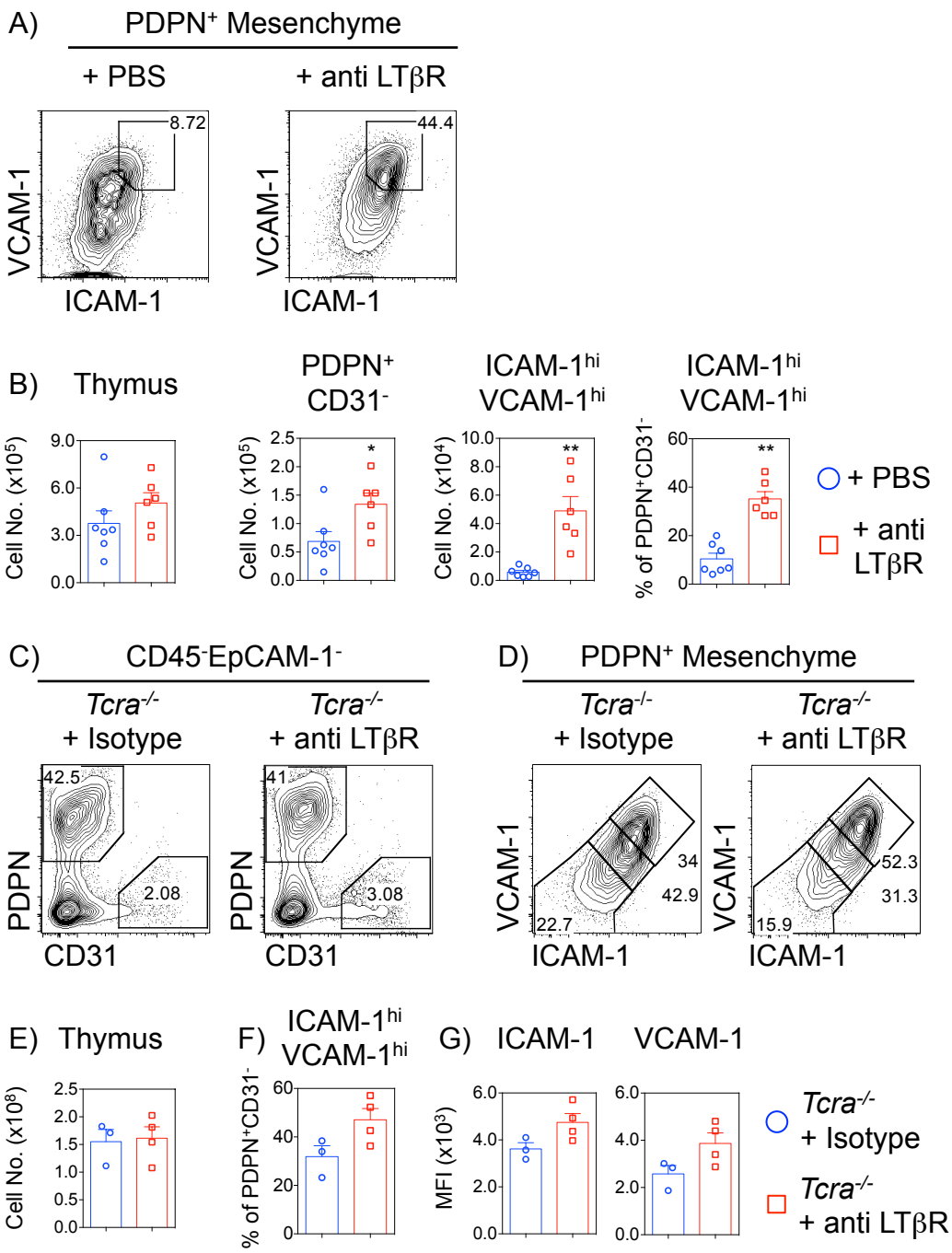
A)
PDPN+ Mesenchyme
+ PBS
+ anti LTβR
8.72
44.4
VCAM-1
ICAM-1
B)
Thymus
PDPN+ CD31-
ICAM-1hi VCAM-1hi
ICAM-1hi VCAM-1hi
Cell No. (x10^5)
Cell No. (x10^4)
% of PDPN+CD31-
+ PBS
+ anti LTβR
C)
CD45-EpCAM-1-
Tcra-/-
+ Isotype
+ anti LTβR
42.5
2.08
41
3.08
PDPN
CD31
D)
PDPN+ Mesenchyme
34
42.9
22.7
52.3
31.3
15.9
E)
Thymus
F)
ICAM-1hi VCAM-1hi
G)
ICAM-1
VCAM-1
MFI (x10^3)
Tcra-/-
+ Isotype
+ anti LTβR

Figure 3.16. *In vivo* Stimulation Of LTβR During Bone Marrow Chimera Boosts ICAM-1 and VCAM-1 Expression

(A) Bone marrow chimeras were generated by giving adult, $CD45.2^+$, B6 WT mice two 500 rad doses of irradiation and reconstituting these mice with $CD45.1^+$ BoyJ WT bone marrow. These mice were subsequently IP injected with 100μg of isotype or agonistic anti-LTβR on days 1, 3, 5, 7 and 9 post-bone marrow transfer and harvested on D10 post- transfer for FACS analysis.

(B) Expression pattern of ICAM-1 and VCAM-1 on $TER119^-Viability^-CD45^-EpCAM\text{-}1^-PDPN^+CD31^-$ thymic mesenchyme of isotype (left) and with anti-LTβR (right) treated mice.

(C) Cell number of total thymus and $PDPN^+$ thymic mesenchyme was calculated for isotype (blue n=7) and anti-LTβR treated (red n=5) mice.

(D) Cell number and percentages of $ICAM\text{-}1^{lo}VCAM\text{-}1^{lo}$, $ICAM\text{-}1^{int}VCAM\text{-}1^{int}$ and $ICAM\text{-}1^{hi}VCAM\text{-}1^{hi}$ $PDPN^+$ mesenchyme was calculated for isotype (blue n=7) and anti-LTβR treated (red n=5).

E) The MFI of ICAM-1 and VCAM-1 on $PDPN^+CD31^-$ mesenchyme of isotype (blue n=7) and anti-LTβR treated (red n=5) mice.

The standard error bars display SEM and a mann-whitney test was performed, where * denotes a statistical significance as $p<0.05$ and ** as $p<0.01$. All data is typical of 2 independent repeats.

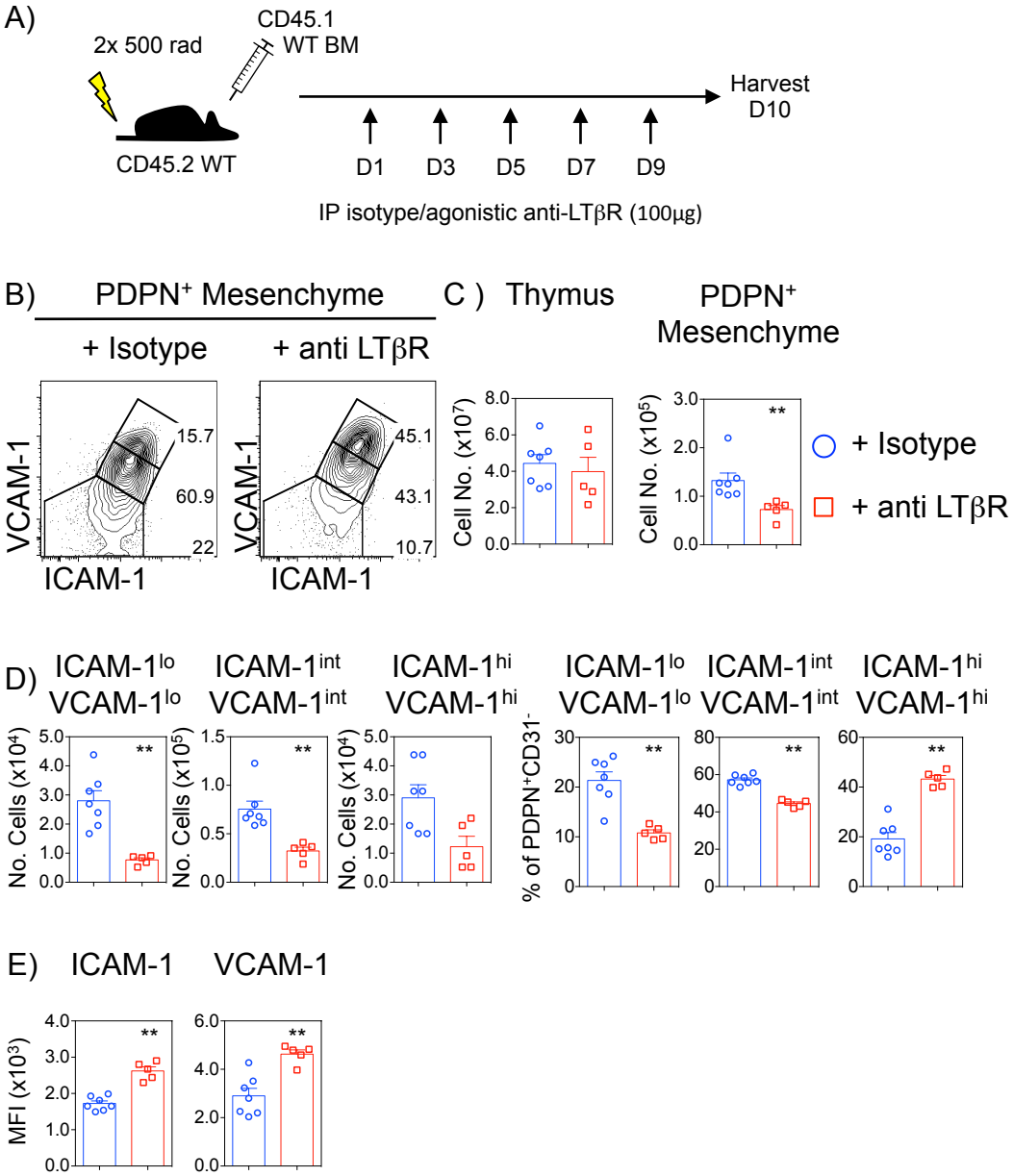
A)
2x 500 rad
CD45.1
WT BM
CD45.2 WT
Harvest
D10
D1
D3
D5
D7
D9
IP isotype/agonistic anti-LTβR (100μg)
B)
PDPN+ Mesenchyme
+ Isotype
+ anti LTβR
VCAM-1
ICAM-1
15.7
60.9
22
45.1
43.1
10.7
C)
Thymus
PDPN+ Mesenchyme
Cell No. (x10^7)
Cell No. (x10^5)
**
+ Isotype
+ anti LTβR
D)
ICAM-1lo VCAM-1lo
ICAM-1int VCAM-1int
ICAM-1hi VCAM-1hi
No. Cells (x10^4)
No. Cells (x10^5)
No. Cells (x10^4)
% of PDPN+CD31-
E)
ICAM-1
VCAM-1
MFI (x10^3)

anti-LTβR antibody every-other day for 10 days (Fig 3.16.A.). Interestingly the mice that received isotype has a much lower population of ICAM-1^{hi}VCAM-1^{hi} thymic mesenchyme compared to the anti-LTβR stimulated mice and had much lower expression of ICAM-1 and VCAM-1 (Fig 16.B-E.). Surprisingly the total population of $PDPN^{+}$ thymic mesenchyme was reduced in the mice receiving the anti-LTβR antibody as well as the percentage and cell number of ICAM-1^{lo}VCAM-1^{lo} and ICAM-1^{int}VCAM-1^{int} thymic mesenchyme (Fig 3.16.D.).

Together these experiments reveal that stimulation of LTβR in the absence of thymocytes is sufficient for the development of ICAM-1^{hi}VCAM-1^{hi} $PDPN^{+}$ thymic mesenchyme. Additionally, not only does anti-LTβR stimulation support ICAM-1^{hi}VCAM-1^{hi} development when thymocytes are missing but it can also boost ICAM-1^{hi}VCAM-1^{hi} development during thymic recovery following TBI and bone marrow grafting.

3.3 DISCUSSION

This chapter aimed to further identify and characterize the non-epithelial stroma populations within the thymus as well as understand pathways involved in their development.

We were able to identify $TER119^{-}CD45^{-}EpCAM\text{-}1^{-}$ stromal cells that could be separated into $PDPN^{+}CD31^{-}$ mesenchyme and $PDPN^{-}CD31^{+}$ endothelium similarly to fibroblastic reticular cells (FRCs) and blood endothelial cells (BECs) of peripheral lymphoid tissues (220). This approach of identifying thymic endothelium and mesenchyme using gp38 and CD31 together for FACS analysis has previously been

used in a study to identify lymphatic endothelial cells (LECs) in the thymus (111). This study identified $PDPN^{+}CD31^{-}$ mesenchyme and $PDPN^{-}CD31^{+}$ endothelium within the thymus but did not further characterize either population. The presence of lymphatic endothelium within the thymus has previously been controversial, the findings of Zacharia *et. al* revealed inconclusive evidence of lymphatic endothelium within the thymus using a $LYVE\text{-}1^{cre}xRosa26^{eYFP}$ fate-mapper mouse model, where LYVE-1 is expressed by lymphatic endothelial cells (111). Our analysis revealed no detectable $PDPN^{+}CD31^{+}$ lymphatic endothelial population within the adult thymus supporting against a lymphatic endothelial population within the thymus. Additional studies have identified thymic mesenchyme using alternative markers to gp38 and CD31 used in our study. Recently a study was published investigating thymic mesenchymal cells and comparing their transcriptional and cell surface protein expression to bone and skin mesenchymal cells (255). The comparative analysis carried out by Patenaude *et. al* provided some insights into a population of thymic mesenchyme defined as lineage $cocktail^{-}Sca\text{-}1^{+}$ cells (255). The analysis of the Lin^{-} $Sca\text{-}1^{+}$ thymic mesenchyme population revealed that 98% ± 2% expressed PDPN, which would suggest this is the same population of thymic mesenchyme identified in our study. Our cell surface phenotypic analysis was consistent with the findings of Patenaude *et. al,* revealing $PDPN^{+}$ thymic mesenchyme expresses the platelet-derived growth factor receptors (PDGFR) α and β. During fetal stages, $PDGFR\alpha^{+}$ mesenchyme have been shown to play a key role in supporting TEC proliferation by the production of fibroblast growth factor 10 (FGF10), our data provide evidence that this population of $PDGFR\alpha^{+}$ cells are persisting into the adult thymus (202). This is also consistent with our PCR analysis, which revealed *Fgf10* expression is

maintained in PDPN$^+$ thymic mesenchyme. The persistence of this population could suggest that PDPN$^+$ thymic mesenchyme is supporting not only the initial development of TEC, but also the maintenance of the TEC compartment. If this hypothesis is correct this could highlight a key role for thymic mesenchyme in regulating TEC within the adult thymus in the steady state and may even implicate a role for mesenchyme-dependent maintenance of TEC in the context of acute or age-associated atrophy and could therefore represent a target in the attempts to reverse these. PDGFRβ is a marker often used to identify thymic pericytes, which are mesenchymal cells that are situated around blood vessels (perivascular) and support the blood vessel structure as well as regulating the exit of egress-competent mature thymocytes through the production of the enzymes SPHK1 and SPHK2 (111,216). The expression of PDGFRβ by PDPN$^+$ thymic mesenchyme is consistent with the perivascular positioning of PDPN$^+$ thymic mesenchyme surrounding CD31$^+$ endothelial cells shown by confocal microscopy. However further analysis of pericyte-associated markers such as NG2 and desmin would be required to definitively identify this population as pericytes (213). Our analysis also identified Ly-51 expression on the thymic mesenchyme. Ly-51 expression has previously been used as a marker to identify what were previously termed cortical mesenchyme based on Ly-51 being a cTEC associated marker and the Ly-51-expressing thymic mesenchyme located within the cortex, before they were later reclassified as thymic NC-derived mesenchyme (NC-Mes) (217,250). These NC-derived mesenchymal cells represent pericytes surrounding the endothelial layer of the vasculature and also express PDGFRβ, phenocopying the PDPN$^+$ thymic mesenchyme identified in our study. Interestingly, the NC-Mes identified in the 2008 study by Muller *et. al*

reportedly did not express PDGFRα, suggesting that PDPN^{+} thymic mesenchyme may incorporate separate PDGFRα and PDGFRβ expressing cells (250). This hypothesis is supported by our confocal analysis which revealed that PDPN^{+} thymic mesenchyme cells were located around CD31^{+} endothelial cells, but also at the capsule of the thymus and within the medulla, where the expression of PDPN was present on both TR5^{+} mTEC but importantly non-epithelial mesenchymal cells.

Our analysis revealed that PDPN^{+} thymic mesenchyme express the adhesion molecules ICAM-1 and VCAM-1. This is consistent with a previous study that identified heterogeneous levels of ICAM-1 and VCAM-1 expression on CD31^{-} PDGFRβ^{+} thymic mesenchyme (211). The expression pattern of ICAM-1 and VCAM-1 on thymic mesenchyme is similar to that of LN FRC. During LN FRC development different populations of ICAM-1/VCAM-1 expressing cells can be identified based on their developmental progression from ICAM-1^{lo}VCAM-1^{lo} to ICAM-1^{int}VCAM-1^{int} and then mature ICAM-1^{hi}VCAM-1^{hi} (232). Through analysis of the expression of ICAM and VCAM on PDPN^{+} mesenchyme during different developmental stages we found that ICAM-1^{hi}VCAM-1^{hi} cells were not present until after birth. This data suggests a development transition from ICAM-1^{lo}VCAM-1^{lo} to ICAM-1^{hi}VCAM-1^{hi} however it does not directly demonstrate this. An experiment to definitively prove this hypothesis would be to sort fluorescently labeled ICAM-1^{lo}VCAM-1^{lo} thymic mesenchyme and introduce them into an RTOC and then look for the presence of ICAM-1^{hi}VCAM-1^{hi} thymic mesenchyme. This would provide evidence for direct precursor-product relationship between the two populations and reveal whether the ICAM-1^{lo}VCAM-1^{lo} thymic mesenchyme are an immature population that give rise to ICAM-1^{hi}VCAM-1^{hi}

mesenchymal cells. Preliminary experiments of this design were carried out to address this hypothesis however technical limitations precluded accurate analysis.

Our analysis of 2-dGuo-treated FTOC, as well as *Tcra*$^{-/-}$ mouse models, revealed that the development of ICAM-1^{hi}VCAM-1^{hi} thymic mesenchyme was dependent on thymocyte:mesenchyme interactions, as absence of these interactions resulted in a loss of ICAM-1^{hi}VCAM-1^{hi} and suggested a potential block at the ICAM-1^{int}VCAM-1^{int} stage. This mirrors the block in development seen in lymph node stromal cells of *Ltbr*$^{-/-}$ mice, where the deletion of LTβR prevents the interaction of LT$\alpha_1\beta_2$ expressing lymphoid tissue inducer (LTi) cells with ICAM-1^{int}VCAM-1^{int} stroma, which is required for the development of ICAM-1^{hi}VCAM-1^{hi} mature LN stromal cells (232). It has been shown that there is an essential requirement of thymocyte crosstalk with thymic epithelial cells for TEC development within the thymus, with one study showing that specific loss of αβ thymocytes in *Tcra*$^{-/-}$ mice have a significant loss of medulla (142). Our analyses reveal an essential requirement for thymocyte interactions with thymic mesenchyme highlighting a novel cellular regulatory mechanism in the development of thymic mesenchyme.

Lymphocyte mediated development of both lymph node stroma and thymic stroma has been shown to occur through signaling of a number of TNFRSF members. Within the thymus, RANK signaling, through provision of RANKL by intrathymic CD4$^+$CD3$^-$ inducer cells, is required for the development of Aire$^+$ mTEC (152). Additionally, RANK signaling is essential for LN development (238). LTβR signaling is also required for stromal development as LTβR-deficient mice have defective medullary

organization and mTEC development (151). Previous studies have shown that both germ line deletion or the specific deletion of LTβR on FRCs, through the use of *Ccl19*^{cre}*Ltbr*$^{fl/fl}$ mice, both result in a complete loss of ICAM-1^{hi}VCAM-1^{hi} cells on lymph node stroma (232,233). Interestingly we found no requirement for RANK signaling but an essential requirement for LTβR signaling for the development of ICAM-1^{hi}VCAM-1^{hi} thymic mesenchyme, consistent with LTβR's role in LN stroma development.

From our analysis it is clear that each of the thymocyte populations SP4, SP8, Treg and iNKT cells express the three known LTBR ligands LTα_3, LT$\alpha_1\beta_2$ and LIGHT and this is consistent with previous reports (159). Therefore it is not surprising that there is only a modest reduction of ICAM-1^{hi}VCAM-1^{hi} thymic mesenchyme in the SP4 and Treg deficient mice and normal ICAM-1^{hi}VCAM-1^{hi} thymic mesenchyme in iNKT cell deficient knockouts. The *Tcra*$^{-/-}$ model disrupts the formation of the αβ TCR, resulting in a loss of all αβ thymocytes and therefore SP4, SP8, Treg and iNKT cells (141). Therefore it was expected that the magnitude of loss of ICAM-1^{hi}VCAM-1^{hi} would be similar to that seen in the dGuo treated FTOC. MHC Class II deletion prevents the development of MHC Class II restricted CD4^{+}CD8^{-} thymocytes, including SP4 and Tregs, but not SP8 (MHC Class I restricted) or iNKT cells (CD1d restricted). Therefore it would appear that the absence of signaling from SP4 and Treg is required for ICAM-1^{hi}VCAM-1^{hi} development to some degree, but there is sufficient LTβR ligand provision by SP8 thymocytes and iNKT cells to limit the loss of ICAM-1^{hi}VCAM-1^{hi} thymic mesenchyme. The data suggested that none of the populations tested above are essential for the development of ICAM-1^{hi}VCAM-1^{hi} thymic

mesenchyme suggesting a redundant mechanism is in place to ensure the development of ICAM-1^{hi}VCAM-1^{hi} thymic mesenchyme.

Building on this, the addition of each population separately in an RTOC system can support the development of the ICAM-1^{hi}VCAM-1^{hi} population. Suggesting that whilst each population is not essential, they are sufficient to support ICAM-1^{hi}VCAM-1^{hi} development on their own. Interestingly the broad expression of LTβR ligands across multiple thymocyte populations differs to that of other TNFRSFs ligands. Whilst RANKL is expressed by SP4, SP8 thymocytes and Tregs, its expression on SP4 thymocytes is enriched on immature SP4 thymocytes (CD69^{+}) (159,162). Additionally the ligand for another TNFRSF member CD40, which is involved in mTEC development, has been shown to be expressed on SP4 but not SP8 thymocytes or Tregs and is thought to be expressed mainly on mature SP4 thymocytes (CD69^{-}) (159,162). This suggests that LTβR regulated development of thymic mesenchyme does not rely on specific populations of thymocytes as with other thymocyte:stroma cross talk mechanisms within the thymus or peripheral lymphoid tissues. An interesting further experiment to directly investigate the role of LTβR within the RTOC system would be the inclusion of an additional control group, which would receive an antagonistic anti-LTβR blocking antibody alongside each of the single thymocyte populations. This would directly test if the development of the ICAM-1^{hi}VCAM-1^{hi} population that each of the single thymocyte populations support is via LTβR signaling.

Not only is the addition of a single LTβR-ligand expressing thymocyte population sufficient for the development of ICAM-1^{hi}VCAM-1^{hi} thymic mesenchyme our data revealed that *in vitro* and *in vivo* anti-LTβR stimulation is also sufficient for ICAM-1^{hi}VCAM-1^{hi} development. This is similar to studies of peripheral lymphoid tissues where anti-LTβR stimulation induces ICAM-1^{hi}VCAM-1^{hi} cells in mLNs in culture (232). In addition to steady state, the effects of LTβR stimulation on thymic mesenchyme within the context of bone marrow chimeras were investigated. This system was used to introduce an absence of SP thymocytes, resulting in a reduction/loss of LTβR-ligand provision and therefore disrupt LTBR signaling. We found that maintaining LTβR signals by injecting anti-LTβR prevented the loss of ICAM-1^{hi}VCAM-1^{hi} thymic mesenchyme observed in the mice receiving the isotype control, suggesting that not only is LTβR signaling required for the initiation of ICAM-1^{hi}VCAM-1^{hi} thymic mesenchyme, but it may also be required for the ongoing maintenance of this population.

A preliminary experiment was carried out to investigate the potential requirement for persistent signaling from thymocytes for the maintenance of ICAM-1^{hi}VCAM-1^{hi} thymic mesenchyme. Using a tetracycline inducible Zap70 mouse model (TetZap70) which have a block at the pre-selection DP stage of thymocyte development unless Zap70 is induced via administering doxycycline (dox), upon which development of SP T-cells is enabled (256). Therefore TetZap70 mice are phenotypically similar to *Tcra*$^{-/-}$ mice, with absence of SP thymocytes resulting in a loss of ICAM-1^{hi}VCAM-1^{hi} thymic mesenchyme. Upon administration of dox, the restored SP T-cell development programme did give rise to ICAM-1^{hi}VCAM-1^{hi} thymic mesenchyme development.

This system would allow us to take the findings of the LTβR BMC experiments a step further by first switching on SP thymocyte development, through administration of dox, and then switching them off, cessation of dox, to investigate whether prolonged interactions with thymocytes are required for the maintenance of ICAM-1^{hi}VCAM-1^{hi} thymic mesenchyme.

A surprising finding of the anti-LTβR treated BMCs was that the total $PDPN^{+}$ population was reduced which had a knock on effect on the size of each of the ICAM-1/VCAM-1 expressing populations. Specifically there was a reduction in the number and percentage of the ICAM-1^{lo}VCAM-1^{lo} and ICAM-1^{int}VCAM-1^{int} thymic mesenchyme populations. This could suggest that the treatment of anti-LTβR is stimulating premature maturation of the immature thymic mesenchyme populations, which may otherwise be required to establish the $PDPN^{+}$ thymic mesenchyme population. Additionally we cannot rule out that the expression of the adhesion molecules themselves is increased due to LTβR stimulation as it has been previously shown that ICAM-1 and VCAM-1 are known target of LTβR signaling (257,258).

Finally our analysis revealed some potential roles for thymic mesenchyme through PCR analysis of genes associated with homeostasis and lymphocyte migration. We found that $PDPN^{+}$ thymic mesenchyme express *Ccl19, Cxcl13* and *Enpp2* but did not express *Ccl21*. *Enpp2* encodes autotaxin (ATX), an ectoenzyme that is required for the production of lysophosphatidic acid (LPA) which plays a role in lymphocyte trafficking into lymph nodes and regulation of lymphocyte migration (252,253). However an intrathymic role for ATX remains to be discovered. CXCL13 is a B-cell

chemoattractant and could therefore play a role in migration of thymic B-cells which have been shown to reside in the medulla at the corticomedullary junction (CMJ) similarly to where our confocal analysis shows thymic mesenchyme (259). Thymic B-cells have been shown to play a role in the generation of Treg and central tolerance suggesting thymic mesenchyme may indirectly regulate these processes through thymic B-cells (260,261).

CCL19 and CCL21 are ligands for CCR7 and have been shown to be essential for the migration of developing thymocytes from the cortex to the medulla as well as thymus colonization by T-cell precursors (21,69). Additionally CCR7 has been shown to play a key role in thymocyte egress in neonatal but not adult mice (69,116). Further PCR analysis was carried out on ICAM-1^{lo} and ICAM-1^{hi} thymic mesenchyme to understand the functional importance of the ICAM-1^{hi} cells, which appeared to be mature cells, based on our ontogeny results. Consistent with lymph node stroma, ICAM-1^{hi}VCAM-1^{hi} thymic mesenchyme expressed higher levels of *Ccl19, Enpp2* and *Sphk1* compared to ICAM-1^{lo}VCAM-1^{lo} thymic mesenchyme. SPHK1 was included as it has been shown to be expressed by thymic pericytes and is essential for the regulation of thymocyte egress by the production and maintenance of an sphingosine-1-phosphate (S1P)-gradient (111). Expression of *Sphk1* is consistent with the pericyte-like phenotype of PDGFRβ expression and perivascular positioning within the thymus identified for the $PDPN^{+}$ thymic mesenchyme.

This chapter identifies a population of thymic mesenchyme within which are ICAM-1^{hi}VCAM-1^{hi} expressing cells whose development is dependent on signaling through

LTβR via interactions with LTβR-ligand bearing $\alpha\beta^+$ T-cells. This ICAM-1^{hi}VCAM-1^{hi} mesenchyme population is positioned at the gateway between the thymus and the periphery and express genes linked with thymocyte migration, precursor entry and T-cells exit; as summarized in Figure 3.17. Together our analyses highlight a potential key, novel role of LTβR regulating thymus colonization and/or mature T-cell egress through regulation of an ICAM-1^{hi}VCAM-1^{hi} thymic mesenchyme population.

Figure 3.17. αβ T-Cell:Thymic Mesenchyme Cross-Talk Via LTβR Is Essential For The Development of ICAM-1^{hi}VCAM-1^{hi} Thymic Mesenchyme

(A) αβ T-cells regulate the development of ICAM-1^{hi}VCAM-1^{hi} PDPN^{+} thymic mesenchyme from ICAM-1^{lo}VCAM-1^{lo} via signaling through LTβR.

Gene analysis of sorted PDPN^{+} thymic mesenchyme as well as the ICAM-1^{lo}VCAM-1^{lo} and ICAM-1^{hi}VCAM-1^{hi} PDPN^{+} thymic mesenchyme populations suggests potential roles of these populations:

(B) Gene analysis reveals ICAM-1^{lo}VCAM-1^{lo} PDPN^{+} thymic mesenchyme express high levels of *Cxcl13* suggesting that they may regulate intrathymic CXCR5^{+} B-cell migration.

(C) Gene analysis reveals PDPN^{+} thymic mesenchyme express *Fgf10* that previous studies have shown regulates TEC proliferation in the embryonic thymus, highlighting a potential role for thymic mesenchyme regulating TEC proliferation in the adult thymus via FGF10.

(D) Gene analysis reveals ICAM-1^{hi}VCAM-1^{hi} PDPN^{+} thymic mesenchyme express high levels of *Ccl19* suggesting that they may regulate CCR7^{+} T-cell and DC migration or entry/egress.

(E) Gene analysis reveals ICAM-1^{hi}VCAM-1^{hi} PDPN^{+} thymic mesenchyme express high levels of *Sphk1* (enzyme that catalyzes production of S1P) suggesting that they may regulate S1P-dependent T-cell egress of S1PR1^{+} T-cells.

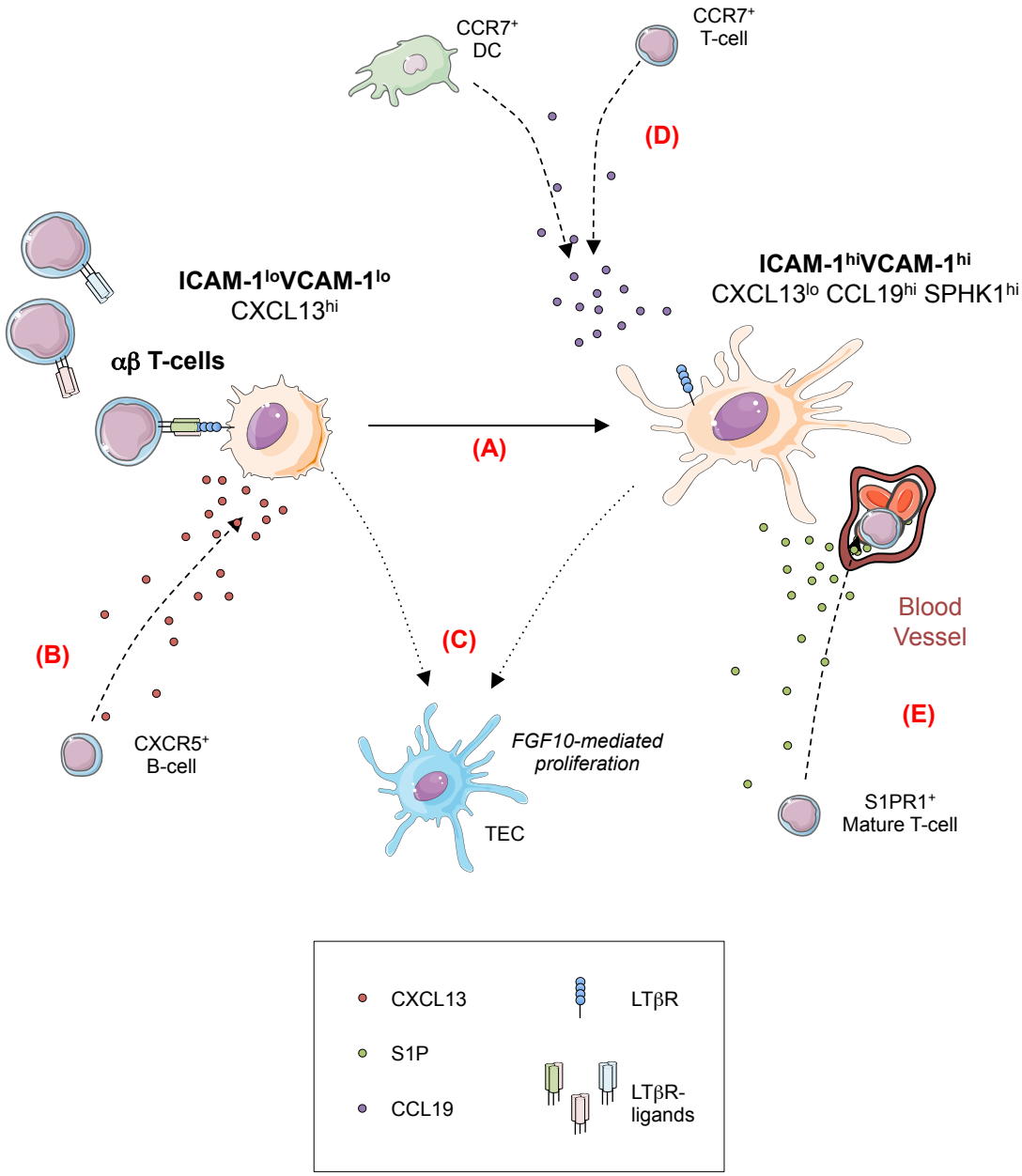
CCR7+
DC
CCR7+
T-cell
(D)
ICAM-1loVCAM-1lo
CXCL13hi
αβ T-cells
ICAM-1hiVCAM-1hi
CXCL13lo CCL19hi SPHK1hi
(A)
(B)
(C)
Blood
Vessel
(E)
CXCR5+
B-cell
FGF10-mediated
proliferation
TEC
S1PR1+
Mature T-cell
CXCL13
S1P
CCL19
LTβR
LTβR-
ligands

CHAPTER FOUR: REGULATION OF THYMOCYTE EGRESS BY THYMIC ENDOTHELIAL CELLS AND LYMPHOTOXIN BETA RECEPTOR SIGNALING

4.1 INTRODUCTION

Thymocytes go through many tightly regulated processes throughout their development from initial early T-cell precursors (ETP), right through to their eventual exit from the thymus. Whilst regulation of developing thymocytes via positive and negative selection are extremely important in ensuring the peripheral T-cell pool is functional, diverse and self tolerant, the egress of the thymocytes must also be regulated and is equally important to ensure only fully mature thymocytes are able to leave the thymus. Previous studies have highlighted two main mechanisms through which thymocyte egress is controlled. Firstly, C-C chemokine receptor type 7 (CCR7) has been shown to play a role in regulating thymocyte egress. Interactions between CCR7 expressed by thymocytes and CCR7 ligands expressed by thymic stroma (CCL19 and CCL21) are essential for the egress of mature thymocytes in neonatal mice (116). Interestingly however this process was subsequently shown to be non-essential for thymocyte egress in the adult thymus indicating that the mechanisms regulating T cell egress may alter in a temporal manner (69). Alternatively the sphingosine-1-phosphate (S1P)-sphingosine-1-phosphate receptor 1 (S1PR1) pathway has been identified as an essential regulatory pathway of thymocyte egress in the adult thymus. S1PR1 is expressed by mature SP thymocytes and mediates the migration of the mature SP thymocyte towards the site of exit via an S1P gradient (95,98,262). Multiple studies have highlighted key roles of many different cell types in regulating thymocyte egress through the maintenance of the S1P gradient where S1PR1-bearing mature thymocytes migrate from low levels of S1P within the thymus to high levels of S1P at the site of exit and in the blood. This regulation occurs either through regulating the production of S1P to maintain high levels of S1P at/near the

site of exit, or the degradation of S1P to maintain low intrathymic S1P levels. An example of the essential role of degrading S1P to maintain low levels of S1P is the production of lipid phosphate phosphatase 3 (LPP3) by TEC and thymic endothelial cells which is a dephosphorylating enzyme that inactivates S1P to maintain low intrathymic S1P levels (112). Endothelial cells also express the S1P transporter spinster homolog 2 (Spns2), which is essential to establish the S1P gradient needed for T-cell egress and thus highlights a positive regulatory role of thymic endothelial cells regulating intrathymic S1P levels (113). Another S1P degrading enzyme, S1P lyase (SGPL), is also produced by bone marrow-derived cells, including thymic dendritic cells, and irreversibly degrades S1P to maintain low intrathymic S1P levels (114). Alternatively thymic pericytes have been show to produce sphingosine kinase 1 (SPHK1) and SPHK2 which are enzymes required for the production of new S1P and its production by PDGFRβ^{+} pericytes is essential for thymocyte egress (111). Although the mechanism of S1P-regulated thymocyte egress is relatively well known, cellular and molecular regulators of this process and thymocyte egress remain poorly understood.

The previous chapter shows that thymic mesenchyme express egress associated molecules such as *Sphk1*, include thymic pericytes, which have previously been linked to regulation of thymocyte egress and are regulated by LTβR signaling through interactions with T-cells. Given that previous studies have suggested that LTβR regulates egress via regulation of thymic stroma, we hypothesized that LTβR regulation of thymic mesenchyme is a critical pathway involved in the control of T-cell output.

Thus the following chapter aimed to further characterize the thymocyte egress defect found within LTβR deficient mice, investigate the mechanism of LTβR-dependent thymocyte egress and identify the thymic population that this is occurring through.

4.2 RESULTS

4.2.1 LTβR Signaling Is Required For Normal Thymocyte Egress

To study thymocyte egress we needed to ensure we had suitable methods in place to correctly measure it when it is altered. The initial phenotypic description of a thymocyte egress defect within LTβR deficient mice used the expression of CD69 and CD62L to separate the single positive $CD4^+CD8^-TCR\beta^{hi}$ (SP4) thymocytes and $CD4^-CD8^+TCR\beta^{hi}$ (SP8) thymocytes into immature ($CD69^+CD62L^-$) and mature ($CD69^{lo}CD62L^+$) cells (151). Using this strategy it was revealed that LTβR-deficient (*Ltbr*$^{-/-}$) mice have a significant intrathymic accumulation of mature thymocytes, indicative of an inability of the mature thymocyte to egress the thymus (151). To refine this analysis, CD25 and FoxP3 were included in our analysis to exclude $CD25^+FoxP3^+$ regulatory T-cells (Tregs) as well a $CD25^+FoxP3^-$ Treg precursors, allowing the investigation of conventional SP4 (cSP4) thymocytes (Fig 4.1.A.). Based on the study by Boehm *et. al,* CD69 and CD62L were used to identify immature and mature populations within SP8 and cSP4 thymocytes of wildtype (WT) mice (Fig 4.1.A.). These WT mice had been crossed with a RAG^{gfp} mouse model, a reporter system first created to identify recent thymic emigrants (RTE) and can also be used to identify different maturational stages of thymocytes within the thymus (74,263). The RAG^{gfp} model works through utilizing the temporal expression of RAG during $CD4^+CD8^+$ DP thymocyte development (263). When the gene is switched off after the

DP stage, residual RAG^{gfp} protein can be used to measure the age of the cell, where the amount of GFP in a cell is inversely proportional to the cell's age (Fig 4.3.A.). Gating using RAG^{gfp} expression also ensures that the SP4 and SP8 cells have recently developed and are not recirculating cells. Within both RAG^{gfp+} cSP4 and SP8 thymocytes it was clear that the immature fraction of each population was distinct from the mature fraction in terms of their expression of RAG^{gfp}, where mature cells had significantly lower levels of RAG^{gfp} and therefore were significantly older than immature cells (Fig 4.1.B.C.). Another important distinction between immature thymocytes and mature thymocytes is the ability to egress the thymus via the sphingosine-1-phosphate pathway by expressing the S1P receptor 1 (S1PR1) on their cell surface (262). Consistent with this, within RAG^{gfp+} cSP4 thymocytes, only mature cSP4 thymocytes express S1PR1 (Fig 4.1.D.). Together these data provide multiple methods of identifying different maturation statuses within cSP4 and SP8 thymocytes.

To confirm the presence of a thymocyte egress defect within LTβR deficient mice we first repeated the CD69/CD62L analysis of immature and mature thymocyte populations using the cSP4 gating strategy identified in Fig 4.1. Consistent with Boehm *et al.*'s analysis, $Ltbr^{-/-}$ mice had increased percentage of $CD4^{+}CD8^{-}$ thymocytes and a significant increase in the percentage and number of mature cSP4 and SP8 thymocytes (Fig 4.2.A-F). Importantly the increase was specific to mature thymocytes with no increase detected within the immature fraction of either cSP4 or SP8 thymocytes (Fig 4.2.C-F). As suggested in Boehm *et al.*'s study, this increase in the number of mature cSP4 and SP8 thymocytes is indicative of an intrathymic

Figure 4.1. Separating Single Positive Thymocytes Into Distinct Immature and Mature Populations

Thymic lobes were harvested from WT RAG^{gfp} reporter mice and mechanically disrupted for FACS analysis of the thymocyte populations.

(A) Conventional single positive CD4 (cSP4) and single positive CD8 (SP8) thymocytes were identified as $CD4^{+}CD8^{-}TCR\beta^{hi}CD25^{-}Foxp3^{-}$ and $CD4^{-}CD8^{+}TCR\beta^{hi}$, respectively. Immature and mature thymocytes were identified as $CD69^{+}CD62L^{-}$ and $CD69^{lo}CD62L^{+}$, respectively.

(B) Within the immature and mature cSP4 thymocytes, RAG^{gfp+} cells were gated on. The RAG^{gfp} MFI was calculated for each population shown on the right.

(C) Within the immature and mature SP8 thymocytes, RAG^{gfp+} cells were gated on. The RAG^{gfp} MFI was calculated for each population shown on the right.

(D) Within the immature and mature cSP4 thymocytes, the expression of S1PR1 was plotted (left) and the S1PR1 MFI was calculated for each population shown on the right.

The standard error bars display the SEM and a mann-whitney test was performed, where ** denotes a significant difference as $p<0.01$. All data is typical of 3 independent repeats where total n=5.

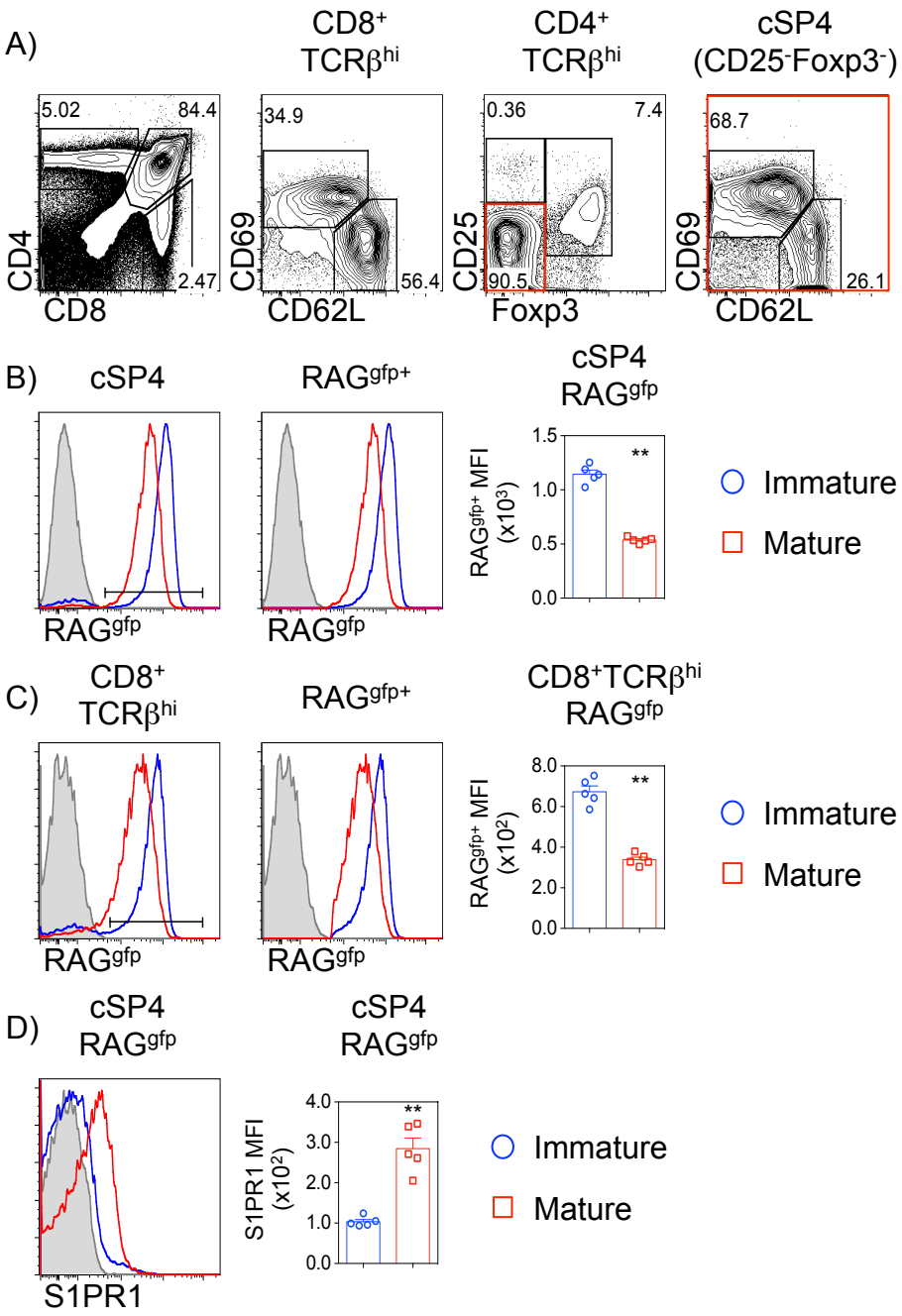
A)
CD8+ TCRβhi
CD4+ TCRβhi
cSP4 (CD25-Foxp3-)
5.02
84.4
2.47
CD4
CD8
34.9
56.4
CD69
CD62L
0.36
7.4
90.5
CD25
Foxp3
68.7
26.1
CD69
CD62L
B)
cSP4
RAGgfp+
cSP4 RAGgfp
RAGgfp
RAGgfp
RAGgfp+ MFI (x10³)
1.5
1.0
0.5
0.0
**
Immature
Mature
C)
CD8+ TCRβhi
RAGgfp+
CD8+TCRβhi RAGgfp
RAGgfp
RAGgfp
RAGgfp+ MFI (x10²)
8.0
6.0
4.0
2.0
0.0
**
Immature
Mature
D)
cSP4 RAGgfp
cSP4 RAGgfp
S1PR1
S1PR1 MFI (x10²)
4.0
3.0
2.0
1.0
0.0
**
Immature
Mature

Figure 4.2. Deletion of LTβR Results In An Intrathymic Accumulation Of Mature Single Positive Thymocytes

Thymic lobes were harvested from control (*Ltbr*$^{+/+}$) and LTβR-deficient (*Ltbr*$^{-/-}$) mice and enzymatically digested for FACS analysis of the thymocyte populations.

(A) Expression pattern of CD4 and CD8 within *Ltbr*$^{+/+}$ (left) and *Ltbr*$^{-/-}$ (right) thymi to identify CD4^{+}CD8^{-} SP4, CD4^{+}CD8^{+} DP and CD4^{-}CD8^{+} SP8 thymocytes.

(B) Cell number of the thymus, cSP4, SP8 and DP thymocytes and percentages of CD4^{+}CD8^{-} and CD4^{-}CD8^{+} were calculated for *Ltbr*$^{+/+}$ (blue, n=13) and *Ltbr*$^{-/-}$ (red, n=12) mice.

(C) Expression pattern of CD69 and CD62L within cSP4 thymocytes of *Ltbr*$^{+/+}$ (left) and *Ltbr*$^{-/-}$ (right) mice.

(D) Cell numbers and percentages of immature and mature cSP4 thymocytes were calculated for *Ltbr*$^{+/+}$ (blue, n=13) and *Ltbr*$^{-/-}$ (red, n=12) mice.

(E) Expression pattern of CD69 and CD62L within SP8 thymocytes of *Ltbr*$^{+/+}$ (left) and *Ltbr*$^{-/-}$ (right) mice.

(F) Cell numbers and percentages of immature and mature SP8 thymocytes were calculated for *Ltbr*$^{+/+}$ (blue, n=13) and *Ltbr*$^{-/-}$ (red, n=12) mice.

The standard error bars display the SEM and a mann-whitney test was performed, where * denotes a significant difference as $p<0.05$, ** $p<0.01$ and **** denotes $p<0.0001$. All data is typical of 3 independent repeats.

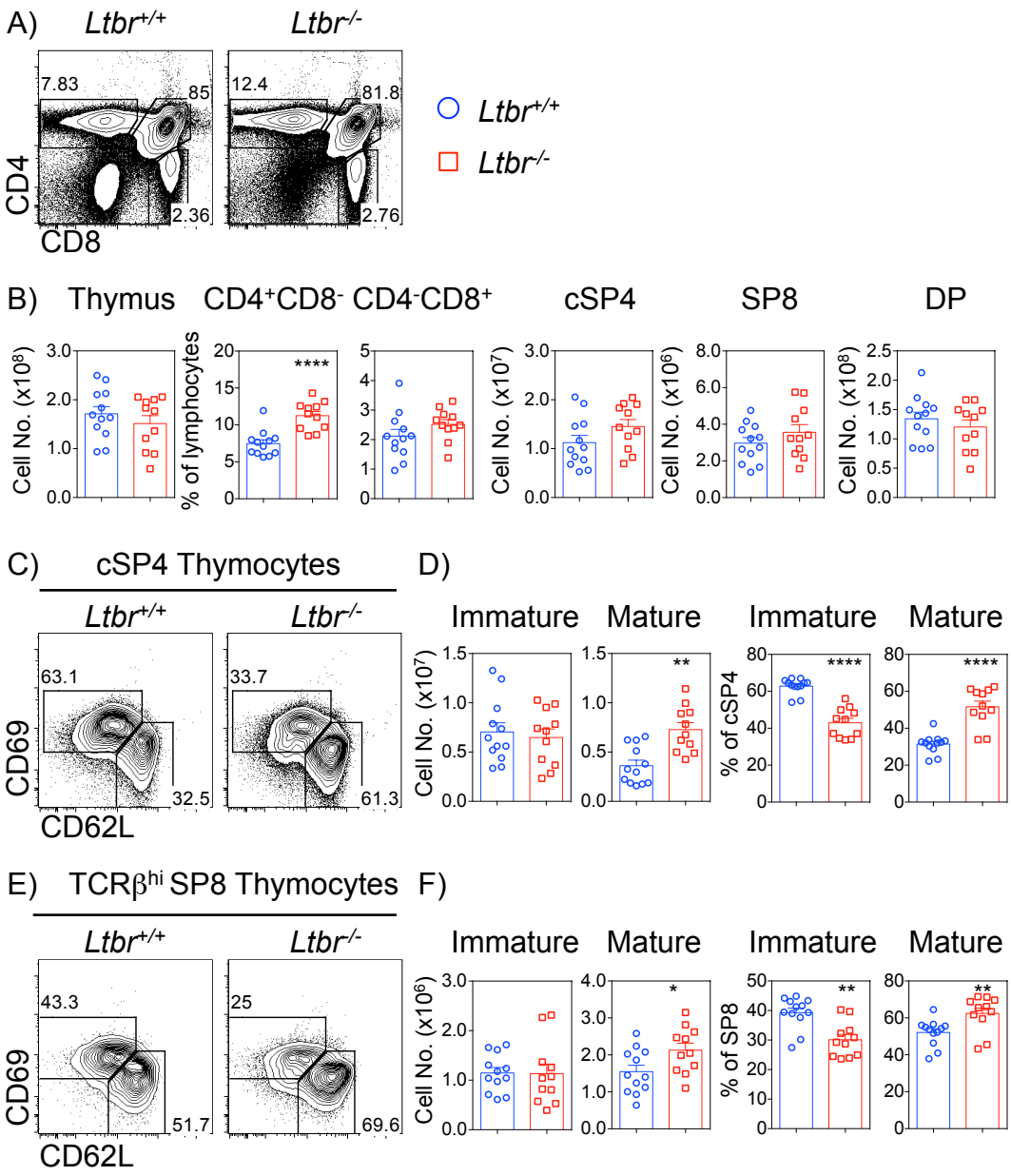
A)
Ltbr+/+
Ltbr-/-
7.83
85
2.36
12.4
81.8
2.76
CD4
CD8
Ltbr+/+
Ltbr-/-
B)
Thymus
CD4+CD8-
CD4-CD8+
cSP4
SP8
DP
Cell No. (x10^8)
% of lymphocytes
****
Cell No. (x10^7)
Cell No. (x10^6)
Cell No. (x10^8)
C)
cSP4 Thymocytes
Ltbr+/+
Ltbr-/-
63.1
32.5
33.7
61.3
CD69
CD62L
D)
Immature
Mature
Immature
Mature
Cell No. (x10^7)
**
% of cSP4
****
****
E)
TCRβhi SP8 Thymocytes
F)
Ltbr+/+
Ltbr-/-
43.3
51.7
25
69.6
CD69
CD62L
Immature
Mature
Immature
Mature
Cell No. (x10^6)
*
% of SP8
**
**

accumulation of cells and is not due to increased proliferation. Following this, *Ltbr*$^{-/-}$ mice were crossed with RAG^{gfp} reporter mice to create *Ltbr*$^{-/-}$RAG^{gfp} mice to directly investigate the impact of LTβR deficiency on intrathymic dwell time and thymocyte egress. Therefore if the increase in mature thymocytes within the *Ltbr*$^{-/-}$ mouse is truly an intrathymic accumulation it would be expected that the mature thymocytes within the *Ltbr*$^{-/-}$ thymus are older, with lower levels of RAG^{gfp}, compared to *Ltbr*$^{+/+}$ controls (Fig 4.3.A.). Through analysis of immature and mature SP4 thymocytes within *Ltbr*$^{-/-}$ RAG^{gfp} mice, it is clear that mature SP4 thymocytes have much lower levels of RAG^{gfp} expression compared to *Ltbr*$^{+/+}$RAG^{gfp} control mice and therefore do have an increased intrathymic dwell time (Fig 4.3.B.C.). Importantly the expression of RAG^{gfp} by immature SP4 thymocytes is the same between both mice indicating the dwell time defect is specific to mature thymocytes (Fig 4.3.B.C.). The RAG^{gfp} model can also be used to identify recent thymic emigrants (RTE) due to the residual RAG^{gfp} present within cells that have recently left the thymus (263). Therefore this can be used to directly investigate whether LTβR deficiency and the accompanied intrathymic accumulation has an impact on the peripheral T-cell pool. Consistent with the increased intrathymic dwell time, SP4 RTE within the spleen of *Ltbr*$^{-/-}$ mice have significantly lower levels of RAG^{gfp} (Fig 4.3.D.E.). As previously reported, *Ltbr*$^{-/-}$ mice have increased splenic cellularity associated with the increased lymphocytes within the spleen as a result of absent peripheral lymph nodes (Fig 4.3.F.) (264). This increase of cells within the spleen resulted in an overall increase in the number of RAG^{gfp-} and RAG^{gfp+} SP4 RTE, however the proportion of RAG^{gfp+} SP4 RTE with the SP4 compartment was reduced, suggesting there are relatively fewer RAG^{gfp+} SP4 RTE in the periphery of LTβR deficient mice (Fig 4.3.F.).

Figure 4.3. Deletion of LTβR Results In Reduced Recent Thymic Emigrants

Thymic lobes and spleens were harvested from control (*Ltbr*$^{+/+}$RAG^{gfp}) and LTβR-deficient (*Ltbr*$^{-/-}$RAG^{gfp}) mice and mechanically disrupted for FACS analysis.

(A) Model of the RAG^{gfp} reporter model. Green fluorescent protein (gfp) is produced when *Rag* is expressed in DP thymocytes. Subsequently the gene is switched off, stopping production of new gfp. The gfp remaining in the cell decays over time and the amount of gfp present within a cell is inversely proportional to its age. Therefore RAG^{gfp} expression can be used to measure intrathymic dwell time and to also identify recent thymic emigrants (RTE).

(B) The expression of RAG^{gfp} on immature (CD4^{+}TCRβ^{hi}CD25^{-}CD69^{+}CD62L^{-}) and mature (CD4^{+}TCRβ^{hi}CD25^{-}CD69^{lo}CD62L^{+}) SP4 thymocytes within *Ltbr*$^{+/+}$RAG^{gfp} (blue) and *Ltbr*$^{-/-}$RAG^{gfp} (red) mice.

(C) RAG^{gfp} MFI for immature and mature SP4 thymocytes from *Ltbr*$^{+/+}$RAG^{gfp} (blue, n=5) and *Ltbr*$^{-/-}$RAG^{gfp} (red, n=5) mice where the data is represented as a ratio of mean RAG^{gfp} MFI of *Ltbr*$^{-/-}$:*Ltbr*$^{+/+}$ for each experiment.

(D) Expression pattern of CD4 and TCRβ to identify SP4 RTE within the spleen within *Ltbr*$^{+/+}$ mice.

(E) Expression of RAG^{gfp} on SP4 RTE of *Ltbr*$^{+/+}$RAG^{gfp} (blue) and *Ltbr*$^{-/-}$RAG^{gfp} (red) mice. RAG^{gfp} MFI for SP4 RTE from *Ltbr*$^{+/+}$RAG^{gfp} (blue, n=5) and *Ltbr*$^{-/-}$RAG^{gfp} (red, n=5) mice where the data is represented as a ratio of mean RAG^{gfp} MFI of *Ltbr*$^{-/-}$:*Ltbr*$^{+/+}$ for each experiment.

(F) Cell numbers of spleen, RAG^{-} SP4 T-cells and RAG^{+} SP4 RTE as well as percentages of SP4 T-cells and SP4 RTE were calculated for *Ltbr*$^{+/+}$ (blue, n=9) and *Ltbr*$^{-/-}$ (red, n=12) mice.

The standard error bars display the SEM and a mann-whitney test was performed, where * denotes a significant difference as $p<0.05$, ** $p<0.01$ and **** denotes $p<0.001$. All data is typical of 5 independent repeats.

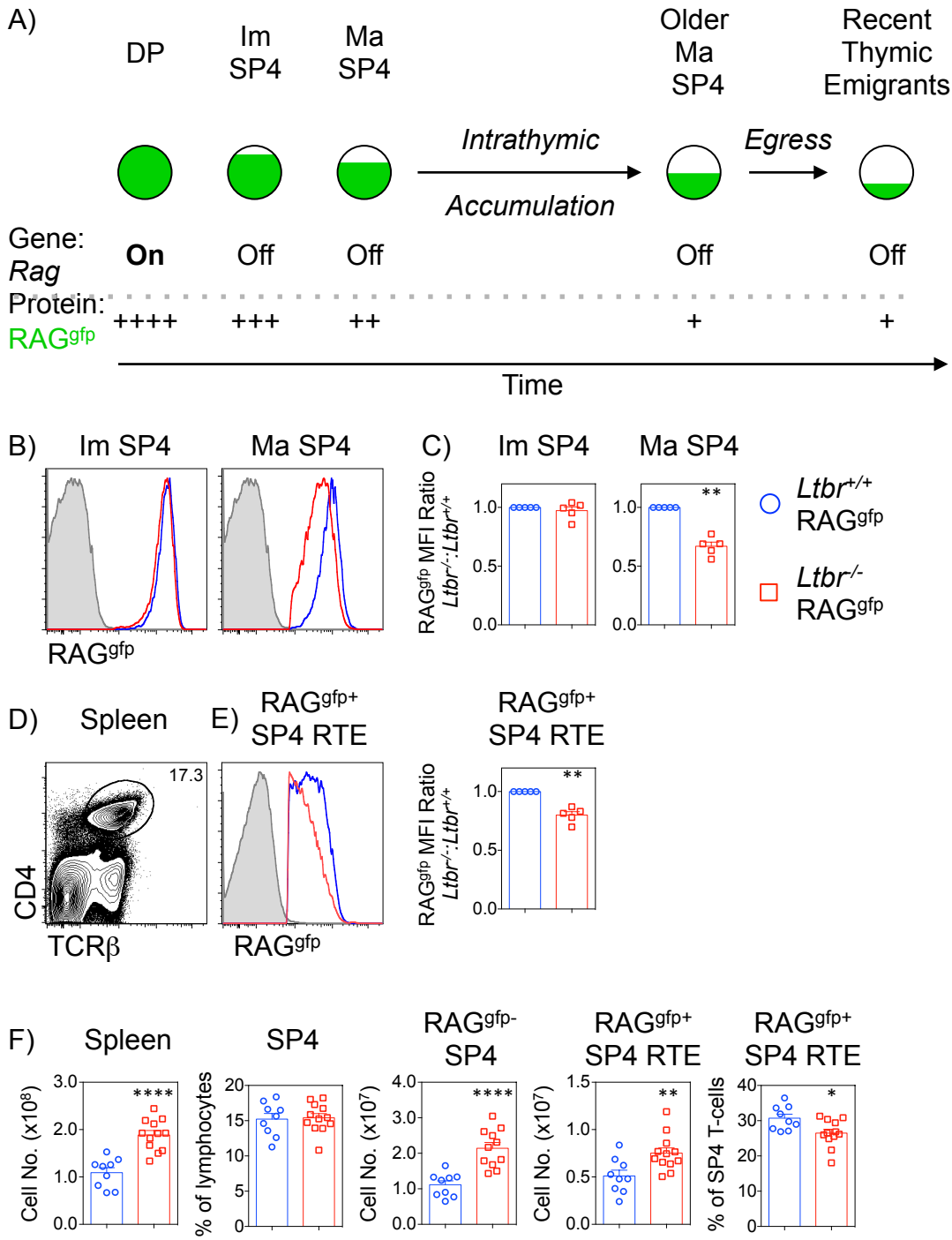
A)
DP
Im SP4
Ma SP4
Older Ma SP4
Recent Thymic Emigrants
Intrathymic Accumulation
Egress
Gene: Rag
On
Off
Off
Off
Off
Protein: RAGgfp
++++
+++
++
+
+
Time
B)
Im SP4
Ma SP4
RAGgfp
C)
Im SP4
Ma SP4
RAGgfp MFI Ratio Ltbr-/-:Ltbr+/+
1.0
0.5
0.0
**
Ltbr+/+ RAGgfp
Ltbr-/- RAGgfp
D)
Spleen
17.3
CD4
TCRβ
RAGgfp
E)
RAGgfp+ SP4 RTE
RAGgfp MFI Ratio Ltbr-/-:Ltbr+/+
**
F)
Spleen
Cell No. (x10^8)
****
SP4
% of lymphocytes
RAGgfp- SP4
Cell No. (x10^7)
****
RAGgfp+ SP4 RTE
Cell No. (x10^7)
**
RAGgfp+ SP4 RTE
% of SP4 T-cells
*

These data provide a more refined analysis of the impact of LTβR deficiency on thymocyte egress and provides a method to directly confirm that LTβR is playing a role in regulating intrathymic dwell time and thymocyte egress of mature thymocytes.

4.2.2 Identifying The Cellular And Molecular Regulators Of LTβR-Dependent Thymocyte Egress

It has previously been shown that multiple cell types of both hematopoietic and stromal origin influence and regulate thymocyte egress through the S1P pathway and the CCR7 pathway (69,111,112,114,116). To identify which cell types may be playing a role in LTβR-dependent thymocyte egress, the expression of LTβR was measured on each of the main cell types within the thymus: $TER119^{-}CD45^{+}EpCAM\text{-}1^{-}$ hematopoietic cells, $TER119^{-}CD45^{-}EpCAM\text{-}1^{+}$ TEC, $TER119^{-}CD45^{-}EpCAM\text{-}1^{-}PDPN^{+}CD31^{-}$ thymic mesenchyme and $TER119^{-}CD45^{-}EpCAM\text{-}1^{-}PDPN^{-}CD31^{+}$ thymic endothelium (Fig 4.4.A.). LTβR expression appeared mainly restricted to the stromal compartment, where it was expressed by TEC, mesenchyme and endothelium (Fig 4.4.B.). However previous studies have shown that LTβR is expressed by thymic dendritic cells (DCs), which make up an extremely small population relative to the $CD45^{+}$ compartment as a whole (157). Therefore our analysis could be diluting the expression of some scarce $CD45^{+}$ thymocyte populations. To address this, two approaches were taken to separate the role of LTβR expressing hematopoietic cells and LTβR expressing thymic stromal cells.

To investigate if hematopoietic expression of LTβR is essential for thymocyte egress, bone marrow chimeras (BMC) were created where $CD45.1^{+}$ WT mice were lethally

Figure 4.4. LTβR Is Expressed By All 3 Of The Main Thymic Stromal Populations

Thymic lobes were harvested from mice and enzymatically digested for FACS analysis of thymic stromal populations.

(A) Identification of $TER119^{-}Viability^{-}CD45^{+}EpCAM\text{-}1^{-}$ hematopoietic cells as well as the three main thymic stromal populations: $TER119^{-}Viability^{-}CD45^{-}EpCAM\text{-}1^{+}$ thymic epithelial cells (TEC), $TER119^{-}Viability^{-}CD45^{-}EpCAM\text{-}1^{-}PDPN^{+}CD31^{-}$ thymic mesenchyme and $TER119^{-}Viability^{-}CD45^{-}EpCAM\text{-}1^{-}PDPN^{-}CD31^{+}$ thymic endothelium of WT mice.

(B) Expression of LTβR on hematopoietic cells as well as TEC, mesenchyme and endothelium from WT mice with an *Ltbr*$^{-/-}$ mouse as a staining control.

All data is typical of 3 independent repeats.

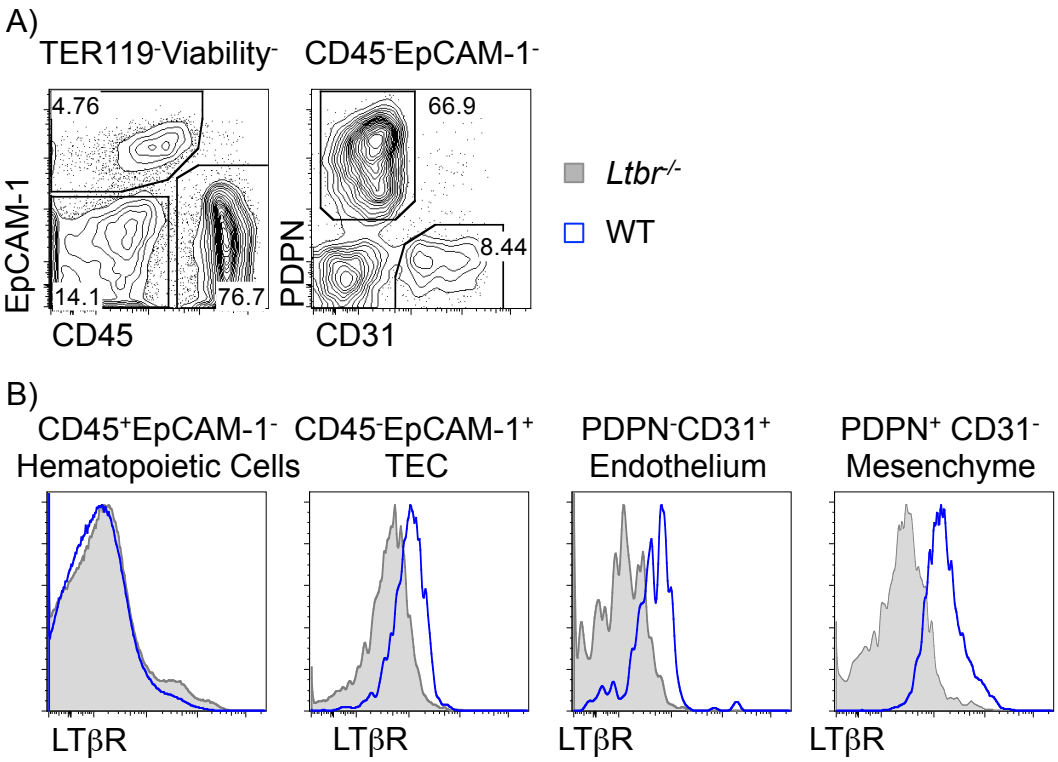
A)
TER119-Viability-
CD45-EpCAM-1-
4.76
14.1
76.7
EpCAM-1
CD45
66.9
8.44
PDPN
CD31
Ltbr-/-
WT
B)
CD45+EpCAM-1-
Hematopoietic Cells
CD45-EpCAM-1+
TEC
PDPN-CD31+
Endothelium
PDPN+ CD31-
Mesenchyme
LTβR
LTβR
LTβR
LTβR

irradiated and reconstituted with CD45.2^{+} control (*Ltbr*$^{+/+}$) or CD45.2^{+} LTβR deficient (*Ltbr*$^{-/-}$) bone marrow and harvested 12 weeks after reconstitution (Fig 4.5.A.). This approach restricts LTβR deficiency to hematopoietic cells, as the host's radio-resistant stromal cells will continue to express LTβR. WT hosts receiving either *Ltbr*$^{+/+}$ or *Ltbr*$^{-/-}$ bone marrow appeared identical, with no increase in the percentage or number of mature SP4 thymocytes (Fig 4.5.B.C.). This data indicates that LTβR expression by hematopoietic cells is dispensable for thymocyte egress however it does not rule out redundancy between stroma and hematopoietic cells. To directly investigate an essential role for LTβR expression by thymic stroma, a complementary experiment was set up to restrict loss of LTβR to thymic stromal cells. Embryonic day 15 (E15) thymic lobes were harvested from *Ltbr*$^{+/+}$ and *Ltbr*$^{-/-}$ mice and cultured in fetal thymic organ culture conditions (FTOC) in the presence of 2-dGuo to deplete hematopoietic cells within the thymus graft prior to transplant. These lobes were then grafted under the kidney capsule of a WT host; therefore host-derived bone marrow and subsequent developing thymocytes will be LTβR sufficient whilst the donor-derived thymic stroma within the grafts will either be LTβR sufficient (*Ltbr*$^{+/+}$) or LTβR deficient (*Ltbr*$^{-/-}$) (Fig 4.5.D.). Analysis of the thymocyte populations within the grafts revealed a reduction of immature cSP4 (Im cSP4) and an increase in the number and percentage of mature cSP4 (Ma cSP4) thymocytes within the *Ltbr*$^{-/-}$ grafts consistent with a blockade in mature thymocyte egress (Fig 4.5.E.). Together these two experiments reveal that LTβR expression by thymic stroma, but not hematopoietic cells, is essential for normal thymocyte egress.

Figure 4.5. Expression Of LTβR By Thymic Stroma Is Essential For Thymocyte Egress

(A) CD45.1 WT mice were lethally irradiated with 2x500 rad doses and reconstituted with CD45.2 *Ltbr*$^{+/+}$ or *Ltbr*$^{-/-}$ bone marrow (BM) and harvested 12 weeks later.

(B) Expression pattern of CD69 and CD62L on CD4^{+}CD8^{-}TCRβ^{hi}CD25^{-}FoxP3^{-} conventional SP4 (cSP4) thymocytes in WT mice receiving *Ltbr*$^{+/+}$ (left) or *Ltbr*$^{-/-}$ (right) BM.

(C) Cell numbers of thymus, cSP4, CD69^{+}CD62L^{-} immature cSP4 (Im cSP4) and CD69^{lo}CD62L^{+} mature cSP4 (Ma cSP4) thymocytes, as well as percentages of Im cSP4 and Ma cSP4 thymocytes, were calculated for WT mice receiving *Ltbr*$^{+/+}$ (blue, n=6) or *Ltbr*$^{-/-}$ (red, n=6) BM.

(D) Thymic lobes were harvested from E15 *Ltbr*$^{+/+}$ or *Ltbr*$^{-/-}$ mice and cultured with dGuo for 7 days and then grafted under the kidney capsule of WT host mice. Grafted mice were then harvested 6 weeks after initial engraftment.

(E) Cell numbers of thymus, cSP4, Im cSP4 and Ma cSP4 thymocytes, as well as percentages of Im cSP4 and Ma cSP4 thymocytes, were calculated for WT mice receiving *Ltbr*$^{+/+}$ (blue, n=17) or *Ltbr*$^{-/-}$ (red, n=20) BM.

The standard error bars display the SEM and a mann-whitney test was performed, where * denotes a significant difference as $p<0.05$, ** $p<0.01$ and *** denotes $p<0.001$. Data of A-C is typical of 2 independent repeats and data of D+E is typical of 3 independent repeats.

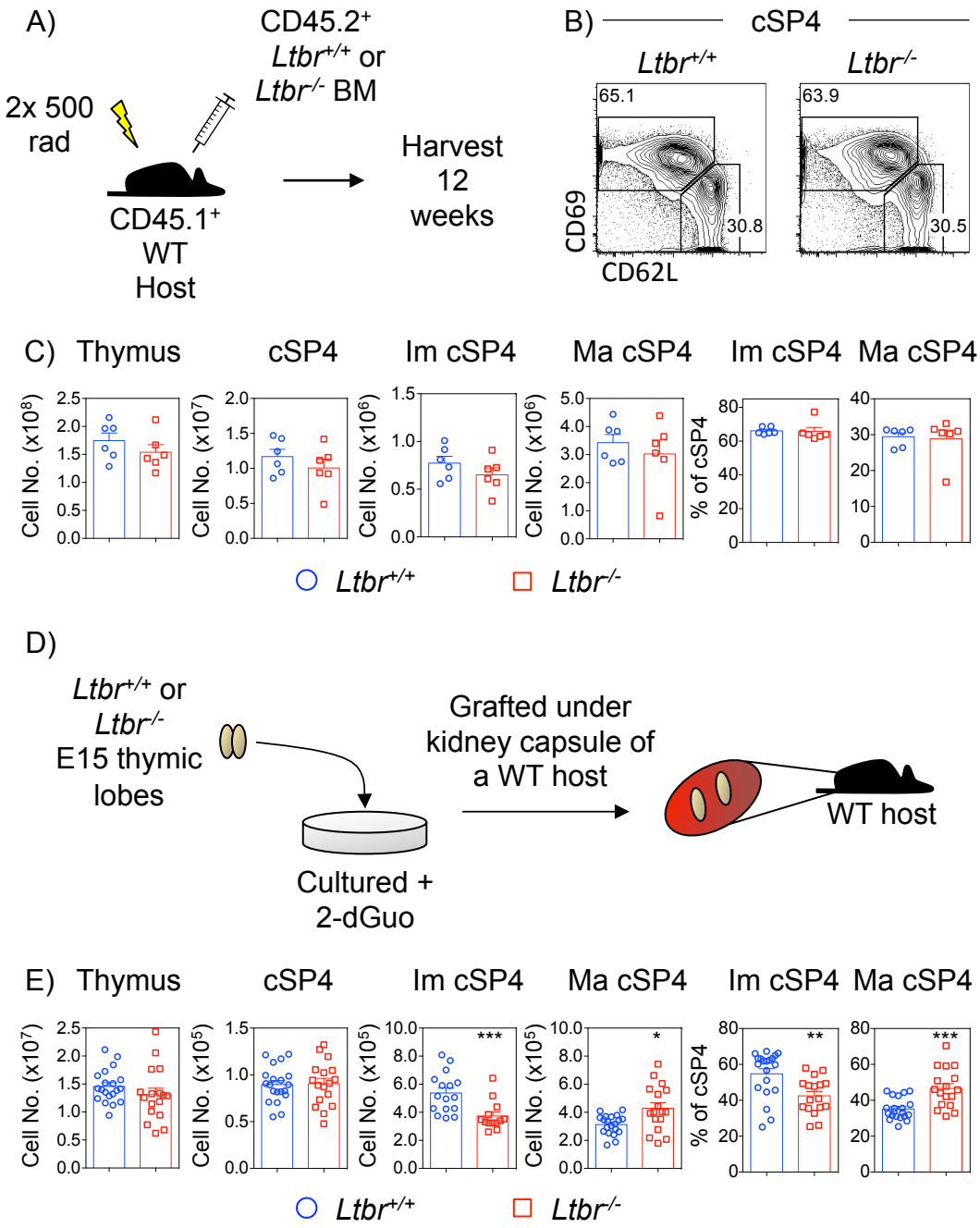
A)
2x 500 rad
CD45.2+ Ltbr+/+ or Ltbr-/- BM
CD45.1+ WT Host
Harvest 12 weeks
B)
cSP4
Ltbr+/+
Ltbr-/-
65.1
30.8
63.9
30.5
CD69
CD62L
C) Thymus
cSP4
Im cSP4
Ma cSP4
Im cSP4
Ma cSP4
Cell No. (x10^8)
Cell No. (x10^7)
Cell No. (x10^6)
Cell No. (x10^6)
% of cSP4
Ltbr+/+
Ltbr-/-
D)
Ltbr+/+ or Ltbr-/- E15 thymic lobes
Cultured + 2-dGuo
Grafted under kidney capsule of a WT host
WT host
E) Thymus
cSP4
Im cSP4
Ma cSP4
Im cSP4
Ma cSP4
Cell No. (x10^7)
Cell No. (x10^5)
Cell No. (x10^5)
Cell No. (x10^5)
% of cSP4
***
*
**
***
Ltbr+/+
Ltbr-/-

The expression profile of LTβR on thymic stromal populations revealed that TEC, mesenchyme and endothelial cells express LTβR (Fig 4.4.B.). Additionally our own data shows that *Ltbr*$^{-/-}$ mice have a reduction of ICAM-1^{hi}VCAM-1^{hi} PDPN^{+} thymic mesenchyme, which express genes known to regulate thymocyte egress such as *Ccl19* and *Sphk1* (Chapter 3). Moreover, thymic mesenchymal production of SPHK1 and SPHK2 is essential for normal S1P-dependent egress of mature thymocytes from the adult thymus (111). This data suggests that thymic mesenchyme may be a candidate for the stromal population that regulates LTβR-dependent thymocyte egress. To directly investigate this, the Cre/LoxP mouse model system was used to specifically delete LTβR on thymic mesenchyme by crossing the mesenchyme specific mouse strain *Pdgfrb*$^{cre/+}$ mice with *Ltbr*$^{flox/flox}$ mice. *Pdgfrb*^{cre} mice have previously been used to successfully target PDGFRβ^{+} perivascular cells within LNs and therefore appeared to be a suitable model to delete *Ltbr* specifically on thymic mesenchyme (265). These mice should have *Ltbr* deleted on all *Pdgfrb*^{cre} expressing cells, which our analysis revealed that PDGFRβ is expressed by all PDPN^{+} thymic mesenchyme cells (Chapter 3). Thymocytes were analyzed from *Pdgfrb*^{cre} control mice and from *Pdgfrb*^{cre}*Ltbr*^{flox} mice however there was no detectable accumulation of mature cSP4 or SP8 thymocytes (Fig 4.6.A-C.).

To ensure that the phenotype observed in the *Pdgfrb*^{cre}*Ltbr*^{flox} mice was truly representative of a non-essential role in regulating thymocyte egress, the efficiency and specificity of the *Pdgfrb*^{cre} strain was tested through two approaches. *Pdgfrb*^{cre} mice were crossed with mT/mG mice, a fate mapper system in which all cells express membrane-targeted tdTomato (mT) prior to Cre excision and membrane-

targeted EGFP (mG) after Cre excision and therefore can be used to accurately identify Cre^- and Cre^+ cells (241). *Pdgfrb*^{cre}mT/mG mice revealed that Cre expression was not specific to thymic mesenchyme (Fig 4.6.D.E.). Whilst Cre activity was detected in 80.9% (± 3.17%) of mesenchyme, it was also expressed by 69.9% (± 7.26%) of thymic endothelium (Fig 4.6.D.E). Alternatively, stroma was isolated from the *Pdgfrb*^{cre}*Ltbr*^{flox} mice and LTβR protein expression was measured on thymic mesenchyme via flow cytometry (Fig 4.6.F.). Despite the *Pdfgrb*^{cre}mT/mG model demonstrating efficient targeting of thymic mesenchyme, there was not a complete loss of LTβR expression on $PDPN^+$ thymic mesenchyme within *Pdgfrb*^{cre}*Ltbr*^{flox} mice suggesting *Pdgfrb*^{cre} is a sub-optimal model to target *Ltbr* deletion to thymic mesenchyme (Fig 4.6.F.). Therefore these data reveal that LTβR deletion in the *Pdgfrb*^{cre}*Ltbr*^{flox} mouse model is inefficient and furthermore the Cre activity of the *Pdgfrb*^{cre} is non-specific. This highlights an essential requirement to test and confirm specificity and efficacy when using mouse models such as the Cre/LoxP system.

Due to the inefficiency of the *Pdgfrb*^{cre} mouse strain, an alternative mesenchyme specific mouse strain was chosen. Previous studies have shown that *Wnt-1*^{cre} mice can target gene deletion to neural crest derived mesenchyme, where it has been used to delete sphingosine kinase on thymic mesenchyme which causes an intrathymic accumulation of mature thymocytes (111). To verify the specificity of the *Wnt-1*^{cre} mouse model, *Wnt-1*^{cre} mice were crossed to mT/mG mice. As expected mT/mG control mice showed no Cre activity within any of the cell populations (Fig 4.7.A.), whereas *Wnt-1*^{cre}mT/mG mice showed Cre activity was specific to thymic

mesenchyme and efficient, with ~75.0% (± 3.35%) of PDPN^{+} thymic mesenchyme switching from mT^{+} to mG^{+} (Fig 4.7.C.D.).

Following confirmation that the *Wnt-1^{cre}* was in fact specifically targeting thymic mesenchyme, *Wnt-1^{cre}* mice were crossed with *Ltbr$^{fl/fl}$* mice to delete LTβR on thymic mesenchyme. The expression of LTβR was significantly reduced and deletion was specific to thymic mesenchyme within *Wnt-1^{cre}Ltbr^{flox}* mice (Fig 4.8.A.B.). It should be noted that expression levels of LTβR were not fully reduced to the levels seen in *Ltbr$^{-/-}$* mice (Fig 4.8.A.B.). As a further test to determine whether the deletion of *Ltbr* within the *Wnt-1^{cre}Ltbr^{flox}* is efficient, the thymic mesenchyme was stained for ICAM-1 and VCAM-1 to identify the ICAM-1^{hi}VCAM-1^{hi} population of PDPN^{+} thymic mesenchyme who's development is dependent on LTβR signaling (Chapter 3). Consistent with *Ltbr$^{-/-}$* mice, there was a significant loss of ICAM-1^{hi}VCAM-1^{hi} PDPN^{+} thymic mesenchyme in *Wnt-1^{cre}Ltbr^{flox}* mice compared to Wnt-1^{cre} controls (Fig 4.8.C.D.). This data confirms the specificity and efficacy of the *Wnt-1^{cre}Ltbr^{flox}* model for targeting LTβR deletion to PDPN^{+} thymic mesenchyme.

To investigate if thymic mesenchyme is required for thymocyte egress the thymocyte populations of *Wnt-1^{cre}Ltbr^{flox}* mice were analyzed. Repeating the analysis that was used for *Ltbr$^{-/-}$* mice revealed no intrathymic accumulation of mature cSP4 or SP8 thymocytes when *Ltbr* was deleted on thymic mesenchyme (Fig 4.9.A-F). This suggests that contrary to our initial hypothesis, which proposed a role for thymic mesenchyme in regulating thymocyte egress in an LTβR-dependent manner, deletion of *Ltbr* on thymic mesenchyme does not impact normal thymocyte egress.

Figure 4.6. Deletion of LTβR On Thymic Mesenchyme Is Not Efficient In *Pdgfrb^{cre}Ltbr^{flox}* Mice

Thymic lobes were harvested from adult mice and enzymatically digested for FACS analysis of stromal populations.

(A) Expression pattern of CD69 and CD62L within CD4^{+}CD8^{-}TCRβ^{hi}CD25^{-}Foxp3^{-} cSP4 thymocytes of control (*Pdgfrb$^{cre/+}$*, left) and mesenchyme specific LTβR-deficient (*Pdgfrb$^{cre/+}$Ltbr$^{fl/fl}$*, right) mice.

(B) Expression pattern of CD69 and CD62L within CD4^{-}CD8^{+}TCRβ^{hi} SP8 thymocytes of *Pdgfrb^{cre}* (left) and *Pdgfrb^{cre}Ltbr^{flox}* (right) mice.

(C) Cell numbers of thymus, cSP4, SP8, CD69^{lo}CD62L^{+} mature cSP4 and CD69^{lo}CD62L^{+} mature SP8 thymocytes were calculated for *Pdgfrb^{cre}* (blue, n=9) and *Pdgfrb^{cre}Ltbr^{flox}* (red, n=9) mice.

(D) Expression of mT and mG within TER119^{-}Viability^{-}CD45^{-}EpCAM-1^{+} thymic epithelial cells (TEC), TER119^{-}Viability^{-}CD45^{-}EpCAM-1^{-}PDPN^{+}CD31^{-} thymic mesenchyme and TER119^{-}Viability^{-}CD45^{-}EpCAM-1^{-}PDPN^{-}CD31^{+} thymic endothelium from *Pdgfrb$^{cre/+}$* mice crossed with mT/mG fate mapper mice (n=10).

(E) Percentage of mT^{-}mG^{+} 'switched' cells within each stroma population.

(F) Deletion of LTβR on PDPN^{+} thymic mesenchyme of *Pdgfrb^{cre},* (blue) *Pdgfrb^{cre}Ltbr^{flox}* (red) and *Ltbr$^{-/-}$* (grey) mice.

The standard error bars display the SEM and a mann-whitney test was performed. All data is typical of 3 independent repeats.

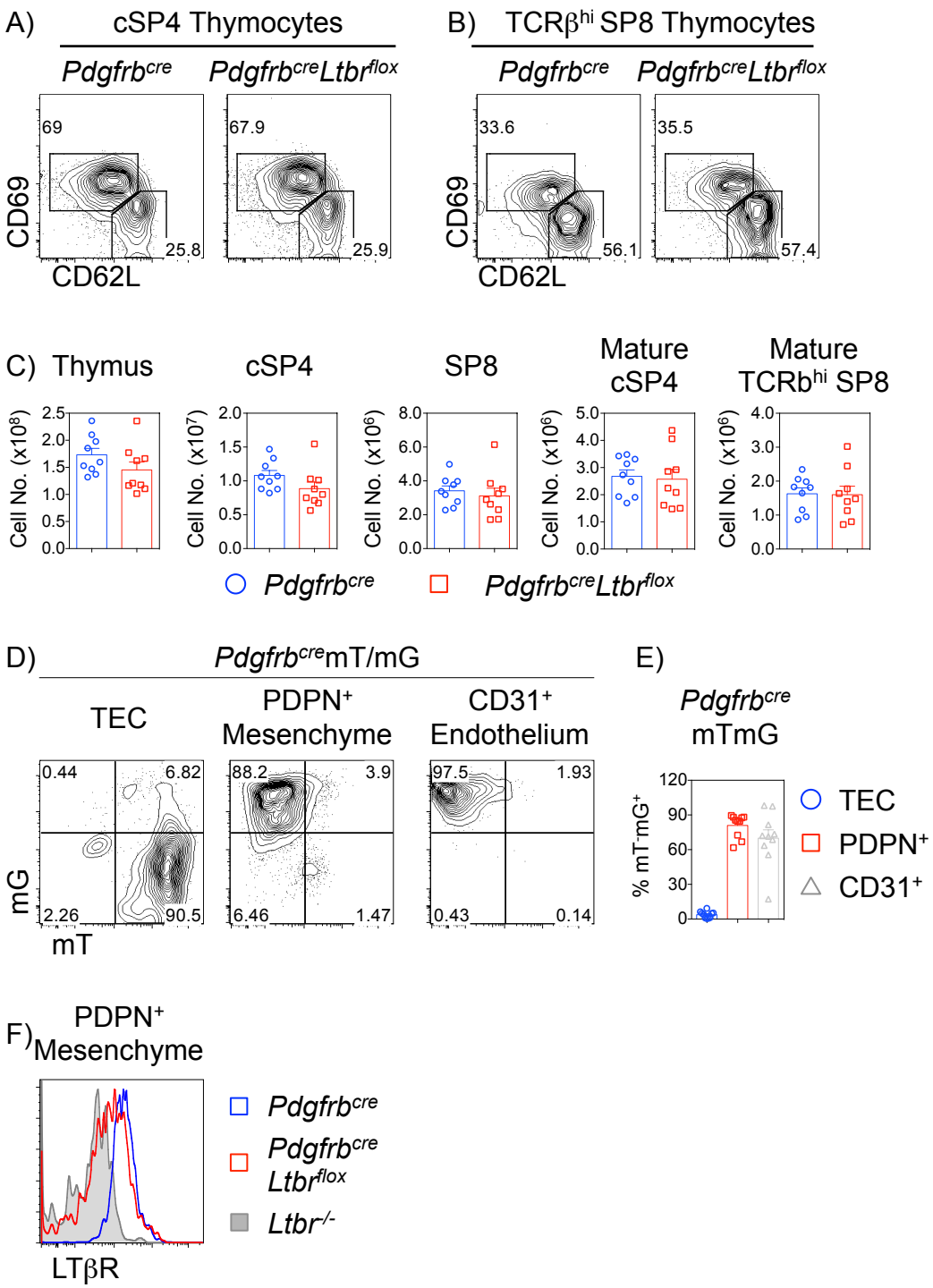
A)
cSP4 Thymocytes
Pdgfrb^cre
Pdgfrb^creLtbr^flox
69
25.8
67.9
25.9
CD69
CD62L
B)
TCRβ^hi SP8 Thymocytes
Pdgfrb^cre
Pdgfrb^creLtbr^flox
33.6
56.1
35.5
57.4
CD69
CD62L
C)
Thymus
cSP4
SP8
Mature cSP4
Mature TCRb^hi SP8
Cell No. (x10^8)
Cell No. (x10^7)
Cell No. (x10^6)
Cell No. (x10^6)
Cell No. (x10^6)
Pdgfrb^cre
Pdgfrb^creLtbr^flox
D)
Pdgfrb^cremT/mG
TEC
PDPN+ Mesenchyme
CD31+ Endothelium
0.44
6.82
2.26
90.5
88.2
3.9
6.46
1.47
97.5
1.93
0.43
0.14
mG
mT
E)
Pdgfrb^cre mTmG
% mT+mG+
TEC
PDPN+
CD31+
F)
PDPN+ Mesenchyme
Pdgfrb^cre
Pdgfrb^cre Ltbr^flox
Ltbr^-/-
LTβR

Figure 4.7. *Wnt-1*^{cre} Specifically Targets PDPN^{+} Thymic Mesenchyme

Thymic lobes were harvested from adult mice and enzymatically digested for FACS analysis of stromal populations.

(A) Expression of mT and mG within TER119^{-}Viability^{-}CD45^{-}EpCAM-1^{+} thymic epithelial cells (TEC), TER119^{-}Viability^{-}CD45^{-}EpCAM-1^{-}PDPN^{+}CD31^{-} thymic mesenchyme and TER119^{-}Viability^{-}CD45^{-}EpCAM-1^{-}PDPN^{-}CD31^{+} thymic endothelium of mT/mG control mice.

(B) Example of gating to identify mT^{+}mG^{-} cells that have not switched and are therefore Cre^{-} and mT^{-}mG^{+} cells that have switched and are Cre^{+}.

(C) Expression of mT and mG within TEC, thymic mesenchyme and CD31^{+} endothelium of *Wnt-1*$^{cre/+}$ mice crossed with mT/mG fate mapper mice (n=9).

(D) Percentage of mT^{-}mG^{+} 'switched' cells within each stroma population.

The standard error bars display the SEM and all data is typical of 3 independent repeats.

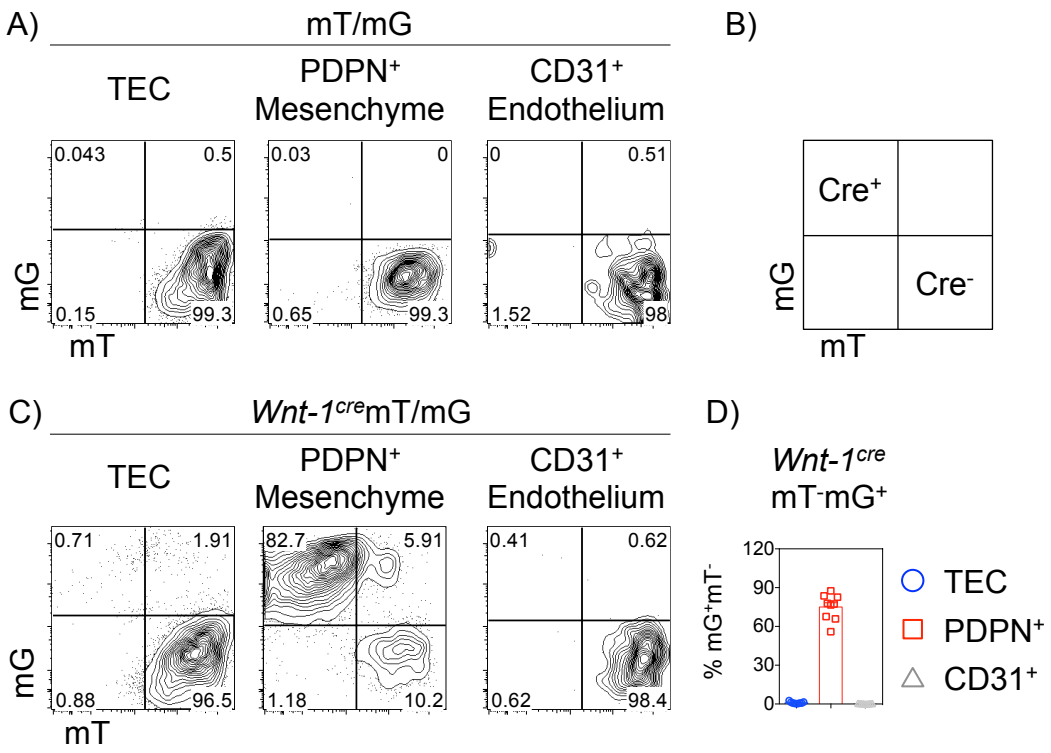
A)
mT/mG
TEC
PDPN+ Mesenchyme
CD31+ Endothelium
0.043
0.5
0.15
99.3
0.03
0
0.65
99.3
0
0.51
1.52
98
mG
mT
B)
Cre+
Cre-
mG
mT
C)
Wnt-1cre mT/mG
TEC
PDPN+ Mesenchyme
CD31+ Endothelium
0.71
1.91
0.88
96.5
82.7
5.91
1.18
10.2
0.41
0.62
0.62
98.4
mG
mT
D)
Wnt-1cre
mT-mG+
% mG+mT-
120
90
60
30
0
TEC
PDPN+
CD31+

Figure 4.8. Targeted Deletion Of *Ltbr* On *Wnt-1^{cre}* Expressing PDPN^{+} Thymic Mesenchyme

Thymic lobes were harvested from adult mice and enzymatically digested for FACS analysis of stromal populations.

(A) Expression of LTβR on TER119^{-}Viability^{-}CD45^{-}EpCAM-1^{+} TEC, TER119^{-}Viability^{-}CD45^{-}EpCAM-1^{-}PDPN^{+}CD31^{-} thymic mesenchyme and TER119^{-}Viability^{-}CD45^{-}EpCAM-1^{-}PDPN^{-}CD31^{+} thymic endothelium on *Wnt-1^{cre}* (blue, n=7) and *Wnt-1^{cre}Ltbr^{flox}* (red, n=9) mice alongside a *Ltbr$^{-/-}$* (grey, n=2) control.

(B) LTβR MFI on TEC, mesenchyme and endothelium of *Wnt-1^{cre}* (blue, n=7) and *Wnt-1^{cre}Ltbr^{flox}* (red, n=9) mice alongside a *Ltbr$^{-/-}$* (grey, n=2) control.

(C) Expression pattern of PDPN and CD31 on TER119^{-}Viability^{-}CD45^{-}EpCAM-1^{-} non-epithelial thymic stroma in *Wnt-1^{cre}* (left) and *Wnt-1^{cre}Ltbr^{flox}* (right) mice.

(D) Expression pattern of ICAM-1 and VCAM-1 on PDPN^{+} thymic mesenchyme from *Wnt-1^{cre}* (left) and *Wnt-1^{cre}Ltbr^{flox}* (right) mice and percentage of ICAM-1^{hi}VCAM-1^{hi} PDPN^{+} thymic mesenchyme.

The standard error bars display the SEM and a mann-whitney test was performed, where *** denotes a significant difference as $p<0.001$. Data of A-C is typical of at least 2 independent repeats and data of D was carried out once.

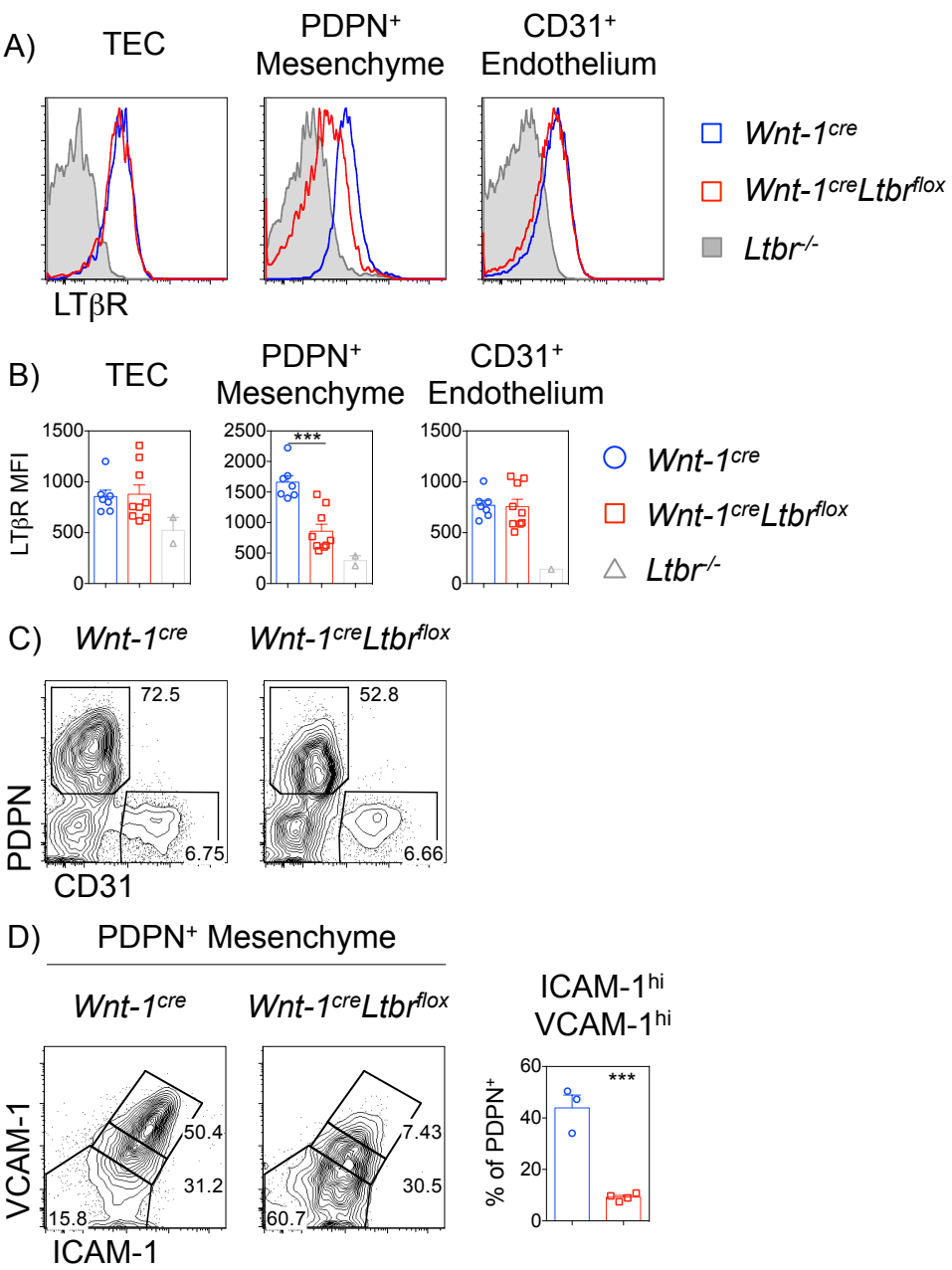
A)
TEC
PDPN+ Mesenchyme
CD31+ Endothelium
LTβR
Wnt-1cre
Wnt-1creLtbrflox
Ltbr-/-
B)
TEC
PDPN+ Mesenchyme
CD31+ Endothelium
LTβR MFI
1500
1000
500
0
2500
2000
1500
1000
500
0
***
1500
1000
500
0
Wnt-1cre
Wnt-1creLtbrflox
Ltbr-/-
C)
Wnt-1cre
Wnt-1creLtbrflox
PDPN
CD31
72.5
6.75
52.8
6.66
D)
PDPN+ Mesenchyme
Wnt-1cre
Wnt-1creLtbrflox
VCAM-1
ICAM-1
50.4
31.2
15.8
7.43
30.5
60.7
ICAM-1hi
VCAM-1hi
% of PDPN+
60
40
20
0
***

Figure 4.9. Deletion of *Ltbr* On Thymic Mesenchyme Does Not Impact Thymocyte Egress

Thymic lobes were harvested from control (*Wnt-1*$^{cre/+}$) and mesenchyme specific LTβR-deficient (*Wnt-1*$^{cre/+}$*Ltbr*$^{fl/fl}$) mice and enzymatically digested for FACS analysis of the thymocyte populations.

(A) Expression pattern of CD4 and CD8 within *Wnt-1*^{cre} (left) and *Wnt-1*^{cre}*Ltbr*^{flox} (right) thymi to identify $CD4^+CD8^-$ SP4, $CD4^+CD8^+$ DP and $CD4^-CD8^+$ SP8 thymocytes.

(B) Cell number of the thymus, cSP4, SP8 and DP thymocytes and percentages of $CD4^+CD8^-$ and $CD4^-CD8^+$ were calculated for *Wnt-1*^{cre} (blue, n=6) and *Wnt-1*^{cre}*Ltbr*^{flox} (red, n=8) mice.

(C) Expression pattern of CD69 and CD62L within cSP4 thymocytes of *Wnt-1*^{cre} (left) and *Wnt-1*^{cre}*Ltbr*^{flox} (right) mice.

(D) Cell numbers and percentages of immature and mature cSP4 thymocytes were calculated for *Wnt-1*^{cre} (blue, n=6) and *Wnt-1*^{cre}*Ltbr*^{flox} (red, n=8) mice.

(E) Expression pattern of CD69 and CD62L within SP8 thymocytes of *Wnt-1*^{cre} (left) and *Wnt-1*^{cre}*Ltbr*^{flox} (right) mice.

(F) Cell numbers and percentages of immature and mature SP8 thymocytes were calculated for *Wnt-1*^{cre} (blue, n=6) and *Wnt-1*^{cre}*Ltbr*^{flox} (red, n=8) mice.

The standard error bars display the SEM and a mann-whitney test was performed. All data is typical of 3 independent repeats.

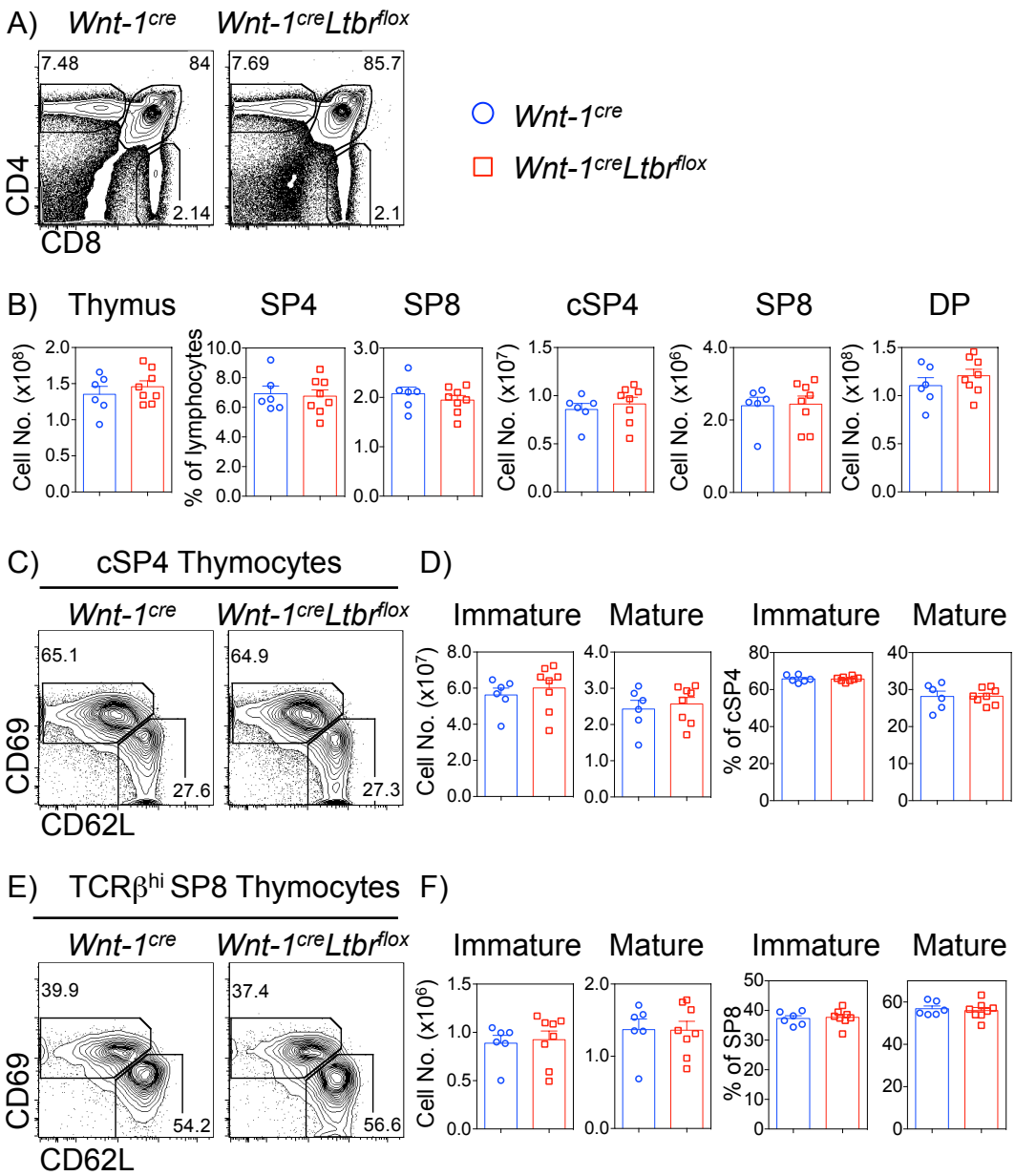
A)
Wnt-1cre
Wnt-1creLtbrflox
7.48
84
2.14
7.69
85.7
2.1
CD4
CD8
Wnt-1cre
Wnt-1creLtbrflox
B)
Thymus
SP4
SP8
cSP4
SP8
DP
Cell No. (x10^8)
% of lymphocytes
Cell No. (x10^7)
Cell No. (x10^6)
Cell No. (x10^8)
C)
cSP4 Thymocytes
D)
Wnt-1cre
Wnt-1creLtbrflox
65.1
27.6
64.9
27.3
CD69
CD62L
Immature
Mature
Immature
Mature
Cell No. (x10^7)
% of cSP4
E)
TCRβhi SP8 Thymocytes
F)
Wnt-1cre
Wnt-1creLtbrflox
39.9
54.2
37.4
56.6
CD69
CD62L
Immature
Mature
Immature
Mature
Cell No. (x10^6)
% of SP8

As our data revealed no role for LTβR expression on thymic mesenchyme for T-cell egress, we attempted to identify which of the remaining stromal populations, TEC or endothelium, is required for LTβR-dependent thymocyte egress. *Ltbr*$^{-/-}$ mice have previously been reported to have an mTEC defect, with a reduction in the population of UEA-1^{+} medullary TEC and a gross disorganization of the medullary architecture (151). Therefore there could be some mechanism that is altered in the absence of normal thymic medulla that is causing a thymocyte egress defect within the *Ltbr*$^{-/-}$ thymus. For this reason we investigated whether LTβR expression on TEC is required for thymocyte egress.

Initially we confirmed the TEC defect of germ-line LTβR knockout mice. Consistent with the initial description of the thymus of LTβR deficient mice, TEC were significantly reduced in *Ltbr*$^{-/-}$ mice (Fig 4.10.A-C). This reduction maps to a reduction of medullary thymic epithelial cells (mTEC) whereas cortical TEC (cTEC) are unaffected (Fig 4.10.A-C). Within the mTEC compartment both CD80^{hi}MHC Class II^{hi} mTEC^{hi} and CD80^{lo}MHC Class II^{lo} mTEC^{lo} are reduced (Fig 4.10.C) and whilst there is a modest reduction of Aire^{+} mTEC^{hi}, there is a substantial reduction of CCL21^{+} mTEC^{lo} consistent with previous reports, however neither population is completely absent (Fig 4.10.C) (156). This data suggests that LTβR plays a key role in the development of both subsets of mTEC and whilst there is a significant reduction in the number of CCL21 expressing mTEC there is not a complete absence which would suggest that CCR7-CCL21 signaling may still occur between thymocytes and mTEC within the LTβR deficient mouse thymus.

Figure 4.10. Absence Of LTβR Signaling Impacts Medullary Thymic Epithelial Cell Development

Thymic lobes were harvested from control (*Ltbr*$^{+/+}$) and LTβR-deficient (*Ltbr*$^{-/-}$) mice and enzymatically digested for FACS analysis of stroma.

(A+B) Identification of CD45^{-}EpCAM-1^{+} thymic epithelial cells (TEC), UEA-1^{+}Ly51^{-} medullary TEC (mTEC), MHC Class II^{hi} (I^{A}I$^{E\ hi}$) CD80^{hi} mTEC^{hi} and I^{A}I$^{E\ lo}$CD80^{lo} mTEC^{lo} cells within *Ltbr*$^{+/+}$ and *Ltbr*$^{-/-}$ mice. Also shown is the expression of Aire and CCL21 within mTEC^{hi} and mTEC^{lo}, respectively.

(C) Cell numbers for thymus, TEC and the different subsets of TEC were calculated for *Ltbr*$^{+/+}$ (blue, n=8) and *Ltbr*$^{-/-}$ (red, n=9) mice.

The standard error bars display the SEM and a mann-whitney test was performed, where * denotes a significant difference as $p<0.05$, ** $p<0.01$ and **** $p<0.0001$. All data is typical of 3 independent repeats.

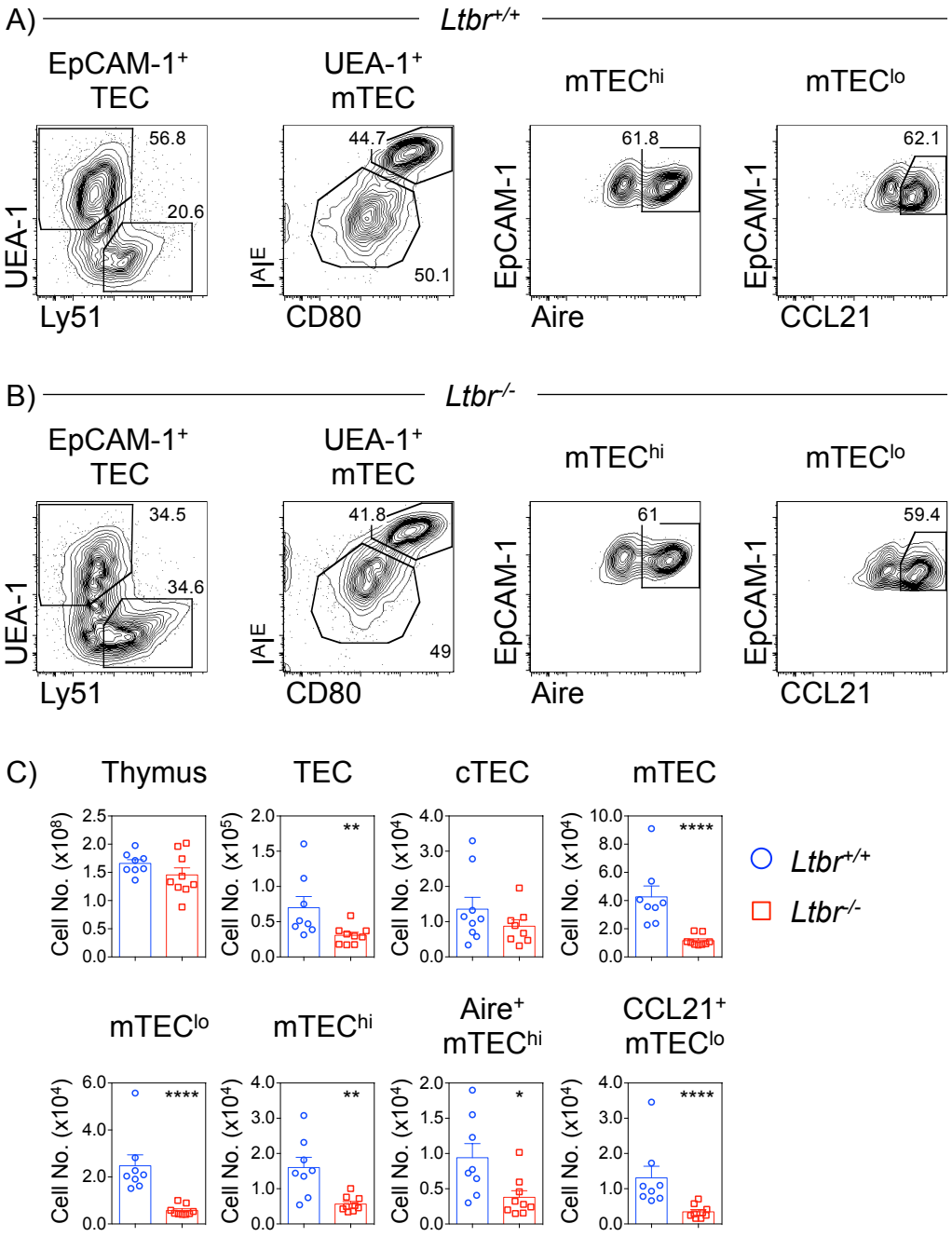
A)
Ltbr+/+
EpCAM-1+ TEC
UEA-1+ mTEC
mTEChi
mTEClo
56.8
20.6
UEA-1
Ly51
44.7
50.1
MHC II
CD80
61.8
EpCAM-1
Aire
62.1
EpCAM-1
CCL21
B)
Ltbr-/-
EpCAM-1+ TEC
UEA-1+ mTEC
mTEChi
mTEClo
34.5
34.6
UEA-1
Ly51
41.8
49
MHC II
CD80
61
EpCAM-1
Aire
59.4
EpCAM-1
CCL21
C)
Thymus
TEC
cTEC
mTEC
Cell No. (x10^8)
Cell No. (x10^5)
Cell No. (x10^4)
**
****
Ltbr+/+
Ltbr-/-
mTEClo
mTEChi
Aire+ mTEChi
CCL21+ mTEClo
****
**
*
****

In addition to flow cytometric analysis, immunofluorescence microscopy was carried out to determine the medullary organization of *Ltbr*$^{-/-}$ mice by staining for ER-TR5 to identify the medulla and CD8 to identify the cortex. CD8 is expressed by $CD4^+CD8^+$ DP thymocytes within the cortex and $CD4^-CD8^+$ SP8 thymocytes within the medulla, however due to the much higher frequency of DP compared to SP8 thymocytes within the thymus CD8 can be used to identify the cortex. Visually it is clear that *Ltbr*$^{-/-}$ mice lack the normal distribution and organization of few, large medullary areas that are characteristic of the steady state thymus and instead have a large number of small medullary areas (Fig 4.11.A.). To quantify this difference in the frequency of differing sizes the area of each ER-TR5$^+$ medullary area was calculated and recorded into three size categories: $<0.1mm^2$, $<0.1mm^2$-$0.5mm^2$ and $\geq 0.5mm^2$. This analysis revealed that *Ltbr*$^{-/-}$ thymi has significantly more medullary areas that are $<0.1mm^2$ and $<0.1mm^2$-$0.5mm^2$ and significantly fewer large ($\geq 0.5mm^2$) medullas (Fig 4.11.B.). Therefore this analysis highlights a key role of LTβR signaling for development of mTEC and medullary organization.

To separate the disorganization phenotype of the *Ltbr*$^{-/-}$ mice we investigated the mature SP thymocyte population within *plt/plt* mice, which lack CCL19 and CCL21 and have a known medullary disorganization phenotype (69,266). Consistent with the previous description of these mice there was no observable intrathymic accumulation of mature thymocytes (Fig 4.12.) (69). This suggested that disorganization of the medulla alone is not sufficient to alter thymocyte egress.

Figure 4.11. Absence Of LTβR Signaling Impacts Medullary Thymic Epithelial Cell Organization

Thymic lobes were harvested from control (*Ltbr*$^{+/+}$) and LTβR-deficient (*Ltbr*$^{-/-}$) mice and snap-frozen on dry ice. Lobes were then cut 7μm thick and stained for immunofluorescence microscopy.

(A) Thymic sections of *Ltbr*$^{+/+}$ (left) and *Ltbr*$^{-/-}$ (right) were stained with ER-TR5 to identify the medulla (red) and CD8 to identify the cortex (green). Scale bars indicated 500μm.

(B) The area of each medulla was measured by drawing round the medullas of thymic sections taken from different depths of the thymic tissue to ensure an accurate average number of medullary areas was calculated. Areas from *Ltbr*$^{+/+}$ (blue, n=3) and *Ltbr*$^{-/-}$ (red, n=3) were sorted into three categories: $<0.1mm^2$, $<0.1mm^2$-$0.5mm^2$ and $\geq 0.5mm^2$.

The standard error bars display the SEM and a parametric T-test was performed, where * denotes a significant difference as $p<0.05$ and ** $p<0.01$. All data is typical of 3 independent repeats, each repeat is an average of quantitation of 3 thymic sections.

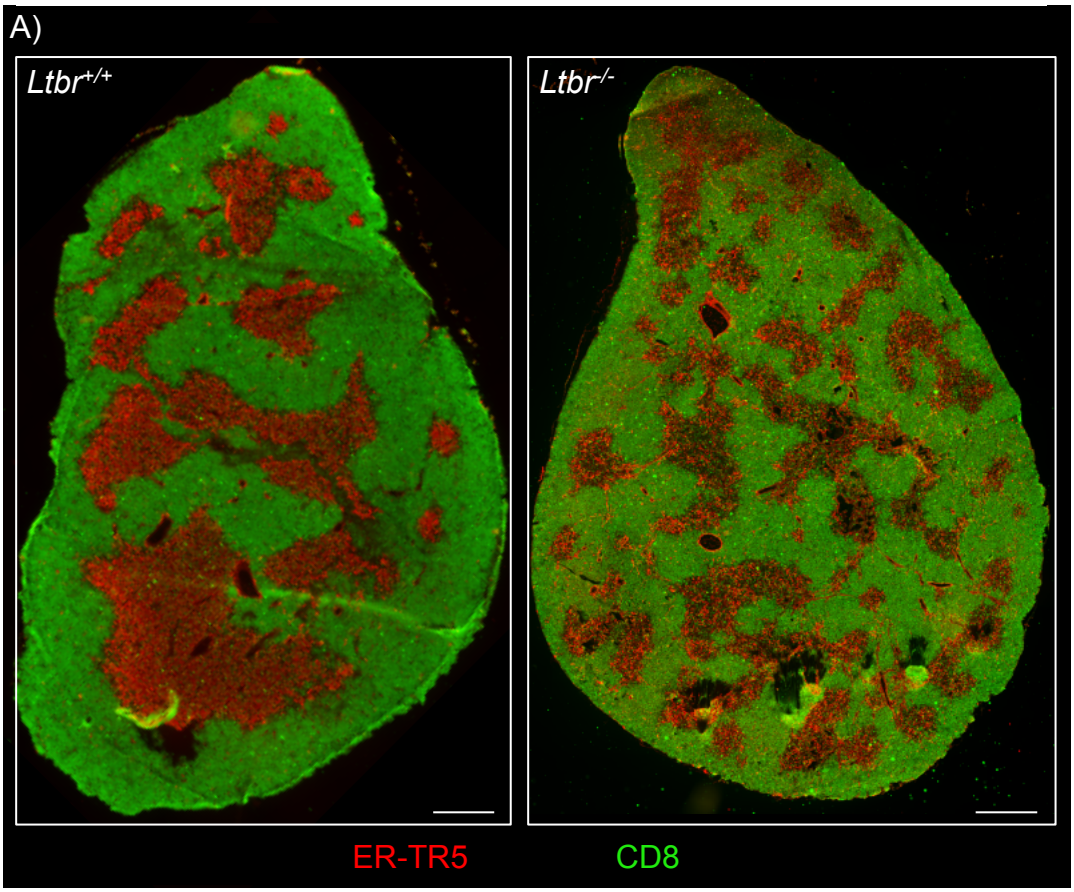
A)
Ltbr+/+
Ltbr-/-
ER-TR5
CD8
B)
No. of medullary areas
25.0
20.0
15.0
10.0
5.0
0.0
*
*
**
<0.1
<0.1-0.5
≥0.5
Area (mm2) of medulla
Ltbr+/+
Ltbr-/-

Figure 4.12. CCR7 Ligands Are Not Essential For Thymocyte Egress

Thymic lobes were harvested from WT and *plt/plt* adult mice and enzymatically digested for FACs analysis.

(A) Expression pattern of CD4 and CD8 within WT (left) and *plt/plt* (right) thymi to identify $CD4^+CD8^-$ SP4, $CD4^+CD8^+$ DP and $CD4^-CD8^+$ SP8 thymocytes.

(B) Cell number of the thymus, cSP4 and SP8 thymocytes and percentages of $CD4^+CD8^-$ and $CD4^-CD8^+$ were calculated for WT (blue, n=6) and *plt/plt* (red, n=6) mice.

(C) Expression pattern of CD69 and CD62L within cSP4 thymocytes of WT (blue, n=6) and *plt/plt* (red, n=6) mice.

(D) Cell numbers and percentages of immature and mature cSP4 thymocytes were calculated for WT (blue, n=6) and *plt/plt* (red, n=6) mice.

(E) Expression pattern of CD69 and CD62L within SP8 thymocytes of WT (blue, n=6) and *plt/plt* (red, n=6) mice.

(F) Cell numbers and percentages of immature and mature SP8 thymocytes were calculated for WT (blue, n=6) and *plt/plt* (red, n=6) mice.

The standard error bars display the SEM and a mann-whitney test was performed, where ** denotes significant difference as $p<0.01$. All data is typical of 2 independent repeat.

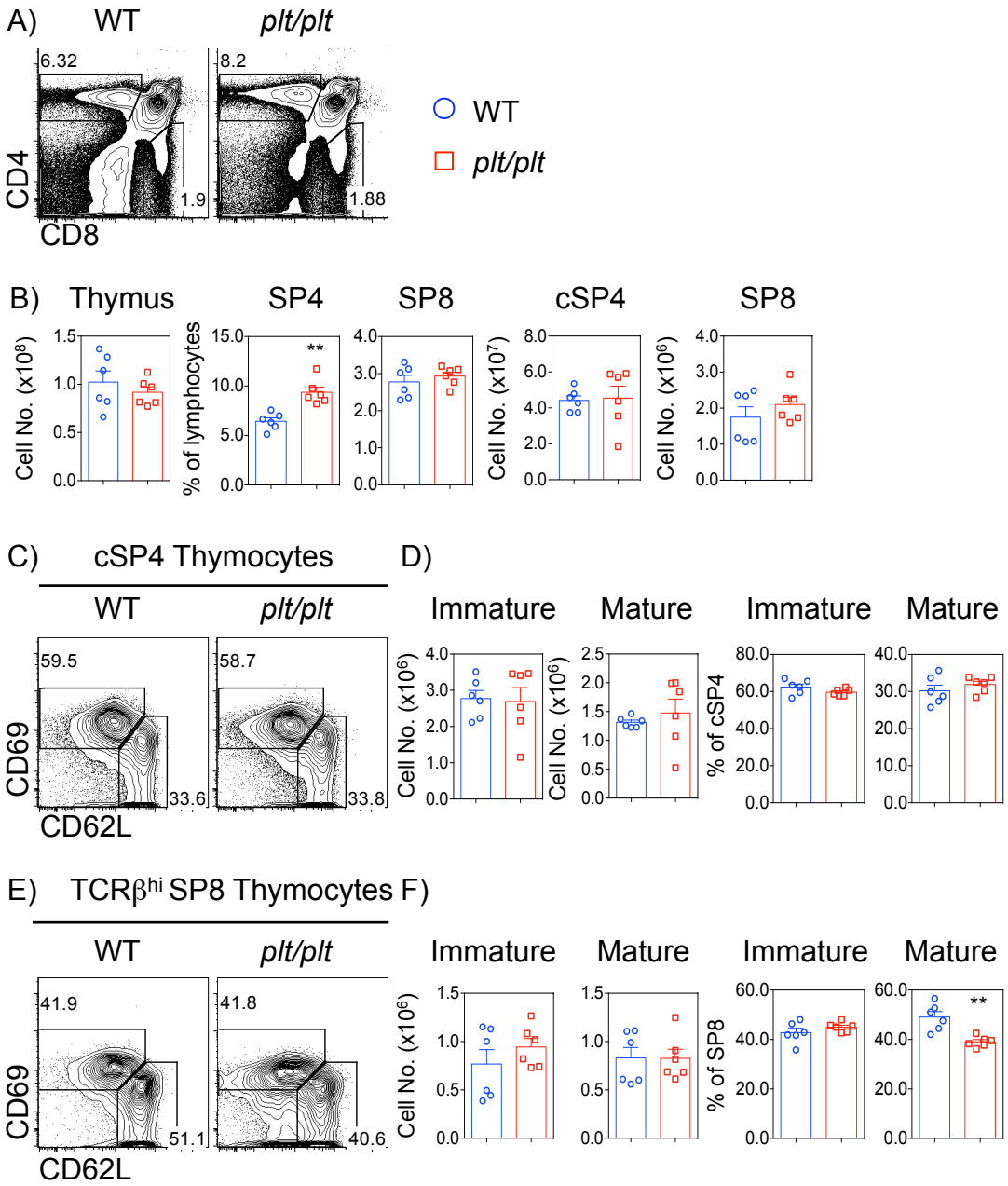
A)
WT
plt/plt
6.32
8.2
CD4
CD8
1.9
1.88
WT
plt/plt
B)
Thymus
SP4
SP8
cSP4
SP8
Cell No. (x10⁸)
% of lymphocytes
Cell No. (x10⁷)
Cell No. (x10⁶)
**
C)
cSP4 Thymocytes
D)
WT
plt/plt
Immature
Mature
Immature
Mature
59.5
58.7
CD69
CD62L
33.6
33.8
Cell No. (x10⁶)
Cell No. (x10⁶)
% of cSP4
E)
TCRβhi SP8 Thymocytes
F)
WT
plt/plt
Immature
Mature
Immature
Mature
41.9
41.8
CD69
CD62L
51.1
40.6
Cell No. (x10⁶)
% of SP8
**

To investigate the role of LTβR expression by TEC in thymocyte egress, *Ltbr* was deleted on TEC by crossing the TEC-specific Cre mouse model *Foxn-1*$^{cre/+}$ with *Ltbr*$^{fl/fl}$ mice (243). LTβR deletion was specific and efficient within the *Foxn-1*^{cre}*Ltbr*^{flox} mice, where only TEC had a significant loss of LTβR expression and the expression was similar to an *Ltbr*$^{-/-}$ used as a staining control (Fig 4.13.A.B.). Consistent with germ line *Ltbr*$^{-/-}$ mice, *Foxn-1*^{cre}*Ltbr*^{flox} mice have reduced numbers of TEC which map to a loss of both mTEC^{hi} and mTEC^{lo}, as well as a small decrease in Aire^{+} mTEC^{hi} and significant loss of CCL21^{+} mTEC^{lo} (Fig 4.13.C.). Whilst CCL21^{+} mTEC^{lo} are significantly reduced, they are not absent, consistent with *Ltbr*$^{-/-}$ mice (Fig 4.13.C.). In addition to this, the medullary disorganization that was prevalent in *Ltbr*$^{-/-}$ mice was also present in *Foxn-1*^{cre}*Ltbr*^{flox} mice, where *Ltbr* deletion on TEC resulted in an increased frequency of smaller medullas (<0.1mm^2 and <0.1mm^2-0.5mm^2) and significantly fewer large medullas (≥0.5mm^2) (Fig 4.14.A.B.). These data indicate that the *Foxn-1*^{cre}*Ltbr*^{flox} mouse model phenocopies *Ltbr*$^{-/-}$ mice and is therefore suitable to investigate the role of TEC in regulating LTβR-dependent T-cell egress.

Thymocytes were isolated from *Foxn-1*^{cre} and *Foxn-1*^{cre}*Ltbr*^{flox} mice and stained for analysis of immature and mature cSP4 and SP8 thymocytes. There was no increase in the number or percentages of immature or mature cSP4 and SP8 thymocytes when *Ltbr* was deleted on TEC (Fig 4.15.A-F). Surprisingly there was a very modest, but significant, reduction in the percentage of CD4^{-}CD8^{+} thymocytes, however this was not matched by a loss of the cell number of these cells (Fig 4.15.B.). Therefore, despite the clear similarities of the medullary defect of the *Ltbr*$^{-/-}$ and the

Figure 4.13. Targeted Deletion Of LTβR on Foxn-1^{cre} Expressing TEC Results In Reduced mTEC

Thymic lobes were harvested from control (*Foxn-1$^{cre/+}$*), thymic epithelial specific LTβR-deficient (*Foxn-1$^{cre/+}$Ltbr$^{fl/fl}$*) and *Ltbr$^{-/-}$* mice and enzymatically digested for stromal analysis by FACS.

A) Expression of LTβR on TER119^{-}Viability^{-}CD45^{-}EpCAM-1^{+} TEC, TER119^{-}Viability^{-}CD45^{-}EpCAM-1^{-}PDPN^{+}CD31^{-} thymic mesenchyme and TER119^{-}Viability^{-}CD45^{-}EpCAM-1^{-}PDPN^{-}CD31^{+} thymic endothelium on *Foxn-1^{cre}* (blue, n=6) and *Foxn-1^{cre}Ltbr^{flox}* (red, n=6) mice alongside a *Ltbr$^{-/-}$* (grey, n=3) control.

B) LTβR MFI on TEC, mesenchyme and endothelium of *Foxn-1^{cre}* (blue, n=6) and *Foxn-1^{cre}Ltbr^{flox}* (red, n=6) mice alongside a *Ltbr$^{-/-}$* (grey, n=3) control.

C) Cell numbers of thymus, CD45^{-}EpCAM-1^{+} thymic epithelial cells (TEC), UEA-1^{-}Ly51^{+} cortical TEC (cTEC), UEA-1^{+}Ly51^{-} medullary TEC (mTEC), MHC Class II^{hi} (I^{A}I^{E} ^{hi}) CD80^{hi} mTEC^{hi} and I^{A}I^{E} ^{lo}CD80^{lo} mTEC^{lo} were calculated as well as the number of Aire^{+} mTEC^{hi} and CCL21^{+}mTEC^{lo} from *Foxn-1^{cre}* (blue, n=12) and *Foxn-1^{cre}Ltbr^{flox}* (red, n=12) mice.

The standard error bars display the SEM and a mann-whitney test was performed, where * denotes a significant difference as $p<0.05$, ** as $p<0.01$ *** $p<0.001$ and **** $p<0.0001$. All data is typical of 3 independent repeats.

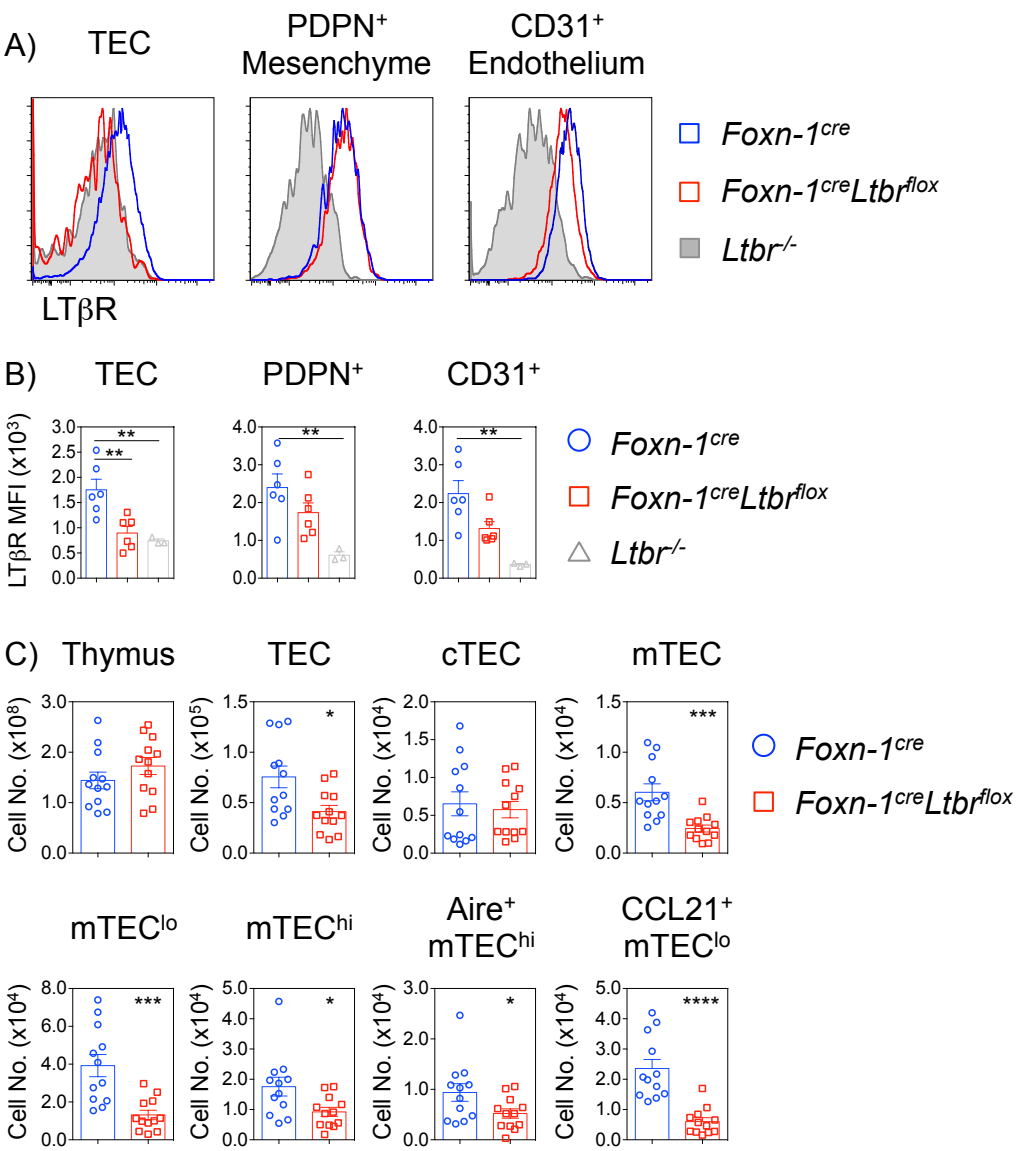
A)
TEC
PDPN+ Mesenchyme
CD31+ Endothelium
LTβR
Foxn-1cre
Foxn-1creLtbrflox
Ltbr-/-
B)
TEC
PDPN+
CD31+
LTβR MFI (x10³)
Foxn-1cre
Foxn-1creLtbrflox
Ltbr-/-
C)
Thymus
TEC
cTEC
mTEC
Cell No. (x10⁸)
Cell No. (x10⁵)
Cell No. (x10⁴)
mTEClo
mTEChi
Aire+ mTEChi
CCL21+ mTEClo
Foxn-1cre
Foxn-1creLtbrflox

Figure 4.14. Absence Of LTβR On Thymic Epithelial Cells Impacts Medullary Thymic Epithelial Cell Organization

Thymic lobes were harvested from control (*Foxn-1*$^{cre/+}$) and thymic epithelial specific LTβR-deficient (*Foxn-1*$^{cre/+}$*Ltbr*$^{fl/fl}$) mice and snap-frozen on dry ice. Lobes were then cut 7μm thick and stained for immunofluorescence microscopy.

A) Thymic sections of *Foxn-1*^{cre} (left) and *Foxn-1*^{cre}*Ltbr*^{flox} (right) were stained with ER-TR5 to identify the medulla (red) and CD8 to identify the cortex (green). Scale bars indicated 500μm.

B) The area of each medulla was measured by drawing round the medullas of thymic sections taken from different depths of the thymic tissue to ensure an accurate average number of medullary areas was calculated. Areas from *Foxn-1*^{cre} (blue, n=3) and *Foxn-1*^{cre}*Ltbr*^{flox} (red, n=3) were sorted into three categories: <0.1mm^2, <0.1mm^2-0.5mm^2 and ≥0.5mm^2.

The standard error bars display the SEM and a parametric T-test was performed, where * denotes a significant difference as $p<0.05$ and ** $p<0.01$. All data is typical of 3 independent repeats, each repeat is an average of quantitation of 3 thymic sections.

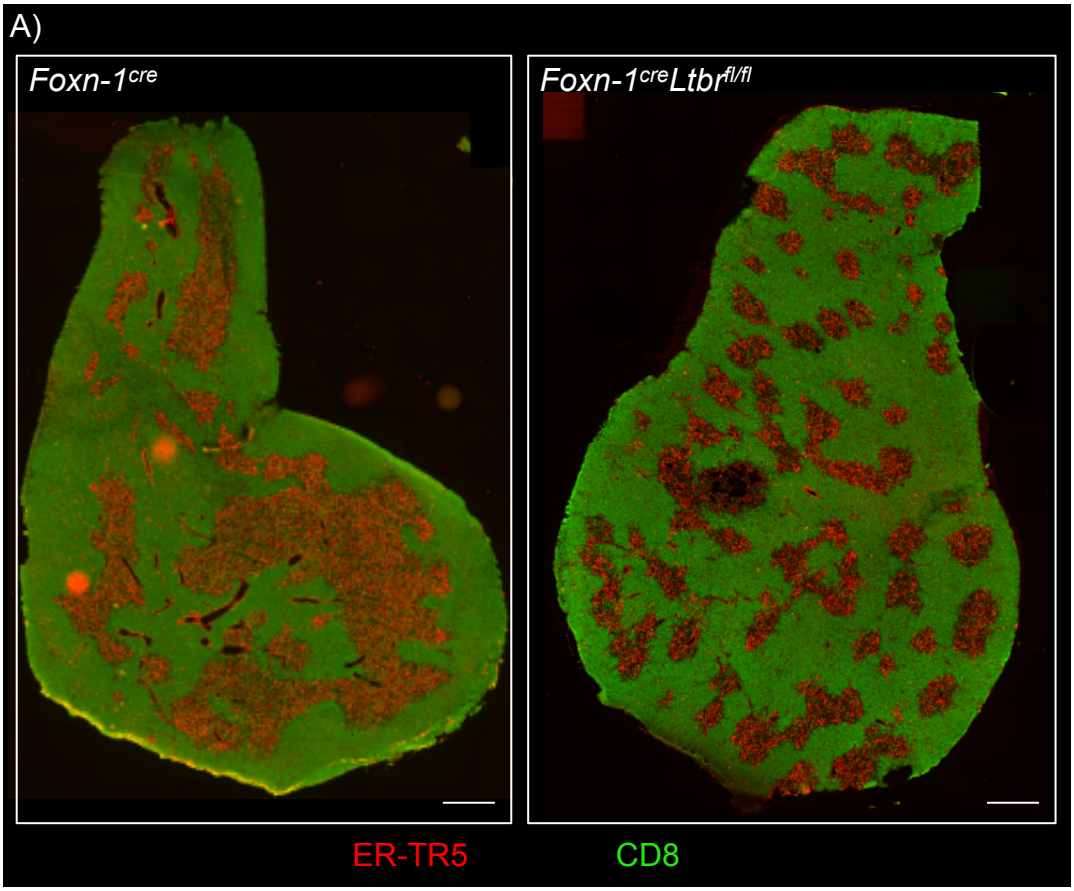
A)
Foxn-1cre
Foxn-1creLtbrfl/fl
ER-TR5
CD8
B)
No. of medullary areas
25.0
20.0
15.0
10.0
5.0
0.0
*
**
*
<0.1
<0.1-0.5
≥0.5
Area (mm2) of medulla
Foxn-1cre
Foxn-1creLtbrfl/fl

Figure 4.15. Deletion of LTβR On Thymic Epithelial Cells Does Not Impact Thymocyte Egress

Thymic lobes were harvested from control (*Foxn-1*$^{cre/+}$) and mesenchyme specific LTβR-deficient (*Foxn-1*$^{cre/+}$*Ltbr*$^{fl/fl}$) mice and enzymatically digested for FACS analysis of the thymocyte populations.

(A) Expression pattern of CD4 and CD8 within *Foxn-1*^{cre} (left) and *Foxn-1*^{cre}*Ltbr*^{flox} (right) thymi to identify $CD4^+CD8^-$ SP4, $CD4^+CD8^+$ DP and $CD4^-CD8^+$ SP8 thymocytes.

(B) Cell number of the thymus, cSP4, SP8 and DP thymocytes and percentages of $CD4^+CD8^-$ and $CD4^-CD8^+$ were calculated for *Foxn-1*^{cre} (blue, n=15) and *Foxn-1*^{cre}*Ltbr*^{flox} (red, n=14) mice.

(C) Expression pattern of CD69 and CD62L within cSP4 thymocytes of *Foxn-1*^{cre} (left) and *Foxn-1*^{cre}*Ltbr*^{flox} (right) mice.

(D) Cell numbers and percentages of immature and mature cSP4 thymocytes were calculated for *Foxn-1*^{cre} (blue, n=15) and *Foxn-1*^{cre}*Ltbr*^{flox} (red, n=14) mice.

(E) Expression pattern of CD69 and CD62L within SP8 thymocytes of *Foxn-1*^{cre} (left) and *Foxn-1*^{cre}*Ltbr*^{flox} (right) mice.

(F) Cell numbers and percentages of immature and mature SP8 thymocytes were calculated for *Foxn-1*^{cre} (blue, n=15) and *Foxn-1*^{cre}*Ltbr*^{flox} (red, n=14) mice.

The standard error bars display the SEM and a mann-whitney test was performed, where * denotes a significant difference as $p<0.05$. All data is typical of 4 independent repeats.

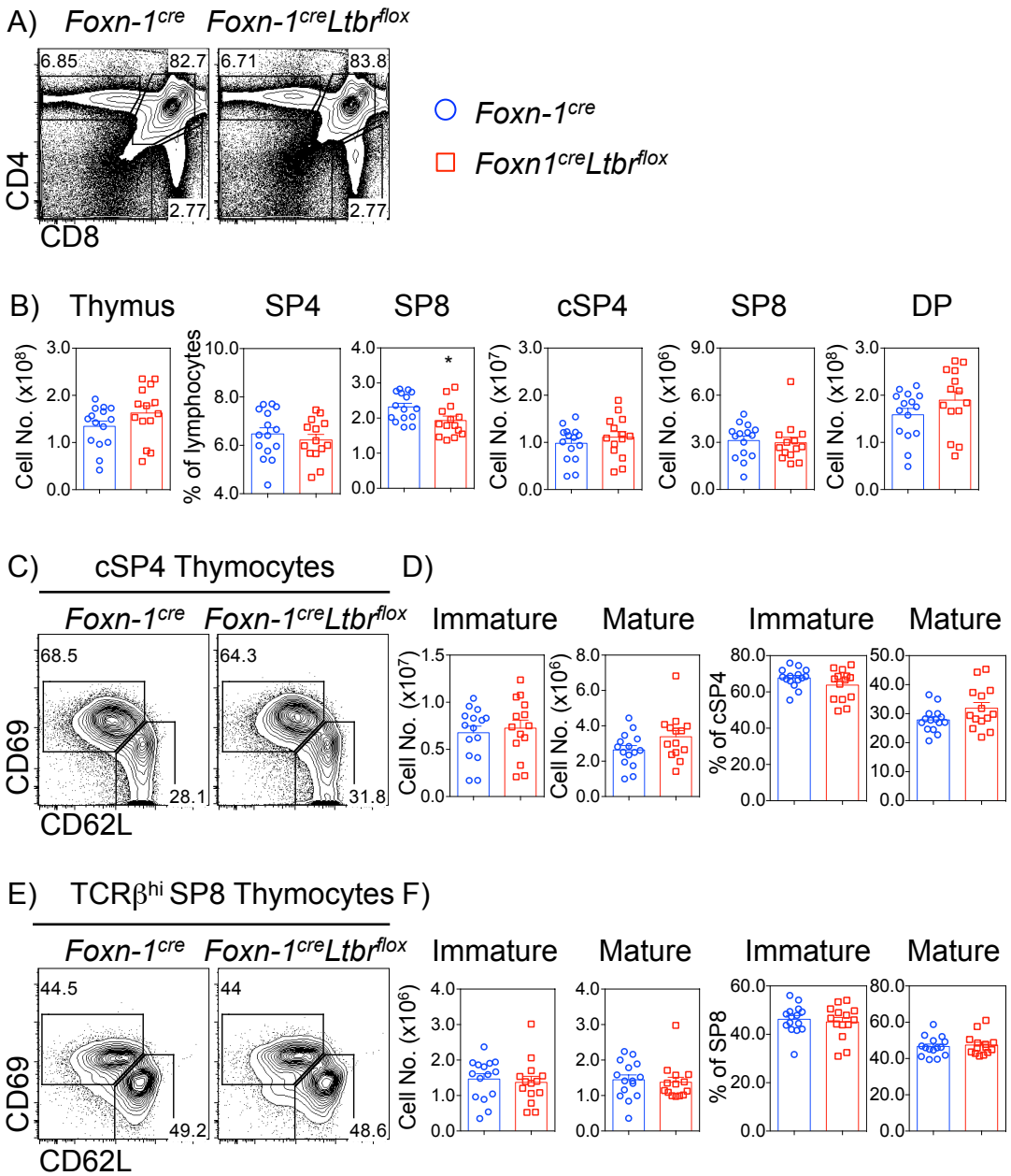
A)
Foxn-1cre
Foxn-1creLtbrflox
6.85
82.7
2.77
6.71
83.8
2.77
CD4
CD8
Foxn-1cre
Foxn1creLtbrflox
B)
Thymus
SP4
SP8
cSP4
SP8
DP
Cell No. (x10^8)
% of lymphocytes
Cell No. (x10^7)
Cell No. (x10^6)
Cell No. (x10^8)
*
C)
cSP4 Thymocytes
D)
Foxn-1cre
Foxn-1creLtbrflox
68.5
28.1
64.3
31.8
CD69
CD62L
Immature
Mature
Immature
Mature
Cell No. (x10^7)
Cell No. (x10^6)
% of cSP4
E)
TCRβhi SP8 Thymocytes
F)
Foxn-1cre
Foxn-1creLtbrflox
44.5
49.2
44
48.6
CD69
CD62L
Immature
Mature
Immature
Mature
Cell No. (x10^6)
% of SP8

Foxn-1^{cre}*Ltbr*^{flox} mice, there was no intrathymic accumulation when *Ltbr* was deleted on TEC and therefore LTβR-dependent thymocyte egress is not regulated by TEC.

So far these analyses have ruled out a role for thymic mesenchyme and thymic epithelium in regulating thymocyte egress through the LTβR pathway, leaving thymic endothelial cells to be investigated. Previous studies have shown thymic endothelium can regulate thymocytes egress, which is logical based on the fact that endothelial cells represent the final barrier to egressing thymocytes to leave the thymus and enter the blood. Additionally thymic endothelial cells regulate LTβR-dependent T-cell progenitor entry (22,24).

As with the TEC and mesenchyme specific models of LTβR deletion, the Cre/LoxP approach was taken to delete *Ltbr* on thymic endothelial cells. The *Tie2*^{cre} model was chosen as previous studies have shown it to be suitable to target deletion to endothelial cells (244). Analysis of *Tie2*^{cre}*Ltbr*^{flox} thymocytes revealed no alteration to the SP4 or SP8 thymocyte percentages nor did they have an intrathymic accumulation of mature cSP4 of SP8 thymocytes (Fig 4.16.A-C.). To ensure that the *Tie2*^{cre} was efficiently and specifically targeting thymic endothelial cells, *Tie2*^{cre} mice were crossed with mT/mG mice. Analysis of the stroma of these mice revealed that whilst *Tie2*^{cre} was specific to thymic endothelial cells, only 27.7% (± 6.83%) of thymic endothelium expressed Cre (Fig 4.16.D.E.). Consistent with the *Tie2*^{cre}mT/mG data there was inefficient deletion of LTβR on CD31^{+} thymic endothelium within *Tie2*^{cre}*Ltbr*^{flox} mice (Fig 4.16.F.). These data further support our previous conclusion that the efficiency and specificity of Cre mouse models need to be scrutinized to

ensure the correct conclusions are being made about data acquired through their use.

Following the inefficiency of the *Tie2*^{cre} an alternative endothelial-specific Cre was chosen. Previous studies have had success at targeting gene deletion to endothelial cells by using the endothelial-specific *Flk-1*$^{cre/+}$ mouse strain (245). *Flk-1*^{cre} mice were crossed with mT/mG mice to check the specificity of the *Flk-1*^{cre}, revealing that 97.7% (± 0.48%) of thymic endothelium is Cre^{+} (Fig 4.17.A-D). *Flk-1*^{cre} mice were then crossed to *Ltbr*^{flox} mice and the thymic stromal populations were stained for LTβR to check for deletion (Fig 4.17.E). There was efficient deletion of LTβR on thymic endothelium, which was reduced to levels similar to *Ltbr*$^{-/-}$ mice (Fig 4.17.E.F.). There was a slight reduction of LTβR on thymic mesenchyme, however this reduction was not comparable to *Ltbr*$^{-/-}$ suggesting deletion of LTβR is occurring mainly within the endothelial compartment (Fig 4.17.E.F.). Therefore, unlike the *Tie2*^{cre}*Ltbr*^{flox} model, the *Flk-1*^{cre}*Ltbr*^{flox} model is a suitable method of deleting *Ltbr* on thymic endothelial cells to look at the impact on thymocyte egress. However a caveat of using endothelial cell Cre models, including the Flk-1^{cre} strain, is that the Cre is also present in hematopoietic cell due to sharing an upstream precursor (245). However our BMC analysis has ruled out a role of LTβR expression by hematopoietic cells for thymocyte egress and therefore this should not impact our findings (Figure 4.5.).

Thymocytes were isolated from *Flk-1*^{cre}*Ltbr*^{flox} and stained to examine the immature and mature fractions of cSP4 and SP8 thymocytes as performed previously. Interestingly there was a large increase in the total number and percentage of cSP4

Figure 4.16. Inefficient And Non-Specific Targeting Of Thymic Endothelium By *Tie2^{cre}*

Thymic lobes were harvested from adult mice and enzymatically digested for FACS analysis of thymocytes populations

(A) Expression pattern of CD69 and CD62L within cSP4 thymocytes of control (*Tie2$^{cre/+}$*, left) and endothelial specific LTβR-deficient (*Tie2$^{cre/+}$Ltbr$^{fl/fl}$*, right) mice.

(B) Expression pattern of CD69 and CD62L within SP8 thymocytes of *Tie2^{cre}* (left) and *Tie2^{cre}Ltbr^{flox}* (right) mice.

(C) Cell numbers of thymus, mature cSP4 and mature SP8 thymocytes were calculated for *Tie2^{cre}* (blue, n=6) and *Tie2^{cre}Ltbr^{flox}* (red, n=6) mice.

(D) Expression of mT and mG within TEC, thymic mesenchyme and thymic endothelium from *Tie2$^{cre/+}$*mice crossed with mT/mG fate mapper mice.

(E) Percentage of $mT^{-}mG^{+}$ 'switched' cells within each stroma population (n=4).

(F) Expression of LTβR on thymic endothelium in *Tie2$^{cre/+}$Ltbr$^{fl/fl}$* mice.

The standard error bars display the SEM and a mann-whitney test was performed. All data is typical of 2 independent repeats.

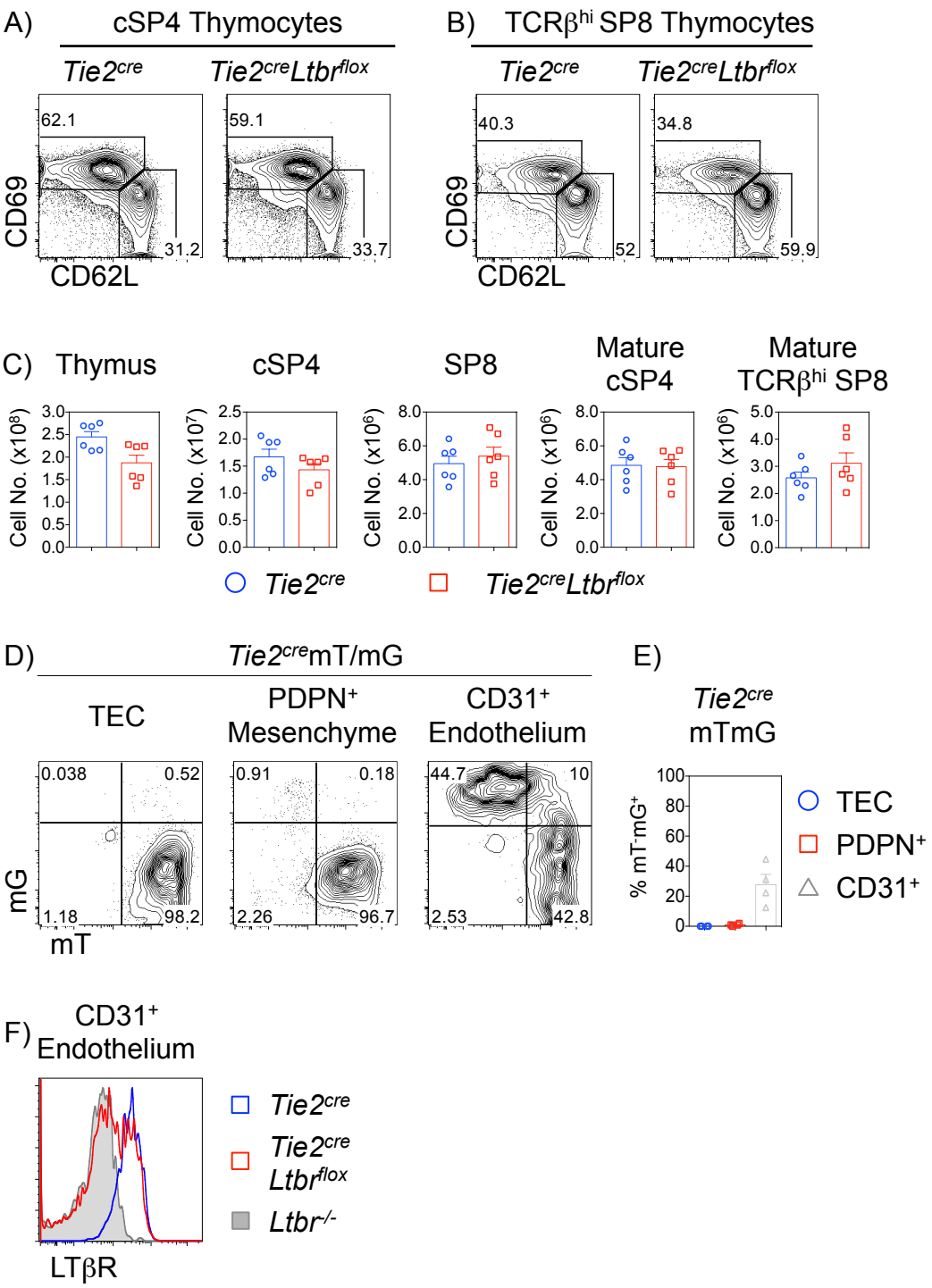
A)
cSP4 Thymocytes
Tie2cre
Tie2creLtbrflox
62.1
31.2
59.1
33.7
CD69
CD62L
B)
TCRβhi SP8 Thymocytes
Tie2cre
Tie2creLtbrflox
40.3
52
34.8
59.9
CD69
CD62L
C)
Thymus
cSP4
SP8
Mature cSP4
Mature TCRβhi SP8
Cell No. (x10^8)
Cell No. (x10^7)
Cell No. (x10^6)
Cell No. (x10^6)
Cell No. (x10^6)
Tie2cre
Tie2creLtbrflox
D)
Tie2cremT/mG
TEC
PDPN+ Mesenchyme
CD31+ Endothelium
0.038
0.52
1.18
98.2
0.91
0.18
2.26
96.7
44.7
10
2.53
42.8
mG
mT
E)
Tie2cre mTmG
% mT+mG+
TEC
PDPN+
CD31+
F)
CD31+ Endothelium
Tie2cre
Tie2cre Ltbrflox
Ltbr-/-
LTβR

Figure 4.17. Targeted Deletion Of LTβR On Flk-1^{cre} Expressing CD31^{+} Thymic Endothelium

Thymic lobes were harvested from adult mice and enzymatically digested for FACS analysis of stromal populations

(A) Expression of mT and mG within TER119^{-}Viability^{-}CD45^{-}EpCAM-1^{+} thymic epithelial cells (TEC), TER119^{-}Viability^{-}CD45^{-}EpCAM-1^{-}PDPN^{+}CD31^{-} thymic mesenchyme and TER119^{-}Viability^{-}CD45^{-}EpCAM-1^{-}PDPN^{-}CD31^{+} thymic endothelium of mT/mG control mice.

(B) Example of gating to identify mT^{+}mG^{-} cells that have not switched and are therefore Cre^{-} and mT^{-}mG^{+} cells that have switched and are Cre^{+}.

(C) Expression of mT and mG within TEC, thymic mesenchyme and CD31^{+} endothelium of *Flk-1$^{cre/+}$* mice crossed with mT/mG fate mapper mice (n=13).

(D) Percentage of mT^{-}mG^{+} 'switched' cells within each stroma population.

(E) Expression of LTβR on TEC, thymic mesenchyme and thymic endothelium of *Flk-1^{cre}* (blue, n=6) and *Flk-1^{cre}Ltbr^{flox}* (red, n=5) mice alongside a *Ltbr$^{-/-}$* (grey, n=2) control.

(F) LTβR MFI on TEC, mesenchyme and endothelium of *Flk-1^{cre}* (blue, n=6) and *Flk-1^{cre}Ltbr^{flox}* (red, n=5) mice alongside a *Ltbr$^{-/-}$* (grey, n=2) control.

The standard error bars display the SEM and a mann-whitney test was performed, where * denotes a significant difference as $p<0.05$ and ** denotes $p<0.01$. Data of A-D is typical of 3 independent experiments and data of E-F is typical of 2 independent experiments.

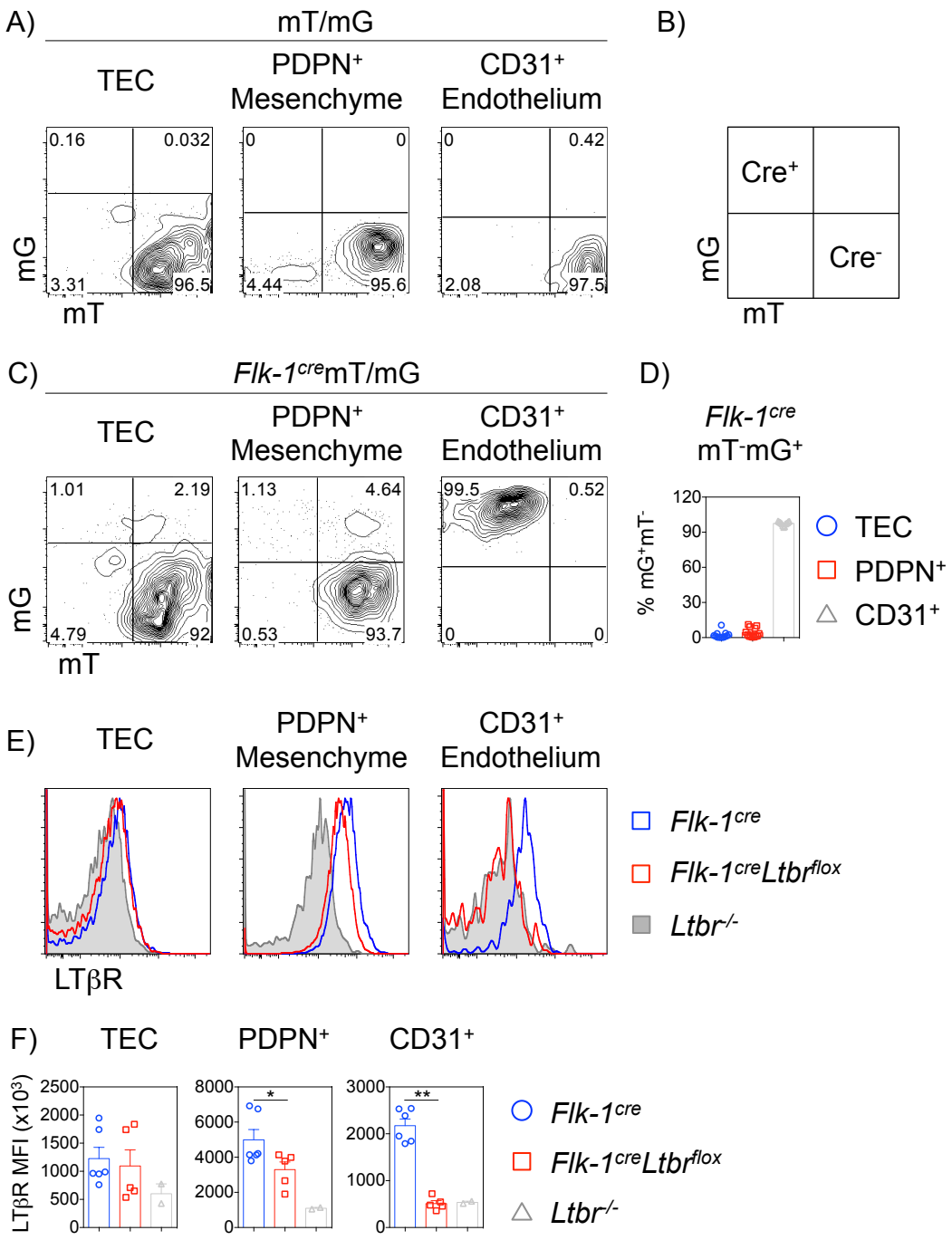
A)
mT/mG
TEC
PDPN+ Mesenchyme
CD31+ Endothelium
0.16
0.032
3.31
96.5
0
0
4.44
95.6
0
0.42
2.08
97.5
mG
mT
B)
Cre+
Cre-
mG
mT
C)
Flk-1cremT/mG
TEC
PDPN+ Mesenchyme
CD31+ Endothelium
1.01
2.19
4.79
92
1.13
4.64
0.53
93.7
99.5
0.52
0
0
mG
mT
D)
Flk-1cre
mT-mG+
% mG+mT-
120
90
60
30
0
TEC
PDPN+
CD31+
E)
TEC
PDPN+ Mesenchyme
CD31+ Endothelium
LTβR
Flk-1cre
Flk-1creLtbrflox
Ltbr-/-
F)
TEC
PDPN+
CD31+
LTβR MFI (x10³)
2500
2000
1500
1000
500
0
8000
6000
4000
2000
0
*
3000
2000
1000
0
**
Flk-1cre
Flk-1creLtbrflox
Ltbr-/-

and SP8 thymocytes within the *Flk-1^{cre}Ltbr^{flox}* mice compared to *Flk-1^{cre}* controls (Fig 4.18.A.B.). Importantly, this increase mapped specifically to the mature fraction of both cSP4 and SP8 populations (Fig 4.18.C-F.). Therefore this data suggests there is an essential role of LTβR expressing thymic endothelial cells in regulating thymocyte egress. Additionally, the phenotype seen within the *Flk-1^{cre}Ltbr^{flox}* mice may be more severe than the germline *Ltbr$^{-/-}$* mice as there is a significant increase in the total number and percentage of cSP4 and SP8 thymocytes that was not present in *Ltbr$^{-/-}$* mice (Fig 4.2.B.; Fig 4.18.B.).

A recent study identified a population of thymic endothelial cells, termed thymic portal endothelial cells (TPEC), whose development is dependent on LTβR signaling (24). This population of P-selectin^{+} (CD62p) Ly6C^{-} thymic endothelium are absent in *Ltbr$^{-/-}$* and have been proposed to be essential for LTβR-dependent ETP entry into the thymus (24). Interestingly this population is also reduced in the *Flk^{cre}Ltbr^{flox}* mice and LTβR is absent on all three sub-populations of endothelium (CD62p^{+}Ly6C^{-}, CD62p^{+}Ly6C^{+} and CD62p^{-}Ly6C^{+}) (Fig 4.19.A-E). Consistent with *Ltbr$^{-/-}$* mice, the total number of CD31^{+} endothelium is not altered in *Flk^{cre}Ltbr^{flox}* mice (Fig 4.19.D). This loss of portal endothelial cells that regulate T-cell progenitor entry correlates nicely with the increased intrathymic accumulation of mature thymocytes and therefore could suggest a potential mechanism by which LTβR is regulating thymocyte egress.

Ltbr$^{-/-}$ and *Flk-1^{cre}Ltbr^{flox}* mice both displayed an intrathymic accumulation of mature thymocytes and to investigate how this block in thymocyte egress is occurring we

Figure 4.18. Deletion of LTβR On Thymic Endothelial Cells Results In A Significant Intrathymic Accumulation Of Mature SP4 Thymocytes

Thymic lobes were harvested from control (*Flk-1*$^{cre/+}$) and mesenchyme specific LTβR-deficient (*Flk-1*$^{cre/+}$*Ltbr*$^{fl/fl}$) mice and enzymatically digested for FACS analysis of the thymocyte populations.

(A) Expression pattern of CD4 and CD8 within *Flk-1*^{cre} (left) and *Flk-1*^{cre}*Ltbr*^{flox} (right) thymi to identify $CD4^+CD8^-$ SP4, $CD4^+CD8^+$ DP and $CD4^-CD8^+$ SP8 thymocytes.

(B) Cell number of the thymus, cSP4, SP8 and DP thymocytes and percentages of $CD4^+CD8^-$ and $CD4^-CD8^+$ were calculated for *Flk-1*^{cre} (blue, n=6) and *Flk-1*^{cre}*Ltbr*^{flox} (red, n=4) mice.

(C) Expression pattern of CD69 and CD62L within cSP4 thymocytes of *Flk-1*^{cre} (left) and *Flk-1*^{cre}*Ltbr*^{flox} (right) mice.

(D) Cell numbers and percentages of immature and mature cSP4 thymocytes were calculated for *Flk-1*^{cre} (blue, n=6) and *Flk-1*^{cre}*Ltbr*^{flox} (red, n=4) mice.

(E) Expression pattern of CD69 and CD62L within SP8 thymocytes of *Flk-1*^{cre} (left) and *Flk-1*^{cre}*Ltbr*^{flox} (right) mice.

(F) Cell numbers and percentages of immature and mature SP8 thymocytes were calculated for *Flk-1*^{cre} (blue, n=6) and *Flk-1*^{cre}*Ltbr*^{flox} (red, n=4) mice.

The standard error bars display the SEM and a mann-whitney test was performed, where * denotes a significant difference as $p<0.05$ and ** denotes $p<0.01$. All data is typical of 2 independent repeats.

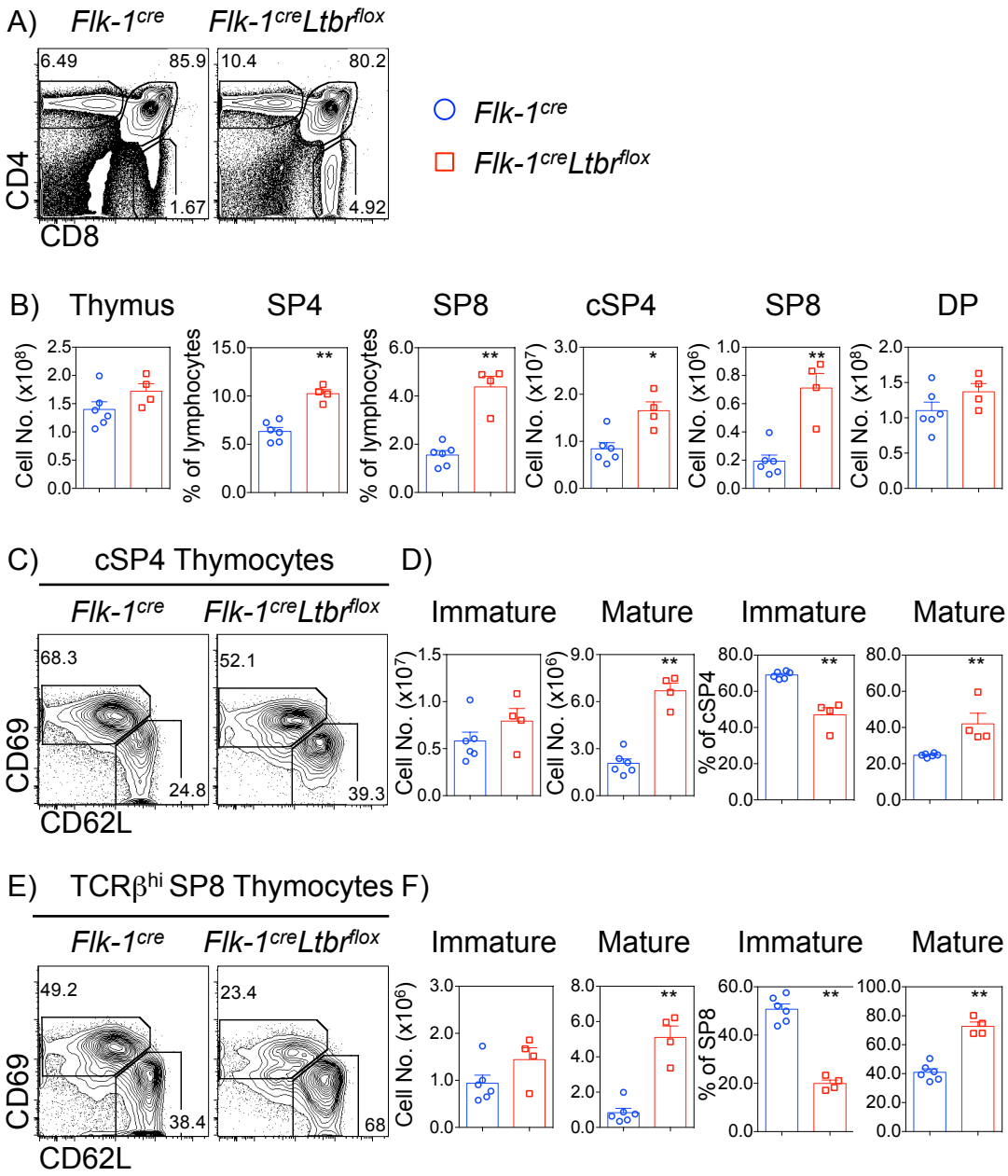
A)
Flk-1cre
Flk-1creLtbrflox
6.49
85.9
1.67
10.4
80.2
4.92
CD4
CD8
Flk-1cre
Flk-1creLtbrflox
B)
Thymus
SP4
SP8
cSP4
SP8
DP
Cell No. (x10^8)
% of lymphocytes
% of lymphocytes
Cell No. (x10^7)
Cell No. (x10^6)
Cell No. (x10^8)
C)
cSP4 Thymocytes
D)
Flk-1cre
Flk-1creLtbrflox
68.3
24.8
52.1
39.3
CD69
CD62L
Immature
Mature
Immature
Mature
Cell No. (x10^7)
Cell No. (x10^6)
% of cSP4
E)
TCRβhi SP8 Thymocytes
F)
Flk-1cre
Flk-1creLtbrflox
49.2
38.4
23.4
68
CD69
CD62L
Immature
Mature
Immature
Mature
Cell No. (x10^6)
% of SP8

Figure 4.19. Targeted Deletion Of LTβR On Flk-1^{cre} Expressing Endothelial Cells Causes Specific Loss Of Thymic Portal Endothelial Cells

Thymic lobes were harvested from adult mice and enzymatically digested for FACS analysis of stromal populations.

(A) Expression pattern of CD62p and Ly6C on TER119$^-$Viability$^-$CD45$^-$EpCAM-1$^-$ PDPN$^-$CD31$^+$ thymic endothelium of *Ltbr*$^{+/+}$, *Ltbr*$^{-/-}$, *Flk-1*^{cre} and *Flk*^{cre}*Ltbr*^{flox} mice.

(B) Expression of LTβR on CD62p$^+$Ly6C$^-$, CD62p$^+$Ly6C$^+$ and CD62p$^-$Ly6C$^+$ thymic endothelium of *Flk-1*^{cre} and *Flk*^{cre}*Ltbr*^{flox} mice alongside *Ltbr*$^{-/-}$ control mice.

(C) LTβR MFI on CD62p$^+$Ly6C$^-$, CD62p$^+$Ly6C$^+$ and CD62p$^-$Ly6C$^+$ thymic endothelium of *Flk-1*^{cre} (blue, n=6) and *Flk*^{cre}*Ltbr*^{flox} (red, n=5) mice alongside *Ltbr*$^{-/-}$ control (grey, n=2) mice.

(D) The cell number and percentage of CD31$^+$ thymic endothelium within TER119$^-$ Viability$^-$CD45$^-$EpCAM-1$^-$ non-epithelial stroma (NES) was calculated for *Flk-1*^{cre} (blue, n=6) and *Flk*^{cre}*Ltbr*^{flox} (red, n=5) mice.

(E) The percentage of CD62p$^+$Ly6C$^-$, CD62p$^+$Ly6C$^+$ and CD62p$^-$Ly6C$^+$ populations with CD31$^+$ thymic endothelium was calculated for *Flk-1*^{cre} (blue, n=6) and *Flk*^{cre}*Ltbr*^{flox} (red, n=5) mice.

The standard error bars display the SEM and a mann-whitney test was performed, where ** denotes a significant difference as $p<0.01$. All data is typical of 2 independent repeats.

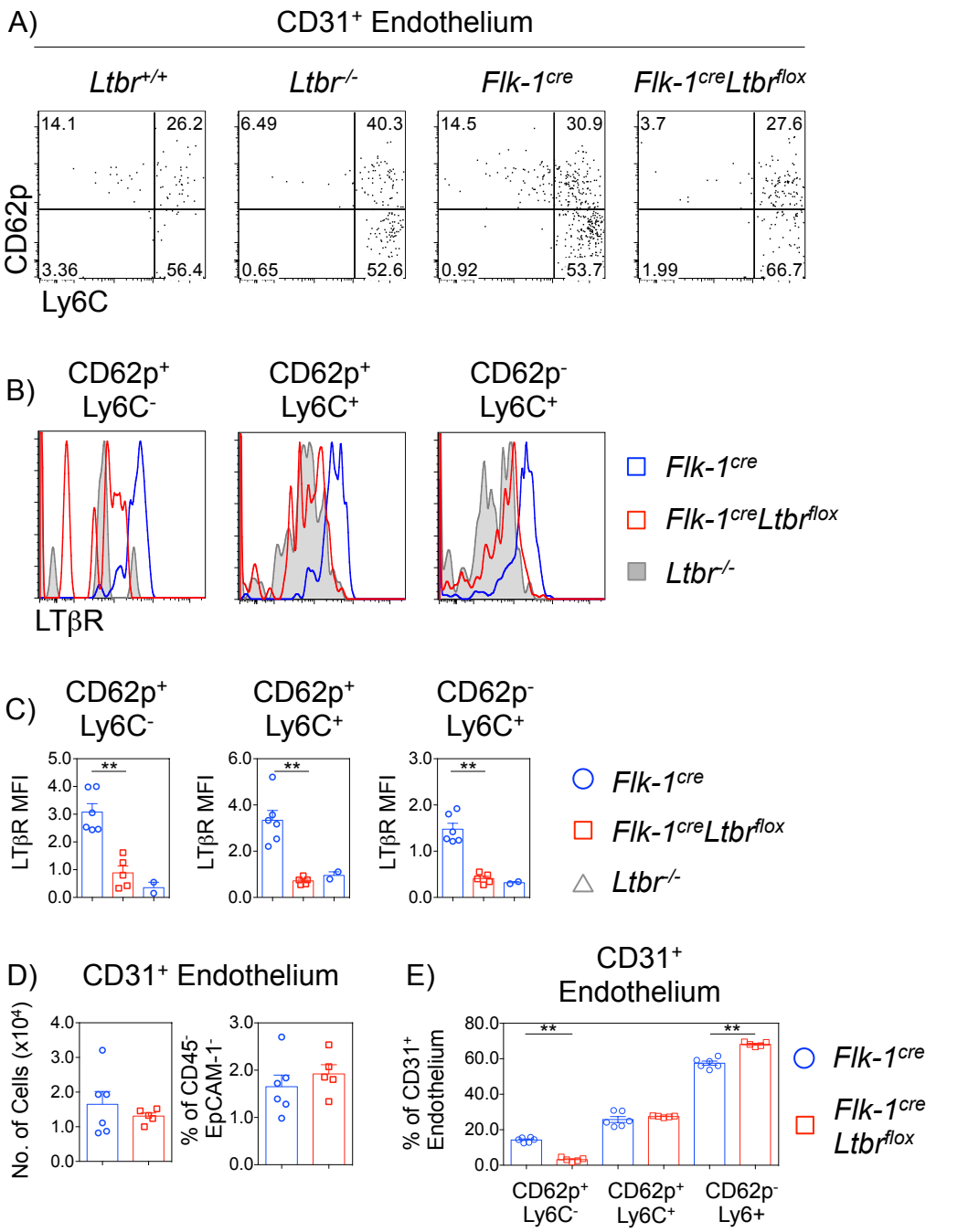
A)
CD31+ Endothelium
Ltbr+/+
Ltbr-/-
Flk-1cre
Flk-1creLtbrflox
CD62p
Ly6C
14.1
26.2
3.36
56.4
6.49
40.3
0.65
52.6
14.5
30.9
0.92
53.7
3.7
27.6
1.99
66.7
B)
CD62p+ Ly6C-
CD62p+ Ly6C+
CD62p- Ly6C+
LTβR
Flk-1cre
Flk-1creLtbrflox
Ltbr-/-
C)
CD62p+ Ly6C-
CD62p+ Ly6C+
CD62p- Ly6C+
LTβR MFI
**
Flk-1cre
Flk-1creLtbrflox
Ltbr-/-
D)
CD31+ Endothelium
No. of Cells (x10⁴)
% of CD45- EpCAM-1-
E)
CD31+ Endothelium
% of CD31+ Endothelium
CD62p+ Ly6C-
CD62p+ Ly6C+
CD62p- Ly6+
Flk-1cre
Flk-1cre Ltbrflox

sought to identify where within the thymus the mature thymocytes are being held. Mice with a thymocyte egress defect/block are often associated with a build up of cells within the perivascular space (PVS), a location within the thymus that exists between perivascular cells and the endothelium of the blood vessels that the perivascular cells surround (111). In instances of PVS accumulation, thymocytes are stuck at the last checkpoint of exit and are not able to enter the blood stream (111). Unlike mice with an intrathymic accumulation of mature thymocytes and an accompanying PVS accumulation as reported in *Il4ra*$^{-/-}$ mice, *Ltbr*$^{-/-}$ do not show any signs of a PVS accumulation (Fig 4.20.A.B.). Perivascular TR7^{+} mesenchyme tightly surround CD31^{+} thymic endothelial cells, with no obvious accumulation of thymocytes in the space between the two basement membranes (Fig 4.20.A.B.). Consistent with this, the same phenotype was observed in *Flk-1*^{cre}*Ltbr*^{flox} mice suggesting that accumulating thymocytes are not located in the PVS (Fig 21.A.B.).

Another method of measuring cells within the PVS that are in the process of egressing the thymus is through the use of I.V. injecting an anti-CD4 antibody to label SP4 thymocytes in contact with the blood (111). This technique has been previously used to identify PVS accumulations by showing an increase in the percentage of cells labeled with the I.V. administered anti-CD4 antibody (IV CD4^{+} cells) (111). Anti-CD4 injection labels a very small fraction of cells within WT mice, which is reduced in WT mice treated with FTY720 to block entry into the PVS (Fig 4.22.A.). *Ltbr*$^{+/+}$ and *Ltbr*$^{-/-}$ mice were injected with the anti-CD4 antibody and, consistent with the immunofluorescence microscopy, there was no increase of IV CD4^{+} cells within *Ltbr*$^{-/-}$ mice (Fig 4.22.B.). Surprisingly there was actually a decrease in the percentage of IV

$CD4^+$ labeled cells and potentially a reduction in number within *Ltbr*$^{-/-}$ mice suggesting that mature cells are struggling to enter the PVS highlighting a potential role of LTβR in thymocyte entry to the PVS (Fig 4.22.B.). The same experiment and analysis were carried out on *Flk-1*^{cre}*Ltbr*^{flox} mice and consistent with *Ltbr*$^{-/-}$ thymic, endothelial specific deletion of *Ltbr* resulted in a similar reduction in the percentage and a significant reduction in the number of IV $CD4^+$ cells (Fig 4.22.C.). These data highlight a role for LTβR in controlling thymocyte entry into the PVS and suggests this could be linked to the thymocyte egress defect found within these mice. Additionally it suggests that this role is carried out by thymic endothelium.

After identifying endothelial cells as the essential population for regulating LTβR-dependent thymocyte egress what remained to investigate was the mechanism through which LTβR is regulating thymocyte egress. The sphingosine-1-phosphate (S1P) pathway is regarded as the primary mechanism of thymocyte egress and is regulated by multiple cell types through the action of enzymes that are required for S1P production or reduction to maintain an S1P gradient that directs thymocyte egress (111,112,114). It has yet to be investigated whether LTβR signaling plays a role in regulating the S1P pathway. To investigate this, stromal cells were isolated from 2-dGuo-treated FTOC lobes stimulated with agonistic anti-LTβR antibody. PCR analysis was carried out for genes associated with the S1P pathway including S1P degrading enzyme *Sgpl1* and dephosphorylating enzyme *Ppap2b*, which reduce the amount of S1P. *Spns2* and *Sphk1*, which are required for the production of S1P, were also included in the analysis. This analysis revealed that *Sgpl1*, *Sphk1* and *Spns2* (to a lesser extent) are increased on total thymic stroma following LTβR

Figure 4.20. *Ltbr*$^{-/-}$ Mice Do Not Have Perivascular Accumulations

Thymic lobes were harvested from control (*Ltbr*$^{+/+}$) and LTβR-deficient (*Ltbr*$^{-/-}$) mice and snap-frozen on dry ice. Lobes were then cut 7μm thick and stained for immunofluorescence microscopy.

(A) Thymic sections of *Ltbr*$^{+/+}$ thymi were stained with CD8 (blue), TR7 (red), CD31 (green) and DAPI (grey). Scale bars indicated a scale of 10μm. Single color images are shown as well as composite images of all colors with (bottom right) or without (top right) DAPI.

(B) Thymi sections of *Ltbr*$^{-/-}$ thymi were stained with CD8 (blue), TR7 (red), CD31 (green) and DAPI (grey). Scale bars indicated a scale of 10μm. Single color images are shown as well as composite images of all colors with (bottom right) or without (top right) DAPI.

Data is representative of 2 mice.

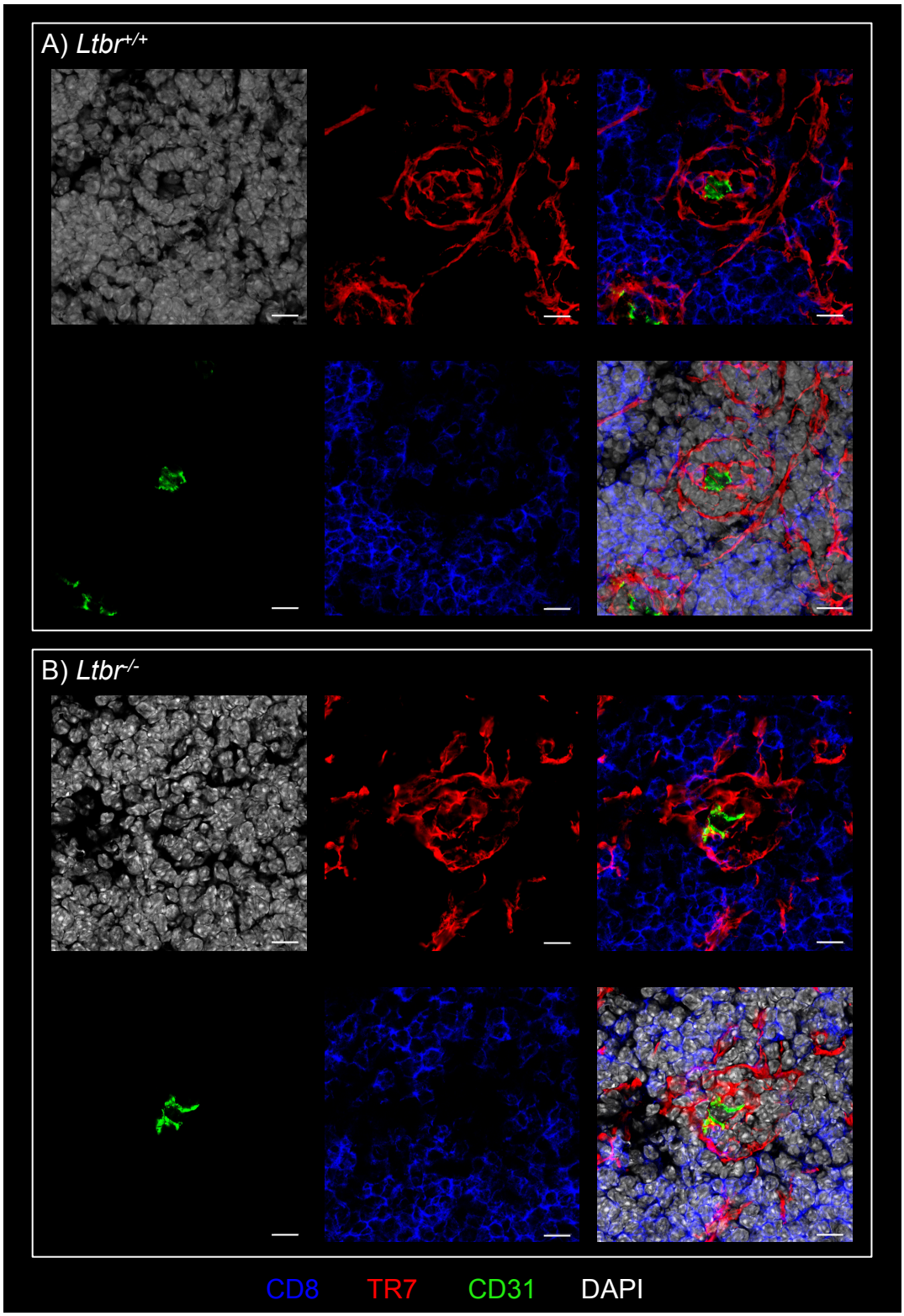
A) Ltbr+/+
B) Ltbr-/-
CD8
TR7
CD31
DAPI

Figure 4.21. *Flk-1^{cre}LtbR^{flox}* Mice Do Not Have Perivascular Accumulations

Thymic lobes were harvested from control (*Flk-1$^{cre/+}$*) and endothelial specific LTβR-deficient (*Flk-1$^{cre/+}$Ltbr$^{fl/fl}$*) mice and snap-frozen on dry ice. Lobes were then cut 7μm thick and stained for immunofluorescence microscopy.

(A) Thymic sections of *Flk-1^{cre}* thymi were stained with CD8 (blue), TR7 (red), CD31 (green) and DAPI (grey). Scale bars indicated a scale of 20μm. Single color images are shown as well as composite images of all colors with (bottom right) or without (top right) DAPI.

(B) Thymi sections of *Flk-1^{cre}Ltbr^{flox}* thymi were stained with CD8 (blue), TR7 (red), CD31 (green) and DAPI (grey). Scale bars indicated a scale of 20μm. Single color images are shown as well as composite images of all colors with (bottom right) or without (top right) DAPI.

Data is representative of 2 mice.

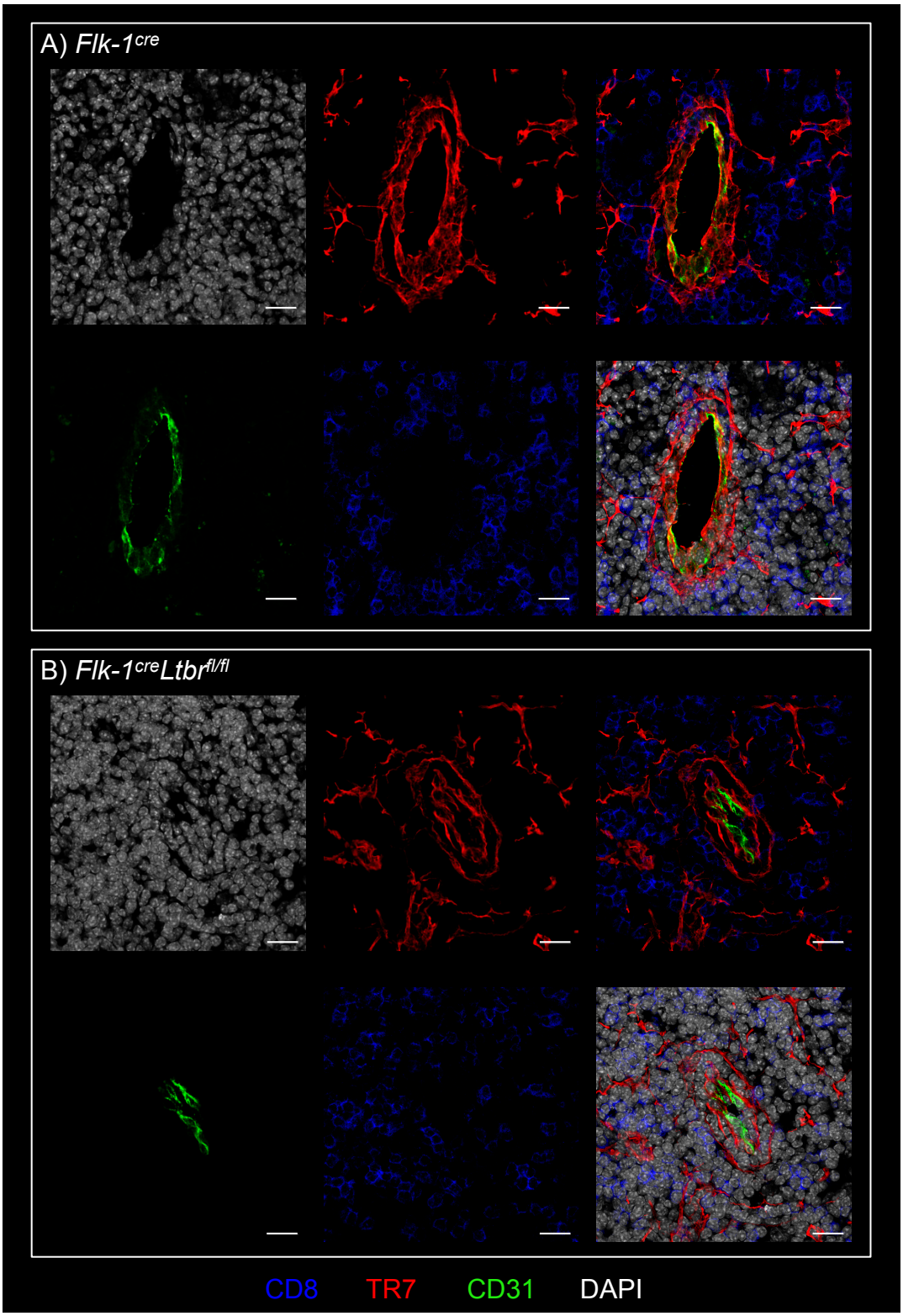
A) Flk-1cre
B) Flk-1creLtbrfl/fl
CD8
TR7
CD31
DAPI

Figure 4.22. LTβR Is Required For Cells To Enter The Perivascular Space During T-cell Egress

Adult control (*Ltbr*$^{+/+}$) and LTβR deficient (*Ltbr*$^{-/-}$) mice were injected I.V. with anti-CD4 PE-conjugated antibody at a concentration of 5μg/ml. Mice were sacrificed three minutes after injection and the thymi were immediately harvested and mechanically disrupted for thymocyte analysis.

(A) Expression of anti-CD4 PE (IV CD4) and CD8 on thymocytes of WT mice of the following conditions: an uninjected control, a mouse injected with FTY720 I.P. the day before anti-CD4 I.V. injections and a mouse just receiving anti-CD4 I.V. injections.

(B) Expression of IV CD4 and CD8 on thymocytes of *Ltbr*$^{+/+}$ (left) and *Ltbr*$^{-/-}$ (right) injected with anti-CD4 I.V. Cell numbers of thymus and IV CD4^{+} labeled cells and percentages of IV CD4^{+} labeled cells from *Ltbr*$^{+/+}$ (blue, n=7) and *Ltbr*$^{-/-}$ (red, n=7) injected with anti-CD4 I.V.

(C) Expression of IV CD4 and CD8 on thymocytes of *Flk-1*$^{cre/+}$ (left) and *Flk-1*$^{cre/+}$*Ltbr*$^{fl/fl}$ (right) injected with anti-CD4 I.V. Cell numbers of thymus and IV CD4^{+} labeled cells and percentages of IV CD4^{+} labeled cells from *Flk-1*$^{cre/+}$ (blue, n=6) and *Flk-1*$^{cre/+}$*Ltbr*$^{fl/fl}$ (red, n=6) injected with anti-CD4 I.V.

The standard error bars display the SEM and a mann-whitney test was performed, where * denotes a significant difference as $p<0.05$ and ** $p<0.01$. All data is typical of 3 independent repeats.

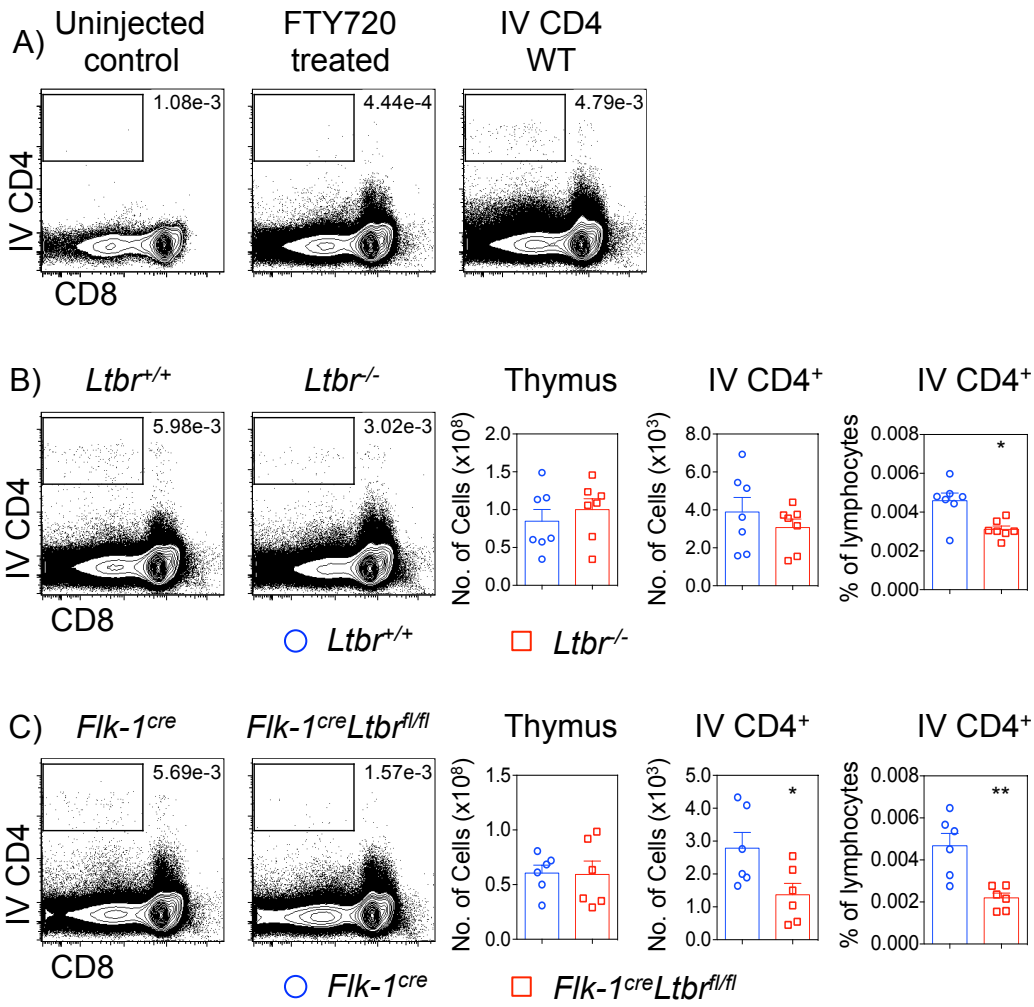
A)
Uninjected control
FTY720 treated
IV CD4 WT
1.08e-3
4.44e-4
4.79e-3
IV CD4
CD8
B)
Ltbr+/+
Ltbr-/-
Thymus
IV CD4+
IV CD4+
5.98e-3
3.02e-3
No. of Cells (x10^8)
No. of Cells (x10^3)
% of lymphocytes
Ltbr+/+
Ltbr-/-
C)
Flk-1cre
Flk-1creLtbrfl/fl
Thymus
IV CD4+
IV CD4+
5.69e-3
1.57e-3
Flk-1cre
Flk-1creLtbrfl/fl

stimulation (Fig 4.23.A.), suggesting LTβR may play a role in regulating S1P. CCL21 and CCL19 are known targets of LTβR and were included to control for successful LTβR stimulation. To ensure the thymocytes within *Ltbr*$^{-/-}$ mice do not have a cell intrinsic defect in S1P-related machinery, PCR analysis was carried out on sorted immature and mature SP4 thymocytes from *Ltbr*$^{+/+}$ and *Ltbr*$^{-/-}$ mice. Mature SP4 thymocytes from *Ltbr*$^{-/-}$ expressed similar levels of *S1pr1*, which is the gene encoding S1PR1 as well *Foxo1* and *Klf2* which are regulators of S1PR1 (Fig 4.23.B.) (99,101). Additionally *Ltbr*$^{+/+}$ and *Ltbr*$^{-/-}$ mature SP4 thymocytes expressed similar levels of Coro1a, which is associated with regulating thymocyte egress (Fig 4.23.B.). Therefore S1P associated thymic machinery is not altered within *Ltbr*$^{-/-}$ thymocytes.

Levels of S1P can be measured indirectly by the expression of S1PR1 on mature thymocytes within the thymus. This can be a useful way to measure whether S1P levels are altered, as the level of S1PR1 expression on the thymocyte surface is inversely correlated with ligand exposure and therefore a reduction of S1P will result in increased surface expression of S1PR1. Therefore measuring S1PR1 on mature thymocytes can be used to explore whether *Ltbr*$^{-/-}$ mice have altered S1P levels within the thymus. Thymocytes were stained with an anti-S1PR1 antibody and its expression is restricted to mature, egress competent, SP4 thymocytes, consistent with previous reports (Fig 4.24.A.B.) (262). Interestingly, the expression of S1PR1 is significantly higher on mature SP4 thymocytes of *Ltbr*$^{-/-}$ mice compared to *Ltbr*$^{+/+}$ controls (Fig 4.24.C.D). To ensure that higher levels of S1PR1 are not being measured due to the increased number of older mature SP4 thymocytes within *Ltbr*$^{-/-}$ mice, RAG^{gfp+} mature SP4 thymocytes from *Ltbr*$^{+/+}$RAG^{gfp} and *Ltbr*$^{-/-}$RAG^{gfp} mice

were split into five different populations of differing RAG^{gfp} levels to target cells of different ages and ensure comparison of S1PR1 between thymocytes of an equivalent age within each strain (Fig 4.24.E.). Consistent with S1PR1 levels on total mature SP4 thymocytes, S1PR1 is significantly increased on *Ltbr*$^{-/-}$ mature thymocytes at all ages groups created (Fig 4.24.E.F.). This indicates a reduction of S1P within the thymus of *Ltbr*$^{-/-}$ mice suggesting that either the S1P gradient is altered or exposure of the mature thymocytes to S1P is altered, resulting in the intrathymic accumulation and egress defects seen within these mice. Additionally the same analysis was carried out on *Flk-1*^{cre}*Ltbr*^{flox} mice, which show a similar increase in S1PR1 is present on mature SP4 thymocytes within *Flk-1*^{cre}*Ltbr*^{flox} mice (Fig 4.24.G.). Interestingly S1PR1 is not altered on mature thymocytes within *Foxn-1*^{cre}*Ltbr*^{flox} thymus consistent with no intrathymic accumulation (Fig 4.24.H.). This suggests that LTβR regulates the S1P gradient through LTβR expressing endothelium, which may be restricted to $CD62P^{+}Ly6C^{-}$ portal endothelial cells that have been proposed to regulate ETP entry.

Together these analyses support a role for LTβR signaling in regulating thymocyte egress. The expression of LTβR was found to be stromal and our analysis revealed that deletion of *Ltbr* specifically on thymic endothelial cells is sufficient to recapitulate the thymocyte egress defect of *Ltbr*$^{-/-}$ mice. Additionally we have shown that S1P levels appear reduced in the germ line and endothelial specific LTβR deletion models and suggest a role for LTβR in regulating thymocyte entry into the perivascular space during thymocyte egress. Therefore we propose a novel role for thymic endothelium in regulating LTβR-dependent thymocyte egress.

Figure 4.23. PCR Analysis Of S1P-S1PR1 Pathway Related Genes

(A) Quantitative real time PCR was performed on stroma isolated from E15 embryonic thymic lobes cultured with dGuo for 7 days, which was then cultured with or without an agonistic anti-LTβR antibody.

(B) Quantitative real time PCR was performed on the following populations sorted from adult *Ltbr*$^{+/+}$ (blue) and *Ltbr*$^{-/-}$ (red) mice:

$CD4^{+}CD8^{-}TCRb^{hi}CD25^{-}RAG^{+}CD69^{+}CD62L^{-}$ **Im SP4**

$CD4^{+}CD8^{-}TCRb^{hi}CD25^{-}RAG^{+}CD69^{-}CD62L^{+}$ **Ma SP4**

Error bars indicate the SEM and mRNA levels were normalized to housekeeping gene β-actin. Data is from at least two independently sorted biological samples; with each gene analyzed a minimum of two times and each PCR ran in triplicates to obtain a SEM.

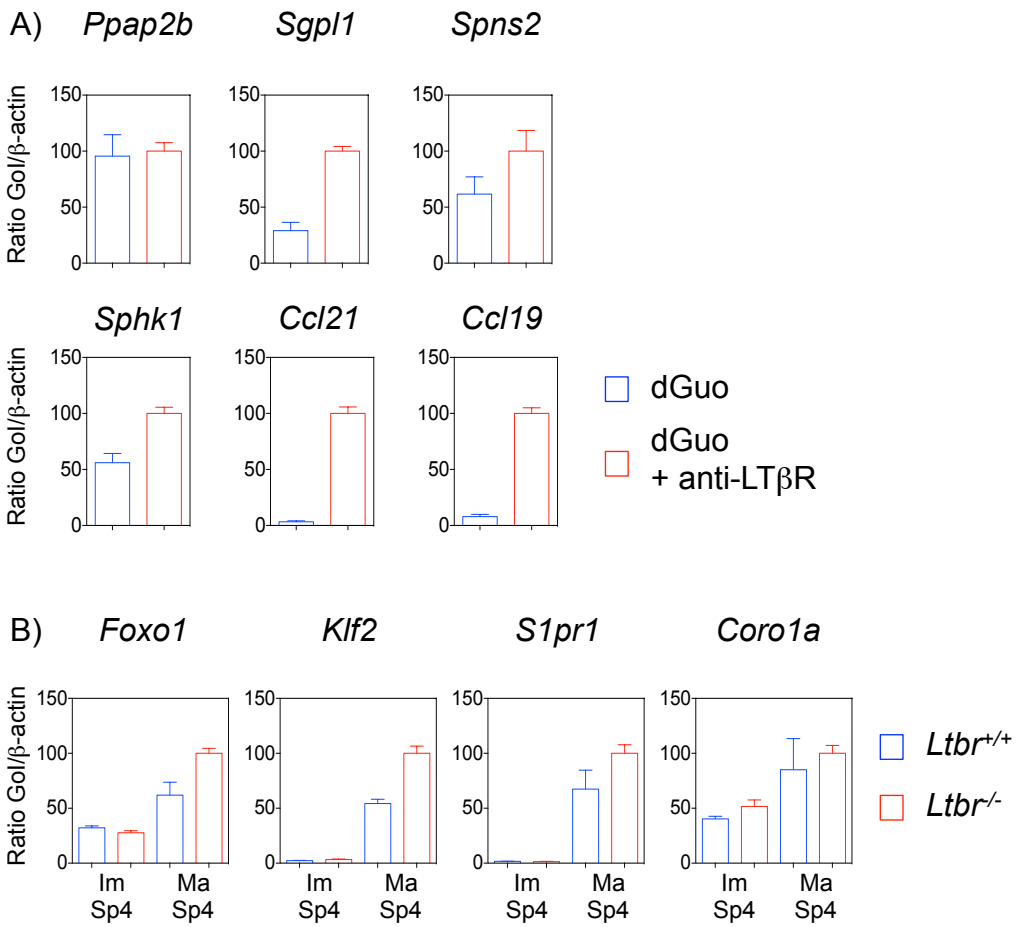
A)
Ppap2b
Sgpl1
Spns2
Sphk1
Ccl21
Ccl19
Ratio GoI/β-actin
150
100
50
0
dGuo
dGuo
+ anti-LTβR
B)
Foxo1
Klf2
S1pr1
Coro1a
Im
Sp4
Ma
Sp4
Ltbr+/+
Ltbr-/-

Figure 4.24. Mature SP4 Thymocytes Of *Ltbr*$^{-/-}$ And *Flk-1*^{cre}*Ltbr*^{flox} Mice Have Altered S1PR1 Expression

Thymic lobes were harvested from control (*Ltbr*$^{+/+}$) and LTβR-deficient (*Ltbr*$^{-/-}$) mice and mechanically disrupted for FACS analysis of thymocytes.

(A) Expression pattern of S1PR1 on $CD4^+CD8^-TCR\beta^{hi}CD25^-CD69^+CD62L^-$ immature (blue) and $CD4^+CD8^-TCR\beta^{hi}CD25^-CD69^{lo}CD62L^+$ mature (red) SP4 thymocytes alongside a staining control (grey).

(B) S1PR1 MFI for immature (blue) and mature (red) $CD25^-$ SP4 thymocytes of *Ltbr*$^{+/+}$ (n=7) mice.

(C) Expression pattern of S1PR1 on mature $CD25^-$ SP4 thymocytes of *Ltbr*$^{+/+}$ (blue, n=7) and *Ltbr*$^{-/-}$ (red, n=7) mice alongside a staining control (grey).

(D) S1PR1 MFI for mature $CD25^-$ SP4 thymocytes of *Ltbr*$^{+/+}$ (blue, n=7) and *Ltbr*$^{-/-}$ (red, n=7) mice.

(E) Expression pattern of CD4 and RAG^{gfp} within RAG^+ mature $CD25^-$ SP4 thymocytes of *Ltbr*$^{+/+}$ (left) and *Ltbr*$^{-/-}$ (right) mice. The RAG^{gfp} population is separated into five slices (1-5) to create five populations of different ages and the S1PR1 MFI is plotted for each population for *Ltbr*$^{+/+}$ (blue, n=7) and *Ltbr*$^{-/-}$ (red, n=7) mice.

(F) Expression of S1PR1 on the five populations of RAG^+ mature $CD25^-$ SP4 thymocytes identified in (**E)** of *Ltbr*$^{+/+}$ (blue, n=7) and *Ltbr*$^{-/-}$ (red, n=7) mice alongside a staining control.

(G) Expression of S1PR1 on $CD25^-$ mature SP4 thymocytes from *Flk-1* (blue, n=3) and *Flk-1*^{cre}*Ltbr*^{flox} mice (red, n=3) alongside a staining control and the S1PR1 MFI is plotted.

(H) S1PR1 MFI plotted for $CD25^-$ mature Sp4 thymocytes from *Foxn-1* (blue, n=6) and *Foxn-1*^{cre}*Ltbr*^{flox} mice (red, n=5).

The standard error bars display the SEM and a mann-whitney test was performed, where * denotes a significant difference as $p<0.05$ and ** $p<0.001$. All data is typical of 3 independent repeats.

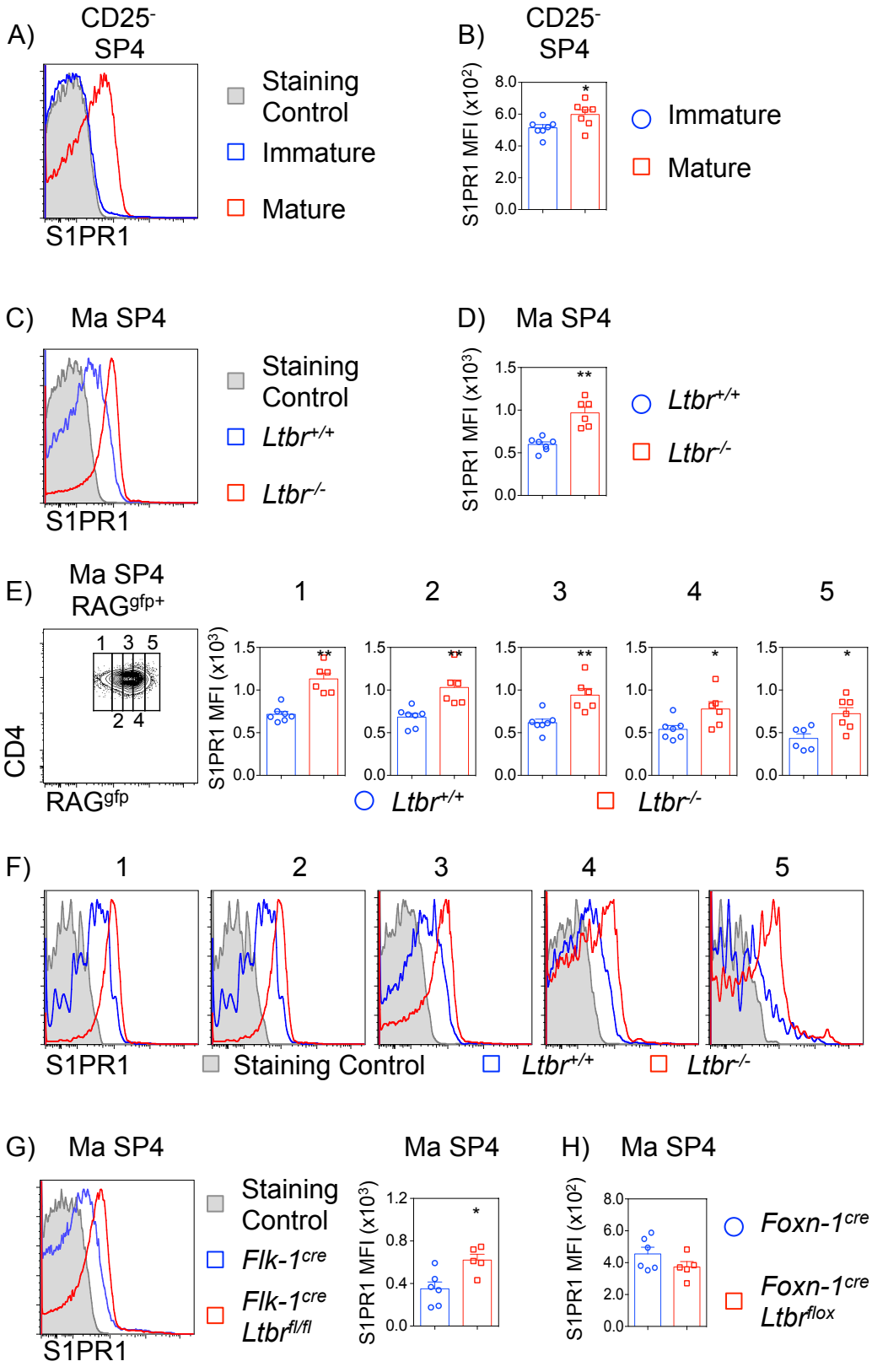
A)
CD25-
SP4
Staining
Control
Immature
Mature
S1PR1
B)
CD25-
SP4
S1PR1 MFI (x10²)
8.0
6.0
4.0
2.0
0.0
*
Immature
Mature
C)
Ma SP4
Staining
Control
Ltbr+/+
Ltbr-/-
S1PR1
D)
Ma SP4
S1PR1 MFI (x10³)
1.5
1.0
0.5
0.0
**
Ltbr+/+
Ltbr-/-
E)
Ma SP4
RAGgfp+
1
2
3
4
5
CD4
RAGgfp
1 3 5
2 4
S1PR1 MFI (x10³)
1.5
1.0
0.5
0.0
**
*
Ltbr+/+
Ltbr-/-
F)
1
2
3
4
5
S1PR1
Staining Control
Ltbr+/+
Ltbr-/-
G)
Ma SP4
Staining
Control
Flk-1cre
Flk-1cre
Ltbrfl/fl
S1PR1
Ma SP4
S1PR1 MFI (x10³)
1.2
0.8
0.4
0.0
*
H)
Ma SP4
S1PR1 MFI (x10²)
8.0
6.0
4.0
2.0
0.0
Foxn-1cre
Foxn-1cre
Ltbrflox

4.3 DISCUSSION

Whilst previous studies have investigated the role of LTβR in regulating thymocyte egress, the precise mechanism whereby LTβR regulates this process remains unknown. This chapter sought to identify the cellular and molecular regulators of thymocyte egress and explore the role that LTβR plays in this process.

LTβR was first identified to be important for thymocyte egress in initial studies by Boehm *et al.*, which investigated the thymic phenotype of *Ltbr*$^{-/-}$ adult mice. The thymus from these mice had an intrathymic accumulation of mature SP4 and SP8 thymocytes, as well as altered medullary organization and mTEC numbers (151). The accumulation of mature thymocytes within these mice was assumed to be due to a block in thymocyte egress as the increase in the number of mature cells was not the result of increased proliferation, a finding we have also observed (not shown). Whilst an intrathymic accumulation may correlate with an egress problem, this was not directly explored in the Boehm *et. al* study. Alternative explanations for increased mature thymocytes could include an increased intrathymic dwell time or reduced rate of T-cell export. In order to directly investigate the impact of LTβR-deficiency on thymocyte egress we used the RAG^{gfp} mouse model to track recent thymic emigrants (RTE) in the periphery of *Ltbr*$^{-/-}$ mice and showed that the proportion of RTE in the T-cell pool was significantly reduced. However, this reduction was not seen at a quantitative level, which is most likely due to the absence of pLN in *Ltbr*$^{-/-}$ which results in an increase in splenocyte cellularity, with the bulk of the peripheral T-cell pool to residing within the spleen. Therefore our data is the first instance where an egress problem has been directly observed within *Ltbr*$^{-/-}$ mice. Interestingly, in

addition to the intrathymic accumulation of mature thymocytes and corresponding reduction in peripheral RTE, our data demonstrates that LTβR directly regulates the kinetics of medullary residency as reflected by increased intrathymic dwell time.

The lack of lymph nodes in *Ltbr*$^{-/-}$ could potentially be a contributing factor to the egress defect within these mice as a lack of periphery lymphoid tissues available for T-cells to migrate to in the periphery may feedback to reduce T-cell output of the thymus. However the kidney capsule grafting experiment showed an intrathymic accumulation within grafted *Ltbr*$^{-/-}$ thymic lobes and in this context the host mouse has normal peripheral lymph nodes. Therefore the presence of peripheral lymph nodes does not rescue the defective egress phenotype of the *Ltbr*$^{-/-}$ thymus.

Because LTβR-deficient mice have a disrupted medullary phenotype, exhibiting both gross medullary disorganization and reduced mTEC populations, as well as a significant intrathymic accumulation of mature thymocytes it was proposed that mTEC and/or the medullary organization could be essential for LTβR-dependent thymocyte egress (151). Our bone marrow chimera (BMC) and kidney capsule transfer experiments, where LTβR-deficiency is limited to thymic stroma or hematopoietic cells, respectively, supported a role for thymic stroma and not hematopoietic cells in regulating thymocyte egress through LTβR signaling. The finding that hematopoietic cells are not required for thymocyte egress was interesting; a recent study found that deleting sphingosine-1-phosphate lyase (SPL) in bone marrow derived cells, thymocytes or dendritic cells (DCs) was sufficient to prevent thymocyte egress and cause an intrathymic accumulation of mature single-

positive (SP) thymocytes (114). The study of Zamora-Pineda *et. al* revealed that deleting SPL in thymic epithelial cells (TEC) or endothelial cells did not impact egress, therefore it seems from our own analysis that LTβR is dispensable for SPL-mediated thymocyte egress.

Thymic epithelial, mesenchymal and endothelial cells all express LTβR (Fig 4.4.B.) and through the use of stromal cell-specific Cre mice crossed with *Ltbr*^{flox} mice we were able to specifically delete *Ltbr* on each of the stromal populations in order to explore the cell-specific role of LTβR in thymic stromal compartments.

There have been previous studies that support a role for TEC regulating thymocyte egress; however there has not been any study to date that directly links LTβR's regulation of TEC and thymocyte egress (112,115). TEC express the CCR7-ligands CCL21 and CCL19, which have been shown to regulate neonatal thymocyte egress (69,116). Additionally TEC have been shown to be essential in maintaining the S1P gradient required for normal thymocyte egress through the production of LPP3 (112). CCR7-ligands are known targets of LTβR signaling however it is not known whether LPP3 is as well (194). However despite these factors there was no observable intrathymic accumulation of mature thymocytes within the epithelial-specific deletion of LTβR mice (*Foxn-1*^{cre}*Ltbr*^{flox}). This was a surprising finding because the disorganization of the medulla and loss of mTEC and CCL21^{+} mTEC^{lo} are such drastic phenotypes within both the constitutive *Ltbr*$^{-/-}$ mouse and the epithelial-specific *Foxn-1*^{cre}*Ltbr*^{flox} mouse. The impact of a disorganized medulla on thymocyte egress has been ruled out through the use of plt/plt mice as well as *Ccr7*$^{-/-}$ mice,

which both have disorganized medullary architecture, complete inhibition of the CCR7-CCR7-L pathway and impaired cortex-medulla migration (69,71,249). Although we have not directly investigated this, Zhu *et. al* proposed that the cortex-medulla migration of SP8 thymocytes was impaired in *Ltbr*$^{-/-}$ mice (155). Because the *Foxn-1*^{cre}*Ltbr*^{flox} mice have a very similar medullary phenotype, these mice may also have the same cortex-medulla migration defect. As there is no accumulation of mature thymocytes within *plt/plt* or *Foxn-1*^{cre}*Ltbr*^{flox} mice, this would suggest that the potential mispositioning of the SP thymocytes does not impact thymocyte egress. Together this suggests that a disrupted medullary environment does not impact the ability of thymocytes to egress and therefore is not the source of the thymocyte egress defect present within the *Ltbr*$^{-/-}$ mouse thymus.

The loss of mTEC within both *Ltbr*$^{-/-}$ and *Foxn-1*^{cre}*Ltbr*^{flox} mice would suggest that there may be reduced thymocyte:mTEC interactions due to the reduced frequency of mTEC within the medullas. Consistent with this, *Ltbr*$^{-/-}$ mice do show signs of reduced interactions between SP4 thymocytes and mTEC by measuring reduced MHC Class II on the surface of SP4 thymocytes which indicates cell contact between SP4 and mTEC (153). This would suggest that interactions with mTEC are not essential for thymocyte egress, which is consistent with the normal programme of SP thymocyte development within *Relb*$^{-/-}$ mice, which have an absence of RelB-dependent mTEC, however experiments directly investigating thymocyte egress within Relb$^{-/-}$ mice remain outstanding (82).

Previously thymic pericytes have been implicated in regulating thymocyte egress through the production of the enzymes sphingosine-1-phosphate kinase (SPHK) 1 and SPHK2 which catalyze the ATP-dependent phosphorylation of sphingosine to produce S1P (111). Our own research has shown that PDPN^{+} thymic mesenchyme have a somewhat pericyte-like phenotype as they have a perivascular positioning and express PDGFRβ (Chapter 3). Interestingly we have also shown that the population of ICAM-1^{hi}VCAM-1^{hi} PDPN^{+} thymic mesenchyme expresses CCL19 and SPHK1, both of which have been implicated in the regulation of thymocyte egress (110,111,116). Additionally, the development of this population of ICAM-1^{hi}VCAM-1^{hi} PDPN^{+} thymic mesenchyme is dependent on LTβR signaling, suggesting that this mesenchyme population may be a candidate for the stromal regulator of LTβR-dependent thymocyte egress.

Using *Wnt-1^{cre}Ltbr^{flox}* we were able to specifically target *Ltbr* deletion to PDPN^{+} thymic mesenchyme and this recapitulated the loss of ICAM-1^{hi}VCAM-1^{hi} PDPN^{+} thymic mesenchyme seen in the constitutive *Ltbr$^{-/-}$* mouse (Fig 4.7. & Fig 4.8.). Additionally *Wnt-1^{cre}Ltbr^{flox}* mice have a thymic dendritic cell (DC) defect that mirrors that of *Ltbr$^{-/-}$* mice, revealing a functional defect in the *Wnt-1^{cre}Ltbr^{flox}* mouse model consistent with successful *Ltbr* deletion (157). However despite these positive identifiers of specific and efficient Cre-mediated deletion of floxed *Ltbr* in thymic mesenchyme, there was no observable intrathymic accumulation of mature thymocytes (Fig 4.9.). Therefore despite the clear role for LTβR in regulating the development of thymic mesenchyme and thymic DC, LTβR signaling is not essential for regulation of thymocyte egress via thymic mesenchyme.

This would suggest that previously identified regulators of thymocyte egress that are expressed by thymic mesenchyme such as SPHK1 and SPHK2 are not dependent on LTβR signaling (111). Staining for S1PR1 on mature thymocytes within the *Wnt-1^{cre}Ltbr^{flox}* thymus could further test this hypothesis, however the lack of an intrathymic accumulation would predict that intrathymic S1P levels are normal.

It was surprising that LTβR expression by PDPN^{+} thymic mesenchyme is not essential for thymocyte egress given their perivascular location around thymic endothelial cells (Chapter 3). Indeed we have not been able to directly identify the location of ICAM-1^{hi}VCAM-1^{hi} mesenchyme within the thymus and therefore one possible explanation as to why this population is not required for thymocyte egress is that these cells may be the non-perivascular thymic mesenchymal cells identified in Chapter 3. However the PCR analysis of gene expression of *Sphk1* within ICAM-1^{hi} PDPN^{+} mesenchyme compared to ICAM-1^{lo} is consistent with a pericyte-like phenotype, which would support a perivascular positioning of the ICAM-1^{hi}VCAM-1^{hi} PDPN^{+} mesenchyme cells.

In addition to the deletion of *Ltbr* within thymic mesenchymal cells resulting in the loss of the ICAM-1^{hi}VCAM-1^{hi} PDPN^{+} population, *Wnt-1^{cre}Ltbr^{flox}* mice have reduced DC populations, which is consistent with the constitutive *Ltbr$^{-/-}$* mice shown in our recently published study (157). This is an interesting observation as thymic DC have been shown to regulate thymocyte egress through their production of S1P lyase which helps to maintain the S1P gradient by degrading interstitial S1P (114). Our BMC results revealed that LTβR operates to regulate egress in a non-hematopoietic

manner and therefore there is no role for LTβR expressed by DCs to regulated thymocyte egress, however the above data also rules out an indirect role of LTβR-expression thymic mesenchyme regulating thymocyte egress via regulation of DC populations within the thymus.

Thymic endothelial cells remained the final stromal cell candidate for LTβR-dependent thymocyte egress. Using *Flk-1*^{cre}*Ltbr*^{flox} mice we were able to specifically and efficiently target *Ltbr* deletion to CD31^{+} thymic endothelial cells. A caveat of using some endothelial-specific Cre lines, including the Flk-1^{cre} model, is that Cre activity does target hematopoietic cells due to an upstream precursor population shared by hematopoietic cells and endothelial cells (245). However in the context of LTβR-dependent thymocyte egress, our BMC experiments reveal no impact on thymocyte egress when LTβR is absent on hematopoietic cells and therefor the Cre activity within hematopoietic cells should not interfere with this analysis. These mice exhibited an intrathymic accumulation that was similar to *Ltbr*$^{-/-}$ mice suggesting they have a thymocyte egress defect, however the impact on RTE has yet to be directly confirmed through the use of *Flk-1*^{cre}*Ltbr*^{flox}RAG^{gfp} mice, which due to time constraints of breeding have yet to investigated. Therefore our data highlights a novel role of thymic endothelium regulating LTβR-dependent thymocyte egress. Thymic endothelial cells have been shown to regulate thymocyte egress before. Deletion of *Ppa2b* (gene encoding LPP3) on thymic endothelial cells resulted in an intrathymic accumulation of mature thymocytes (112). However our PCR analysis of 2-dGuo treated fetal thymic organ cultures (FTOC) stimulated with anti-LTβR revealed that expression of *Ppa2b* was not increased upon stimulation of anti-LTβR. To directly

investigate this, cell sorting of thymic endothelial cells from *Ltbr*$^{+/+}$, *Ltbr*$^{-/-}$ as well as from *Flk-1*^{cre} and *Flk-1*^{cre}*Ltbr*^{flox} mice is currently underway to identify potential regulators of S1P, including *Ppa2b*. Vascular endothelium has been previously reported to be a major source of plasma S1P in addition to the hematopoietic system (267). Findings from Venkataraman *et. al* have shown that cultured endothelial cells express *Sphk1* and *Sphk2* which are required for the production of S1P, but also express *Sgpp2* and *Sgpl* which degrade S1P (267). Whilst the production of S1P by endothelial cells may be counterintuitive due to their expression of *Sgpp2* and *Sgpl* which degrade S1P, *in vitro* analysis appeared to show that under conditions of laminar shear stress there was a down regulation of *Sgpp2* and *Sgpl* and a concomitant release of S1P. Whilst these findings are from *in vitro* endothelial cell cultures there may be scope for thymic endothelial cells to contribute to the S1P gradient beyond as a negative regulator of S1P, which we hope our PCR analysis will reveal. Additionally, expression of the S1P transporter spinster homolog 2 (Spns2) on thymic endothelial cells is essential for thymocyte egress, suggesting another possible mechanism for LTβR regulation of thymocyte egress via thymic endothelium (113).

We believe the S1P pathway is involved in LTβR-dependent thymocyte egress due to the altered expression of the S1P receptor 1 (S1PR1) on mature thymocytes, which is significantly higher on mature thymocytes within *Ltbr*$^{-/-}$ and *Flk-1*^{cre}*Ltbr*^{flox} mice. Importantly using *Ltbr*$^{-/-}$RAG^{gfp} mice we were able to gate mature SP4 thymocyte populations of a comparable age between *Ltbr*$^{+/+}$ and *Ltbr*$^{-/-}$ mice and showed that mature cells of a comparable age from *Ltbr*$^{-/-}$ mice have significantly higher

expression of S1PR1. Therefore the increase of S1PR1 is likely due to altered interstitial free S1P and not due to the increased maturity of mature SP4 thymocytes within *Ltbr*$^{-/-}$ mice. Another important result was that *Foxn-1*^{cre}*Ltbr*^{flox} mature SP4 thymocytes have normal levels of S1PR1, which suggests that disorganization and potential mispositioning within the *Ltbr*$^{-/-}$ thymus does not cause an increase of S1PR1 on mature SP4 thymocytes. However this finding does not rule out that increased S1PR1 is due to altered exposure of the mature cells to S1P rather than altered levels of S1P within the thymus.

Therefore our analysis highlights a novel role of LTβR regulating the S1P-S1PR1 pathway to regulate thymocyte egress, however the exact mechanism through which this occurs requires further research.

It was recently revealed in a study of the role of LTβR in T-cell progenitor entry into the thymus that the total CD31^{+} thymic endothelial population could be further subdivided into distinct populations (24). The findings of Shi *et al.* revealed that *Ltbr*$^{-/-}$ mice have a specific loss of CD62p^{+} (P-selectin) Ly6C^{-} endothelial cells that they termed thymic portal endothelial cells (TPECs) due to their localization with perivascular spaces and thymic seeding progenitor cells, and these TPECs are crucial to the entry of T-cell progenitors into the thymus (24). Therefore *Ltbr*$^{-/-}$ mice have a mature thymocyte egress defect as well as an ETP entry defect both correlating with altered thymic endothelial cells at the CMJ which is the proposed site of entry and exit (22,24,268). Our analysis revealed that *Flk-1*^{cre}*Ltbr*^{flox} mice have a significant loss of TPECs and that TPECs express LTβR in control mice but have a

loss of LTβR expression in *Flk-1^{cre}Ltbr^{flox}* mice. Therefore our analysis suggests that LTβR is regulating thymocyte egress through its control of thymic endothelial cells and this may map to a specific population of portal endothelial cells, whose development is dependent on LTβR. Furthermore, stromal cells that regulate thymocyte egress may also regulate ETP entry into the thymus raising an interesting hypothesis that LTβR-dependent ETP entry and thymocyte egress could be linked.

An interesting observation to come out of our immunofluorescence microscopy analysis was the lack of accumulating cells within the PVS of *Ltbr$^{-/-}$* and *Flk-1^{cre}Ltbr^{flox}* mice. In previous studies of mice within an intrathymic accumulation of mature thymocyte and/or a thymocyte egress defect there can be an associated accumulation of cells in the PVS (111). It was previously shown that S1PR1-transgenic mice which had premature expression of S1PR1 on DP thymocytes showed an accumulation of cells within the PVS (111). Additionally a recent study showed that in the absence of IL-4Rα there is reduced RTE as well as an intrathymic accumulation of mature cells within the PVS (115). Both studies used a technique of labeling cells in the process of thymocyte egress within the PVS space, which involves injecting anti-CD4 PE antibody intravenously (I.V) for a short period of time. Both studies revealed an increase in the proportion of labeled cells and consistent with our microscopy we did not see an increase. Rather there was a decrease in the percentage and number of cells entering the PVS, suggesting that a potential reason as to why thymocytes might not be leaving the thymus efficiently is that they have a reduced capacity to access the PVS. Whilst this does suggest that entry into the PVS is faulty, it does not rule out a potentially compounding effect of defective egress from

the PVS into the periphery. As previously discussed, the regulation of the S1P gradient by endothelial cells through both the negative and positive regulators of S1P levels (degrading S1P via S1P lyase or increased release/production of S1P via Spns2 or SPHK) may compound the egress defect. Future experiments exploring the differential expression of genes within endothelial cells of *Ltbr*$^{-/-}$ and *Flk-1*^{cre}*Ltbr*^{flox} mice will attempt to address this.

As the intrathymic accumulation of mature thymocytes does not appear to be occurring within the PVS, current experiments are underway to directly investigate where the intrathymic accumulation of mature thymocytes is occurring which we hypothesis may be found within the medulla due to it being the final site of maturation prior to thymocyte egress. Preliminary analysis is indicating that this may be the case in both the *Ltbr*$^{-/-}$ and the *Flk-1*^{cre}*Ltbr*^{flox} thymus. An interesting hypothesis as to why this may occur comes from observations of the balance of the CCR7 and S1P-S1PR1 pathway in lymph nodes. For cells to enter the lymph nodes they must express CCR7 and due to the high levels of S1P in the blood these cells do not express S1PR1 (269). Subsequent exit of the LN is dependent on downregulation of CCR7 and expression of S1PR1 to overcome CCR7-CCR7-L mediated retention within the LN (270). The observation that cells within *Ltbr*$^{-/-}$ and *Flk-1*^{cre}*Ltbr*^{flox} have increased S1PR1 (suggesting reduced S1P) and still have presence of CCR7-ligands within the medulla (although reduced in the *Ltbr*$^{-/-}$) may suggest a similar mechanism is in place within the thymus. The hypothesis being that in these mice, intrathymic S1P is reduced; preventing the cells to efficiently leave the medulla via overcoming CCR7-CCR7-L signals. This would also be consistent with *Foxn-1*^{cre}*Ltbr*^{flox} mice,

which have reduced CCL21+ mTEC, but normal S1P levels which is sufficient for normal thymocyte egress. To investigate this hypothesis directly we have begun preliminary analysis of *Ltbr*$^{-/-}$*plt/plt* "double KO (dKO)" mice, which will have the proposed S1P-reduction of the *Ltbr*$^{-/-}$ but a complete loss of CCL21. Therefore if our hypothesis is correct the complete absence of CCR7-ligands should rescue the egress defect of the *Ltbr*$^{-/-}$ mice. Our preliminary analysis of these mice may suggest that dKO mice do not have an intrathymic accumulation defect and intrathymic dwell time appears normal. If these findings are consistent this would provide evidence that CCR7-L and S1P-S1PR1 pathways are opposing each other within the thymus to regulate thymocyte egress. This would highlight a novel role within the thymus for LTβR, S1P-S1PR1 and CCR7-CCR7-L signals regulating thymocyte egress through a mechanism where fine balance of retention and egress signals determines thymocyte egress.

As well as the S1P-S1PR1 pathway, alternative pathways have been proposed to regulate thymocyte egress. CXCR4 has previously been suggested to regulate thymocyte egress however if or how CXCR4 regulates thymocyte egress was unclear due to the embryonic lethality of CXCR4-deficient mouse models (118–120). However a recent study using a more refined model of CXCR4 deletion, where *Cd4*^{cre}*Cxcr4*^{flox} mice were used to avoid the embryonic lethality and deleted *Cxcr4* specifically in DP thymocytes and their downstream progeny, revealed no role for CXCR4 in thymocyte egress (122). As previously discussed, IL-4Rα was recently identified as a novel regulator of thymocyte egress, however a distinct phenotype of the *Il4ra*$^{-/-}$ thymus was large accumulations of cells within the PVS (115). As *Ltbr*$^{-/-}$

mice lack PVS accumulation it is unlikely that this type 2 cytokine axis is being regulated via LTβR. Moreover *Il4ra*$^{-/-}$ mice show no impact on S1P-mediated signaling, further suggesting LTβR is not regulating IL-4Rα-dependent egress.

Based on these findings, summarized in Figure 4.25, our analysis does not rule out the role of multiple stromal cell types regulating thymocyte egress, on the contrary there are many different mechanisms and cell types regulating thymocyte egress. We propose that thymic endothelial cells are essential for the regulation of LTβR-dependent thymocyte egress and this may be occurring specifically at the stage of T-cell entry into the perivascular space. Therefore our analysis highlights this as a novel mechanism for LTβR regulation of T-cell egress.

Figure 4.25. LTβR Regulation Of Thymic Endothelium Is A Critical Regulatory Pathway Of T-Cell Egress

(A) Under normal steady-state conditions, T-cell egress within the adult thymus occurs following maturation of immature SP thymocytes from a $CD69^{+}CD62L^{-}RAG^{gfp+++}$ population into a $CD69^{lo}CD62L^{+}S1PR1^{+}RAG^{gfp++}$ population. This expression of S1PR1 signifies the mature SP thymocytes ability to egress the thymus, which it undergoes via blood vessels at the corticomedullary junction (CMJ).

(B) Adult LTβR-deficient mice have a significant T-cell egress defect. S1PR1-expressing mature SP thymocytes do not exit the thymus properly and instead accumulate within the thymus. These cells have significantly higher expression of S1PR1, which indicates that intrathymic levels of S1P are reduced, which may be the cause of the altered T-cell egress. These cells also have lower RAG^{gfp} expression indicative of their increased time within the thymus due to their inability to exit the thymus properly.

(C) We generated $Flk\text{-}1^{cre}Ltbr^{flox}$ mice within which Ltbr is specifically deleted on endothelial cells, including all the endothelial cells within the thymus. These mice phenotypically mirrored LTβR-deficient mice, exhibiting the same intrathymic accumulation defect and increased S1PR1 expression on the mature thymocytes. Interestingly deleting LTβR on thymic mesenchyme or epithelial cells did not result in an egress defect despite the essential role for LTβR regulation of medullary thymic epithelial cell development. Thus our data indicated that LTβR regulation of thymic endothelium is an essential pathway in controlling T-cell egress.

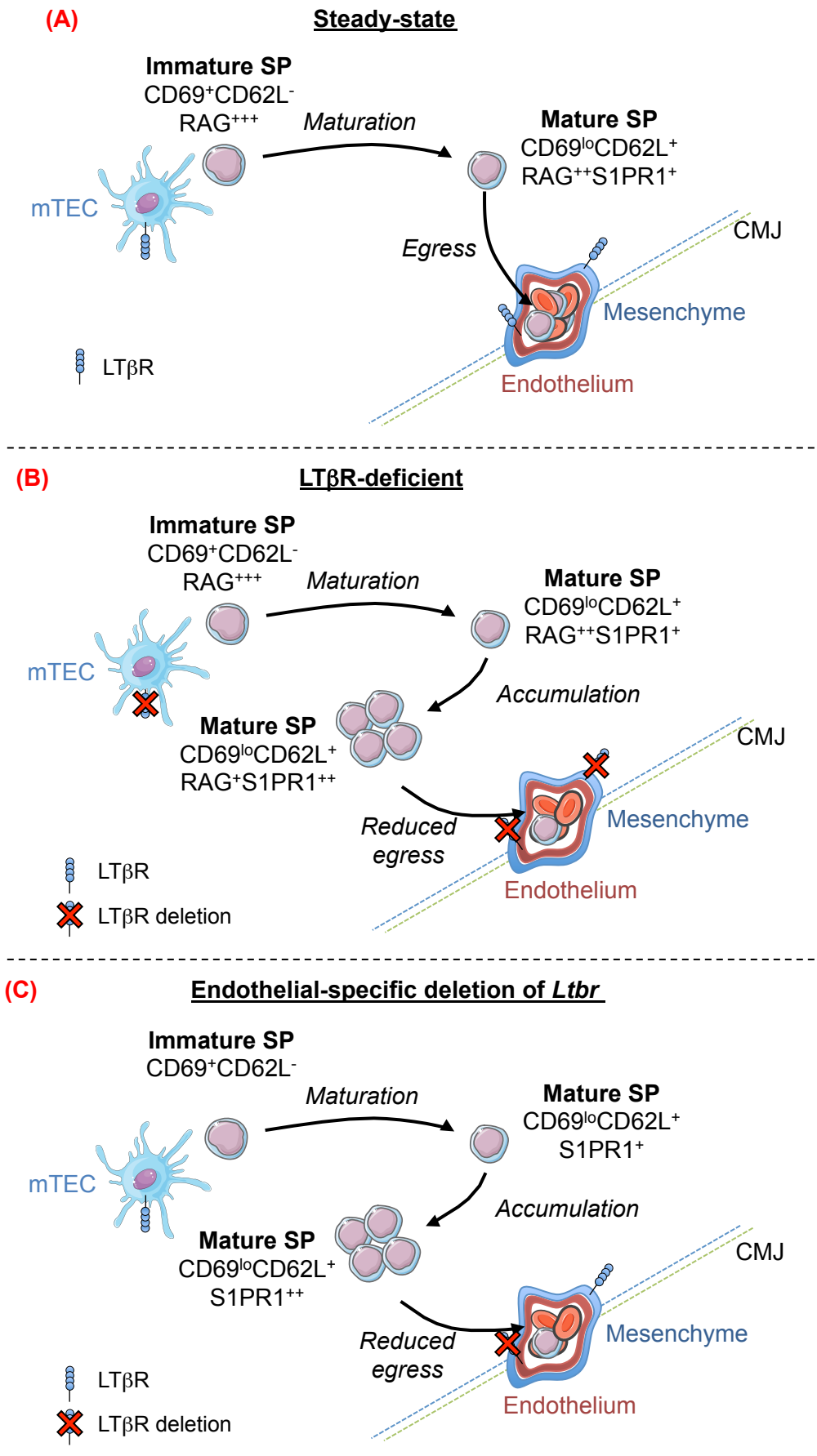
(A)
Steady-state
Immature SP
CD69+CD62L-
RAG+++
Maturation
Mature SP
CD69loCD62L+
RAG++S1PR1+
mTEC
Egress
CMJ
Mesenchyme
Endothelium
LTβR
(B)
LTβR-deficient
Immature SP
CD69+CD62L-
RAG+++
Maturation
Mature SP
CD69loCD62L+
RAG++S1PR1+
mTEC
Accumulation
Mature SP
CD69loCD62L+
RAG+S1PR1++
CMJ
Reduced
egress
Mesenchyme
Endothelium
LTβR
LTβR deletion
(C)
Endothelial-specific deletion of Ltbr
Immature SP
CD69+CD62L-
Maturation
Mature SP
CD69loCD62L+
S1PR1+
mTEC
Accumulation
Mature SP
CD69loCD62L+
S1PR1++
CMJ
Reduced
egress
Mesenchyme
Endothelium
LTβR
LTβR deletion

CHAPTER FIVE: UNDERSTANDING THE TIMING OF THYMOCYTE EGRESS

5.1 INTRODUCTION

Once thymocytes have undergone positive and negative selection the final stage in their development is maturation to an egress competent mature cell that expresses molecules essential for their exit, such as the S1P-receptor 1 (S1PR1) (98,262). Whilst regulators of thymus egress, including mediators of the S1P-S1PR1 pathway, have been identified through many studies including our own, the finer details of egress remain in debate (115,271). There are two main hypotheses regarding thymocyte egress; the stochastic model and the conveyor-belt model (272). The former suggests that thymocyte egress is a random process; once thymocytes have reached maturation and are egress competence e.g. express S1PR1, they are able to leave the thymus at random. However the latter suggests that only the cells that have reached maturation first leave the thymus before the newer mature cells in a strictly ordered linear manner.

There is supporting evidence for both models and which of these models are correct still remains in contention. In 1995 Scollay and Godfrey reviewed the evidence that supported these models, highlighting how much of the studies up until that point supported either model and definitive evidence for one over the other was lacking (272–276). Since then studies that attempt to definitively investigate the timing and order of thymocyte egress have been lacking and even the recent studies of this topic are still not clear.

Supporting the conveyor-belt model, McCaughtry *et. al* separated SP thymocytes into subsets based on the expression of RAG^{gfp} (277). The GFP^{lo} cells were identified as

the most mature, expressing the lowest levels of CD69 and HSA and were egress competent as evidenced by their expression of *S1pr1* (277). Using a method of intrathymically labeling thymocytes with biotin, McCaughtry *et. al* were able to identify the newest RTE and show that these cells expressed similar levels of HSA as the GFP^{lo} fraction and concluded that the most mature SP thymocytes are exiting the thymus first and therefore proposed the conveyor-belt model to be the mode of thymocyte egress.

Around a similar time Jin *et. al* published a study investigating the dynamics of medullary thymocyte development and separated the SP4 population into 4 fractions of different maturational status based on their expression of the T-cell activation marker CD69 and markers of T-cell maturation 6C10 and QA2 (278–281). Using an adoptive transfer technique, Jin *et. al* reintroduced sorted populations of the 4 SP4 fractions, Sp1 (youngest), Sp2, Sp3 and Sp4 (oldest) into the thymus and monitored their development (278). This approach revealed that these fractions displayed ordered maturational progression within the medulla with Sp1 giving rise to Sp2, Sp2 giving rise to Sp3 and Sp3 giving rise to Sp4 (278). Whilst their analyses revealed that, consistent with their expression of S1PR1, the older Sp3 and Sp4 fractions were detected in the periphery before the younger Sp1 and Sp2 fractions, Sp3 thymocytes were detectable in the peripheral before all of the Sp4 thymocyte had left, suggesting that once SP thymocytes reach egress-competence their egress from the thymus is stochastic (278).

Both of these studies, as well as others published prior to these, provide well-

reasoned arguments, backed up with clear data, to support either of the thymocyte egress models (263,272–278). Therefore this chapter aims to adopt a more accurate and detailed approach to identify SP thymocytes of differing maturational stages and to investigate whether the egress of these mature SP thymocytes follow a random or ordered program of egress.

5.2 RESULTS

5.2.1 Is Thymic Egress A Random Or Ordered Process

The kinetics and timing of thymocyte egress remains a point of contention. The two main schools of thought are the stochastic (random) model and the conveyor-belt (ordered) model. The former suggests that once a cell has become egress competent it can exit the thymus at any time, regardless of that cells age relative to the other egress-competent SP thymocytes amongst that cell, whereas the latter suggests that the oldest egress-competent mature cells will leave before the newer mature cells in a strictly linear manner.

To investigate whether cells leave in an ordered or random process, the $CD69^{lo}CD62L^{+}$ mature fraction of conventional SP4 (cSP4) thymocytes needed to be separated into subsets of different ages. To do this, the $CD69^{lo}CD62L^{+}$ fraction was separated into four distinct populations (M1-M4) based on their expression of CD69 (M1 has highest CD69 expression, M4 has the lowest) (Fig 5.1.A.). This was carried out in RAG^{gfp} mice to determine the sequential maturation of these different M1-M4 subpopulations. The analysis of RAG^{gfp} MFI on each population revealed significant reduction of RAG^{gfp} between M1-M4 populations of mature SP4 thymocytes,

revealing a positive correlation of CD69 and RAG^{gfp} expression and identifying M1 cells as the youngest population whilst M4 cells are the oldest (Fig 5.1.B.). A defining characteristic of the most mature cells is their expression of molecular regulators of thymic exit, including the sphingosine-1-phosphate receptor 1 (S1PR1), expression of which correlates with egress competency (97). Expression of S1PR1 was found to be present on all four M1-M4 subsets and expression levels of S1PR1 increase, correlating with reduced RAG^{gfp} indicating higher levels of S1PR1 on older mature SP thymocytes (Fig 5.1.C.) Plotting MFI for both RAG^{gfp} and S1PR1 on a dual axis plot clearly demonstrates this positive relationship between the age of the mature cell and its expression of S1PR1 (Fig 5.1.D.). These analyses support both stochastic and conveyor-belt models of thymocytes egress; the mature population as a whole possesses the ability to egress the thymus via S1PR1 expression, however older mature SP4 fractions do express higher levels of S1PR1 and therefore may have a greater propensity to egress the thymocyte compared to the younger mature SP4 fractions and thus may egress the thymus first.

As this analysis provided data to support stochastic and conveyor-belt egress models we sought to investigate the timing of thymocyte egress using additional fine-grain experimental analysis. The method of injecting anti-CD4 antibody intravenously (IV CD4) is often used to identify cells within the perivascular space (PVS) and therefore is a robust method of labeling cells in the act of egress (111,115). Therefore the stochastic model would suggest that PVS resident IV $CD4^+$ labeled cells will be a mix of SP thymocytes at differing stages of maturation, whereas the conveyor-belt model would predict only the most mature cells would be in the act of egress.

Figure 5.1. Mature SP4 Thymocytes Can Be Separated Into Four Distinct Fractions

Thymic lobes were harvested from WT RAG^{gfp} reporter mice and mechanically disrupted for FACS analysis of the thymocyte populations.

(A) Conventional single positive CD4 (cSP4) thymocytes were identified as $CD4^{+}CD8^{-}TCR\beta^{hi}CD25^{-}Foxp3^{-}$. Immature and mature thymocytes were identified as $CD69^{+}CD62L^{-}$ and $CD69^{lo}CD62L^{+}$, respectively and the $CD69^{lo}CD62L^{+}$ mature fraction was further separated based on levels of CD69 in to M1 (red), M2 (blue), M3 (green) and M4 (orange) populations.

(B) RAG^{gfp} expression for each of M1-M4 population and the RAG^{gfp} MFI was calculated for each population; M1 (red), M2 (blue), M3 (green) and M4 (orange).

(C) S1PR1 expression for each M1-M4 population and the S1PR1 MFI was calculated for each population; M1 (red), M2 (blue), M3 (green) and M4 (orange).

(D) Graph plotting RAG^{gfp} (blue circle) and S1PR1 (red square) MFI for each M1-M4 population as previously calculated for (B) and (C).

The standard error bars display the SEM and an one-way ANOVA test was performed, where ** denotes a significant difference as $p<0.01$, *** as $p<0.001$ and **** as $p<0.0001$. All data is typical of 3 independent repeats where total n=5.

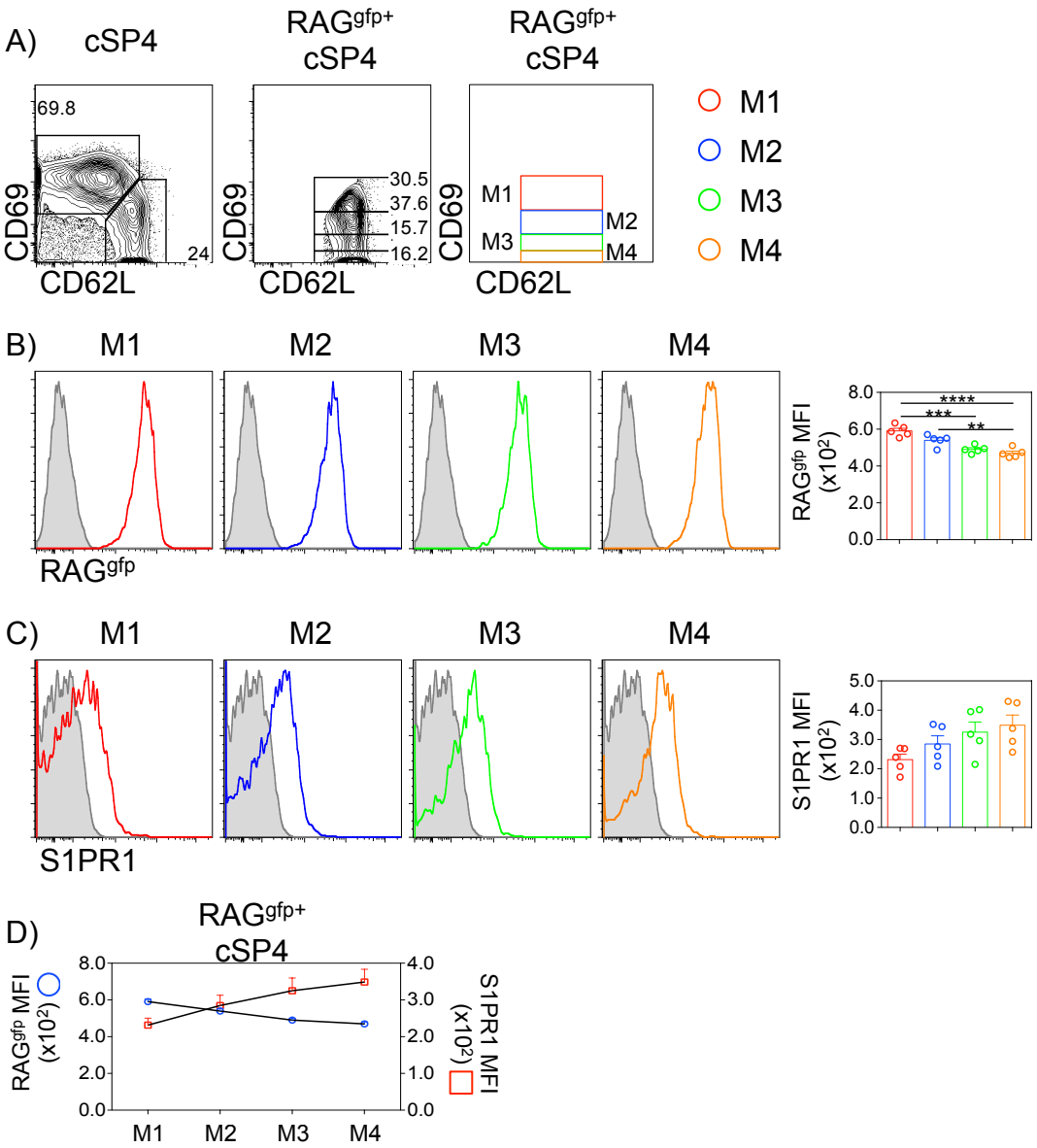
A)
cSP4
RAGgfp+ cSP4
RAGgfp+ cSP4
69.8
24
30.5
37.6
15.7
16.2
CD69
CD62L
M1
M2
M3
M4
B)
M1
M2
M3
M4
RAGgfp
RAGgfp MFI (x10²)
****
***
**
C)
S1PR1
S1PR1 MFI (x10²)
D)
RAGgfp+ cSP4
RAGgfp MFI (x10²)
S1PR1 MFI (x10²)

IV $CD4^+$ labeled cells were identifiable in adult wild type mice that have been I.V. injected with the anti-CD4 PE antibody (Fig 5.2.A.) by flow cytometric analysis. Surprisingly more than half of the IV $CD4^+$ cells were RAG^{gfp-} which may indicate that these cells are recirculating cells and are entering the thymus rather than exiting the thymus, therefore only RAG^{gfp+} cells were gated on to ensure the analysis was accurately investigating newly generated thymocytes exiting the thymus (Fig 5.2.A.). RAG^+ IV $CD4^+$ cells expressed high levels of TCRβ and were $CD25^-$ suggesting these cells were conventional SP4 thymocytes (Fig 5.2.A.). Within the $CD25^-$ SP4 thymocytes the majority of the labeled cells were $CD69^{lo}CD62L^+$ mature thymocytes consistent with egressing cells and S1PR1 expression (Fig 5.2.B.). Using the gating method to split the mature population into four subsets based on CD69 expression revealed that all subsets were labeled with the anti-CD4 antibody (Fig 5.2.C.). This suggests that all mature SP4 cells, regardless of their age, can enter the PVS and therefore are able to exit the thymus.

The observation that over half of IV $CD4^+$ cells are RAG^{gfp-} is an interesting finding and required further analysis. Previous studies have used I.V. anti-CD4 antibody injections to label cells in the PVS and suggested these cells are exiting the thymus, yet no studies have used this technique in combination with RAG^{gfp} (111). Separating the IV $CD4^+$ thymocyte population based on RAG^{gfp} revealed that over 50% of IV $CD4^+$ cells are RAG^{gfp-} (Fig 5.3.A.). Within the RAG^{gfp+} fraction the majority of cells were $CD25^-$ and these cells fell within the $CD69^{lo}CD62L^+$ gate consistent with mature cells leaving the thymus (Fig 5.3.B.). The RAG^{gfp-} cells may represent recirculating cells and Tregs are well known to recirculate to the thymus (282). However within the

RAG^{gfp-} fraction of IV CD4^{+} cells there was no skewing towards CD25^{+} cells or obvious bias towards mature cells (Fig 5.3.C.). This suggests that IV CD4^{+} cells may be labeling cells that are not only exiting the thymus but also entering the thymus and therefore analysis using this technique requires the inclusion of RAG^{gfp} to more accurately measure cells with the PVS that are recirculating.

If mature thymocytes are leaving in an ordered manner then the conveyor-belt model predicts that mice with egress defects and an intrathymic accumulation of mature thymocytes such as *Ltbr*$^{-/-}$ mice would have a selective increase in the number of the most mature fraction of these cells, defined here as M4. CD69^{lo}CD62L^{+} mature cSP4 thymocytes from *Ltbr*$^{+/+}$and *Ltbr*$^{-/-}$ mice were separated into the M1-M4 fractions as before (Fig 5.4.A.). There was no specific increase in the oldest fraction of mature cSP4 thymocytes (M4), instead there was a significant increase in the number of M2 and M3 fractions and M1 and M4 followed the same trend, consistent with the stochastic model of thymocyte egress and our IV CD4 analysis (Fig 5.4.B.). Uptake of BrdU reveals cells that are proliferating and the mature subset of cSP4 thymocytes have reduced proliferation consistent with previous reports (Fig 5.4.C.) (151). To exclude the possibility that the increase in the M2 and M3 fractions was not simply due to increased proliferation, the percentage of BrdU^{+} cells within each M1-M4 fraction was calculated. Fractions M2-M4 all had significantly lower BrdU^{+} cells consistent with the mature population as a whole, whereas M1 had normal proportions of BrdU^{+} cells (Fig 5.4.C.). This data suggests that in the context of altered egress and an intrathymic accumulation of mature thymocytes the stochastic model of thymocyte egress is occurring.

Figure 5.2. Each M1-M4 Subpopulation of Mature SP4 Thymocytes Can Enter The Perivascular Space

Adult WT RAG^{gfp} reporter mice were injected I.V. with anti-CD4 PE-conjugated antibody at a concentration of 5µg/ml. Mice were sacrificed three minutes after injection and the thymi were immediately harvested and mechanically disrupted for thymocyte analysis.

(A) Gating strategy to identify RAG^{gfp+} $CD25^{-}$ IV $CD4^{+}$ labeled cells within the perivascular space (PVS).

(B) Gating for immature ($CD69^{+}CD62L^{-}$) and mature ($CD69^{lo}CD62L^{+}$) cells within IV $CD4^{+}$ RAG^{gfp+} $CD25^{-}$ SP4 thymocytes. The proportions of immature (blue circle) and mature (red square) cells with $CD4^{+}$ RAG^{gfp+} $CD25^{-}$ SP4 thymocytes reveal mature cells as the dominant population within the PVS.

(C) The mature IV $CD4^{+}$ labeled cells as identified in (B) separated into M1-M4 to identify each population within the PVS; M1 (red), M2 (blue), M3 (green) and M4 (orange).

The standard error bars display the SEM. A mann-whitney test was performed in (B), where ** denotes a significant difference as $p<0.01$. An one-way ANOVA as performed in (C), where ** denotes a significant difference as $p<0.01$, *** denotes $p<0.001$ and **** denotes $p<0.0001$. All data is typical of 3 independent repeats where total n=7.

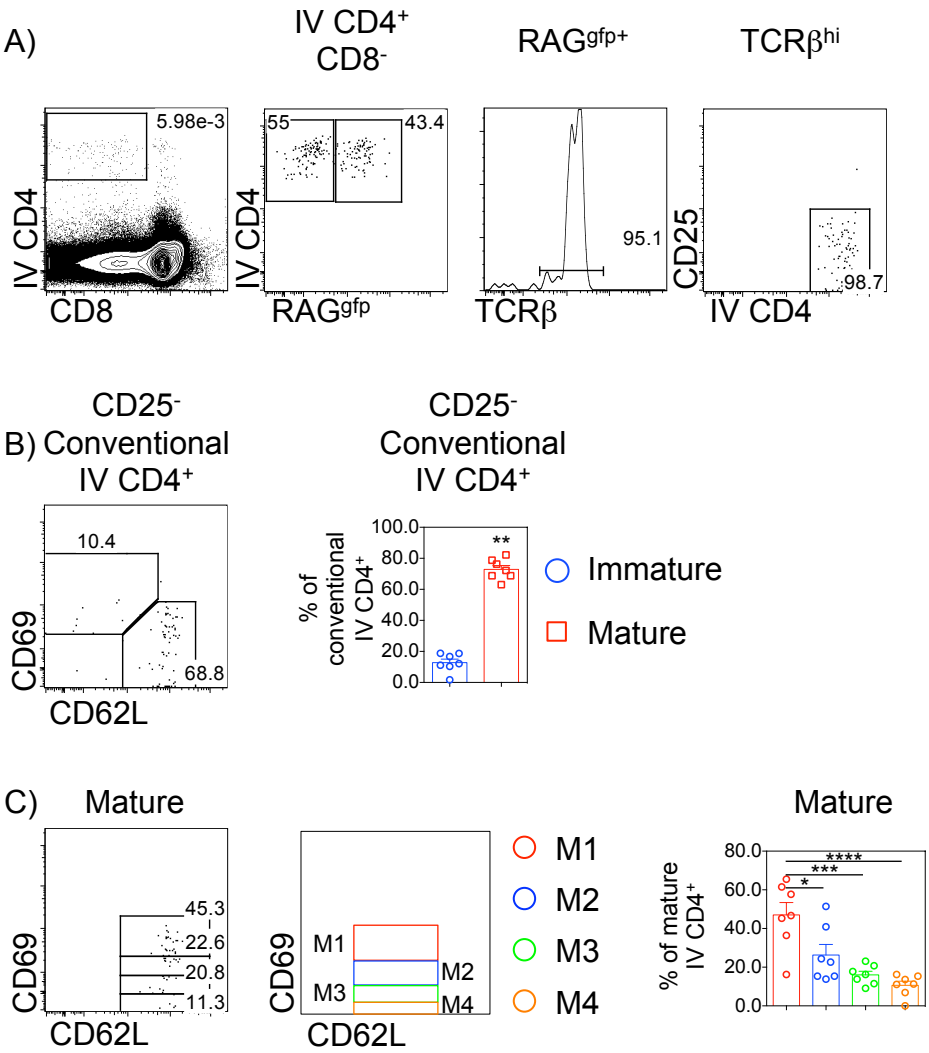
A)
IV CD4+ CD8-
RAGgfp+
TCRβhi
5.98e-3
IV CD4
CD8
55
43.4
IV CD4
RAGgfp
95.1
TCRβ
CD25
98.7
IV CD4
B) Conventional IV CD4+
CD25-
10.4
68.8
CD69
CD62L
CD25- Conventional IV CD4+
% of conventional IV CD4+
100.0
80.0
60.0
40.0
20.0
0.0
**
Immature
Mature
C) Mature
45.3
22.6
20.8
11.3
CD69
CD62L
M1
M2
M3
M4
CD69
CD62L
M1
M2
M3
M4
Mature
% of mature IV CD4+
80.0
60.0
40.0
20.0
0.0
****
***
*

Figure 5.3. IV CD4 Labeled Cells Contain Both RAG^{gfp-} And RAG^{gfp+} Cells Within The Perivascular Space

Adult WT RAG^{gfp} reporter mice were injected I.V. with anti-CD4 PE-conjugated antibody at a concentration of 5µg/ml. Mice were sacrificed three minutes after injection and the thymi were immediately harvested and mechanically disrupted for thymocyte analysis.

(A) Expression of anti-CD4 PE (IV CD4) and CD8 on thymocytes of WT RAG^{gfp} mice. Expression of RAG^{gfp} expression within the IV CD4^{+} population (middle) and the proportions of RAG^{gfp-} (blue circle) and RAG^{gfp+} (red square) IV CD4^{+} cells were calculated (right).

(B) RAG^{gfp+} IV CD4^{+} cells were separated based on expression of CD25 and the expression of pattern CD69 and CD62L was plotted for CD25^{+} (middle) and CD25^{-} (right) RAG^{gfp+} IV CD4^{+}.

(C) RAG^{gfp-} IV CD4^{+} cells were separated based on expression of CD25 and the expression of pattern CD69 and CD62L was plotted for CD25^{+} (middle) and CD25^{-} (right) RAG^{gfp-} IV CD4^{+}.

The standard error bars display the SEM and a mann-whitney test was performed. All data is typical of 3 independent repeats where total n=7.

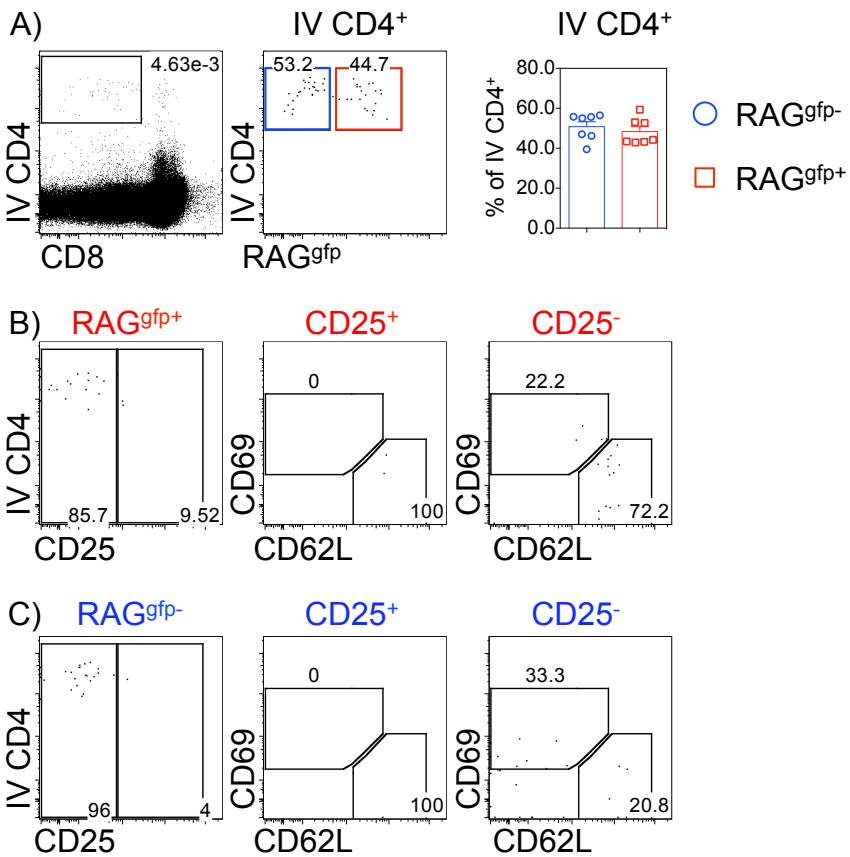
A)
IV CD4+
IV CD4+
4.63e-3
IV CD4
CD8
53.2
44.7
IV CD4
RAGgfp
% of IV CD4+
80.0
60.0
40.0
20.0
0.0
RAGgfp-
RAGgfp+
B)
RAGgfp+
CD25+
CD25-
IV CD4
85.7
9.52
CD25
0
100
CD69
CD62L
22.2
72.2
CD69
CD62L
C)
RAGgfp-
CD25+
CD25-
IV CD4
96
4
CD25
0
100
CD69
CD62L
33.3
20.8
CD69
CD62L

Figure 5.4. Each Of The M1-M4 Subpopulations Of Mature SP4 Thymocytes Accumulate Within The Adult LTβR-deficient Mouse Thymus

Thymic lobes were harvested from control (*Ltbr*$^{+/+}$) and LTβR-deficient (*Ltbr*$^{-/-}$) mice and mechanically disrupted for FACS analysis of thymocytes.

(A) Expression pattern of CD69 and CD62L on mature conventional single positive CD4 (cSP4) thymocytes, identified as CD4^{+}CD8^{-}TCRβ^{hi}CD25^{-}Foxp3^{-}CD69^{lo}CD62L. The CD69^{lo}CD62L^{+} mature fraction was further separated based on levels of CD69 in to M1, M2, M3 and M4.

(B) Cell numbers for each M1-M4 fraction were calculated for *Ltbr*$^{+/+}$ (blue, n=12) and *Ltbr*$^{-/-}$ (red, n=11).

(C) *Ltbr*$^{+/+}$ and *Ltbr*$^{-/-}$ adult mice were administered BrdU to measure proliferation within mature cSP4 thymocytes and the M1-M4 subpopulations within the mature cSP4 population. The percentage of BrdU^{+} cells was calculated for each population within *Ltbr*$^{+/+}$ (blue, n=5) and *Ltbr*$^{-/-}$ (red, n=6) mice.

The standard error bars display the SEM and a mann-whitney test was performed, where ** denotes a significant difference as $p<0.01$, *** denotes $p<0.001$ and **** denotes $p<0.0001$. (A-B) is typical of 3 independent repeats and (C) is typical of 2 independent repeats.

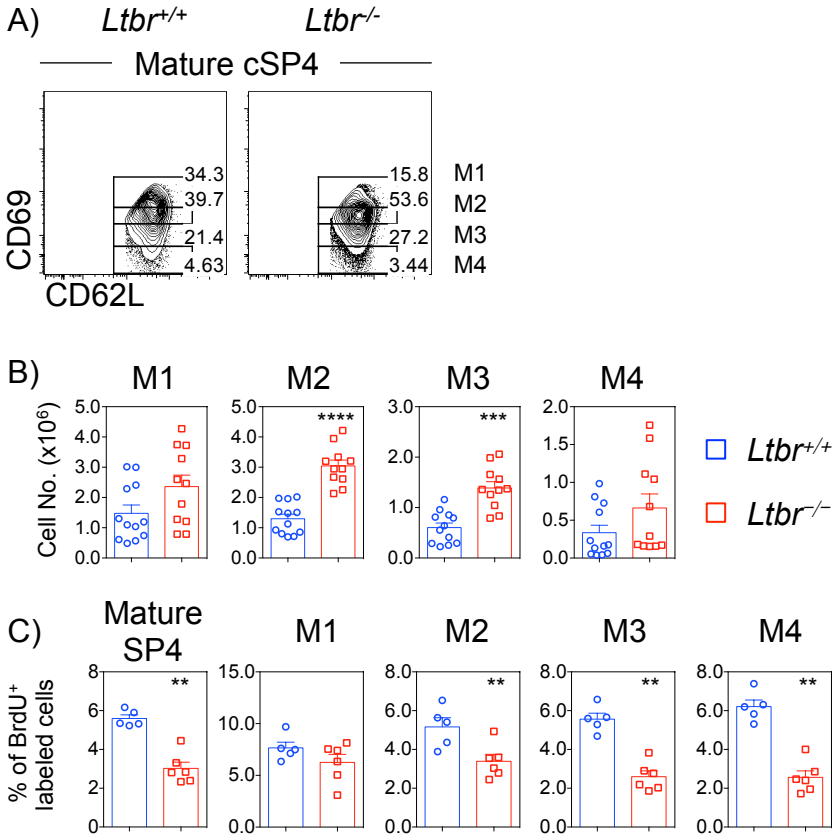
A)
Ltbr+/+
Ltbr-/-
Mature cSP4
CD69
CD62L
34.3
39.7
21.4
4.63
15.8
53.6
27.2
3.44
M1
M2
M3
M4
B)
M1
M2
M3
M4
Cell No. (x10^6)
****
***
Ltbr+/+
Ltbr-/-
C)
Mature SP4
M1
M2
M3
M4
% of BrdU+ labeled cells
**

This supports our previous data suggesting that once mature thymocytes reach egress competence they can leave the cell in a random timing and are not restricted to an ordered program of egress where the oldest cells must leave first.

Data from the *Ltbr*$^{-/-}$RAG^{gfp} mouse model revealed how mature thymocytes within the *Ltbr*$^{-/-}$ thymus have a much longer intrathymic dwell time compared to the control counterparts (Chapter 4). This model could also help provide insight into the dwell time of each of the M1-M4 fractions and if the dwell time of each of the fractions were similarly increased it would support the stochastic egress model. To investigate this a similar approach was applied to data acquired from *Ltbr*$^{-/-}$RAG^{gfp} data. The RAG^{gfp+} mature subset of SP4 thymocytes was separated into the M1-M4 fractions based on CD69 expression (Fig 5.5.A.). For each fraction the RAG^{gfp} expression was plotted comparing *Ltbr*$^{+/+}$RAG^{gfp} and *Ltbr*$^{-/-}$RAG^{gfp} mice (Fig 5.5.B.). Analysis of the MFI of RAG^{gfp} on each fraction revealed RAG^{gfp} is significantly lower on each of the M2-M4 fractions of *Ltbr*$^{-/-}$RAG^{gfp} mature thymocytes (Fig 5.5.C.). Therefore this suggests that all fractions within the mature subset of SP4 thymocytes are accumulating rather than accumulation of just the most mature M4 fraction, further supporting the stochastic model.

Finally, the method of splitting the mature fraction into M1-M4 was used for the IV CD4^{+} cells within *Ltbr*$^{-/-}$ mice. Gating was consistent with previous experiments where RAG^{gfp+} IV CD4^{+} CD25^{-} cells were gated on and split into immature and mature cells based on CD69 and CD62L expression (Fig 5.6.A.). CD69^{lo}CD62L^{+} mature cells were gated on and separated into the M1-M4 fraction. Importantly, there was no

specific skewing of IV $CD4^+$ cells within any of the M1-4 fractions within the perivascular space (Fig 5.6.B.). This indicates that accumulating thymocytes in the process of active emigration consisted of all stages of mature thymocytes, further supporting the stochastic model of thymocyte egress.

These results reveal that the $CD69^{lo}CD62L^+$ mature fraction can be split based on CD69 expression into subsets that exhibit sequential maturation. All of these subset can be found within the PVS indicating that they are actively undergoing thymic egress and each of these fractions were found among accumulating mature thymocytes within a model of disrupted thymocyte egress (*Ltbr*$^{-/-}$ mice). Together these analyses provide novel evidence to support the stochastic model of thymocyte egress, where egress-competent mature thymocytes do not exit in an ordered, linear manner.

Figure 5.5. RAG^{gfp} And S1PR1 Are Increased On Each Of The M1-M4 Subpopulations Of Mature SP4 Thymocytes Within Adult LTβR-deficient Mice

Thymic lobes were harvested from control (*Ltbr*$^{+/+}$RAG^{gfp}) and LTβR-deficient (*Ltbr*$^{-/-}$ RAG^{gfp}) mice and mechanically disrupted for FACS analysis.

(A) Expression pattern of CD69 and CD62L on mature conventional single positive CD4 (cSP4) thymocytes, identified as CD4^{+}CD8^{-}TCRβ^{hi}CD25^{-}Foxp3^{-} RAG^{gfp+}CD69^{lo}CD62L. The CD69^{lo}CD62L^{+} mature fraction was further separated based on levels of CD69 in to M1 (red), M2 (blue), M3 (green) and M4 (orange).

(B) The expression of RAG^{gfp} on M1-M4 fraction of CD69^{lo}CD62L^{+} mature SP4 thymocytes within *Ltbr*$^{+/+}$RAG^{gfp} (blue) and *Ltbr*$^{-/-}$RAG^{gfp} (red) mice. Expression of RAG^{gfp} is also compared to a non-fluorescent control (grey) for each population.

(C) RAG^{gfp} MFI for each M1-M4 population of mature SP4 thymocytes was calculated. **Left:** RAG^{gfp} MFI is compared between *Ltbr*$^{+/+}$RAG^{gfp} (left bar) and *Ltbr*$^{-/-}$ RAG^{gfp} (right bar) for M1 (red), M2 (blue), M3 (green) and M4 (orange). **Right:** RAG^{gfp} MFI is compared between *Ltbr*$^{+/+}$RAG^{gfp} (blue) and *Ltbr*$^{-/-}$RAG^{gfp} (red) for M1-M4.

The standard error bars display the SEM and an one-way ANOVA test was performed, where * denotes a significant difference as $p<0.05$. All data is typical of 3 independent repeats where total n=8.

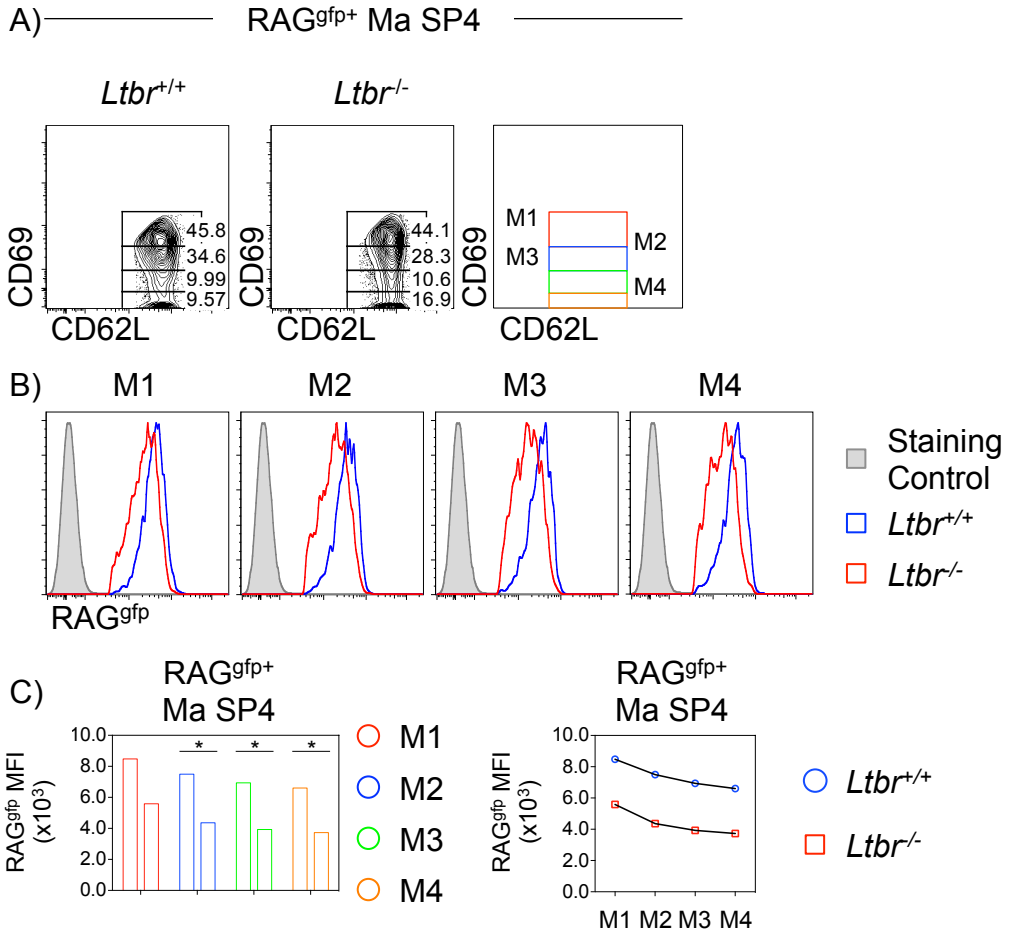
A)
RAGgfp+ Ma SP4
Ltbr+/+
Ltbr-/-
CD69
CD62L
45.8
34.6
9.99
9.57
44.1
28.3
10.6
16.9
M1
M2
M3
M4
B)
M1
M2
M3
M4
RAGgfp
Staining Control
Ltbr+/+
Ltbr-/-
C)
RAGgfp+ Ma SP4
RAGgfp MFI (x10³)
10.0
8.0
6.0
4.0
2.0
0.0
*
*
*
M1
M2
M3
M4
RAGgfp+ Ma SP4
RAGgfp MFI (x10³)
10.0
8.0
6.0
4.0
2.0
0.0
M1 M2 M3 M4
Ltbr+/+
Ltbr-/-

Figure 5.6. Each Of The M1-M4 Subpopulations Of Mature SP4 Thymocytes Within The Adult LTβR-deficient Mouse Thymus Are Present Within The PVS

Adult LTβR deficient (*Ltbr*$^{-/-}$RAG^{gfp}) mice were injected I.V. with anti-CD4 PE-conjugated antibody at a concentration of 5μg/ml. Mice were sacrificed three minutes after injection and the thymi were immediately harvested and mechanically disrupted for thymocyte analysis.

(A) Gating strategy to reveal immature (CD69^{+}CD62L^{-}) and mature (CD69^{lo}CD62L^{+}) cells within IV CD4^{+} RAG^{gfp+} CD25^{-} SP4 thymocytes.

(B) Mature (CD69^{lo}CD62L^{+}) IV CD4^{+} RAG^{gfp+} CD25^{-} SP4 thymocytes were separated into M1-M4 fractions based on CD69 expression and the proportions of M1 (red), M2 (blue), M3 (green) and M4 (orange) were calculated.

The standard error bars display the SEM and an one-way ANOVA test was performed. All data is typical of 3 independent repeats where total n=7.

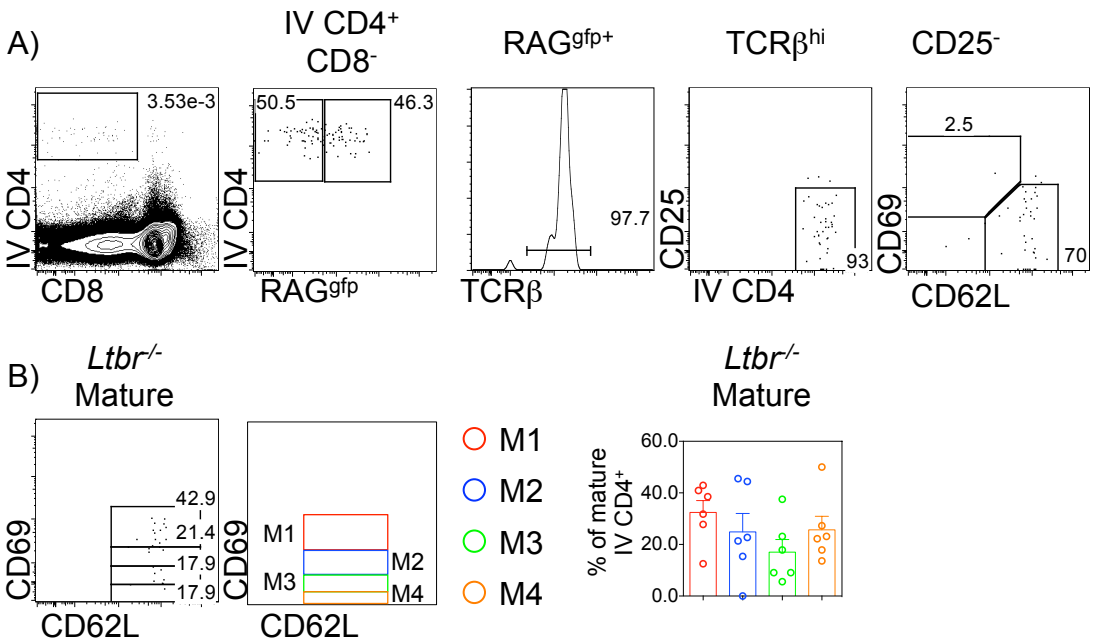
A)
IV CD4+ CD8-
RAGgfp+
TCRβhi
CD25-
3.53e-3
IV CD4
CD8
50.5
46.3
IV CD4
RAGgfp
97.7
TCRβ
CD25
93
IV CD4
2.5
CD69
70
CD62L
B)
Ltbr-/-
Mature
42.9
21.4
17.9
17.9
CD69
CD62L
M1
M2
M3
M4
CD69
CD62L
M1
M2
M3
M4
Ltbr-/-
Mature
% of mature IV CD4+
60.0
40.0
20.0
0.0

5.3 DISCUSSION

Thymocyte development is a highly regulated, multi-step programme, which ensures that T-cells generated by the thymus express a functional T-cell receptor and are self-tolerant. The final step in this process is thymocyte egress and the timing and regulation of this is highly important in ensuring that only functionally mature thymocytes that have undergone a full developmental programme leave the thymus to generate and maintain the peripheral T-cell pool. Although multiple cellular and molecular regulators of thymocyte egress have been identified, specific details of egress timing, such as the order of cells leaving the thymus, remain contentious topics. The aim of this chapter was to develop an approach to enable a more accurate investigation of the timing and order of thymocyte egress, which may be important for further studies of the regulators of thymocyte egress or approaches to manipulate the T-cell immune system via thymocyte egress.

Different models have been proposed for how maturation and timing of thymocyte egress occurs with studies supporting two models in particular, the conveyor-belt model and the stochastic model. The conveyor-belt model proposes that thymocytes follow a linear, strictly ordered pattern of egress, where only the most mature cells can exit following a specified period of medullary residency. Alternatively the stochastic, or random, thymocyte egress model proposes that once a thymocyte has matured and has become egress competent it can leave the thymus, regardless if there are cells that are older than itself that have not yet undergone egress.

Previous studies have separated the SP4 population as a whole to investigate which

of the two models of egress is occurring. The study by McCaughtry *et al.* took an approach where the SP4 thymocyte population was separated into three subsets based on their expression of RAG^{gfp}: GFP^{hi}, GFP^{mid} and GFP^{lo} (94). Their analysis revealed that GFP^{lo} cells had the most mature phenotype, expressing high levels of maturation associated molecules such as CD62L and Qa2 and low levels of CD69, consistent with our own gating of mature SP4 thymocytes, which are $CD69^{lo}CD62L^{+}$ and express lower levels of RAG^{gfp} compared to $CD69^{+}CD62L^{-}$ immature SP4 thymocytes. The findings of McCaughtry *et al.* revealed that GFP^{mid} and GFP^{lo} cells both express *S1pr1,* whereas GFP^{hi} cells do not and that GFP^{lo} SP4 thymocytes had the highest expression of *S1pr1*. Additionally intrathymic (I.T.) injection of biotin was used to directly track RTE which revealed that RTE have a phenotype resembling the most mature GFP^{lo} SP4 fraction. Because GFP^{lo} SP4 thymocytes were more mature than GFP^{mid} and RTE resembled only the GFP^{lo} it was concluded that this data supported the conveyor belt method.

Because this gating strategy using RAG^{gfp} levels was used to separate the SP4 population as a whole it will include both egress incompetent immature SP4 thymocytes and egress competent mature SP4 thymocytes. Therefore it is most likely that the GFP^{hi} population is the $CD69^{+}CD62L^{-}$ immature population, which our own analysis reveals have higher levels of RAG^{gfp} compared to the $CD69^{lo}CD62L^{+}$ population. GFP^{mid} and GFP^{lo} express S1PR1 and CD62L and our analysis reveals that S1PR1 expression is restricted to the $CD69^{lo}CD62L^{+}$ population and although the McCaughtry *et al.* study suggests that the more mature, GFP^{lo}, SP4 thymocytes have higher levels of *S1pr1* gene expression, there is only a modest increase in

S1PR1 expression between our M1-M4 SP4 populations (M1<M2<M2<M4). Therefore it appears that the populations identified in the McCaughtry *et al.* study most likely reveal differences between the $CD69^{+}CD62L^{-}$ immature and $CD69^{lo}CD62L^{+}$ mature population. Thus the approach utilized by McCaughtry *et. al* fails to separate the mature population in order to definitively measure the order of thymocyte egress whereas our strategy of separating the mature SP4 fraction into subsets of differing maturational statuses allows for a more fine-grain analysis of thymocyte maturation.

Another study used a similar approach to separate the SP4 thymocyte population as a whole into four different maturation fractions based on CD69, Qa2 and 6C10 expression to create Sp1 $CD69^{+}6C10^{+}$, Sp2 $CD69^{+}6C10^{-}$, Sp3 $CD69^{-}6C10^{-}QA2^{-}$ and Sp4 $CD69^{-}6C10^{-}QA2^{+}$ populations (278). The findings of Jin *et al.* revealed that the Sp3 and Sp4 fractions, which are $CD69^{-}$, expressed higher levels of *S1pr1* compared to Sp1 and Sp2, which are both $CD69^{+}$ (278). This difference in *S1pr1* gene expression is perhaps not surprising due to the antagonistic nature of CD69 and S1PR1 expression (102,103,106). The Jin *et al.* study nicely showed a precursor-product relationship between the Sp1, Sp2, Sp3 and Sp4 populations (developing in that order) and adoptive transfer of these four populations revealed that Sp3 and Sp4 fractions were found in the periphery sooner than Sp1 and Sp2. However Sp3 cells were found in the periphery when some Sp4 thymocytes were still within the thymus suggesting that egress may not be occurring in an ordered manner. The Jin *et al.* study faces the same caveat as the McCaughtry *et al* study which is that the SP4 thymocyte population as a whole is being separated into different maturational

subsets. Thus many of the differences identified between the different SP4 fractions are key differences previously identified between immature and mature SP4 thymocytes, such as the expression of S1PR1 and thus do not offer enough depth to accurately investigate the order of mature thymocyte egress. Together the results of both studies do not clearly conclude whether thymocyte egress is a random or ordered process.

An additional caveat of the study by Jin *et al.* is the use of Qa2 to distinguish between the Sp3 and Sp4 populations. Xing *et al.* showed that the expression of Qa2 is dependent on type 1 interferon signaling in SP thymocytes and is not associated with the maturation status of the thymocyte itself (262). Therefore the use of Qa2 to define different maturation subsets with the SP4 thymocyte population is inherently flawed. Instead Xing *et al.* proposed the use of CD69 and MHC Class I to separate SP4 thymocytes into three distinct populations, $CD69^{+}$Class I^{-} SM, $CD69^{+}$Class I^{+} M1 and $CD69^{-}$Class I^{+} M2 and showed that the Sp3 and Sp4 populations shown in the study by Jin *et al.* can be identified as $CD69^{-}$Class I^{+} M2. Interestingly the M2 population of SP4 thymocytes express CD62L, S1PR1 and are $CD69^{-}$ which would make them the equivalent population to the $CD69^{lo}CD62L^{+}$ mature SP4 population we have used for our own analysis.

Our approach to understand which of the two models operates to regulate thymocyte egress was similar but, in contrast to previous studies, we separated the $CD69^{lo}CD62L^{+}$ mature SP4 cells into sub fractions. This allowed us to focus on SP4 thymocytes that are egress competent and possess the potential to exit the thymus,

a point that extends the findings of the previous studies discussed above. We used the expression levels of CD69 to split the $CD69^{lo}CD62L^{+}$ SP4 population into four populations termed M1-M4 and analysis of RAG^{gfp} expression across the four populations revealed sequential populations of different ages, with M1>M2>M3>M4 for RAG^{gfp}. Additionally all four M1-4 populations expressed S1PR1 suggesting that all cells are egress competent allowing us to directly compare cells capable of thymus exit and investigate whether the more mature M4 cells leave before the relatively less mature M1 cells. Interestingly the use of I.V. injection of an anti-CD4 antibody, to label cells in the thymic PVS as previously reported, revealed that all four populations are present in the perivascular space (PVS) and therefore likely to be in the process of egress (111,115). Therefore this revealed that younger (higher RAG^{gfp}) mature cells possess the capacity to undergo the first step of egress via entry to the PVS at the same time as the older (lower RAG^{gfp}) mature cells, providing evidence for a stochastic model of thymocyte egress at the level of PVS entry. Additionally our analysis revealed that in the context of an intrathymic accumulation of mature SP4 thymocytes, as observed in *Ltbr*$^{-/-}$ mice, there was an increase in each of the M1-M4 mature subpopulations and thus no specific build up of the most mature, M4, subset of SP4 thymocytes. There was also an increase in the intrathymic dwell time for each M1-M4 fraction not just the more mature M4 fraction. These are also indicative of a stochastic model of egress, as it could be predicted that ordered egress would result in the most mature M4 cells preferentially accumulating within the thymus.

Our data therefore support the stochastic model of thymocyte egress, revealing that PVS entry occurs randomly within the mature, egress-competent SP thymocyte population. However, whether the whole process of thymocyte egress is stochastic remains to be determined as PVS entry is only one step of the egress process and cells within the PVS must then undergo reverse transendothelial migration into the blood. To determine whether reverse transendothelial migration from the PVS into the blood subsequently occurs in a stochastic manner requires further experiments to analyze RTE in the periphery and compare their phenotype to the M1-M4 mature populations. Using our approach to identify M1-M4 populations of mature thymocytes in conjunction with the biotin intrathymic labeling technique used in the McCaughtry *et al.* study would allow us to specifically show whether younger mature cells can leave before older mature cells and experiments are currently underway to address this.

Our analysis to identify different mature populations within the PVS through I.V. injections of anti-CD4 revealed an interesting observation. Over half of the IV $CD4^+$ cells were RAG^{gfp-} suggesting that I.V. anti-CD4 labels cells in the PVS that are exiting but also entering the thymus. Preliminary analysis of the RAG^{gfp-} population interestingly did not suggest a skewing to $CD25^+$ cells. $CD25^+$ cells will include activated T-cells but could also potentially include $CD25^+$ regulatory T-cells (Treg) and previous studies have shown that a large portion of thymic Treg are recirculating and would therefore be RAG^{gfp-} (282,283). This RAG^{gfp-} IV $CD4^+$ population may also include the long-term thymic resident population of iNKT cells which have recently been implicated in the regulation of thymocyte egress via type 2 cytokines (115,284).

Thus the potential localization of iNKT cells to points of conventional T-cell egress may have interesting implications for how these cells are capable of contributing to the regulation of T-cell egress. These observations highlight an important requirement for the inclusion of RAG^{gfp} when interpreting IV $CD4^+$ cells. Further experiments are currently underway to identify these RAG^{gfp-} cells through the use of a more diverse staining panel to include DC, iNKT and Treg markers. Once the RAG^{gfp-} population(s) within PVS have been identified it would be interesting to investigate whether this population is interacting with the egressing cells also within the PVS and whether there is a requirement for these cells for normal egress or PVS entry.

An additional interesting observation came from the analysis of the M1-M4 fractions of mature SP4 thymocytes in *Ltbr*$^{-/-}$$RAG^{gfp}$ mice. Our analysis revealed that not only is RAG^{gfp} expression lower on each fraction compared to *Ltbr*$^{+/+}$$RAG^{gfp}$ control mice, but that the RAG^{gfp} expression of *Ltbr*$^{-/-}$ M1 cells is lower than the RAG^{gfp} expression of *Ltbr*$^{+/+}$ M1. This would suggest that the length of time spent by all mature SP4 thymocytes in *Ltbr*$^{-/-}$ thymus exceeds the time spent by even the most mature SP4 thymocytes within the control mice. As described in Chapter 4, RAG^{gfp} reduction does not occur in immature SP thymocytes, thus only egress-competent SP thymocytes accumulate and this occurs at all mature stages within $CD69^{lo}CD62L^+$ mature SP thymocytes supporting the stochastic model of egress.

Together this chapter uses an alternative approach of identifying populations of different ages within the mature fraction of SP4 thymocytes to show that, beyond the

acquisition of egress capability, egress of these cells does not depend on the age of the cell. Our data show that once a SP4 thymocyte has reached the $CD69^{lo}CD62L^{+}$ mature stage it expresses S1PR1 and can enter the PVS and potentially egress the thymus regardless of the mature cells around it, supporting the stochastic model of thymocyte egress. Thus thymocyte egress as a whole process may actually be thought of as a mixture of both the stochastic and conveyor belt models. Conveyor belt, because immature SP thymocytes must undergo maturation before becoming egress-competent and thus there is a specific timing and order to when cells have the ability to exit. However once this maturation occurs entry into the PVS can occur randomly, independent of the residency within the thymus of the mature cell, supporting the stochastic model. As discussed above, whether the final step of thymocyte egress from the PVS into the blood remains to be determined.

An implication of the stochastic model is that the mature SP thymocytes can leave once they reach egress-competence and therefore must undergo sufficient maturation prior to this point. It has been shown that HSA^{hi} immature SP thymocytes are sensitive to negative selection upon TCR stimulation but once these cells mature into HSA^{lo} SP thymocytes they are resistant to this and instead have a proliferative capacity following TCR stimulation which is vital to the T-cell response to their cognate Ag (96). Thus the ability to egress the thymus is limited to the mature thymocytes to ensure that this functional transition has occurred. Development into the mature phenotype is also associated with cytokine licensing of the SP thymocyte, i.e. the ability to produce cytokines, which a recent study by Xing *et. al* shows is restricted to M2 mature fraction (97). Both studies restrict these functional abilities to

the mature SP population as a whole, therefore our approach of separating the mature population into different fractions based on their maturation may provide further insight into these functional abilities in relation to the maturational status of the mature cell.

An interesting extension of this would be that if functional capacity differed between the M1-M4 populations, which all have the capacity to exit the thymus, it would imply that T-cells entering the peripheral pool may potentially have different functional capacities. There has been evidence that may support this which reveals medullary residency time is important in the acquisition of functional phenotype for mature SP thymocytes. Jin *et. al* intrathymically injected the most mature, Sp4, SP thymocyte population and studied their phenotypic and functional changes following either 1 day or 4 days within the thymus (278). Their analysis revealed increased frequencies of IL-4 and interferon (IFN)-γ producing cells when cells were in the thymus for 4 days suggesting functional changes increased with increased medullary residency (278). Thus this may support the hypothesis that T-cells of the M1 fraction may not undergo full medullary residency-dependent acquisition of functional capacities. Investigation of this hypothesis would require functional analysis of each of the M1-M4 fractions of the $CD69^{lo}CD62L^{+}$ mature SP population to show that the older fractions have a greater functional capacity compared to the younger fractions. An alternative to this could be that functional maturation has already occurred within the M1 fraction of $CD69^{lo}CD62L^{+}$ thymocytes, thus whether the M1 fraction exits the thymus prior to their maturation to the older M2-M4 fractions has no consequence on their function.

Alternatively mature thymocytes may leave the thymus at different maturation states and then undergo further maturation within the periphery. Boursalian *et. al* provide evidence that such continued maturation of T-cells can occur in the periphery through the use of RAG^{gfp} mice (263). RTE continued phenotypic maturation within the periphery, such as reduced HSA expression, as well as continued functional maturation as evidenced by RAG^{gfp+} RTE secreting less IL-2 and have lower expression of the high-affinity IL-2 receptor resulting in reduced antibody-induced proliferation compared to RAG^{gfp-} T-cells (263). Thus current evidence may suggest that if T-cells leave the thymus at the earliest M1 stage they may undergo further maturation within the periphery, however directly investigating this using our new approach would be required to confirm this.

Together our analysis, summarized in Figure 5.7, not only provides evidence that thymocyte entry into the PVS, a key step in the egress of mature thymocytes, occurs stochastically but also provides a novel approach of identifying different maturation subsets of SP thymocytes within the $CD69^{lo}CD62L^{+}$ mature population which will increase the accuracy of further investigations of thymocyte egress.

Figure 5.7. T-cell Egress Is Not An Exclusively Stochastic Or Linear Process

(A) The initial stage of T-cell egress requires the maturation of $CD69^{+}CD62L^{-}$ immature cells to become egress-competent $S1PR1^{+}CD69^{lo}CD62L^{+}$ mature SP thymocytes. This indicates that the initial stage of T-cell egress is linear and ordered.

(B) We have identified four populations within mature SP thymocytes that differ by RAG^{gfp} and S1PR1 expression, where the most immature $CD69^{lo}CD62L^{+}$ cells (M1) have high RAG^{gfp} and lower S1PR1 compared to the most mature $CD69^{lo}CD62L^{+}$ cells (M4).

(C) Each of the M1, M2, M3 and M4 subpopulations can enter the perivascular space; an essential stage of T-cell egress, thus supporting that egress at this stage is stochastic.

(D) The final stage of T-cell egress requires the reverse transendothelial migration of mature cells within the perivascular space to enter the blood. It has yet to be determined whether this process is linear or stochastic and is area of research that demands further testing as it may have implications on the function of the T-cells leaving the thymus.

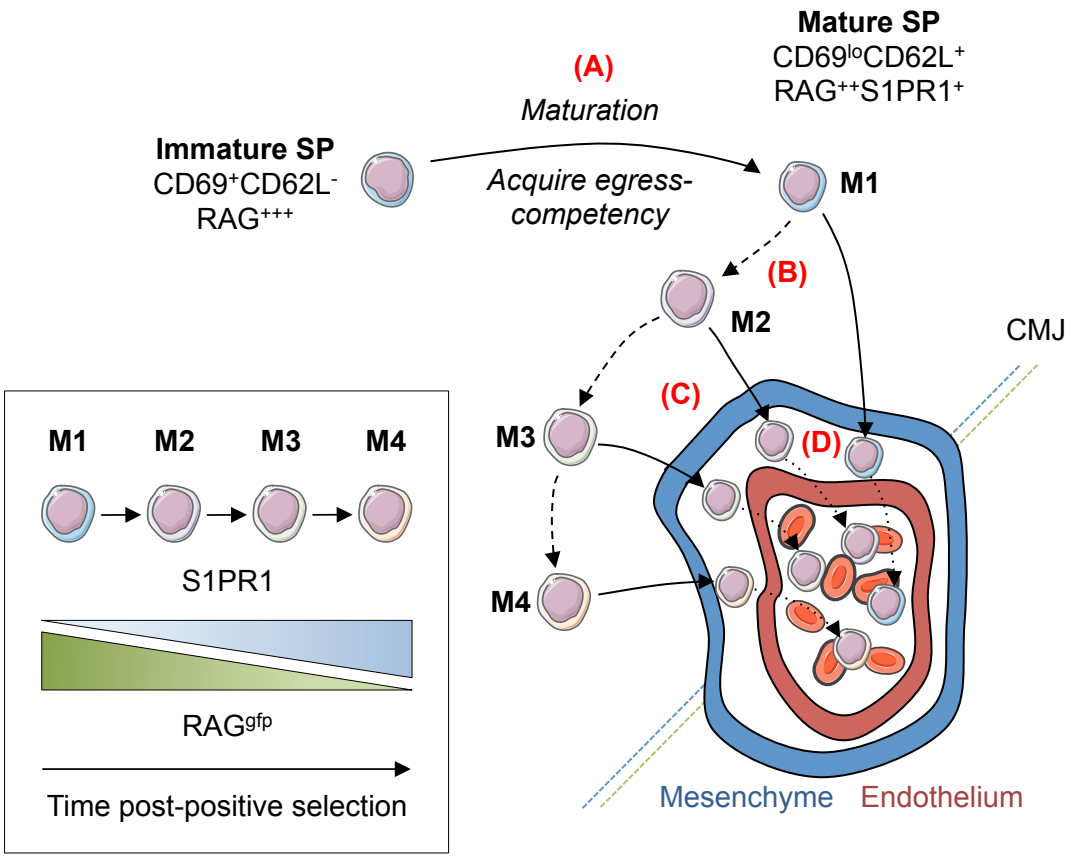
Mature SP
CD69loCD62L+
RAG++S1PR1+
(A)
Maturation
Immature SP
CD69+CD62L-
RAG+++
Acquire egress-competency
M1
(B)
M2
CMJ
(C)
M3
(D)
M4
Mesenchyme
Endothelium
M1
M2
M3
M4
S1PR1
RAGgfp
Time post-positive selection

CHAPTER SIX: GENERAL DISCUSSION

6.1 BACKGROUND AND OVERALL AIMS

The thymus is a complex organ made up of a heterogeneous mix of hematopoietic and stromal cells, where the stromal cells can be separated into epithelium, endothelium and mesenchyme populations. The current literature surrounding thymic mesenchymal cells, including their function and developmental regulation, is lacking. Although the phenotype and function of the thymic mesenchyme within the embryonic thymus has in part been revealed, thymic mesenchyme within the adult thymus has lacked significant investigation. This is not to say that thymic mesenchyme in the adult is completely unknown; thymic mesenchyme has previously been shown to contribute to the structure of the adult thymus including the capsule and may also regulate thymocyte migration through the production of chemokines such as CXCL12 (214,251). A particularly important role of thymic mesenchyme was recently identified in pericytes regulating thymocyte egress via expression of SPHK1 and 2, which regulate S1P-mediated thymocyte egress through catalyzing the phosphorylation of sphingosine to generate S1P (111). The cellular and molecular regulators of thymic mesenchyme also represent an area of research that requires further investigation, as it is unknown how the development and maintenance of thymic mesenchyme occurs.

Through our review of the literature we found that lymph node (LN) and thymic microenvironments may share some cellular and molecular similarities that could inform our own study of the thymic mesenchymal compartment. For example, stromal cells within LNs and the thymus express CCR7-ligands which attract $CCR7^{+}$ T-cells and dendritic cells (DC) (21,69–71,220,222,223). One particular similarity of note was

the essential requirement for signaling through the TNFRSF member lymphotoxin beta receptor (LTβR) for the development of LN mesenchyme as well as thymic stromal microenvironments (22,24,149,151,153,194,231,232). However this also revealed that whilst LTβR was important for mTEC and thymic endothelial cell development and function, it's role in regulating thymic mesenchyme had not been investigated (22,24,151,153,194). In addition to regulating the thymic stromal microenvironment, studies of LTβR-deficient mouse thymi revealed a role for LTβR in regulating thymocyte egress, however it remained unknown precisely how LTβR was regulating this process (151).

Therefore the general aims of this study were to address the following questions:

- What are the phenotypic and functional characteristics of adult thymic mesenchyme?
- How is adult thymic mesenchyme regulated at both the cellular and molecular levels?
- What are the cellular and molecular regulators of LTβR-dependent thymocyte egress?

6.2 DEFINING THE ROLE OF LTβR IN REGULATING THYMIC MESENCHYME

Using flow cytometric analysis we sought to define the phenotype and potential heterogeneity of thymic mesenchyme within the adult murine thymus. Within the adult thymus we were able to identify thymic mesenchyme as $PDPN^{+}CD31^{-}$ non-epithelial stroma using a gating strategy similar to that used to identify stromal populations within LNs (220). This $PDPN^{+}CD31^{-}$ population expressed a number of markers previously associated with thymic mesenchyme such as PDGFRα, also

expressed by embryonic mesenchyme and PDGFRβ, reported to identify thymic pericytes, as well as the adhesion molecules ICAM-1 and VCAM-1 (111,202). Our analysis revealed that the development of the ICAM-1^{hi}VCAM-1^{hi} mesenchyme population was critically dependent on LTβR signaling mediated via αβ T-cell interactions with thymic mesenchyme and ICAM-1^{hi}VCAM-1^{hi} are a significant population as they expressed *Sphk1, Ccl19* and *Autotaxin* linking their potential function to regulating thymocyte migration and egress. This dependency on interactions between mesenchyme and T-cells reflects a similar mechanism of crosstalk that operates for thymocyte-TEC development, which are both dependent on signaling to each other for their development. The initial discovery of the thymic phenotype of LTβR-deficient mice by Boehm *et. al* revealed a potential role for LTβR in thymocyte egress (151). Thus together with a reported role for thymic mesenchyme for regulation of thymic egress and our own results indicating an essential requirement for LTβR for mesenchyme development, we hypothesized that LTβR regulation of thymic mesenchyme is a critical regulatory pathway of T-cell egress (151). What made this hypothesis attractive was that, if correct, it would suggest that developing T-cells signal LTβR-dependent development of thymic mesenchyme. The mesenchyme, acting as gatekeepers of T-cell exit, would in turn produce mediators enabling T-cell egress, thus suggesting that T-cells enable their own egress through their regulation of thymic mesenchyme.

To directly investigate this hypothesis we generated a mouse model to specifically delete *Ltbr* on thymic mesenchyme. We crossed the previously reported neural-crest derived mesenchyme specific Cre mouse model, *Wnt-1^{cre}*, to an mT/mG fate mapper,

wherein all cells express mT but switch to mG following Cre excision, which can be identified by flow cytometry (111,241). The *Wnt-1*^{cre}mT/mG mice revealed efficient and specific activity of Cre within PDPN^{+} thymic mesenchyme. We crossed the *Wnt-1*^{cre} strain to the *Ltbr*^{flox} strain to specifically delete *Ltbr* on *Wnt-1*^{cre} thymic mesenchyme to investigate the role of LTβR regulation of thymic mesenchyme in regulating T-cell egress. Analysis of the thymus of these mice revealed that despite a loss of ICAM-1^{hi}VCAM-1^{hi} thymic mesenchyme, thymocyte egress was unperturbed disproving our hypothesis that LTβR regulation of thymic mesenchyme acts to control thymic T cell exit. Therefore despite the essential role of LTβR in the development of ICAM-1^{hi}VCAM-1^{hi} thymic mesenchyme, this regulatory pathway is not essential for thymocyte egress. Importantly our analysis is focusing on LTβR regulation of thymic mesenchyme controlling egress and therefore does not rule out a role for thymic mesenchyme to regulate LTβR-independent thymocyte egress. The study of thymic pericytes, which are thymic mesenchymal cells, clearly supports thymic mesenchyme regulating thymocyte egress via SPHK production and therefore our analysis shows that LTβR is not regulating this process (111). Our preliminary gene-expression analysis of thymic stroma from WT and *Ltbr*$^{-/-}$ mice appears to support this, with *Ltbr*$^{-/-}$ thymic mesenchyme having no major reduction in *Sphk.* Our analysis centered on a role for LTβR regulation of thymic mesenchyme in regulating thymocyte egress however an alternative function of these cells could be regulating the entry of progenitor cells which is also dysfunctional in LTβR-deficient mice (22,24). The case for thymic mesenchyme regulating T-cell progenitor entry is similar to that for regulating T-cell egress, in that thymic mesenchymal cells are situated around blood vessels which are the site of T-cell progenitor entry and mature T-cell egress, making

them well positioned to regulate these processes. Although endothelial cells have currently been identified in recent studies to regulate the process of T-cell progenitor entry into the thymus, these studies have not investigated a role for thymic mesenchyme in this LTβR-dependent process (22,24). This may be of interest as thymus colonization is regulated by CCR7-CCR7-ligands and our own analysis shows that thymic mesenchyme express *Ccl19* and therefore thymic mesenchyme may have a role in this process. Analysis of the ETP population within the *Wnt-1^{cre}Ltbr^{flox}* mice would allow us to investigate this potential function of thymic mesenchyme. Our recently published study revealed that *Wnt-1^{cre}Ltbr^{flox}* mice had a significant reduction of a subpopulation of dendritic cells termed cDC1 and this reduction of cDC1 in *Wnt-1^{cre}Ltbr^{flox}* mice mirrored the reduction found in *Ltbr$^{-/-}$* mice (157). cDC1 cells arise from a progenitor that migrate into the thymus, suggesting that the reduction of cDC1 in the *Wnt-1^{cre}Ltbr^{flox}* could be due to reduced colonization of the thymus by cDC1 progenitors or impaired development of the cDC1 from the progenitors. Therefore this highlights a potential role for thymic mesenchyme in regulating the intrathymic DC populations, which have essential roles in negative selection to prevent autoimmunity.

The other main defect within LTβR-deficient thymi is the drastic medullary disorganization and reduced mTEC, particularly CCL21^{+} mTEC^{lo}. Our analysis of *Foxn-1^{cre}Ltbr^{flox}* mice reveal that this defect is primarily cell intrinsic, however early studies of thymocyte function within the embryonic thymus found that thymic mesenchyme regulate TEC proliferation through the production of growth factors such as FGF10, which our own gene analysis shows is expressed in adult thymic

mesenchymal cells (201,202). Therefore an experiment to analyze the TEC populations within *Wnt-1^{cre}Ltbr^{flox}* would be interesting to investigate whether LTβR regulation of thymic mesenchyme is indirectly regulating TEC.

Alternatively thymic mesenchyme express *Ccl19* which may suggest a role in regulating thymocyte egress in the neonatal thymus rather than the adult. The CCR7 pathway has been shown to regulate the cortical to medullary migration of T-cells however this is regulated through CCL21 and not CCL19 (220,249). However The CCR7-dependent control of T-cell egress in neonates was shown to be regulated by CCL19 (69,116). Therefore the CCR7 pathway of neonatal T-cell egress may be controlled by LTβR regulation of thymic mesenchyme. Therefore investigation of *Ltbr$^{-/-}$* and *Wnt-1^{cre}Ltbr^{flox}* neonates could be a very interesting avenue to pursue in the future. Alternatively transwell migration assays could be carried out to explore a role for thymic mesenchyme in regulating intrathymic migration of thymocytes as well as other lymphocytes such as thymic B-cells in the context of mesenchyme expression of *Cxcl13*. This potential regulation of intrathymic B-cells is interesting as thymic B-cells have recently been identified to contribute to negative selection (260). Furthermore, as our analysis indicates a potential role of thymic mesenchyme in regulating DC migration into the thymus, this could indicate a common mechanism for hematopoietic entry of cells associated with negative selection. Our preliminary analysis found that sorted PDPN^{+} thymic mesenchyme could successfully be sorted and maintained in culture and thus a transwell migration assay would be feasible.

It would be very interesting to investigate whether our strategy of identifying thymic mesenchyme is possible within human thymic tissues and whether the ICAM-1^{hi}VCAM-1^{hi} population is present similarly to the mouse thymus. A recent study which engineered a human thymic microenvironment isolated and cultured thymic mesenchyme and briefly phenotyped them using mesenchyme markers including PDGFRα (285). Interestingly Chung *et. al* found that they were able to reaggregate cultured human TEC and thymic mesenchyme to form a functional thymus which supported thymopoiesis (285). Therefore thymic mesenchyme within the human thymus may play a similar role to embryonic mice for the development of the thymus however additional functions of human thymic mesenchyme could also be investigated. We were fortunate to be able to carry out pilot experiments to investigate the mesenchyme population within human neonatal thymus tissue from patients undergoing cardiac surgery. In these experiments we were able to identify $PDPN^{+}CD31^{-}$ thymic mesenchyme, however due to the size of the thymus tissue itself and the accompanying large number of thymocytes it was difficult to enrich for the thymic mesenchyme population for further in-depth analysis. We are aiming to repeat these pilot analyses using different techniques to deplete the thymocyte population in order to enrich the stromal populations, however lack of availability of human tissue has currently prevented this.

During age-related thymic involution there is a loss of TEC with a concomitant increase in adipocytes, with thymic involution ultimately resulting in reduced thymopoiesis (286,287). The increased adiposity of the thymus is believed to occur through epithelial-mesenchymal transition (EMT) where epithelial cells lose their

epithelial phenotype and differentiate into mesenchyme cells, followed by transdifferentiation of EMT-derived thymic mesenchyme cells into adipocytes (288). This EMT process was observed using *Foxn-1^{cre}ROSA26RstoplacZ* fate mapper mice which showed LacZ^{+} cells (therefore cells that expressed *Foxn-1^{cre}*) expressing Fibroblast Specific Protein-1 (FSP1), an EMT specific marker therefore indicating that these cells were previously epithelial cells that have undergone EMT (289). EMT is an important process that is not restricted to the thymus and is involved in many aspects of development and is characterized by reduced expression of epithelial markers and increased expression of mesenchymal markers (290,291). Thus a population within the total thymic mesenchyme pool identified, as PDPN^{+}CD31^{-} in our analysis may have previously been TEC that have undergone EMT and may also be a population that will transition to pre-adipocytes within the aging thymus. Within peripheral LNs LTβR operates to direct adipocyte precursors into lymphoid stroma (231). Thus LTβR may have a similar role within the thymus to inhibit adipogenesis and maintain mesenchyme phenotype of the cells. Therefore an interesting study would be to investigate the adiposity of LTβR-deficient thymus, which may be increased due to absent LTβR-mediated inhibition of adipogenesis.

Together our study of thymic mesenchyme has revealed a novel role of αβ T-cell mediated conditioning of ICAM-1^{hi}VCAM-1^{hi} thymic mesenchyme and these interactions occur through LTβR. Although thymic mesenchyme express genes associated with T-cell exit, LTβR regulation of thymic mesenchyme is not involved in the control of T-cell egress. Therefore further investigations are required to identify the functional role of ICAM-1^{hi}VCAM-1^{hi} thymic mesenchyme within the adult thymus.

6.3 IDENTIFYING THE MECHANISM OF LTβR-REGULATED T-CELL EGRESS

Our data indicated that the initial hypothesis that LTβR regulation of thymic mesenchyme is an essential pathway involved in thymocyte egress was incorrect. However LTβR-deficient mice have a clear thymocyte egress defect, which led us to identify the cellular regulator of LTβR-dependent egress. Through *in vivo* models to separate hematopoietic and stromal sources of LTβR we were able to show that LTβR expression by stromal cells is required for T-cell egress. As our analysis had already ruled out an essential role for thymic mesenchyme, the other stromal populations to explore were TEC and endothelium. Boehm *et. al* proposed that the strong medullary phenotype and T-cell egress defect of the LTβR-deficient thymus may be linked, we therefore hypothesized that LTβR regulation of TEC may be an essential pathway regulating T-cell egress (151). Using a *Foxn-1^{cre}Ltbr^{flox}* model to delete *Ltbr* on TEC we were able to show that, despite medullary disorganization and reduced mTEC populations, *Foxn-1^{cre}Ltbr^{flox}* mice had no intrathymic accumulation and therefore LTβR regulation of TEC is not an essential regulator of T-cell egress. Our finding of normal intrathymic mature T-cells is important as Zhu *et. al* proposed that LTβR controls CCR7-ligands and absence of this pathway results in SP thymocytes in the cortex as a result of defective CCR7-mediate cortex-medulla migration (155). Therefore not only do our results reveal that thymic medullary disorganization does not impact T-cell egress, it shows that reduced mTEC populations, including CCL21^{+} mTEC^{lo} which are the primary source of CCL21 in the thymus, are not the source of the T-cell egress defect within LTβR-deficient mice. Therefore the proposed role for LTβR regulating cortex-medulla migration via CCR7 is not the mechanism regulating T-cell egress. The last stromal candidate for

regulation of LTβR-dependent T-cell egress was the thymic endothelium. Endothelial cells have been shown to regulated LTβR-dependent T-cell progenitor entry and have previously been implicated in regulating S1P-dependent T-cell egress (22,24,112,113). Using the same approach as to delete *Ltbr* in mesenchyme and TEC, we crossed the endothelial-specific *Flk-1*^{cre} mouse strain to the *Ltbr*^{flox} strain to generate *Flk-1*^{cre}*Ltbr*^{flox}. Interestingly these mice appeared to have an intrathymic accumulation of mature thymocytes of a similar magnitude found within *Ltbr*$^{-/-}$ mice, suggesting that LTβR regulation of thymic endothelial cells is critical for LTβR-dependent T-cell egress. Additionally our analysis found that both *Ltbr*$^{-/-}$ and *Flk-1*^{cre}*Ltbr*^{flox} mice had a significant loss of TEPC which are thought to regulated T-cell progenitor entry (24). Thus our data reveal a novel role for LTβR regulation of thymic endothelial cells as a critical pathway to control T-cell egress and suggests that TEPCs may have an additional role of regulating T-cell egress as well as their previously identified role of regulating T-cell progenitor entry. If this secondary hypothesis of a dual role of endothelial cells regulating entry and exit is correct it could have potential implications for attempts to manipulate one of these processes as it may result in affecting both pathways simultaneously.

Examples of this can be seen in the recent studies of the role of the LTβR pathway in T-cell progenitor entry. Lucas *et. al* found that *in vivo* stimulation of LTβR following bone marrow reconstitution of lethally irradiated mice enhanced the reconstitution of the thymus, as revealed by increased donor cells within the thymus (22). Interestingly this study by Lucas *et. al* found increased frequencies of T-cell populations within the periphery of mice receiving agonistic anti-LTβR (22). Whilst this increase is likely

due, in part, to increased T-cell production downstream of increased thymus reconstitution, it may also indicate that T-cell egress is increased upon anti-LTβR stimulation. Additionally it was shown that this agonistic anti-LTβR treatment increased the frequency of the thymic portal endothelial cells (TPEC) which are thought to regulate T-cell progenitor entry (24). We saw a similar reduction of TPEC in the *Flk-1*^{cre}*Ltbr*^{flox} accompanying the T-cell egress defect and therefore the effects of anti-LTβR stimulation observed by Lucas *et. al* are likely via stimulation of TPEC.

Whilst in this context manipulating T-cell progenitor entry to boost thymic reconstitution and boost egress for thymic output sound like attractive outcomes for therapies, affecting both of these pathways simultaneously may actually be disadvantageous. As our analysis has shown, T-cell egress, or at least the first stage of entry into the PVS, occurs randomly once the cell has acquired egress competence. However we do not fully know whether there is a requirement for different mature T-cells to spend longer in the medulla prior to exit. If a therapy aimed to boost thymus reconstitution by stimulating increased progenitor entry into the thymus, it may also directly increase T-cell egress which could potentially reduce the intramedullary dwell time of the mature thymocytes prior to exit. Further studies would be required to investigate whether this could have any negative impact on the function of these T-cells, which would clearly be counterproductive to the therapy.

An important point to consider regarding our findings of LTβR-dependent T-cell egress is that the altered egress of LTβR-deficient mice does not result in peripheral T-cell lymphopenia. Therefore even though T-cell egress is defective it does not

appear to impact peripheral T-cell-mediated immunity at the quantitative level, however it remains to be determined whether the reduced T-cell egress influences the quality of the T-cells and the repertoire of the peripheral T-cell pool. A consequence of reduced T-cell egress in these mice could be more evident and significant in neonates during the initial establishment of the peripheral T-cell pool and may even cause reduced T-cell diversity within the T-cell pool. As discussed in the previous section, *Ccr7*$^{-/-}$ and *plt/plt* neonates have reduced T-cell egress and this results in a severe T-cell lymphopenia that is present for the first two weeks neonates (69,116). Therefore the role of LTβR in T-cell egress may have more significance during early stages if further experiments revealed a similar phenotype within *Ltbr*$^{-/-}$ neonates. An additional experiment investigating the TCR Vβ repertoire would be very interesting both at the neonatal and adult stages to explore the long term consequences of reduced T-cell egress in these mice.

It is important to note that another major phenotype of *Ltbr*$^{-/-}$ mice is the loss of peripheral lymph nodes due to the essential role of LTβR in their development (149,232). This lack of peripheral LNs may complicate the interpretation of the results from LTβR-deficient mice, however there is no intrathymic accumulation of mature thymocytes in LTα-deficient mice (data not shown), which lack peripheral lymph nodes (237). In addition to this, an intrathymic accumulation is present in WT mice grafted with LTβR-deficient thymic lobes as well as *Flk-1*^{cre}*Ltbr*^{flox} mice, which also have peripheral LNs (although it has yet to be determined whether there is any consequence on LN development within these mice). Therefore the absence of lymph nodes is not a causative factor in regulating T-cell egress from the thymus.

During our experiments investigating the role LTβR in T-cell egress and upon reviewing the current literature surrounding T-cell egress, we found that the understanding of the timing of thymocyte egress was lacking. Therefore an additional aim of our study was to examine the timing and order of T-cell egress to understand whether this process was occurring randomly or in an ordered fashion. What our analysis revealed was that T-cell egress is likely occurring both stochastically and ordered. Previous studies of T-cell egress, particularly the studies by McCaughtry *et. al* and Jin *et. al,* supported the hypothesis that the initial stage of T-cell egress is ordered (277,278). This first stage of T-cell egress involves the maturation of SP thymocytes to become egress-competent and therefore is a linear process, as this must first occur before T-cells have the ability to leave the thymus. However our own analyses suggest that the next step of T-cell egress, where egress-competent T-cells migrate into the PVS, occurs randomly. What currently remains unknown following this study is whether the final step of reverse transendothelial migration of T-cells from the PVS into the blood remains stochastic or is an ordered process. We aim to test this by using a method used by McCaughtry *et. al* to intrathymically label thymocytes with biotin to identify newly generated T-cells within the periphery (277). By using this technique in conjunction with IV anti-CD4 to label T-cells within the PVS, we aim to compare the phenotype of RTE with $CD69^{lo}CD62L^{+}$ T-cells of different maturation within the thymus and the PVS. This will allow us to investigate whether RTE resemble the most mature subset (M4), or are heterogeneous and includes all of the mature subsets of the $CD69^{lo}CD62L^{+}$ population. This experiment

would then allow us to understand the finer details of the timing of T-cell egress and would contribute to further experiments of function and phenotype of RTE.

6.4 CONCLUDING REMARKS

In summary, the two main arms of this thesis have furthered our understanding of the mesenchyme compartment of the thymus, revealing a novel mechanism of αβ T-cell conditioning of thymic mesenchyme via LTβR signaling. Additionally this thesis has also revealed a novel mechanism for LTβR regulation of thymic endothelial cells to control T-cell, as summarized in Figure 6.1. Our observation that thymic mesenchyme development is dependent on LTβR signaling provided by αβ T-cells highlights a potential mechanism through which to manipulate this stromal population, however the functional importance of LTβR-dependent regulation of thymic mesenchyme requires further investigation. Our analysis provides evidence that LTβR regulation of thymic epithelial cells is dispensable for T-cell egress, a hypothesis proposed following the initial discovery of LTβR-dependent T-cell egress. Instead our experiments revealed a previously unrecognized role for LTβR regulation of thymic endothelial cells impacting on T-cell egress, specifically at the stage of entry into the PVS. Furthermore our data demonstrates that entry into the PVS is a stochastic process, addressing an important, previously outstanding question regarding when and in what order does the process of T-cell egress occur. Further experiments to explore the molecular basis for this novel finding may prove an important avenue of future research into the mechanisms of T-cell egress.

Figure 6.1. LTβR Regulation Of Thymic Endothelium Is A Critical Pathway In Controlling T-Cell Egress And T-Cell Egress Is Both A Linear And Stochastic Process.

(A) LTβR regulation of thymic endothelium is essential for T-cell egress and this regulation is likely critical for entry of T-cells into the PVS.

(B) Once thymocytes have matured from a $CD69^{+}CD62L^{-}$ phenotype to an egress-competent $CD69^{lo}CD62L^{+}$ phenotype they have the ability to enter the PVS. This initial maturation is essential for T-cell egress and therefore suggests that T-cell egress fits a linear model. However our analysis has revealed that subsets of cells within the $CD69^{lo}CD62L^{+}$ mature T-cell population that differ on their age and expression of S1PR1 are all able to enter the PVS, supporting the stochastic model of T-cell egress.

(C) What remains to be tested is whether the transendothelial migration of T-cells within the PVS is a linear or stochastic process. If this process were linear we would expect only the most mature (M4) fraction of $CD69^{lo}CD62L^{+}$ cells in the PVS to enter the periphery. Alternatively if this process were stochastic then all cells within the PVS would be found in the periphery and therefore can leave the PVS randomly. Whether or not each of these processes is occurring will require further investigation as it may have important implications on the function of the RTE once in the periphery and may determine whether these cells require further maturation once they have left the thymus.

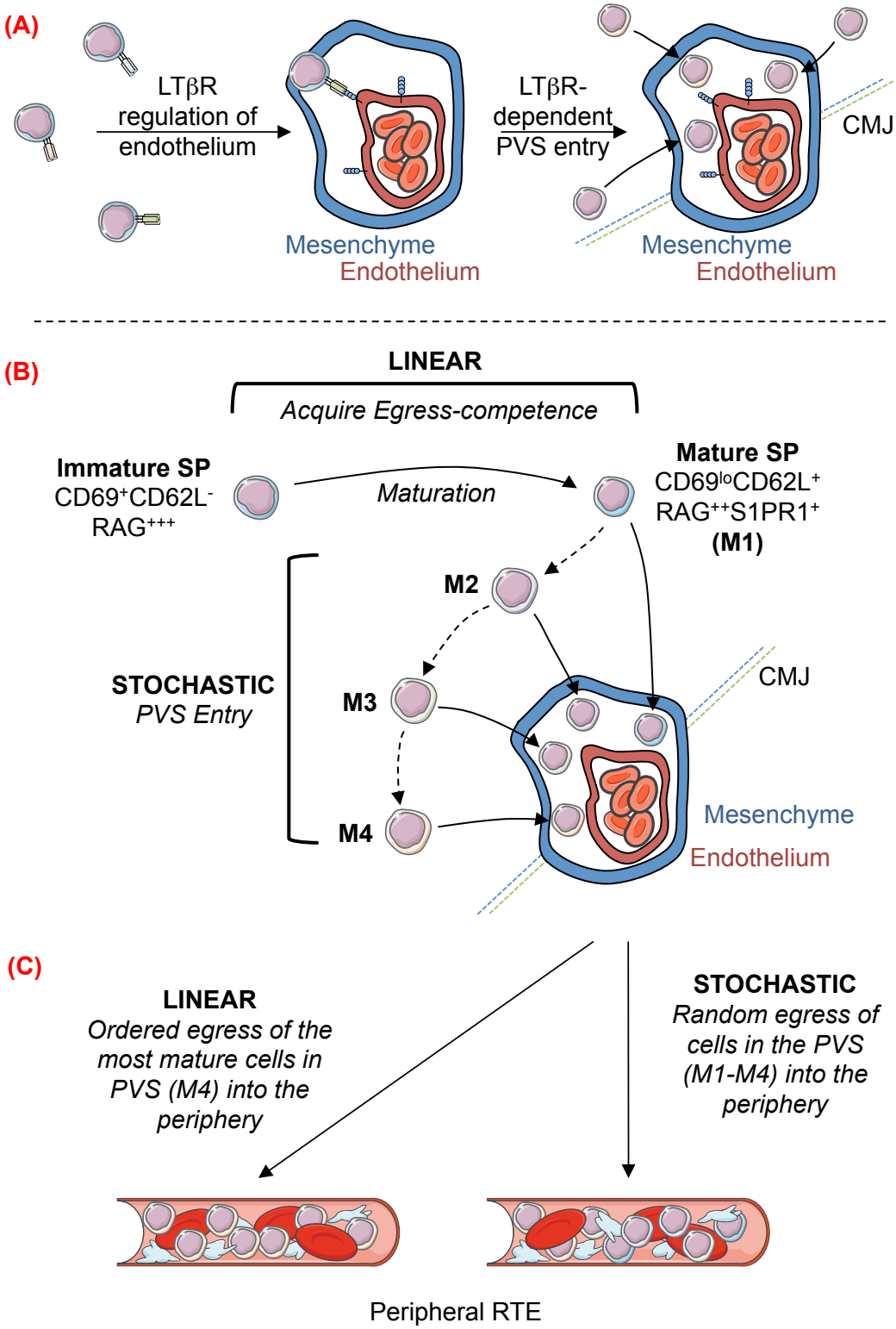
(A)
LTβR
regulation of
endothelium
Mesenchyme
Endothelium
LTβR-
dependent
PVS entry
CMJ
Mesenchyme
Endothelium
(B)
LINEAR
Acquire Egress-competence
Immature SP
CD69+CD62L-
RAG+++
Maturation
Mature SP
CD69loCD62L+
RAG++S1PR1+
(M1)
M2
STOCHASTIC
PVS Entry
M3
M4
CMJ
Mesenchyme
Endothelium
(C)
LINEAR
Ordered egress of the
most mature cells in
PVS (M4) into the
periphery
STOCHASTIC
Random egress of
cells in the PVS
(M1-M4) into the
periphery
Peripheral RTE

CHAPTER SEVEN: REFERENCES

1. Miller JFAP. Immunological Function Of The Thymus. Lancet. 1961;2:748–9.
2. Luckheeram RV, Zhou R, Verma AD, Xia B. CD4 +T cells: Differentiation and functions. Clin Dev Immunol. 2012;2012.
3. Ekkens MJ, Shedlock DJ, Jung E, Troy A, Pearce EL, Shen H, et al. Th1 and Th2 cells help CD8 T-cell responses. Infect Immun. 2007;75(5):2291–6.
4. Smith KM, Pottage L, Thomas ER, Leishman AJ, Doig TN, Xu D, et al. Th1 and Th2 CD4+ T Cells Provide Help for B Cell Clonal Expansion and Antibody Synthesis in a Similar Manner In Vivo. J Immunol [Internet]. 2000;165(6):3136–44.
5. Andersen MH, Schrama D, thor Straten P, Becker JC. Cytotoxic T Cells. J Invest Dermatol [Internet]. 2006;126(1):32–41.
6. Mullbacher A, Lobigs M, Hla RT, Tran T, Stehle T, Simon MM. Antigen-dependent release of IFN-gamma by cytotoxic T cells up- regulates Fas on target cells and facilitates exocytosis-independent specific target cell lysis. J Immunol [Internet]. 2002;169(1):145–50.
7. Kägi D, Vignaux F, Ledermann B, Bürki K, Depraetere V, Nagata S, et al. Fas and perforin pathways as major mechanisms of T cell-mediated cytotoxicity. Science. 1994;265(5171):528–30.
8. Kägi D, Ledermann B, Bürki K, Seiler P, Odermatt B, Olsen KJ, et al. Cytotoxicity mediated by T cells and natural killer cells is greatly impaired in perforin-deficient mice. Nature. 1994;369:31–7.
9. Harty JT, Tvinnereim AR, White DW. Cd8+ T Cell Effector Mechanisms in Resistance To Infection. Annu Rev Immunol. 2000;25:275–308.
10. Donskoy E, Goldschneider I. Thymocytopoiesis is maintained by blood-borne precursors throughout postnatal life. A study in parabiotic mice. J Immunol. 1992;148(6):1604–12.
11. Itoi M, Kawamoto H, Katsura Y, Amagai T. Two distinct steps of immigration of hematopoietic progenitors into the early thymus anlage. Int Immunol. 2001;13(9):1203–11.
12. Le Douarin NM, Jotereau F V. Tracing of cells of the avian thymus through embryonic life in interspecific chimeras. J Exp Med [Internet]. 1975;142(1):17–40.
13. Jenkinson EJ, Jenkinson WE, Rossi SW, Anderson G. The thymus and T-cell commitment: the right niche for Notch? Nat Rev Immunol [Internet]. 2006;6(7):551–5.
14. Lind EF, Prockop SE, Porritt HE, Petrie HT. Mapping precursor movement through the postnatal thymus reveals specific microenvironments supporting defined stages of early lymphoid development. J Exp Med. 2001;194(2):127–34.
15. Foss DL, Donskoy E, Goldschneider I. The Importation of Hematogenous Precursors by the Thymus Is a Gated Phenomenon in Normal Adult Mice. J Exp Med [Internet]. 2001;193(3):365–74.
16. Havran WL, Allison JP. Developmentally ordered appearance of thymocytes expressing different T-cell antigen receptors. Vol. 335, Nature. 1988. p. 443–5.
17. Bhandoola A, Sambandam A. From stem cell to T cell: one route or many? Nat Rev Immunol [Internet]. 2006;6(2):117–26.
18. Allman D, Sambandam A, Kim S, Miller JP, Pagan A, Well D, et al. Thymopoiesis independent of common lymphoid progenitors. Nat Immunol. 2003;4(2):168–74.
19. Godfrey DI, Zlotnik A, Suda T, Godfrey DI, Zlotnik A. Phenotypic and functional characterization of c-kit expression during intrathymic T cell development DURING INTRATHYMIC T CELL DEVELOPMENT ’. J Immunol. 2010;
20. Rossi FM V, Corbel SY, Merzaban JS, Carlow D a, Gossens K, Duenas J, et al. Recruitment of adult thymic progenitors is regulated by P-selectin and its ligand PSGL-1. Nat Immunol. 2005;6(6):626–34.
21. Zlotoff DA, Sambandam A, Logan TD, Bell JJ, Schwarz BA, Bhandoola A. CCR7 and CCR9 together recruit hematopoietic progenitors to the adult thymus. Blood. 2010;115(10):1897–905.
22. Lucas B, James KD, Cosway EJ, Parnell SM, Tumanov A V., Ware CF, et al. Lymphotoxin Receptor Controls T Cell Progenitor Entry to the Thymus. J Immunol [Internet]. 2016;
23. Scimone ML, Aifantis I, Apostolou I, von Boehmer H, von Andrian UH. A multistep adhesion cascade for lymphoid progenitor cell homing to the thymus. Proc Natl Acad Sci U S A. 2006;103(18):7006–11.
24. Shi Y, Wu W, Chai Q, Li Q, Hou Y, Xia H, et al. LTβR controls thymic portal endothelial cells for haematopoietic progenitor cell homing and T-cell regeneration. Nat Commun [Internet]. 2016;7:12369.
25. Ardavin C, Wu L, Li CL, Shortman K. Thymic dendritic cells and T cells develop simultaneously

in the thymus from a common precursor population. Nature. 1993;362(6422):761–3.
26. Rothenberg E V, Moore JE, Yui M a. Launching the T-cell-lineage developmental programme. Nat Rev Immunol [Internet]. 2008;8(1):9–21.
27. Rothenberg E V. T Cell Lineage Commitment: Identity and Renunciation. J Immunol [Internet]. 2011;186(12):6649–55.
28. Masuda K, Kakugawa K, Nakayama T, Minato N, Katsura Y, Kawamoto H. T Cell Lineage Determination Precedes the Initiation of TCR Gene Rearrangement. J Immunol [Internet]. 2007;179(6):3699–706.
29. Shortman K, Egerton M, Spangrude GJ, Scollay R. The generation and fate of thymocytes. SeminImmunol. 1990;2(1044–5323):3–12.
30. Plotkin J, Prockop SE, Lepique A, Petrie HT. Critical role for CXCR4 signaling in progenitor localization and T cell differentiation in the postnatal thymus. J Immunol. 2003;171(9):4521–7.
31. Buono M, Facchini R, Matsuoka S, Thongjuea S, Waithe D, Luis TC, et al. A dynamic niche provides Kit ligand in a stage-specific manner to the earliest thymocyte progenitors. Nat Cell Biol [Internet]. 2016;(January).
32. Wang H, Pierce LJ, Spangrude G. Distinct roles of IL-7 and stem cell factor in the OP9-DL1 T-cell differentiation culture system. Exp Hematol. 2006;34(12):1730–40.
33. Massa S, Balciunaite G, Ceredig R, Rolink AG. Critical role for c-kit (CD117) in T cell lineage commitment and early thymocyte development in vitro. Eur J Immunol. 2006;36:526–32.
34. Balciunaite G, Ceredig R, Fehling H, Rolink AG. The role of Notch and IL-7 signaling in early thymocyte proliferation and differentiation. Eur J Immunol. 2005;1292–300.
35. Radtke F, Wilson A, Stark G, Bauer M, Van Meerwijk J, MacDonald HR, et al. Deficient T cell fate specification in mice with an induced inactivation of Notch1. Immunity. 1999;10(5):547–58.
36. Prockop SE, Palencia S, Ryan CM, Gordon K, Gray D, Petrie HT, et al. Stromal Cells Provide the Matrix for Migration of Early Lymphoid Progenitors Through the Thymic Cortex. J Immunol. 2002;16(4354):4361.
37. Dudley EC, Petrie HT, Shah LM, Owen MJ, Hayday AC. T Cell Receptor p Chain Gene Rearrangement and Selection during Thymocyte Development in Adult Mice. Immunity. 1994;1:83–93.
38. Davis M, Bjorkman P. T-cell antigen receptor genes and T-cell recognition. Nature. 1988;334:395–402.
39. Mombaerts P, Johnson RS, Herrup K, Tonegawa S, Papaioannouo VE. RAG-l-Deficient M ice Have No Mature 8 and T Lymphocytes. Cell. 1992;68:869–77.
40. Shinkai Y, Rathbun G, Oltz EM, Stewart V, Mendelsohn M, Charron J, et al. RAG-2-Deficient Mice Lack Mature Lymphocytes Owing to Inability to Initiate V (D) J Rearrangement. Cell. 1992;68:855–67.
41. Mombaerts P, Clarke A, Rudnicki M, Iacomini J, Itohara S, Lafaille JJ, et al. Mutations in T-cell antigen receptor genes α and β block thymocyte development at different stages. Nature. 1992;360:225–31.
42. Taghon T, Yui MA, Pant R, Diamond RA, Rothenberg E V. Developmental and Molecular Characterization of Emerging b - and gd -Selected Pre-T Cells in the Adult Mouse Thymus. Immunity. 2006;(January):53–64.
43. Yamasaki S, Saito T. Molecular basis for pre-TCR-mediated autonomous signaling. Trends Immunol. 2006;28(1):39–43.
44. Fehling H, Krotkova A, Saint-Ruf C, Boehmer H von. Crucial role of the pre-T-cell receptor α gene in development of αβ but not γδ T cells. Nature. 1995;375:795–8.
45. Falk I, Nerz G, Haidl I, Krotkova A, Eichmann K. Immature thymocytes that fail to express TCR b and / or TCRyd proteins die by apoptotic cell death in the CD44 - CD25 - (DN4) subset. 2001;31:3308–17.
46. Ciofani M, Schmitt TM, Ciofani A, Michie M, Çuburu N, Aublin A, et al. Obligatory Role for Cooperative Signaling by Pre-TCR and Notch during Thymocyte Differentiation. J Immunol. 2004;172:5230–9.
47. Ciofani M, Zuniga-Pflucker JC. Notch promotes survival of pre – T cells at the b -selection checkpoint by regulating cellular metabolism. 2005;6(9):881–8.
48. Trampont PC, Shen Y, Duley AK, Bender TP, Sutherland AE, Littman DR, et al. CXCR4 acts as a costimulator during thymic β selection. Nat Immunolt. 2010;11(2):162–70.
49. Teague TK, Tan C, Marino JH, Davis BK, Taylor AA, Huey RW, et al. CD28 expression redefines thymocyte development during the pre-T to DP transition. Int Immunol.

2010;22(5):387–97.
50. Meerwijk JPM Van, Marguerat S, Lees RK, Germain RN, Fowlkes BJ, Macdonald HR. Quantitative Impact of Thymic Clonal Deletion on the. J Exp Med. 1997;185(3):377–83.
51. Palmer E. Negative selection - Clearing out the bad apples from the T-cell repertoire. Nat Rev Immunol. 2003;3(May):383–91.
52. Laufer T, DeKoning J, Markowitz J, Lo D, Glimcher L. Unopposed positive selection and autoreactivity in mice expressing class II MHC only on thymic cortex. Nature. 1996;383:81–5.
53. Surh CD, Sprent J. T-cell apoptosis detected in situ during positive and negative selection in the thymus. Nature. 1994;372:100–3.
54. Ioannidis V, Beermann F, Clevers H, Held W. The β -catenin – TCF-1 pathway ensures CD4 + CD8 + thymocyte survival. Nat Immunol. 2001;2(8):691–7.
55. Sun Z, Unutmaz D, Zou Y, Sunshine MJ, Pierani A, Brenner-morton S, et al. Requirement for RORγ in Thymocyte Survival and Lymphoid Organ Development. Science (80-). 2000;288(June):2369–74.
56. Brandle D, Mullert C, Rulicke T, Hengartner H. Engagement of the T-cell receptor during positive selection in the thymus down-regulates RAG-I expression. Immunology. 1992;89(October):9529–33.
57. Borgulya P, Kishi H, Boehmer H Von. Exclusion and Inclusion of α and β T Cell Receptor Alleles. Cell. 1992;69:529–37.
58. Singer A, Adoro S, Park J. Lineage fate and intense debate: myths, models and mechanisms of CD4/CD8 lineage choice. Nat Rev Immunol. 2008;8(10):788–801.
59. Itano BA, Salmon P, Kioussis D, Tolaini M, Corbella P, Robey E. The cytoplasmic domain of CD4 promotes the development of CD4 lineage T cells. J Exp Med. 1996;183(3):731–41.
60. Seong R, Chamberlin J, Parnes J. Signal for T-cell differentiation to a CD4 cell lineage is delivered by CD4 transmembrane region and/or cytoplasmic tail. Nature. 1992;356:718–20.
61. Chan SH, Cosgrove D, Waltxinger C, Benoist C, Mathis D. Another View of the Selective Model of Thymocyte Selection. Cell. 1993;73:225–36.
62. Davis CB, Killeen N, Crooks MEC, Raulet D, Littman DR. Evidence for a Stochastic Mechanism in the Differentiation of Mature Subsets of T Lymphocytes. Cell. 1993;73:237–47.
63. Brugnera E, Bhandoola A, Cibotti R, Yu Q, Guinter TI, Yamashita Y, et al. Coreceptor Reversal in the Thymus : Signaled CD4 □ 8 □ Thymocytes Initially Terminate CD8 Transcription Even When Differentiating into CD8 □ T Cells. Immunity. 2000;13:59–71.
64. Singer A. New perspectives on a developmental dilemma : the kinetic signaling model and the importance of signal duration for the CD4 / CD8 lineage decision. Curr Opin Immunol. 2002;14(2):207–15.
65. Taniuchi I, Osato M, Egawa T, Sunshine MJ, Bae S, Komori T, et al. Differential Requirements for Runx Proteins in CD4 Repression and Epigenetic Silencing during T Lymphocyte Development. Cell. 2002;111:621–33.
66. He X, He X, Dave VP, Zhang Y, Hua X, Nicolas E, et al. The zinc finger transcription factor Th-POK regulates CD4 versus CD8 T-cell lineage commitment. Nature. 2005;433(2):826–33.
67. Dave VP, Allman D, Keefe R, Hardy R, Kappes DJ. HD mice : A novel mouse mutant with a specific defect in the generation of CD4+ T cells. Proc Natl Acad Sci U S A. 1998;95(7):8187–92.
68. Muroi S, Naoe Y, Miyamoto C, Akiyama K, Ikawa T, Masuda K, et al. Cascading suppression of transcriptional silencers by ThPOK seals helper T cell fate. Nat Immunol. 2008;9(10):1113–21.
69. Ueno T, Saito F, Gray DHD, Kuse S, Hieshima K, Nakano H, et al. CCR7 Signals Are Essential for Cortex-Medulla Migration of Developing Thymocytes. J Exp Med [Internet]. 2004;200(4):493–505.
70. Nitta T, Nitta S, Lei Y, Lipp M, Takahama Y. CCR7-mediated migration of developing thymocytes to the medulla is essential for negative selection to tissue-restricted antigens. Proc Natl Acad Sci U S A. 2009;106(40):17129–33.
71. Kurobe H, Liu C, Ueno T, Saito F, Ohigashi I, Seach N, et al. CCR7-dependent cortex-to-medulla migration of positively selected thymocytes is essential for establishing central tolerance. Immunity. 2006;24(2):165–77.
72. Cowan JE, Parnell SM, Nakamura K, Caamano JH, Lane PJL, Jenkinson EJ, et al. The thymic medulla is required for Foxp3+ regulatory but not conventional CD4+ thymocyte development. J Exp Med [Internet]. 2013 Apr 8;210(4):675–81.

73. Choi YI, Duke-cohan JS, Ahmed WB, Handley MA, Epstein JA, Clayton LK, et al. PlexinD1 controls migration of positively-selected thymocytes into the medulla. Immunity. 2008;29(6):888–98.
74. Cowan JE, Mccarthy NI, Parnell SM, White AJ, Bacon A, Serge A, et al. Differential Requirement for CCR4 and CCR7 during the Development of Innate and Adaptive ab T Cells in the Adult Thymus. J Immunol. 2014;199(2):1204–12.
75. Hu Z, Lancaster JN, Sasiponganan C, Ehrlich LIR. CCR4 promotes medullary entry and thymocyte-dendritic cell interactions required for central tolerance. J Exp Med [Internet]. 2015;
76. Strasser A, Walter T, Hall E. The role of BH3-only proteins in the immune system. Nat Rev Immunol. 2005;5(3):189–200.
77. Gray D, Kupresanin, Berzins SP, Herold M, O'Reilly L, Bouillet P, et al. The BH3-only proteins Bim and Puma cooperate to impose deletional T-cell tolerance to organ-specific antigens. Immunity. 2012;37(3):451–62.
78. Bouillet P, Zhang L, Coultas L, Puthalakath H, Pellegrini M, Cory S, et al. BH3-only Bcl-2 family member Bim is required for apoptosis of autoreactive thymocytes. Nature. 2002;415(2):2–7.
79. McCaughtry TM, Baldwin TA, Wilken MS, Hogquist KA. Clonal deletion of thymocytes can occur in the cortex with no involvement of the medulla. J Exp Med [Internet]. 2008;205(11):2575–84.
80. Baldwin KK, Trenchak BP, Altman JD, Davis MM. Negative Selection of T Cells Occurs Throughout Thymic Development. J Immunol. 1999;163:689–98.
81. Stritesky GL, Xing Y, Erickson JR, Kalekar L a, Wang X, Mueller DL, et al. Murine thymic selection quantified using a unique method to capture deleted T cells. Proc Natl Acad Sci U S A [Internet]. 2013;110:4679–84.
82. Cowan JE, Parnell SM, Nakamura K, Caamano JH, Lane PJL, Jenkinson EJ, et al. The thymic medulla is required for Foxp3+ regulatory but not conventional CD4+ thymocyte development. J Exp Med [Internet]. 2013;210(4):675–81.
83. Ohashi P, Pircher H, Burki K, Zinkernagel R, Hengartner H. Distinct sequence of negative or positive selection implied by thymocyte T-cell receptor densities. Nature. 1990;346(8):861–3.
84. Rincón M, Whitmarsh A, Yang DD, Weiss L, Dérijard B, Jayaraj P, et al. The JNK Pathway Regulates the In Vivo Deletion of. J Immunol. 1998;188(10):1817–30.
85. Gong Q, Cheng AM, Akk AM, Alberola-ila J, Gong G, Pawson T, et al. Disruption of T cell signaling networks and development by Grb2 haploid insufficiency. Nature. 2001;2(1):29–36.
86. McNeil LK, Starr TK, Hogquist KA. A requirement for sustained ERK signaling during thymocyte positive selection in vivo. PNAS. 2005;2005:1–6.
87. Daniels MA, Teixeiro E, Gill J, Hausmann B, Roubaty D, Holmberg K, et al. Thymic selection threshold defined by compartmentalization of Ras / MAPK signalling. Nature. 2006;444(12):4–9.
88. Moran AE, Holzapfel KL, Xing Y, Cunningham NR, Maltzman JS, Punt J, et al. T cell receptor signal strength in Treg and iNKT cell development demonstrated by a novel fluorescent reporter mouse. J Exp Med [Internet]. 2011;208(6):1279–89.
89. Fontenot JD, Rasmussen JP, Williams LM, Dooley JL, Farr AG, Rudensky AY. Regulatory T cell lineage specification by the forkhead transcription factor foxp3. Immunity [Internet]. 2005 Mar;22(3):329–41.
90. Fontenot JD, Gavin M a, Rudensky AY. Foxp3 programs the development and function of CD4+CD25+ regulatory T cells. Nat Immunol [Internet]. 2003;4(4):330–6.
91. Asseman C, Mauze S, Leach MW, Coffman RL, Powrie F. An Essential Role for Interleukin 10 in the Function of Regulatory T Cells That Inhibit Intestinal Inflammation. J Exp Med [Internet]. 1999;190(7):995–1004.
92. Burkly L, Hession C, Ogata L, Reilly C, Marconi L a, Olson D, et al. Expression of relB is required for the development of thymic medulla and dendritic cells [Internet]. Vol. 373, Nature. 1995. p. 531–6.
93. Weih F, Carrasco D, Durham SK, Barton DS, Rizzo CA, Ryseck RP, et al. Multiorgan inflammation and hematopoietic abnormalities in mice with a targeted disruption of RelB, a member of the NF-??B/Rel family. Cell. 1995;80(2):331–40.
94. McCaughtry TM, Wilken MS, Hogquist K a. Thymic emigration revisited. J Exp Med [Internet]. 2007;204(11):2513–20.
95. Mouri Y, Nishijima H, Kawano H, Hirota F, Sakaguchi N, Morimoto J, et al. NF- B-Inducing Kinase in Thymic Stroma Establishes Central Tolerance by Orchestrating Cross-Talk with Not

Only Thymocytes but Also Dendritic Cells. J Immunol [Internet]. 2014;193(9):4356–67.
96. Kishimoto H, Sprent J. Negative selection in the thymus includes semimature T cells. J Exp Med [Internet]. 1997;185(2):263–71.
97. Xing Y, Wang X, Jameson SC, Hogquist KA. Late stages of T cell maturation in the thymus involve NF-κB and tonic type I interferon signaling. Nat Immunol [Internet]. 2016;9(October 2015):1–10.
98. Allende ML, Dreier JL, Mandala S, Proia RL. Expression of the Sphingosine 1-Phosphate Receptor, S1P1, on T-cells Controls Thymic Emigration. J Biol Chem. 2004;279(15):15396–401.
99. Carlson CM, Endrizzi BT, Wu J, Ding X, Weinreich M a, Walsh ER, et al. Kruppel-like factor 2 regulates thymocyte and T-cell migration. Nature. 2006;442(7100):299–302.
100. Bai A, Hu H, Yeung M, Chen J. Kruppel-Like Factor 2 Controls T Cell Trafficking by Activating L-Selectin (CD62L) and Sphingosine-1-Phosphate Receptor 1 Transcription. J Immunol [Internet]. 2007;178(12):7632–9.
101. Fabre S, Carrette F, Chen J, Lang V, Semichon M, Denoyelle C, et al. FOXO1 Regulates L-Selectin and a Network of Human T Cell Homing Molecules Downstream of Phosphatidylinositol 3-Kinase. J Immunol [Internet]. 2008;181(5):2980–9.
102. Alfonso C, McHeyzer-Williams MG, Rosen H. CD69 down-modulation and inhibition of thymic egress by short- and long-term selective chemical agonism of sphingosine 1-phosphate receptors. Eur J Immunol [Internet]. 2006;36(1):149–59.
103. Shiow LR, Rosen DB, Brdicková N, Xu Y, An J, Lanier LL, et al. CD69 acts downstream of interferon-alpha/beta to inhibit S1P1 and lymphocyte egress from lymphoid organs. Nature. 2006;440(7083):540–4.
104. Yagi H, Kamba R, Chiba K, Soga H, Yaguchi K, Nakamura M, et al. Immunosuppressant FTY720 inhibits thymocyte emigration. Eur J Immunol [Internet]. 2000;30(5):1435–44.
105. Rosen H, Alfonso C, Surh CD, McHeyzer-Williams MG. Rapid induction of medullary thymocyte phenotypic maturation and egress inhibition by nanomolar sphingosine 1-phosphate receptor agonist. Proc Natl Acad Sci U S A. 2003;100(19):10907–12.
106. Mandala S, Hajdu R, Bergstrom J, Quackenbush E, Xie J, Milligan J, et al. Alteration of Lymphocyte Trafficking by Sphingosine- 1-Phosphate Receptor Agonists. Science (80-). 2011;346(2002):346–50.
107. Brinkmann V, Davis MD, Heise CE, Albert R, Cottens S, Hof R, et al. The immune modulator FTY720 targets sphingosine 1-phosphate receptors. J Biol Chem. 2002;277(24):21453–7.
108. Blackburn CC, Manley NR, Boehm T, Martins VC, Ruggiero E, Schlenner SM, et al. Thymus-autonomous T cell development in the absence of progenitor import. J Exp Med [Internet]. 2012;209(8):1397–400.
109. Gräler MH, Goetzl EJ. The immunosuppressant FTY720 down-regulates sphingosine 1-phosphate G-protein-coupled receptors. FASEB J. 2004;18(3):551–3.
110. Pappu R, Schwab SR, Cornelissen I, Pereira JP, Regard JB, Xu Y, et al. Promotion of lymphocyte egress into blood and lymph by distinct sources of sphingosine-1-phosphate. Science (80-). 2007;316(5822):295–8.
111. Zachariah MA, Cyster JG. Neural Crest-Derived Pericytes Promote Egress of Mature Thymocytes at the Corticomedullary Junction. Science (80-) [Internet]. 2010;328(5982):1129–35.
112. Breart B, Ramos-Perez WD, Mendoza a., Salous a. K, Gobert M, Huang Y, et al. Lipid phosphate phosphatase 3 enables efficient thymic egress. J Exp Med [Internet]. 2011;208(6):1267–78.
113. Fukuhara S, Simmons S, Kawamura S, Inoue A, Orba Y, Tokudome T, et al. The sphingosine-1-phosphate transporter Spns2 expressed on endothelial cells regulates lymphocyte trafficking in mice. 2012;122(4):21–8.
114. Zamora-Pineda J, Kumar A, Suh JH, Zhang M, Saba JD. Dendritic cell sphingosine-1-phosphate lyase regulates thymic egress. J Exp Med [Internet]. 2016;jem.20160287.
115. White AJ, Baik S, Parnell SM, Holland AM, Brombacher F, Jenkinson WE, et al. A type 2 cytokine axis for thymus emigration. J Exp Med [Internet]. 2017;jem.20170271.
116. Ueno T, Hara K, Willis MS, Malin M a., Höpken UE, Gray DHD, et al. Role for CCR7 ligands in the emigration of newly generated T lymphocytes from the neonatal thymus. Immunity. 2002;16:205–18.
117. Jin R, Aili A, Wang Y, Wu J, Sun X, Ge Q. Critical role of SP thymocyte motility in regulation of

thymic output in neonatal Aire - / - mice. Oncotarget. 2016;1:83–94.
118. Zou Y-R, Kottmann AH, Kuroda M, Taniuchi I, Littman DR. Function of the chemokine receptor CXCR4 in haematopoiesis and in cerebellar development. Nature [Internet]. 1998;393(6685):595–9.
119. Vianello F, Kraft P, Mok YT, Hart WK, White N, Poznansky MC. A CXCR4-dependent chemorepellent signal contributes to the emigration of mature single-positive CD4 cells from the fetal thymus. J Immunol [Internet]. 2005;175(8):5115–25.
120. Poznansky MC, Olszak IT, Evans RH, Wang Z, Foxall RB, Olson DP, et al. Thymocyte emigration is mediated by active movement away from stroma-derived factors. J Clin Invest. 2002;109(8):1101–10.
121. Zhanzhuo Li Q, Gao J-L, Wan W, Ganesan S, McDermott D, Murphy P. The CXCR4 antagonist AMD3100 redistributes leukocytes from primary immune organs to secondary immune organs, lung and blood in mice. Eur J Immunol. 2015;45(6):1855–67.
122. Lucas B, White AJ, Parnell SM, Henley PM, Jenkinson WE, Anderson G. Progressive Changes in CXCR4 Expression That Define Thymocyte Positive Selection Are Dispensable For Both Innate and Conventional αβT-cell Development. Sci Rep [Internet]. 2017;7(1):5068.
123. Bockman D, Kirby M. Dependence of Thymus Development on Derivatives of the Neural Crest. 1983;223:498–500.
124. Gordon J, Wilson VA, Blair NF, Sheridan J, Farley A, Wilson L, et al. Functional evidence for a single endodermal origin for the thymic epithelium. Nat Immunol [Internet]. 2004;5(5):546–53.
125. Suniara RK, Jenkinson EJ, Owen JJ. An essential role for thymic mesenchyme in early T cell development. J Exp Med [Internet]. 2000 Mar 20;191(6):1051–6.
126. Pantelouris E. Absence of Thymus in a Mouse Mutant. Nature. 1968;217:370–1.
127. Blackburn CC, Augustine CL, Li R, Harvey RP, Malin M a, Boyd RL, et al. The nu gene acts cell-autonomously and is required for differentiation of thymic epithelial progenitors. Proc Natl Acad Sci U S A [Internet]. 1996;93(12):5742–6.
128. Nowell CS, Bredenkamp N, Tetelin S, Jin X, Tischner C, Vaidya H, et al. Foxn1 regulates lineage progression in cortical and medullary thymic epithelial cells but is dispensable for medullary sublineage divergence. PLoS Genet. 2011;7(11).
129. Rossi SW, Jenkinson WE, Anderson G, Jenkinson EJ. Clonal analysis reveals a common progenitor for thymic cortical and medullary epithelium. Nature. 2006;441(7096):988–91.
130. Bleul CC, Corbeaux T, Reuter A, Fisch P, Mönting JS, Boehm T. Formation of a functional thymus initiated by a postnatal epithelial progenitor cell. Nature. 2006;441(7096):992–6.
131. Baik S, Jenkinson EJ, Lane PJL, Anderson G, Jenkinson WE. Generation of both cortical and Aire+ medullary thymic epithelial compartments from CD205+ progenitors. Eur J Immunol. 2013;43(3):589–94.
132. Ohigashi I, Zuklys S, Sakata M, Mayer CE, Zhanybekova S, Murata S, et al. Aire-expressing thymic medullary epithelial cells originate from beta5t-expressing progenitor cells. Proc Natl Acad Sci U S A [Internet]. 2013;110(24):9885–90.
133. Alves NL, Takahama Y, Ohigashi I, Ribeiro AR, Baik S, Anderson G, et al. Serial progression of cortical and medullary thymic epithelial microenvironments. Eur J Immunol. 2014;44(1):16–22.
134. Ribeiro AR, Rodrigues PM, Meireles C, Di Santo JP, Alves NL. Thymocyte selection regulates the homeostasis of IL-7-expressing thymic cortical epithelial cells in vivo. J Immunol [Internet]. 2013;191(3):1200–9.
135. Sekai M, Hamazaki Y, Minato N. Medullary Thymic Epithelial Stem Cells Maintain a Functional Thymus to Ensure Lifelong Central T Cell Tolerance. Immunity [Internet]. 2014 Nov;41(5):753–61.
136. Baik S, Sekai M, Hamazaki Y, Jenkinson WE, Anderson G. Relb acts downstream of medullary thymic epithelial stem cells and is essential for the emergence of RANK+ medullary epithelial progenitors. Eur J Immunol. 2016;46(4):857–62.
137. McCarthy NI, Cowan JE, Nakamura K, Bacon a., Baik S, White a. J, et al. Osteoprotegerin-Mediated Homeostasis of Rank+ Thymic Epithelial Cells Does Not Limit Foxp3+ Regulatory T Cell Development. J Immunol [Internet]. 2015;
138. Akiyama N, Takizawa N, Miyauchi M, Yanai H, Tateishi R, Shinzawa M, et al. Identification of embryonic precursor cells that differentiate into thymic epithelial cells expressing autoimmune regulator. J Exp Med [Internet]. 2016;213(8):1441–58.
139. Shakib S, Desanti GE, Jenkinson WE, Parnell SM, Jenkinson EJ, Anderson G. Checkpoints in

the development of thymic cortical epithelial cells. J Immunol [Internet]. 2009;182(1):130–7.
140. van Ewijk W, Shores EW, Singer A. Crosstalk in the mouse thymus. Trends Immunol. 1994;15(5):214–7.
141. Philpott KL, Viney JL, Kay G, Rastan S, Gardiner EM, Chae S, et al. Lymphoid development in mice congenitally lacking T cell receptor αβ-expressing cells. Science (80-). 1992;256(June):1448–52.
142. Palmer DB, Viney JL, Ritter MA, Hayday AC, Owen MJ. Expression of the αβ T-Cell Receptor is Necessary for the Generation of the Thymic Medulla. Dev Immunol. 1993;3(3):175–9.
143. Grusby MJ, Johnson RS, Papaioannou VE, Glimcher LH. Depletion of CD4+ T cells in major histocompatibility complex class II-deficient mice. Science. 1991;253(12):1417–20.
144. Nasreen M, Ueno T, Saito F, Takahama Y. In vivo treatment of class II MHC-deficient mice with anti-TCR antibody restores the generation of circulating CD4 T cells and optimal architecture of thymic medulla. J Immunol [Internet]. 2003;171(7):3394–400.
145. Irla M, Hugues S, Gill J, Nitta T, Hikosaka Y, Williams IR, et al. Autoantigen-Specific Interactions with CD4+ Thymocytes Control Mature Medullary Thymic Epithelial Cell Cellularity. Immunity. 2008;29(3):451–63.
146. White AJ, Jenkinson WE, Cowan JE, Parnell SM, Bacon A, Jones ND, et al. An essential role for medullary thymic epithelial cells during the intrathymic development of invariant NKT cells. J Immunol [Internet]. 2014;192(6):2659–66.
147. Akiyama T, Maeda S, Yamane S, Ogino K, Kasai M, Kajiura F, et al. Dependence of self-tolerance on TRAF6-directed development of thymic stroma. Science. 2005;308(April):248–51.
148. Kajiura F, Sun S, Nomura T, Izumi K, Ueno T, Bando Y, et al. NF- B-Inducing Kinase Establishes Self-Tolerance in a Thymic Stroma-Dependent Manner. J Immunol [Internet]. 2004;172(4):2067–75.
149. Fütterer A, Mink K, Luz A, Kosco-Vilbois MH, Pfeffer K. The lymphotoxin β receptor controls organogenesis and affinity maturation in peripheral lymphoid tissues. Immunity. 1998;9:59–70.
150. Randall TD, Carragher DM, Rangel-moreno J. Development of secondary lymphoid organs. Annu Rev Immunol. 2009;26:627–50.
151. Boehm T, Scheu S, Pfeffer K, Bleul CC. Thymic medullary epithelial cell differentiation, thymocyte emigration, and the control of autoimmunity require lympho-epithelial cross talk via LTbetaR. J Exp Med. 2003;198(5):757–69.
152. Rossi SW, Kim M-Y, Leibbrandt A, Parnell SM, Jenkinson WE, Glanville SH, et al. RANK signals from CD4(+)3(-) inducer cells regulate development of Aire-expressing epithelial cells in the thymic medulla. J Exp Med. 2007;204(6):1267–72.
153. Martins VC, Boehm T, Bleul CC. Ltbr Signaling Does Not Regulate Aire-Dependent Transcripts. J Immunol. 2008;181(1):400–7.
154. Seach N, Ueno T, Fletcher AL, Mattesich M, Engwerda CR, Scott S, et al. The Lymphotoxin Pathway Regulates Aire-Independent Expression of Ectopic Genes and Chemokines in Thymic Stromal Cells. J Immunol. 2008;(180):5384–92.
155. Zhu M, Chin RK, Tumanov A V, Liu X, Fu YX. Lymphotoxin beta receptor is required for the migration and selection of autoreactive T cells in thymic medulla. J Immunol [Internet]. 2007;179(12):8069–75.
156. Lkhagvasuren E, Sakata M, Ohigashi I, Takahama Y. Lymphotoxin β receptor regulates the development of CCL21-expressing subset of postnatal medullary thymic epithelial cells. J Immunol [Internet]. 2013;190:5110–7.
157. Cosway EJ, Lucas B, James KD, Parnell SM, Carvalho-Gaspar M, White AJ, et al. Redefining thymus medulla specialization for central tolerance. J Exp Med [Internet]. 2017;jem.20171000.
158. Schneider K, Potter KG, Ware CF. Lymphotoxin and LIGHT signaling pathways and target genes. Immunol Rev. 2004;202:49–66.
159. White AJ, Withers DR, Parnell SM, Scott HS, Finke D, Lane PJL, et al. Sequential phases in the development of Aire-expressing medullary thymic epithelial cells involve distinct cellular input. Eur J Immunol. 2008;38(4):942–7.
160. Takaba H, Morishita Y, Tomofuji Y, Danks L, Nitta T, Komatsu N, et al. Fezf2 Orchestrates a Thymic Program of Self-Antigen Expression for Immune Tolerance. Cell [Internet]. 2015;163(4):975–87.
161. Hikosaka Y, Nitta T, Ohigashi I, Yano K, Ishimaru N, Hayashi Y, et al. The Cytokine RANKL Produced by Positively Selected Thymocytes Fosters Medullary Thymic Epithelial Cells that Express Autoimmune Regulator. Immunity. 2008;29(3):438–50.

162. Desanti GE, Cowan JE, Baik S, Parnell SM, White AJ, Penninger JM, et al. Developmentally regulated availability of RANKL and CD40 ligand reveals distinct mechanisms of fetal and adult cross-talk in the thymus medulla. J Immunol [Internet]. 2012;189(12):5519–26.
163. Akiyama T, Shimo Y, Yanai H, Qin J, Ohshima D, Maruyama Y, et al. The Tumor Necrosis Factor Family Receptors RANK and CD40 Cooperatively Establish the Thymic Medullary Microenvironment and Self-Tolerance. Immunity. 2008;29(3):423–37.
164. Groettrup M, Kirk CJ, Basler M. Proteasomes in immune cells: more than peptide producers? Nat Rev Immunol [Internet]. 2010;10(1):73–8.
165. Murata S, Sasaki K, Kishimoto T, Niwa S, Hayashi H, Takahama Y, et al. Regulation of CD8+ T Cell Development by Thymus-Specific Proteasomes. Science (80-). 2007;316:1349–53.
166. Sasaki K, Takada K, Ohte Y, Kondo H, Sorimachi H, Tanaka K, et al. Thymoproteasomes produce unique peptide motifs for positive selection of CD8(+) T cells. Nat Commun [Internet]. 2015;6(May):7484.
167. Nitta T, Murata S, Sasaki K, Fujii H, Ripen AM, Ishimaru N, et al. Thymoproteasome Shapes Immunocompetent Repertoire of CD8+ T Cells. Immunity [Internet]. 2010;32(1):29–40.
168. Xing Y, Jameson SC, Hogquist KA. Thymoproteasome subunit-β5T generates peptide-MHC complexes specialized for positive selection. Proc Natl Acad Sci [Internet]. 2013;110(17):6979–84.
169. Takada K, Van Laethem F, Yan X, Akane K, Suzuki H, Murata S, et al. TCR affinity for thymoproteasome-dependent positively selecting peptides conditions antigen responsiveness in CD8+ T cells. Nat Immunol. 2015;16(10):1069–76.
170. Honey K, Nakagawa T, Peters C, Rudensky A. Cathepsin L regulates CD4+ T cell selection independently of its effect on invariant chain: a role in the generation of positively selecting peptide ligands. J Exp Med [Internet]. 2002;195(10):1349–58.
171. Chyi-Song Hsieh, DeRoos P, Honey K, Beers C, Rudensky AY. Presentation Peptide Generation for MHC Class II A Role for Cathepsin L and Cathepsin S in A Role for Cathepsin L and Cathepsin S in Peptide Generation for MHC Class II Presentation Chyi-Song. J Immunol [Internet]. 2002;168:2618–25.
172. Bowlus CL, Ahn J, Chu T, Gruen JR. Cloning of a novel MHC-encoded serine peptidase highly expressed by cortical epithelial cells of the thymus. Cell Immunol. 1999;196:80–6.
173. Gommeaux J, Grégoire C, Nguessan P, Richelme M, Malissen M, Guerder S, et al. Thymus-specific serine protease regulates positive selection of a subset of CD4+ thymocytes. Eur J Immunol [Internet]. 2009 Apr;39(4):956–64.
174. Viret C, Lamare C, Guiraud M, Fazilleau N, Bour A, Malissen B, et al. Thymus-specific serine protease contributes to the diversification of the functional endogenous CD4 T cell receptor repertoire. J Exp Med [Internet]. 2011;208(1):3–11.
175. Nedjic J, Aichinger M, Emmerich J, Mizushima N, Klein L. Autophagy in thymic epithelium shapes the T-cell repertoire and is essential for tolerance. Nature [Internet]. 2008;455(7211):396–400.
176. Mizushima N, Yamamoto A, Matsu M, Yoshimori T, Ohsumi Y. In Vivo Analysis of Autophagy in Response to Nutrient Starvation Using Transgenic Mice Expressing a Fluorescent Autophagosome Marker. Mol Biol Cell. 2004;15:1101–11.
177. Wekerle H, Ketelsen U-P, Ernst M. Thymic Nurse Cells Lymphoepithelial Cell Complexes In Murine Thymuses: Morphological And Serological Characterization. J Exp Med. 1980;151(April):925–44.
178. Nakagawa Y, Ohigashi I, Nitta T, Sakata M, Tanaka K, Murata S, et al. Thymic nurse cells provide microenvironment for secondary T cell receptor α rearrangement in cortical thymocytes. Proc Natl Acad Sci U S A [Internet]. 2012;109(50):20572–7.
179. Fiorini E, Ferrero I, Merck E, Favre S, Pierres M, Luther SA, et al. Cutting Edge: Thymic Crosstalk Regulates Delta-Like 4 Expression on Cortical Epithelial Cells. J Immunol [Internet]. 2008;181(12):8199–203.
180. Koch U, Fiorini E, Benedito R, Besseyrias V, Schuster-Gossler K, Pierres M, et al. Delta-like 4 is the essential, nonredundant ligand for Notch1 during thymic T cell lineage commitment. J Exp Med. 2008;205(11):2515–23.
181. Hozumi K, Mailhos C, Negishi N, Hirano K, Yahata T, Ando K, et al. Delta-like 4 is indispensable in thymic environment specific for T cell development. J Exp Med [Internet]. 2008;205(11):2507–13.
182. Takahama Y, Letterio JJ, Suzuki H, Farr AG, Singer A. Early progression of thymocytes along

the CD4/CD8 developmental pathway is regulated by a subset of thymic epithelial cells expressing transforming growth factor beta. J Exp Med [Internet]. 1994;179(5):1495–506.
183. Liu C, Saito F, Liu Z, Lei Y, Uehara S, Love P, et al. Coordination between CCR7- and CCR9-mediated chemokine signals in prevascular fetal thymus colonization. Blood. 2006;108(8):2531–9.
184. Heinzel K, Benz C, Bleul CC. A silent chemokine receptor regulates steady-state leukocyte homing in vivo. Proc Natl Acad Sci U S A [Internet]. 2007;104(20):8421–6.
185. Lucas B, White AJ, Ulvmar MH, Nibbs RJB, Sitnik KM, Agace WW, et al. CCRL1/ACKR4 is expressed in key thymic microenvironments but is dispensable for T lymphopoiesis at steady state in adult mice. Eur J Immunol. 2015;45(2):574–83.
186. Janas ML, Varano G, Gudmundsson K, Noda M, Nagasawa T, Turner M. Thymic development beyond beta-selection requires phosphatidylinositol 3-kinase activation by CXCR4. J Exp Med [Internet]. 2010;207(1):247–61.
187. Derbinski J, Gäbler J, Brors B, Tierling S, Jonnakuty S, Hergenhahn M, et al. Promiscuous gene expression in thymic epithelial cells is regulated at multiple levels. J Exp Med [Internet]. 2005;202(1):33–45.
188. Gray D, Abramson J, Benoist C, Mathis D. Proliferative arrest and rapid turnover of thymic epithelial cells expressing Aire. J Exp Med [Internet]. 2007;204(11):2521–8.
189. Takahama Y, Ohigashi I, Baik S, Anderson G. Generation of diversity in thymic epithelial cells. Nat Rev Immunol. 2017;
190. Derbinski J, Schulte a, Kyewski B, Klein L. Promiscuous gene expression in medullary thymic epithelial cells mirrors the peripheral self. Nat Immunol [Internet]. 2001;2(11):1032–9.
191. Anderson MS, Venanzi ES, Klein L, Chen Z, Berzins SP, Turley SJ, et al. Projection of an immunological self shadow within the thymus by the aire protein. Science. 2002;298(November):1395–401.
192. Zuklys S, Balciunaite G, Agarwal A, Fasler-Kan E, Palmer E, Hollander GA. Normal Thymic Architecture and Negative Selection Are Associated with Aire Expression, the Gene Defective in the Autoimmune-Polyendocrinopathy-Candidiasis-Ectodermal Dystrophy (APECED). J Immunol [Internet]. 2000;165(4):1976–83.
193. Peterson P, Pitkänen J, Sillanpää N, Krohn K. Autoimmune polyendocrinopathy candidiasis ectodermal dystrophy (APECED): A model disease to study molecular aspects of endocrine autoimmunity. Clin Exp Immunol. 2004;135(3):348–57.
194. Seach N, Ueno T, Fletcher AL, Lowen T, Mattesich M, Engwerda CR, et al. The lymphotoxin pathway regulates Aire-independent expression of ectopic genes and chemokines in thymic stromal cells. J Immunol. 2008;180:5384–92.
195. Lei Y, Ripen AM, Ishimaru N, Ohigashi I, Nagasawa T, Jeker LT, et al. Aire-dependent production of XCL1 mediates medullary accumulation of thymic dendritic cells and contributes to regulatory T cell development. J Exp Med. 2011;208(2):383–94.
196. Hubert FX, Kinkel SA, Davey GM, Phipson B, Mueller SN, Liston A, et al. Aire regulates the transfer of antigen from mTECs to dendritic cells for induction of thymic tolerance. Blood. 2011;118(9):2462–72.
197. Laan M, Kisand K, Kont V, Möll K, Tserel L, Scott HS, et al. Autoimmune regulator deficiency results in decreased expression of CCR4 and CCR7 ligands and in delayed migration of CD4+ thymocytes. J Immunol [Internet]. 2009;183(12):7682–91.
198. Auerbach R. Morphogenetic interactions in the development of the mouse thymus gland. Dev Biol [Internet]. 1960;2:271–84.
199. Auerbach R. Developmental studies of mouse thymus and spleen. Natl Cancer Inst Monogr. 1963;11:23–33.
200. Jiang X, Rowitch DH, Soriano P, McMahon a P, Sucov HM. Fate of the mammalian cardiac neural crest. Development [Internet]. 2000 Apr;127(8):1607–16.
201. Jenkinson WE, Jenkinson EJ, Anderson G. Differential requirement for mesenchyme in the proliferation and maturation of thymic epithelial progenitors. J Exp Med [Internet]. 2003 Jul 21;198(2):325–32.
202. Jenkinson WE, Rossi SW, Parnell SM, Jenkinson EJ, Anderson G. PDGFRalpha-expressing mesenchyme regulates thymus growth and the availability of intrathymic niches. Blood [Internet]. 2007 Feb 1;109(3):954–60.
203. Shinohara T, Honjo T. Epidermal growth factor can replace thymic mesenchyme in induction of embryonic thymus morphogenesis in vitro. Eur J Immunol. 1996;26:747–52.

204. Griffith A V, Cardenas K, Carter C, Gordon J, Iberg A, Engleka K, et al. Increased thymus- and decreased parathyroid-fated organ domains in Splotch mutant embryos. Dev Biol [Internet]. 2009 Mar 1;327(1):216–27.
205. Revest J-M, Suniara RK, Kerr K, Owen JJT, Dickson C. Development of the Thymus Requires Signaling Through the Fibroblast Growth Factor Receptor R2-IIIb. J Immunol [Internet]. 2001 Aug 15;167(4):1954–61.
206. Itoi M, Amagai T. Inductive role of fibroblastic cell lines in development of the mouse thymus anlage in organ culture. Cell Immunol [Internet]. 1998 Jan 10;183(1):32–41.
207. Shinohara T, Honjo T. Studies in vitro on the mechanism of the epithelial / mesenchymal interaction in the early fetal thymus. 1997;522–9.
208. Anderson G, Jenkinson EJ, Moore NC, Owen JJT. MHC Class II-positive epithelium and mesenchyme cells are both required for T-cell developent in the thymus. Nature. 1993;362:70–3.
209. Anderson G, Anderson KL, Tchilian EZ, Owen JJ, Jenkinson EJ. Fibroblast dependency during early thymocyte development maps to the CD25+ CD44+ stage and involves interactions with fibroblast matrix molecules. Eur J Immunol [Internet]. 1997 May;27(5):1200–6.
210. Sultana DA, Tomita S, Hamada M, Iwanaga Y, Kitahama Y, Khang N Van, et al. Gene expression profile of the third pharyngeal pouch reveals role of mesenchymal MafB in embryonic thymus development. Blood [Internet]. 2009 Mar 26;113(13):2976–87.
211. Sitnik KM, Kotarsky K, White AJ, Jenkinson WE, Anderson G, Agace WW. Mesenchymal cells regulate retinoic acid receptor-dependent cortical thymic epithelial cell homeostasis. J Immunol [Internet]. 2012 May 15;188(10):4801–9.
212. Yamazaki H, Sakata E, Yamane T, Yanagisawa A, Abe K, Yamamura KI, et al. Presence and distribution of neural crest-derived cells in the murine developing thymus and their potential for differentiation. Int Immunol. 2005;17(5):549–58.
213. Foster K, Sheridan J, Veiga-Fernandes H, Roderick K, Pachnis V, Adams R, et al. Contribution of neural crest-derived cells in the embryonic and adult thymus. J Immunol [Internet]. 2008 Mar 1;180(5):3183–9.
214. Gray DHD, Tull D, Ueno T, Seach N, Classon BJ, Chidgey A, et al. A unique thymic fibroblast population revealed by the monoclonal antibody MTS-15. J Immunol. 2007;178:4956–65.
215. Sitnik KM, Wendland K, Weishaupt H, Anderson G, Kotarsky K, Agace WW. Context-Dependent Development of Lymphoid Article Context-Dependent Development of Lymphoid Stroma from Adult CD34 + Adventitial Progenitors. CellReports [Internet]. 2016;1–14.
216. Ozerdem U, Stallcup WB. Early contribution of pericytes to angiogenic sprouting and tube formation. Angiogenesis. 2003;6(3):241–9.
217. Müller SM, Terszowski G, Blum C, Haller C, Anquez V, Kuschert S, et al. Gene targeting of VEGF-A in thymus epithelium disrupts thymus blood vessel architecture. Proc Natl Acad Sci U S A [Internet]. 2005 Jul 26;102(30):10587–92.
218. Fletcher AL, Acton SE, Knoblich K. Lymph node fibroblastic reticular cells in health and disease. Nat Rev Immunol [Internet]. 2015;15(6):350–61.
219. Katakai T, Hara T, Sugai M, Gonda H, Shimizu A. Lymph node fibroblastic reticular cells construct the stromal reticulum via contact with lymphocytes. J Exp Med [Internet]. 2004 Sep 20;200(6):783–95.
220. Link A, Vogt TK, Favre S, Britschgi MR, Acha-Orbea H, Hinz B, et al. Fibroblastic reticular cells in lymph nodes regulate the homeostasis of naive T cells. Nat Immunol [Internet]. 2007 Nov;8(11):1255–65.
221. Bajénoff M, Egen J, Koo LY, Laugier JP, Brau F, Germain RN, et al. Stromal Cell Networks Regulate Lymphocyte Entry, Migration, and Territoriality in Lymph Nodes. Immunity. 2006;25(6):989–1001.
222. Malhotra D, Fletcher AL, Astarita JL, Lukacs-Kornek V, Tayalia P, Hemler M, et al. Transcriptional profiling of stroma from inflamed and resting lymph nodes defines immunological hallmarks. Nat Immunol. 2012;13(5):499–510.
223. Gunn MD, Kyuwa S, Tam C, Kakiuchi T, Matsuzawa A, Williams LT, et al. Mice lacking expression of secondary lymphoid organ chemokine have defects in lymphocyte homing and dendritic cell localization. J Exp Med [Internet]. 1999;189(3):451–60.
224. Mori S, Nakano H, Aritomi K, Wang CR, Gunn MD, Kakiuchi T. Mice lacking expression of the chemokines CCL21-ser and CCL19 (plt mice) demonstrate delayed but enhanced T cell immune responses. J Exp Med. 2001;193(2):207–18.

225. Nakano H, Tamura T, Yoshimoto T, Yagita H, Miyasaka M, Butcher EC, et al. Genetic defect in T lymphocyte-specific homing into peripheral lymph nodes. Eur J Immunol. 1997;27(1):215–21.
226. Nakano H, Mori S, Yonekawa H, Nariuchi H, Matsuzawa a, Kakiuchi T. A novel mutant gene involved in T-lymphocyte-specific homing into peripheral lymphoid organs on mouse chromosome 4. Blood. 1998;91(8):2886–95.
227. Gretz JE, Norbury CC, Anderson a O, Proudfoot a E, Shaw S. Lymph-borne chemokines and other low molecular weight molecules reach high endothelial venules via specialized conduits while a functional barrier limits access to the lymphocyte microenvironments in lymph node cortex. J Exp Med. 2000;192(10):1425–40.
228. Roozendaal R, Mempel TR, Pitcher LA, Santiago F, Verschoor A, Mebius RE, et al. Conduits mediate transport of low molecular weight antigen to lymph node follicles. Immunity. 2009;30(2):264–76.
229. Pavert SA Van De, Olivier BJ, Goverse G, Vondenhoff MF, Greuter M, Beke P, et al. CXCL13 Is Essential For Lymph Node Intiation and Is Induced By Retinoic Acid and Neuronal Stimulation. 2009;10(11):1193–9.
230. Pavert SA Van De, Olivier BJ, Goverse G, Vondenhoff MF, Greuter M, Beke P, et al. CXCL13 is essential for lymph node initiation and is induced by retinoic acid and neuronal stimulation. Nat Immunol. 2009;10(11):1193–9.
231. Bénézech C, Mader E, Desanti G, Khan M, Nakamura K, White A, et al. Lymphotoxin-β receptor signaling through NF-κB2-RelB pathway reprograms adipocyte precursors as lymph node stromal cells. Immunity [Internet]. 2012 Oct 19;37(4):721–34.
232. Bénézech C, White A, Mader E, Serre K, Parnell S, Pfeffer K, et al. Ontogeny of stromal organizer cells during lymph node development. J Immunol [Internet]. 2010 Apr 15;184(8):4521–30.
233. Chai Q, Onder L, Scandella E, Gil-Cruz C, Perez-Shibayama C, Cupovic J, et al. Maturation of lymph node fibroblastic reticular cells from myofibroblastic precursors is critical for antiviral immunity. Immunity [Internet]. 2013 May 23;38(5):1013–24.
234. Yu W, Nagaoka H, Jankovic M, Misulovin Z, Suh H, Rolink A, et al. Continued RAG expression in late stages of B cell development and no apparent re-induction after immunization. Nature [Internet]. 1999;400(6745):682–7.
235. Hare KJ, Jenkinson EJ, Anderson G. CD69 expression discriminates MHC-dependent and -independent stages of thymocyte positive selection. J Immunol [Internet]. 1999;162(7):3978–83.
236. Mendiratta SK, Martin WD, Hong S, Boesteanu A, Joyce S, Van Kaer L. CD1d1 Mutant Mice Are Deficient in Natural T Cells That PromptlyProduce IL-4. Immunity. 1997;6(4):469–77.
237. Banks T a, Rouse BT, Kerley MK, Blair PJ, Godfrey VL, Kuklin N a, et al. Lymphotoxin-alpha-deficient mice. Effects on secondary lymphoid organ development and humoral immune responsiveness. J Immunol [Internet]. 1995;155:1685–93.
238. Dougall WC, Glaccum M, Charrier K, Rohrbach K, Brasel K, De Smedt T, et al. RANK is essential for osteoclast and lymph node development. Genes Dev. 1999;13(18):2412–24.
239. Wang Y, Koroleva EP, Kruglov AA, Kuprash D V, Sergei A, Fu Y, et al. Lymphotoxin beta receptor signaling in intestinal epithelial cells orchestrates innate immune responses against mucosal bacterial infection. Immunity. 2010;32(3):403–13.
240. Foo SS, Turner CJ, Adams S, Compagni A, Aubyn D, Kogata N, et al. Ephrin-B2 controls cell motility and adhesion during blood-vessel-wall assembly. Cell. 2006;124(1):161–73.
241. Muzumdar M, Tasic B, Miyamichi K, Ling L, Liqun L. A Global Double-Fluorescent Cre Reporter Mouse. Genesis. 2007;45(6):593–605.
242. Lewis A, Vasudevan H, O'neill A, Soriano P, Bush J. The widely used Wnt1-Cre transgene causes developmental phenotypes by ectopic activation of Wnt signaling. Dev Biol. 2013;379(2):229–34.
243. Gordon J, Xiao S, Hughes B, Su D, Navarre SP, Condie BG, et al. Specific expression of lacZ and cre recombinase in fetal thymic epithelial cells by multiplex gene targeting at the Foxn1 locus. BMC Dev Biol [Internet]. 2007;7:69.
244. Kisanuki YY, Hammer RE, Miyazaki J, Williams SC, Richardson JA, Yanagisawa M. Tie2-Cre Transgenic Mice: A New Model for Endothelial Cell-Lineage Analysis in Vivo. Dev Biol [Internet]. 2001;230(2):230–42.
245. Motoike T, Markham DW, Rossant J, Sato TN. Evidence for novel fate of Flk1+ progenitor: Contribution to muscle lineage. Genesis. 2003;35(3):153–9.

246. Jenkinson EJ, Anderson G, Owen JJ. Studies on T cell maturation on defined thymic stromal cell populations in vitro. J Exp Med [Internet]. 1992;176(3):845–53.
247. Farr AG. Characterization and cloning of a novel glycoprotein expressed by stromal cells in T-dependent areas of peripheral lymphoid tissues. J Exp Med [Internet]. 1992;176(5):1477–82.
248. van Vliet E, Melis M, Van Ewijk W. Monoclonal antibodies to stromal cell types of the mouse thymus. Eur J Immunol. 1984;14(6):524–9.
249. Kozai M, Kubo Y, Katakai T, Kondo H, Kiyonari H, Schaeuble K, et al. Essential role of CCL21 in establishment of central self- tolerance in T cells. J Exp Med [Internet]. 2017;214(7):1–11.
250. Müller SM, Stolt CC, Terszowski G, Blum C, Amagai T, Kessaris N, et al. Neural Crest Origin of Perivascular Mesenchyme in the Adult Thymus. J Immunol. 2008;180:5344–51.
251. Odaka C. Localization of mesenchymal cells in adult mouse thymus: their abnormal distribution in mice with disorganization of thymic medullary epithelium. J Histochem Cytochem [Internet]. 2009 Apr;57(4):373–82.
252. Katakai T, Kondo N, Ueda Y, Kinashi T, Alerts E. Autotaxin Produced by Stromal Cells Promotes LFA-1 − Independent and Rho-Dependent Interstitial T Cell Motility in the Lymph Node Paracortex. 2014;
253. Kanda H, Newton R, Klein R, Morita Y, Gunn M, Rosen S. Autotaxin, A Lysophosphatidic Acid-Producing Ectoenzyme, Promostes Lymphocyte Entry Into Secondary Lymphoid Organs. Nat Immunol. 2008;9(4):415–23.
254. Shores EW, Van Ewijk W, Singer A. Disorganization and restoration of thymic medullary epithelial cells in T cell receptor-negative scid mice: Evidence that receptor-bearing lymphocytes influence maturation of the thymic microenvironment. Eur J Immunol. 1991;21(7):1657–61.
255. Patenaude J, Perreault C. Thymic Mesenchymal Cells Have a Distinct Transcriptomic Profile. J Immunol [Internet]. 2016;
256. Saini M, Sinclair C, Marshall D, Tolaini M, Sakaguchi S, Seddon B. Regulation of Zap70 expression during thymocyte development enables temporal separation of CD4 and CD8 repertoire selection at different signaling thresholds. Sci Signal. 2010;3(114):ra23.
257. Dejardin E, Droin NM, Delhase M, Haas E, Cao Y, Makris C, et al. The lymphotoxin-beta receptor induces different patterns of gene expression via two NF-kappaB pathways. Immunity [Internet]. 2002;17(4):525–35.
258. Vondenhoff MF, Greuter M, Goverse G, Elewaut D, Dewint P, Ware F, et al. LTBR Signaling Induces Cytoking Expressino and Up-Regulates Lymphangiogenic Factors in Lymph Node Anlagen. J Immunol. 2010;182(9):5439–45.
259. Perera J, Huang H. The Development And Function Of Thymic B Cells. Cell Mol Life Sci. 2015;72(14):2657–63.
260. Yamano T, Nedjic J, Hinterberger M, Steinert M, Koser S, Pinto S, et al. Thymic B Cells Are Licensed to Present Self Antigens for Central T Cell Tolerance Induction. Immunity [Internet]. 2015;42(6):1048–61.
261. Walters SN, Webster KE, Daley S, Grey ST. A role for intrathymic B cells in the generation of natural regulatory T cells. J Immunol [Internet]. 2014 Jul 1;193(1):170–6.
262. Xing Y, Wang X, Jameson SC, Hogquist KA. Late stages of T cell maturation in the thymus involve NF-κB and tonic type I interferon signaling. Nat Immunol [Internet]. 2016;17(5).
263. Boursalian TE, Golob J, Soper DM, Cooper CJ, Fink PJ. Continued maturation of thymic emigrants in the periphery. Nat Immunol. 2004;5(4):418–25.
264. De Trez C, Schneider K, Potter K, Droin N, Fulton J, Norris PS, et al. The inhibitory HVEM-BTLA pathway counter regulates lymphotoxin receptor signaling to achieve homeostasis of dendritic cells. J Immunol (Baltimore, Md 1950) [Internet]. 2008;180(1):238–48.
265. Krautler N., Kana V, Kranich J, Tian Y, Perera D, Lemm D, et al. Follicular dendritic cells emerge from ubiquitous perivascular precursors. Cell. 2012;150(1):358–66.
266. Kozai M, Kubo Y, Katakai T, Kondo H, Kiyonari H, Schaeuble K, et al. Essential role of CCL21 in establishment of central self-tolerance in T cells Mina Kozai1, Yuki Kubo1,2, Tomoya Katakai3, Hiroyuki Kondo1, Hiroshi Kiyonari4, Karin Schaeuble5, Sanjiv A. Luther5, Naozumi Ishimaru6, Izumi Ohigashi1*, Yousuke Takahama1*.
267. Venkataraman K, Lee Y-M, Michaud J, Thangada S, Ai Y, Bonkovsky H, et al. Vascular Endothelium As A Contributor Of Plasma Sphingosine-1-Phosphate. Circ Res. 2008;102(6):669–76.
268. Mori K, Itoi M, Tsukamoto N, Kubo H, Amagai T. The perivascular space as a path of

hematopoietic progenitor cells and mature T cells between the blood circulation and the thymic parenchyma. Int Immunol. 2007;19(6):745–53.
269. Förster R, Schubel A, Breitfeld D, Kremmer E, Renner-Müller I, Wolf E, et al. CCR7 coordinates the primary immune response by establishing functional microenvironments in secondary lymphoid organs. Cell. 1999;99(1):23–33.
270. Hunter MC, Teijeira A, Halin C. T cell trafficking through lymphatic vessels. Front Immunol. 2016;7(DEC).
271. Weinreich, M and Hogquist KA. Thymic emigration: when and how T cells leave home. J Immunol. 2008;181(4):2265–70.
272. Scollay R, Godfrey DI. Thymic emigration: conveyor belts or lucky dips? Immunol Today. 1995;16(6):268–73.
273. Huesmann M, Scott B, Kisielow P, von Boehmer H. Kinetics and efficacy of positive selection in the thymus of normal and T cell receptor transgenic mice. Cell. 1991;66(3):533–40.
274. Lucas B, Vasseur F, Penit C. Production, selection, and maturation of thymocytes with high surface density of TCR. J Immunol [Internet]. 1994;153(1):53–62.
275. Egerton M, Scollay R, Shortman K. Kinetics of mature T-cell development in the thymus. Proc Natl Acad Sci [Internet]. 1990;87(7):2579–82.
276. Kelly KA, Scollay R. Analysis of recent thymic emigrants with subse- and maturity-related markers. Int Immunol. 1990;2(5):419–25.
277. McCaughtry TM, Wilken MS, Hogquist K a. Thymic emigration revisited. J Exp Med. 2007;204(11):2513–20.
278. Jin R, Wang W, Yao J-Y, Zhou Y-B, Qian X-P, Zhang J, et al. Characterization of the in vivo dynamics of medullary CD4+CD8- thymocyte development. J Immunol [Internet]. 2008;180(4):2256–63.
279. Gui M, Wiest DL, Li J, Kappes D, Hardy RR, Hayakawa K. Peripheral CD4+ T cell maturation recognized by increased expression of Thy-1/CD90 bearing the 6C10 carbohydrate epitope. J Immunol [Internet]. 1999;163(9):4796–804.
280. Vernachio J, Li M, Donnenberg AD, Soloski MJ. Qa-2 expression in the adult murine thymus. A unique marker for a mature thymic subset. J Immunol [Internet]. 1989;142(1):48–56.
281. Ziegler SF, Ramsdell F, Alderson MR. The activation antigen CD69. Stem Cells. 1994;12(5):456–65.
282. Cowan JE, McCarthy NI, Anderson G. CCR7 Controls Thymus Recirculation, but Not Production and Emigration, of Foxp3+ T Cells. Cell Rep [Internet]. 2016;14(5):1041–8.
283. Hale JS, Fink PJ. Back to the Thymus: Peripheral T Cells Come Home. Immunol Cell Biol. 2009;87(1):58–64.
284. Berzins SP, Mcnab FW, Jones CM, Smyth MJ, Godfrey DI. Long-term retention of mature NK1.1+ NKT cells in the thymus. J Immunol [Internet]. 2006;176(7):4059–65.
285. Chung B, Montel-Hagen A, Ge S, Blumberg G, Kim K, Klein S, et al. Engineering the human thymic microenvironment to support thymopoiesis in vivo. Stem Cells [Internet]. 2014 May 6;
286. Steinmann G G. Changes in the human thymus during aging. Curr Top Pathol der Pathol. 1986;75(Table 1):43–88.
287. Yang H, Youm YH, Vandanmagsar B, Rood J, Kumar KG, Butler AA, et al. Obesity accelerates thymic aging. Blood. 2009;114(18):3803–12.
288. Tan J, Wang Y, Zhang N, Zhu X. Induction of Epithelial to Mesenchymal Transition (EMT) and Inhibition on Adipogenesis: Two Different Sides of the Same Coin? Feasible Roles and Mechanisms of Transforming Growth Factor β1 (TGF-β1) in Age-Related Thymic Involution. Cell Biol Int [Internet]. 2016;9999:1–5.
289. Youm YH, Yang H, Sun Y, Smith RG, Manley NR, Vandanmagsar B, et al. Deficient ghrelin receptor-mediated signaling compromises thymic stromal cell microenvironment by acceleratingthymic adiposity. J Biol Chem. 2009;284(11):7068–77.
290. Thiery JP, Acloque H, Huang RYJ, Nieto MA. Epithelial-Mesenchymal Transitions in Development and Disease. Cell. 2009;139(5):871–90.
291. Lamouille S, Xu J, Derynck R. Molecular mechanisms of epithelial-mesenchymal transition. Natl Rev Mol Cell Biol. 2014;15(3):178–96.